



Asia-Pacific  
Economic Cooperation

*Asia Pacific Economic Cooperation*

Assessment of Geological Storage Potential of Carbon Dioxide in the APEC Region - Phase 1

**CO<sub>2</sub> Storage Prospectivity of Selected  
Sedimentary Basins in the Region of  
China and South East Asia**

*APEC Energy Working Group EWG Project 06/2003*

**June 2005**



**Prepared by  
Innovative Carbon Technologies Pty Ltd.  
on behalf of the Cooperative Research Centre for Greenhouse Gas Technologies (CO2CRC)**

GPO Box 463, Canberra, ACT 2601  
Tel: +61 2 6200 3366 Fax: +61 2 6230 0448  
Email: [dhilditch@ictpl.com.au](mailto:dhilditch@ictpl.com.au)  
Website: [www.ictpl.com.au](http://www.ictpl.com.au)

**FOR THE ASIA-PACIFIC ECONOMIC COOPERATION  
SECRETARIAT**

35 Heng Mui Keng Terrace Singapore 119616  
Tel: (65) 6775-6012 Fax: (65) 6775-6013  
Email: [info@apec.org](mailto:info@apec.org)  
Website: [www.apec.org](http://www.apec.org)

© 2005 APEC Secretariat  
APEC#205-RE-01.6.



*Asia Pacific Economic Cooperation*

Assessment of Geological Storage Potential of Carbon Dioxide in the APEC Region - Phase 1

# **CO<sub>2</sub> Storage Prospectivity of Selected Sedimentary Basins in the Region of China and South East Asia**

*APEC Energy Working Group EWG Project 06/2003*

**June 2005**

Prepared and published by  
Innovative Carbon Technologies Pty Ltd.



Asia-Pacific  
Economic Cooperation



**Prepared by**

**Innovative Carbon Technologies Pty Ltd and Geoscience Australia  
on behalf of the Cooperative Research Centre for Greenhouse Gas Technologies  
(CO2CRC)**

GPO Box 463, Canberra, ACT 2601

Tel: +61 2 6200 3366 Fax: +61 2 6230 0448

Email: [dhilditch@ictpl.com.au](mailto:dhilditch@ictpl.com.au)

Website: [www.ictpl.com.au](http://www.ictpl.com.au)

**FOR THE ASIA-PACIFIC ECONOMIC COOPERATION  
SECRETARIAT**

35 Heng Mui Keng Terrace Singapore 119616

Tel: (65) 6775-6012 Fax: (65) 6775-6013

Email: [info@apec.org](mailto:info@apec.org)

Website: [www.apec.org](http://www.apec.org)

© 2005 APEC Secretariat

APEC#205-RE-01.6.

# Acknowledgements

The work reported here was initiated in 2001 by the APEC Expert Group on Clean Fossil Energy (EGCFE) as the first phase of a multi-phase program on carbon dioxide capture and geological storage in the APEC region. The EGCFE operates under the APEC Energy Working Group (EWG), one of whose key roles is to promote sustainable energy development within the APEC community.

Essential to the development of this report was the expertise and substantial effort contributed by authors Ian Newlands and Robert Langford from Geoscience Australia and CO2CRC, and the contributions they received from John Bradshaw, Rick Causebrook, Timothy Robertson and Catherine Martin, also from Geoscience Australia and CO2CRC.

The production of this report would not have been possible without the support of CO2CRC and the contributions of CO2CRC and ICTPL staff, particularly those made by Andy Rigg, David Hilditch, Lee-Anne Shepherd and Amie Cupitt.

Thanks also go to Frank Mourits and Scott Smouse from the EGCFE and Joel Tu from APEC for initiating the project and providing ongoing guidance; and to both Stefan Bachu and Bill Gunter for their invaluable advice.



# Contents

<b>Executive Summary</b> .....	<b>17</b>
<b>Overview Summary</b> .....	<b>19</b>
<b>Technical Summary</b> .....	<b>21</b>
Conclusion .....	24
<b>1. Introduction</b> .....	<b>25</b>
<b>2. Definition</b> .....	<b>27</b>
2.1 Geological Storage.....	27
2.2 Methodology and assumptions .....	30
2.3 Current CO <sub>2</sub> Storage Pilot Sites .....	34
<b>3. China</b> .....	<b>35</b>
3.1 Source Characterisation .....	35
3.2 Geological Storage Summary .....	37
3.2.1 Basin Fill.....	38
3.2.2 Hydrocarbon fields.....	44
3.2.3 Coal.....	46
3.2.4 Summary.....	50
<b>4. Indonesia</b> .....	<b>51</b>
4.1 Source Characterisation .....	51
4.2 Geological Storage Summary .....	52
<b>5. South Korea</b> .....	<b>55</b>
5.1 Source Characterisation .....	55
5.2 Geological Storage Summary .....	56
<b>6. Malaysia</b> .....	<b>57</b>
6.1 Source Characterisation .....	57
6.2 Geological Storage Summary .....	58
<b>7. Philippines</b> .....	<b>59</b>
7.1 Source Characterisation .....	59
7.2 Geological Storage Summary .....	60
<b>8. Chinese Taipei</b> .....	<b>61</b>
8.1 Source Characterisation .....	61
8.2 Geological Storage Summary .....	62
<b>9. Thailand</b> .....	<b>64</b>
9.1 Source Characterisation .....	64
9.2 Geological Storage Summary .....	65
<b>10. References</b> .....	<b>67</b>
<b>Appendices</b> .....	<b>69</b>

<b>Appendix A: Additional Basin Discussion .....</b>	<b>71</b>
<b>A1. China .....</b>	<b>71</b>
A1.1 Bohai (North China) Basin .....	71
A1.1.1 CO <sub>2</sub> Sources .....	71
A1.1.2 Basin Overview .....	71
A1.1.3 Basin Fill .....	74
A1.1.4 Hydrocarbon fields .....	77
A1.1.5 Coal Occurrence .....	78
A1.1.6 Potential CO <sub>2</sub> Storage Options .....	78
A1.1.7 References .....	78
A1.2 East China Sea Basin .....	79
A1.2.1 CO <sub>2</sub> Sources .....	79
A1.2.2 Basin Overview .....	79
A1.2.3 Basin Fill .....	83
A1.2.4 Hydrocarbon Fields .....	87
A1.2.5 Coal Occurrence .....	87
A1.2.6 Potential CO <sub>2</sub> Storage Options .....	88
A1.2.7 References .....	88
A1.3 Hefei (Hehuai) Basin .....	89
A1.3.1 CO <sub>2</sub> Sources .....	89
A1.3.2 Basin Overview .....	89
A1.3.3 Basin Fill .....	92
A1.3.4 Hydrocarbon Fields .....	93
A1.3.5 Coal Occurrence .....	94
A1.3.6 Potential CO <sub>2</sub> Storage Options .....	94
A1.3.7 References .....	94
A1.4 Jiangnan Basin .....	95
A1.4.1 CO <sub>2</sub> Sources .....	95
A1.4.2 Basin Overview .....	95
A1.4.3 Basin Fill .....	99
A1.4.4 Hydrocarbon Fields .....	99
A1.4.5 Coal Occurrence .....	99
A1.4.6 Potential CO <sub>2</sub> Storage Options .....	100
A1.4.7 References .....	100
A1.5 Nanpanjiang .....	101
A1.5.1. CO <sub>2</sub> Sources .....	101
A1.5.2 Basin Overview .....	101
A1.5.3 Basin Fill .....	101
A1.5.4 Hydrocarbon Fields .....	101
A1.5.5 Coal Occurrence .....	101
A1.5.6 Potential CO <sub>2</sub> Storage Options .....	101
A1.5.7 References .....	102
A1.6 Nanyang .....	102
A1.6.1 CO <sub>2</sub> Sources .....	102
A1.6.2 Basin Overview .....	102
A1.6.3 Potential CO <sub>2</sub> Storage Options .....	102

A1.7 Ordos Basin.....	103
<i>A1.7.1 CO<sub>2</sub> Sources</i> .....	103
<i>A1.7.2 Basin Overview</i> .....	103
<i>A1.7.3 Basin Fill</i> .....	107
<i>A1.7.4 Hydrocarbon Fields</i> .....	107
<i>A1.7.5 Coal Occurrence</i> .....	110
<i>A1.7.6 Potential CO<sub>2</sub> Storage Options</i> .....	110
<i>A1.7.7 References</i> .....	110
A1.8 Pearl River Mouth Basin.....	111
<i>A1.8.1 CO<sub>2</sub> Sources</i> .....	111
<i>A1.8.2 Basin Overview</i> .....	111
<i>A1.8.3 Basin Fill</i> .....	113
<i>A1.8.4 Hydrocarbon Fields</i> .....	119
<i>A1.8.5 Coal Occurrence</i> .....	119
<i>A1.8.6 Potential CO<sub>2</sub> Storage Options</i> .....	119
<i>A1.8.7 References</i> .....	120
A1.9 Sanshui Basin.....	121
<i>A1.9.1 CO<sub>2</sub> Sources</i> .....	121
<i>A1.9.2 Basin Overview</i> .....	121
<i>A1.9.3 Basin Fill</i> .....	121
<i>A1.9.4 Hydrocarbon Fields</i> .....	121
<i>A1.9.5 Coal Occurrence</i> .....	121
<i>A1.9.6 Potential CO<sub>2</sub> Storage Options</i> .....	121
<i>A1.9.7 References</i> .....	122
A1.10 Shiwan Dashan Basin.....	123
<i>A1.10.1 CO<sub>2</sub> Sources</i> .....	123
<i>A1.10.2 Basin Overview</i> .....	123
<i>A1.10.3 Basin Fill</i> .....	123
<i>A1.10.4 Hydrocarbon Fields</i> .....	123
<i>A1.10.5 Coal Occurrence</i> .....	123
<i>A1.10.6 Potential CO<sub>2</sub> Storage Options</i> .....	123
<i>A1.10.7 References</i> .....	124
A1.11 Sichuan Basin.....	125
<i>A1.11.1 CO<sub>2</sub> Sources</i> .....	125
<i>A1.11.2 Basin Overview</i> .....	125
<i>A1.11.3 Basin Fill</i> .....	127
<i>A1.11.4 Hydrocarbon Fields</i> .....	128
<i>A1.11.5 Coal</i> .....	130
<i>A1.11.6 Potential CO<sub>2</sub> Storage Options</i> .....	130
<i>A1.11.7 References</i> .....	130
A1.12 Songliao Basin.....	131
<i>A1.12.1 CO<sub>2</sub> Sources</i> .....	131
<i>A1.12.2 Basin Overview</i> .....	131
<i>A1.12.3 Basin Fill</i> .....	131
<i>A1.12.4 Hydrocarbon Fields</i> .....	135
<i>A1.12.5 Coal Occurrence</i> .....	135

<i>A1.12.6 Potential CO<sub>2</sub> Storage Options</i> .....	137
<i>A1.12.7 References</i> .....	137
A1.13 Subei (Jiangsu-Yellow Sea) Basins.....	139
<i>A1.13.1 CO<sub>2</sub> Sources</i> .....	139
<i>A1.13.2 Basin Overview</i> .....	139
<i>A1.13.3 Basin Fill</i> .....	140
<i>A1.13.4 Hydrocarbon Fields</i> .....	140
<i>A1.13.5 Coal Occurrence</i> .....	140
<i>A1.13.6 Potential CO<sub>2</sub> Storage Options</i> .....	142
<i>A1.13.7 References</i> .....	142
A.1.14 Yinggehai Basin (China Section).....	143
<i>A.1.14.1 CO<sub>2</sub> Sources</i> .....	143
<i>A.1.14.2 Basin Overview</i> .....	143
<i>A.1.14.3 Basin Fill</i> .....	145
<i>A.1.14.4 Hydrocarbon Fields</i> .....	146
<i>A.1.14.5 Coal Occurrence</i> .....	146
<i>A.1.14.6 Potential CO<sub>2</sub> Storage Options</i> .....	146
<i>A.1.14.7 References</i> .....	148
<b>A2. Indonesia</b> .....	<b>149</b>
A2.1 NW Java Basin.....	149
<i>A2.1.1 CO<sub>2</sub> Sources</i> .....	149
<i>A2.1.2 Basin Overview</i> .....	149
<i>A2.1.3 Basin Fill</i> .....	150
<i>A2.1.4 Hydrocarbon Fields</i> .....	150
<i>A2.1.5 Coal Occurrence</i> .....	152
<i>A2.1.6 Potential CO<sub>2</sub> Storage Options</i> .....	152
<i>A2.1.7 References</i> .....	152
A2.2 East Java Basin.....	153
<i>A2.2.1 CO<sub>2</sub> Sources</i> .....	153
<i>A2.2.2 Basin Overview</i> .....	153
<i>A2.2.3 Basin Fill</i> .....	154
<i>A2.2.4 Hydrocarbon fields</i> .....	154
<i>A2.2.5 Coal Occurrence</i> .....	155
<i>A2.2.6 Potential CO<sub>2</sub> Storage Options</i> .....	155
<i>A2.2.7 References</i> .....	156
A2.3 Kutei Basin.....	157
<i>A2.3.1 CO<sub>2</sub> Sources</i> .....	157
<i>A2.3.2 Basin Overview</i> .....	157
<i>A2.3.3 Basin Fill</i> .....	159
<i>A2.3.4 Hydrocarbon Fields</i> .....	161
<i>A2.3.5 Coal Occurrence</i> .....	161
<i>A2.3.6 Potential CO<sub>2</sub> Storage Options</i> .....	161
<i>A2.3.7 References</i> .....	162
A2.4 North Sumatra Basin.....	163
<i>A2.4.1 CO<sub>2</sub> Sources</i> .....	163
<i>A2.4.2 Basin Overview</i> .....	163

A2.4.3 Basin Fill .....	165
A2.4.4 Hydrocarbon fields .....	165
A2.4.5 Coal Occurrence.....	165
A2.4.6 Potential CO <sub>2</sub> storage Options .....	165
A2.4.7 References .....	170
A2.5 Central Sumatra Basin .....	171
A2.5.1 CO <sub>2</sub> Sources.....	171
A2.5.2 Basin Overview.....	171
A2.5.3 Basin Fill .....	172
A2.5.4 Hydrocarbon Fields .....	172
A2.5.5 Coal Occurrence.....	174
A2.5.6 Potential CO <sub>2</sub> Storage Options.....	176
A2.5.7 References.....	176
A2.6 Southern Sumatra Basin.....	177
A2.6.1 CO <sub>2</sub> Sources .....	177
A2.6.2 Basin Overview.....	177
A2.6.3 Basin Fill .....	178
A2.6.4 Hydrocarbon fields.....	178
A2.6.5 Coal Occurrence.....	178
A2.6.6 Potential CO <sub>2</sub> Storage Options.....	178
A2.6.7 References.....	180
<b>A3. South Korea .....</b>	<b>181</b>
A3.1 Kunsan Basin (South Korean Sector: North Yellow Sea Basin).....	181
3.1.1 CO <sub>2</sub> Sources .....	181
3.1.2 Basin Overview .....	181
3.1.3 Basin Fill.....	181
3.1.4 Hydrocarbon Fields .....	182
3.1.5 Coal Occurance .....	182
3.1.6 Potential CO <sub>2</sub> Storage Options .....	184
3.1.7 References .....	184
A3.2 Northern most East China Sea Basin .....	185
A3.2.1 CO <sub>2</sub> Sources.....	185
A3.2.2 Basin Overview.....	185
A3.2.3 Basin Fill .....	187
A3.2.4 Hydrocarbon Fields.....	187
A3.2.5 Coal Occurrence .....	187
A3.2.6 Potential CO <sub>2</sub> Storage Options.....	188
A3.2.7 References.....	188
A3.3 Ulleung Basin.....	189
A3.3.1 CO <sub>2</sub> Sources.....	189
A3.3.2 Basin Overview.....	189
A3.3.3 Basin Fill .....	191
A3.3.4 Hydrocarbon Fields.....	193
A3.3.5 Coal Occurrence .....	193
A3.3.6 Potential CO <sub>2</sub> Storage Options.....	193
A3.3.7 References.....	193

<b>A4. Malaysia</b> .....	<b>195</b>
A4.1 Malay Basin .....	195
A4.1.1 CO <sub>2</sub> Sources .....	195
A4.1.2 Basin Overview.....	195
A4.1.3 Basin Fill .....	195
A4.1.4 Hydrocarbon Fields.....	198
A4.1.5 Coal Occurrence .....	198
A4.1.6 Potential CO <sub>2</sub> Storage Options.....	198
A4.1.7 References.....	198
<b>A5. Philippines</b> .....	<b>199</b>
A5.1 Luzon Basin .....	199
A5.1.1 CO <sub>2</sub> Sources .....	199
A5.1.2 Basin Overview.....	201
A5.1.3 Basin Fill .....	201
A5.1.4 Hydrocarbon Fields.....	201
A5.1.5 Coal Occurrence.....	201
A5.1.6 Potential CO <sub>2</sub> Storage Options.....	202
A5.1.7 References.....	202
<b>A6 Chinese Taipei</b> .....	<b>203</b>
A6.1 West of Chinese Taipei.....	203
A6.1.1 CO <sub>2</sub> Sources .....	203
A6.1.2 Basin Overview.....	203
A6.1.3 Basin Fill .....	203
A6.1.4 Hydrocarbon Fields.....	203
A6.1.5 Coal Occurrence .....	207
A6.1.6 Potential CO <sub>2</sub> Storage Options.....	207
A6.1.7 References.....	207
<b>A7. Thailand</b> .....	<b>209</b>
A7.1 Thai Gulf Basin (NW Basins & Pattani).....	209
A7.1.1 CO <sub>2</sub> Sources .....	209
A7.1.2 Basin Overview.....	209
A7.1.3 Basin Fill .....	210
A7.1.4 Hydrocarbon Fields.....	210
A7.1.5 Coal Occurrence.....	210
A7.1.6 Potential CO <sub>2</sub> Storage Options.....	211
A7.1.7 References.....	212
<b>A8. Table of Basin Attributes</b> .....	<b>213</b>
<b>Appendix B: Depleted Field Calculations and Data</b> .....	<b>219</b>
<b>Glossary</b> .....	<b>223</b>
<b>Acronyms and Units</b> .....	<b>227</b>

# Figures

<b>Figure 1.</b> Diagrammatic representation of various means of CO <sub>2</sub> storage in geologic media .....	17
<b>Figure 2.</b> Stationary source CO <sub>2</sub> emissions vs prospectivity .....	19
<b>Figure 3.</b> Stationary source CO <sub>2</sub> emissions vs prospectivity with geological notes.....	21
<b>Figure 4.</b> A tentative ranking of the CO <sub>2</sub> storage prospectivity of sedimentary basins in eastern China together with stationary CO <sub>2</sub> emissions. ....	22
<b>Figure 5.</b> APEC economies that are a focus of this report.....	25
<b>Figure 6.</b> Diagrammatic representation of various means of CO <sub>2</sub> storage in geologic media .....	27
<b>Figure 7.</b> Variation of CO <sub>2</sub> density with depth in sedimentary basins.....	29
<b>Figure 8.</b> APEC stationary source CO <sub>2</sub> emissions, Mt/year.....	30
<b>Figure 9.</b> APEC geological storage groups. ....	30
<b>Figure 10.</b> Global point source emissions - APEC contributions. ....	31
<b>Figure 11.</b> APEC - East and South East Asia significant sedimentary basins. ....	31
<b>Figure 12.</b> CO <sub>2</sub> emissions from stationary sources .....	31
<b>Figure 13.</b> Stationary source CO <sub>2</sub> emissions and arbitrary nodes.....	32
<b>Figure 14.</b> Sedimentary basins which fall within 300 kms of nodes. ....	32
<b>Figure 15.</b> Selected basin set.....	32
<b>Figure 16.</b> World and regional storage capacity estimates .....	33
<b>Figure 17.</b> Some of the CO <sub>2</sub> storage pilot projects in the study region. ....	34
<b>Figure 18.</b> China aggregated CO <sub>2</sub> sources and basins in proximity to concentrated emissions.....	35
<b>Figure 19.</b> Eastern China aggregated CO <sub>2</sub> sources and basins in proximity to emissions. ....	36
<b>Figure 20.</b> China CO <sub>2</sub> Emissions.....	37
<b>Figure 21.</b> Structural elements of China (from Korsh et al., 1991). ....	37
<b>Figure 22.</b> Classification of China's sedimentary basins .....	38
<b>Figure 23.</b> Eastern China approximate totals for annual stationary source CO <sub>2</sub> emissions in generalised 'geological' regions.....	39
<b>Figure 24.</b> The southern coastal region of the southern fold belt. ....	40
<b>Figure 25.</b> Cross-sections of the Bohai Basin illustrating the early, syn and late phases of rift base evolution .	41
<b>Figure 26.</b> Model of heterogeneity and buoyancy.....	42
<b>Figure 27.</b> The effect of CO <sub>2</sub> buoyancy and heterogeneity on the efficiency of CO <sub>2</sub> geological storage .....	42
<b>Figure 28.</b> China: relative prospectivity of the basins studied with aggregated CO <sub>2</sub> emissions.....	43
<b>Figure 29.</b> Summary hydrocarbon pore space per member economy .....	45
<b>Figure 30.</b> Comparison of the magnitude of hydrocarbon space equivalent CO <sub>2</sub> stored with annual CO <sub>2</sub> emissions .....	45
<b>Figure 31.</b> China coal map .....	46
<b>Figure 32.</b> Location of coal mines in China practicing methane drainage .....	48
<b>Figure 32.</b> Location of coal bed methane projects in China. ....	49
<b>Figure 34.</b> Indonesia stationary CO <sub>2</sub> emissions and basins studied .....	51
<b>Figure 35.</b> Indonesia stationary CO <sub>2</sub> emissions. ....	51

<b>Figure 36.</b> <i>The geology and hydrocarbon potential of the Island of Java and its adjoining offshore areas</i> .....	<b>53</b>
<b>Figure 37.</b> <i>South East Asia major stationary CO<sub>2</sub> emissions (aggregated) and coal deposits.</i> .....	<b>54</b>
<b>Figure 38.</b> <i>South Korea stationary CO<sub>2</sub> emissions and study basins.</i> .....	<b>55</b>
<b>Figure 38.</b> <i>South Korea stationary CO<sub>2</sub> emissions.</i> .....	<b>56</b>
<b>Figure 40.</b> <i>Malaysia stationary CO<sub>2</sub> emissions and study basins.</i> .....	<b>57</b>
<b>Figure 41.</b> <i>Malaysia stationary CO<sub>2</sub> emissions.</i> .....	<b>58</b>
<b>Figure 42.</b> <i>Simplified structural map of the Gulf of Thailand and Malay basins</i> .....	<b>58</b>
<b>Figure 43.</b> <i>Philippines stationary CO<sub>2</sub> emissions and study basins.</i> .....	<b>59</b>
<b>Figure 44.</b> <i>Phillipines stationary CO<sub>2</sub> emissions.</i> .....	<b>60</b>
<b>Figure 45.</b> <i>Chinese Taipei stationary CO<sub>2</sub> emissions and study basins.</i> .....	<b>61</b>
<b>Figure 46.</b> <i>Chinese Taipei stationary CO<sub>2</sub> emissions.</i> .....	<b>62</b>
<b>Figure 47.</b> <i>Basins in the Chinese Taipei region</i> .....	<b>63</b>
<b>Figure 48.</b> <i>Thailand stationary CO<sub>2</sub> emissions and study basins.</i> .....	<b>64</b>
<b>Figure 49.</b> <i>Thailand stationary CO<sub>2</sub> emissions.</i> .....	<b>65</b>
<b>Figure 50.</b> <i>Simplified structural map of the Gulf of Thailand and Malay basins</i> .....	<b>65</b>

# Figures in Appendices

<b>Figure A1.</b> Bohai Basin location and structure map of China .....	72
<b>Figure A2.</b> Regional structure setting of the Bohai Basin.....	72
<b>Figure A3.</b> Bohai Basin cross-sections .....	73
<b>Figure A4.</b> Bohai Basin stratigraphy .....	74
<b>Figure A5.</b> Sedimentary facies maps in the offshore Bohai Basin .....	76
<b>Figure A6.</b> Facies variation for the low stand sediments of the lower Guantao member .....	76
<b>Figure A7.</b> Facies variation for the high stand sediments of the lower Guantao member .....	77
<b>Figure A8.</b> The character of the basement of the East China Sea .....	79
<b>Figure A9.</b> The structural divisions of the East China Sea .....	80
<b>Figure A10.</b> Structural cross-section of the East China Sea.....	81
<b>Figure A11.</b> Isopach maps of the Cenozoic sediments in the East China Sea .....	82
<b>Figure A12.</b> Distribution of Cenozoic sediments of the East China Sea.....	83
<b>Figure A13.</b> The paleogeography of the Cenozoic sediments .....	84
<b>Figure A14.</b> Cenozoic stratigraphy of the East China Sea .....	85
<b>Figure A15.</b> Stratigraphic correlation of the East China Sea .....	86
<b>Figure A16.</b> Schematic cross-section showing the predictive types of traps.....	87
<b>Figure A17.</b> Hefei Basin location.....	89
<b>Figure A18.</b> Structure map showing the locations of the basins including Hefei .....	90
<b>Figure A19.</b> Structural cross-sections from the Dabieshan area .....	91
<b>Figure A20.</b> Upper Triassic through Lower Tertiary unit names for foreland and rift basins, age data for ultrahigh-pressure rocks, and formation and rapid exhumation of UHP rocks and rapid doming episode of Dabieshan core. ....	92
<b>Figure A21.</b> Distribution map of the residual Jurassic and Cretaceous formations, Hehuai Basin. ....	93
<b>Figure A22.</b> Seismic section and its interpretation along seismic line 840, Shenqui Depression .....	93
<b>Figure A23.</b> Diagram of the tectonic elements in the Jiangnan Basin .....	95
<b>Figure A24.</b> Jiangnan cross-section .....	96
<b>Figure A25.</b> Stratigraphy in the Qianjiang depression of the Jiangnan Basin .....	97
<b>Figure A26.</b> Salt bearing basins in eastern China .....	98
<b>Figure A27.</b> Ordos Basin location map.....	104
<b>Figure A28.</b> North-south and east-west cross-sections accross the Ordos Basin .....	105
<b>Figure A29.</b> Triassic palaeogeography map of China .....	105
<b>Figure A30.</b> Ordos Basin stratigraphy.....	106
<b>Figure A31.</b> Paleogeography of the Ordos Basin from the Permian to cretaceous .....	108
<b>Figure A32.</b> Ordos Basin scheme showing the locus of the Mezoic depocenter .....	109
<b>Figure A33.</b> Ordos Basin, porosity and permeability data .....	109
<b>Figure A34.</b> Ordos Basin with location of hydrocarbon fields.....	109
<b>Figure A35.</b> Location map of the Pearl River Basin and other South China Sea basins .....	111

<b>Figure A36.</b> <i>Location and tectonic element map of the Pearl River Mouth Basin</i> .....	112
<b>Figure A37.</b> <i>Structural profile of the Pearl River Mouth Basin</i> .....	112
<b>Figure A38.</b> <i>Pearl River Mouth Basin detailed cross section of the Wenchang B sag</i> .....	113
<b>Figure A39.</b> <i>Pearl River Mouth Basin stratigraphy</i> .....	114
<b>Figure A40.</b> <i>Tertiary Shenhu-Wenchang Formation: facies map of the Peral River Mouth Basin</i> .....	115
<b>Figure A41.</b> <i>Tertiary Enping Formation (T8-T7): facies map of the Peral River Mouth Basin</i> .....	115
<b>Figure A42.</b> <i>Delta systems in the Lower Zhuhai Formation</i> .....	116
<b>Figure A43.</b> <i>Sandstone distribution in the Upper Zhuhai Formation</i> .....	116
<b>Figure A44.</b> <i>Sandstone distribution in the Middle Zhujiang Formation</i> .....	117
<b>Figure A45.</b> <i>Sand distribution in the delta systems of the Upper Zhujiang Formation</i> .....	117
<b>Figure A46.</b> <i>Sandstone distribution in the delta system of the Lower Hanjiang Formation</i> .....	118
<b>Figure A47.</b> <i>Seismic section Zhu III depression</i> .....	118
<b>Figure A48.</b> <i>Shoreline migration 22Ma to present</i> .....	119
<b>Figure A49.</b> <i>Location of the Shiwan-Dashan Basin</i> .....	124
<b>Figure A50.</b> <i>Oil and gas exploration and development block in Suchuan Basin</i> .....	125
<b>Figure A51.</b> <i>Formation of the Sichuan Basin</i> .....	126
<b>Figure A52.</b> <i>Sketch map of the sedimentation and structure in Sichuan Basin</i> .....	127
<b>Figure A53.</b> <i>Triangle plot of the genetic types of reservoir pore space in the Sichuan Basin</i> .....	127
<b>Figure A54.</b> <i>Gas pool section of Xiaoqan-Fenggu structural zone in western Sichuan depression</i> .....	129
<b>Figure A55.</b> <i>Lithofacies map of the continental strata in the Sichuan Basin</i> .....	129
<b>Figure A56.</b> <i>The location of the Songliao Basin</i> .....	132
<b>Figure A57.</b> <i>Structural cross-section of the Songliao Basin</i> .....	133
<b>Figure A58.</b> <i>Mesozoic and Cenozoic stratigraphy of the Sonliao Basin</i> .....	133
<b>Figure A59.</b> <i>Facies distribution in the Qingshankou Formation during Qn1 and Qu2 time</i> .....	134
<b>Figure A60.</b> <i>Burial depth of the Qingshankou Formation</i> .....	134
<b>Figure A61.</b> <i>Cross-section of the Zhenlai to Shengping area</i> .....	135
<b>Figure A62.</b> <i>Songlio Basin Daqing oilfield</i> .....	136
<b>Figure A63.</b> <i>Jiangsu Basin map</i> .....	139
<b>Figure A64.</b> <i>Generalised geological cross-section showing Northern Jiangsu Basin</i> .....	140
<b>Figure A65.</b> <i>Stratigraphy and half graben detail of the Dongtai sub-basin of the Jiangsu Basin</i> .....	141
<b>Figure A66.</b> <i>Palaeogeography of the Funning and Dainan Formations</i> .....	142
<b>Figure A67.</b> <i>Yinggehai Basin location map</i> .....	143
<b>Figure A68.</b> <i>Cross-section of the Ynggehai Basin</i> .....	144
<b>Figure A69.</b> <i>Organic chemistry and pressure profile for well LD301 Yinggehai Basin</i> .....	144
<b>Figure A70.</b> <i>Generalised stratigraphy of the south eastern flank of the Yinggehai Basin</i> .....	145
<b>Figure A71.</b> <i>Dongfang field cross-section showing heterogeneity of reservoir and temperature</i> .....	147
<b>Figure A72.</b> <i>NW Java Basin with distribution of hydrocarbon fields</i> .....	149
<b>Figure A73.</b> <i>Sundaland palaeogeology</i> .....	150
<b>Figure A74.</b> <i>Generalised stratigraphic column of Northwest Java</i> .....	151

<b>Figure A75.</b> <i>The geology and hydrocarbon potential of the Island of Java and its adjoining offshore areas</i>	<b>151</b>
<b>Figure A76.</b> <i>Tectono-stratigraphic development of the East Java Sea Basin</i>	<b>153</b>
<b>Figure A77.</b> <i>The geology and hydrocarbon potential of the Island of Java and its adjoining offshore areas</i>	<b>154</b>
<b>Figure A78.</b> <i>The geology and hydrocarbon potential of the Island of Java and its adjoining offshore areas</i>	<b>155</b>
<b>Figure A79.</b> <i>Kutei stratigraphy</i>	<b>157</b>
<b>Figure A80.</b> <i>Litho-stratigraphic and chrono-stratigraphic column of the Kutei Basin with hydrocarbon reserves</i>	<b>158</b>
<b>Figure A81.</b> <i>Kutei sequence stratigraphic interpretation section</i>	<b>159</b>
<b>Figure A82.</b> <i>North Sumatra Basin map</i>	<b>160</b>
<b>Figure A83.</b> <i>North Sumatra/Mergui Basins Thai sector well results</i>	<b>163</b>
<b>Figure A84.</b> <i>General physiography of the Mergui and North Sumatran basins showing the primary depocenters of the Thailand Andaman Sea: the West Mergui, East Mergui, and sub-basins</i>	<b>164</b>
<b>Figure A85.</b> <i>Generalised stratigraphic column for the Thailand sector of the Mergui and the North Sumatra basins showing the major sequences</i>	<b>166</b>
<b>Figure A86.</b> <i>Stratigraphy of the North Sumatran Basin</i>	<b>167</b>
<b>Figure A87.</b> <i>Palaeogeography of the Late Oligocene to Early Miocene, Northern Sumatra</i>	<b>168</b>
<b>Figure A88.</b> <i>Palaeogeography Middle Miocene to Upper Miocene, Northern Sumatra</i>	<b>168</b>
<b>Figure A89.</b> <i>Generalised cross-section across the Thailand Andaman Sea and the North Sumatra Basin</i>	<b>169</b>
<b>Figure A90.</b> <i>Central and Sumatran Basin regional map</i>	<b>171</b>
<b>Figure A91.</b> <i>Schematic section across the Central Sumatra Basin</i>	<b>172</b>
<b>Figure A92.</b> <i>Stratigraphic chart of the Central Sumatra Basin</i>	<b>173</b>
<b>Figure A93.</b> <i>Extent of Miocene Duri-Minas sequence in the Central Sumatra Basin</i>	<b>174</b>
<b>Figure A94.</b> <i>Diagrammatic cross-section of producing and prospective plays in Central Sumatra syn-rift sequences</i>	<b>175</b>
<b>Figure A95.</b> <i>South Sumatra Basin regional location map</i>	<b>177</b>
<b>Figure A96.</b> <i>Stratigraphy and tectonics of the South Sumatra Basin</i>	<b>179</b>
<b>Figure A97.</b> <i>Structural framework of the South Yellow Sea Basin, offshore western Korea, and location of the wells examined</i>	<b>182</b>
<b>Figure A98.</b> <i>Generalised lithological log of the Haeme-1 well showing sample horizons</i>	<b>183</b>
<b>Figure A99.</b> <i>Cheju (Fuke) Basin location</i>	<b>185</b>
<b>Figure A100.</b> <i>Cheju (Fuke) Basin cross-section</i>	<b>186</b>
<b>Figure A101.</b> <i>Cheju stratigraphy</i>	<b>186</b>
<b>Figure A102.</b> <i>Seismic section line with overlaid geological interpretation</i>	<b>187</b>
<b>Figure A103.</b> <i>Bathymetry of the Ulleung Basin</i>	<b>189</b>
<b>Figure A104.</b> <i>Ulleung Basin seismic section</i>	<b>190</b>
<b>Figure A105.</b> <i>Total sediment thickness (isopach) between the top of the acoustic basement and the seafloor</i>	<b>190</b>
<b>Figure A106.</b> <i>A schematic model illustrating the stratigraphic evolution of the Ulleung Basin</i>	<b>191</b>
<b>Figure A107.</b> <i>Lithologic columns of the Dolgorae- 1 well and the dummy well</i>	<b>192</b>
<b>Figure A108.</b> <i>Schematic cross-sectional diagram showing main rock types</i>	<b>193</b>
<b>Figure A109.</b> <i>Simplified structural map of the Gulf of Thailand and Malay Basins</i>	<b>196</b>
<b>Figure A111.</b> <i>Malay Basin composite stratigraphy</i>	<b>197</b>

<b>Figure A110.</b> <i>Palaeogeographic map of the Oligocene to Miocene period in the region of the Thai and Malay basins</i> .....	<b>197</b>
<b>Figure A112.</b> <i>Phillipines stationary CO<sub>2</sub> emissions and Luzon Basin</i> .....	<b>199</b>
<b>Figure A113.</b> <i>The Luzon Central Valley fore-arc basin</i> .....	<b>200</b>
<b>Figure A114.</b> <i>Basins in the Chinese Taipei region</i> .....	<b>204</b>
<b>Figure A115.</b> <i>Profiles showing the upper crustal structures across the northern margin of the South China Sea in the Chinese Taipei region</i> .....	<b>205</b>
<b>Figure A116.</b> <i>Stratigraphy of Chinese Taipei basins and other structural elements</i> .....	<b>206</b>
<b>Figure A117.</b> <i>Simplified structural map of the Gulf of Thailand and Malay Basins</i> .....	<b>209</b>
<b>Figure A118.</b> <i>Depositional environment during the Oligocene and Miocene</i> .....	<b>210</b>
<b>Figure A119.</b> <i>Litostratigraphic column of the Bongkot Field</i> .....	<b>211</b>
<b>Figure A120.</b> <i>Stratigraphic summary of the major depositional sequences within the Pattani Basin</i> .....	<b>212</b>

## Tables

<b>Table 1.</b> <i>Factors for consideration for CO<sub>2</sub> storage in deep saline reservoirs</i> .....	<b>28</b>
<b>Table A1.</b> <i>Details of the calculations used to estimated stored CO<sub>2</sub> from hydrocarbon volumes are in the report text of Appendix B</i> .....	<b>220</b>

# Executive Summary

This report is a desk top study of the geological prospectivity (see Glossary) for carbon dioxide subsurface storage in selected member economies of the APEC (Asia Pacific Economic Cooperation) region. The focus regions were selected by excluding those that have undertaken, or are about to complete, a CO<sub>2</sub> (carbon dioxide) geological storage assessment, and those with very low emissions as documented by IEA (2000). The regions assessed within APEC are China, Indonesia, South Korea, Malaysia, Philippines, Chinese Taipei and Thailand.

The three main options for subsurface storage of CO<sub>2</sub> are deep saline reservoirs, depleted oil and gas fields and deep unmineable coal beds (Figure 1).

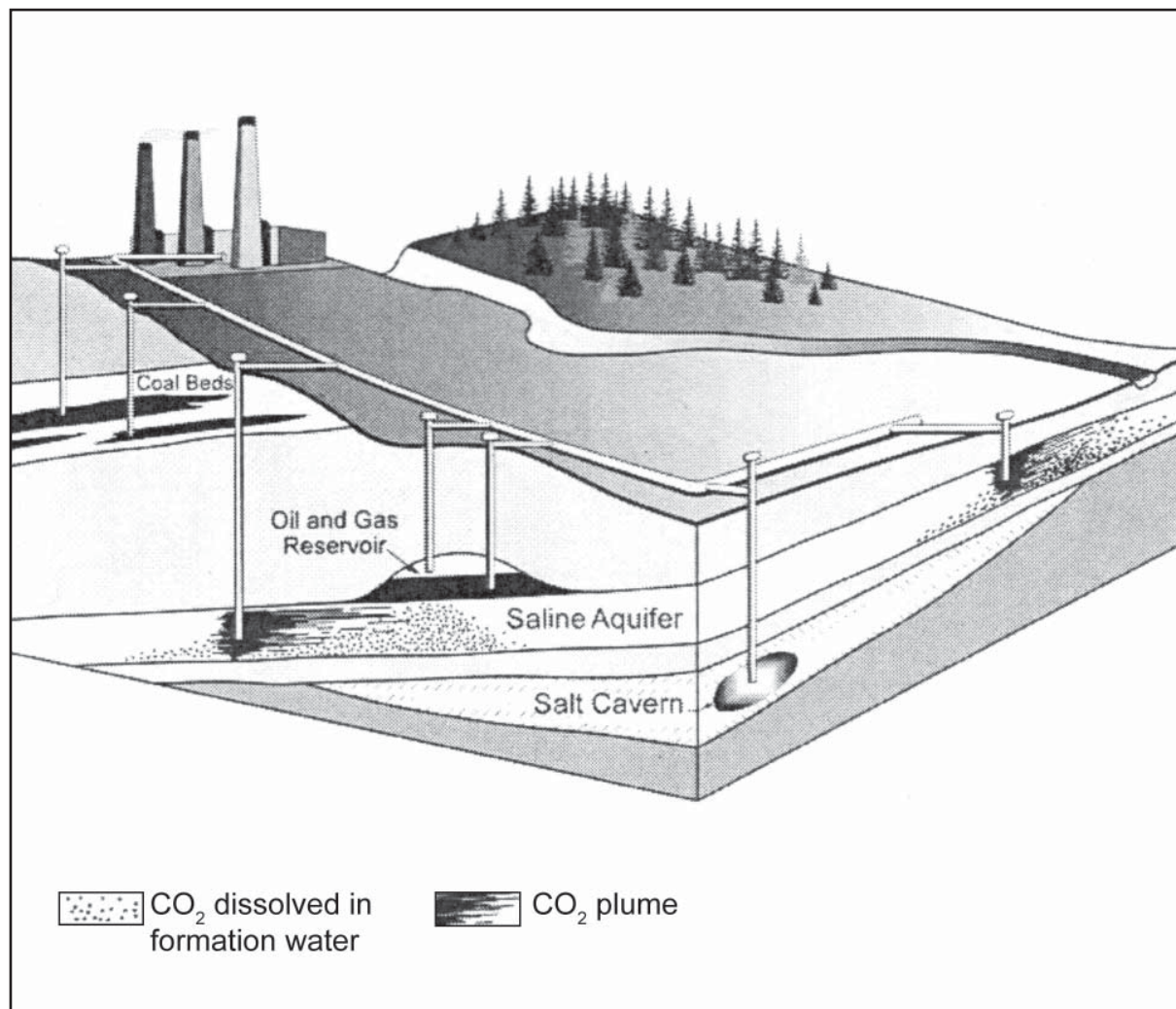


**Figure 1. Diagrammatic representation of various means of CO<sub>2</sub> storage in geologic media (Modified after Bachu, 2003)**

Within each member economy, prospective sedimentary basins for CO<sub>2</sub> subsurface storage were selected on the basis of proximity to significant point CO<sub>2</sub> sources. The significance of these internal emissions was assessed relative to the CO<sub>2</sub> output of the specific economy and not in absolute terms across member economies. The term “emissions” in this report means point source emissions as estimated by the IEA (International Energy Agency) (2000); this includes power generation, cement manufacture and other industrial processes. Transport, agriculture and other distributed sources are not considered in this report.

This study is based on published literature and seeks to summarise CO<sub>2</sub> storage prospectivity. This report does not attempt to quantify storage capacity. Quantifying storage capacity without examination of seismic and well data is of limited value, despite being attempted in the literature on several occasions. There is little or no published literature on CO<sub>2</sub> prospectivity for most of these regions. The principles for assessment that were utilised are akin to assessment of a region for viable hydrocarbon accumulations.

This report has several levels of detail. This summary section contains an overview summary followed by a technical summary. The body of the report is a moderately detailed technical discussion of each selected member economy and its basins. An appendix is included for readers requiring additional technical information, diagrams and references.

# Overview Summary

The prospectivity of each potentially viable sedimentary basin was assessed by examining basin evolution and geological characteristics in the published literature. Prospectivity is a term used in the exploration for any geological resource; in this case CO<sub>2</sub> storage space. Prospectivity is a perception of the likelihood that an industry resource is present in a given area based on the available information (See Glossary). When the level of uncertainty is very high (as in this report), the prospectivity of an area can and will change with new knowledge and changes in economic and technological factors.

Prospectivity has been plotted against the scale of stationary emissions for the selected economies (Figure 2). In general, the selected member economies fall into four categories being;

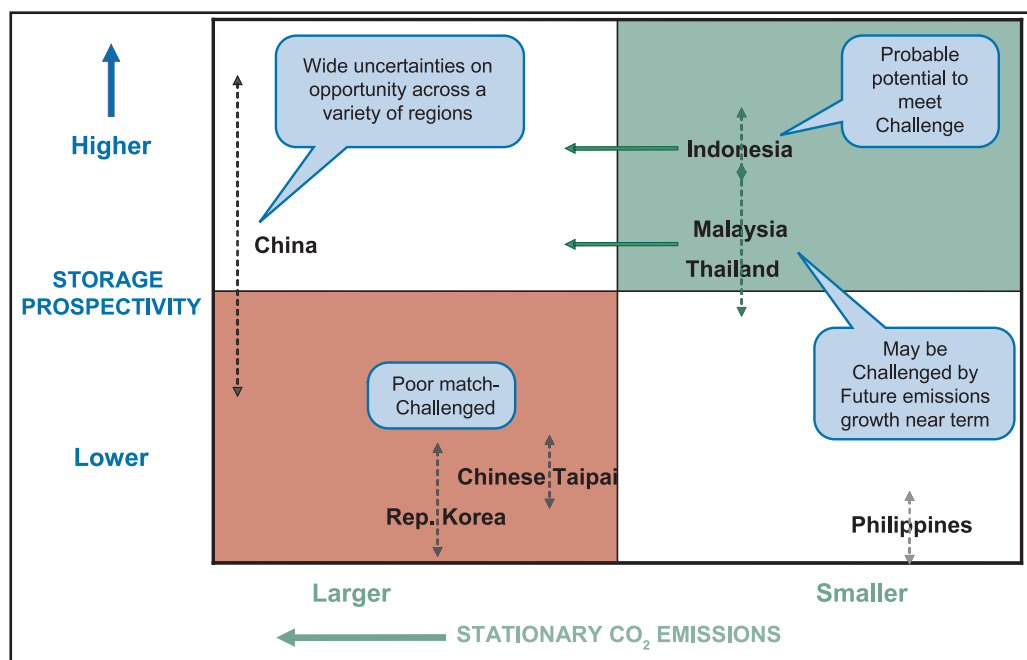


**Figure 2.**  
Stationary source CO<sub>2</sub> emissions vs prospectivity

## 1. Very high emissions (10<sup>3</sup> Mt/yr) and moderate to high prospectivity for storage

### China

- ◆ Stationary emissions of 2970 Mt CO<sub>2</sub> /yr (IEA, 2000)
- ◆ Sources in western China are negligible in relative terms. Sources are concentrated in northern China. A number of well explored basins with good prospectivity underlie this area.
- ◆ Southern areas (eg Guangzhou) are challenged due to the absence of obvious high prospectivity onshore basins –offshore basins may offer a solution.
- ◆ Uncertainty exists regarding the offshore basins, however they are probably moderately prospective. Despite uncertainty, the Pearl River Basin may be the most prospective of the fully offshore basins.
- ◆ The annual stationary source CO<sub>2</sub> emissions in China are of the same order of magnitude as China’s ultimate hydrocarbon field CO<sub>2</sub> storage capacity. Storage in depleted fields would be a favourable place to start using Carbon Capture and Storage (CCS) technology, but their potential cannot match the scale of China’s longer term emissions. Significant depleted field capacity may not be available in the near term due to the continuing productivity of the largest fields.
- ◆ Prospectivity of saline reservoirs for storage may be adequate to make a worthwhile impact on emissions reduction.

## 2. Moderate emissions ( $10^2$ Mt/yr) and moderate storage prospectivity

### Indonesia

- ◆ The main source areas are near Jakarta on Java and gas processing in Kalimantan.
- ◆ There are basins with widespread high prospectivity reservoir-seal pairs adjacent to the main source areas, e.g. Jakarta – NW Java Basin, Kalimantan – Kutei Basin.

### Malaysia and Thailand

- ◆ Both economies have moderate emissions. Their moderate storage prospectivity may become an issue as emissions grow.

## 3. Low emissions ( $10^1$ Mt/yr) and low storage prospectivity

### Philippines

- ◆ Philippines emissions are the lowest in this study but prospectivity for storage is very low: as emissions grow the challenge will become greater.

## 4. High emissions ( $10^2$ Mt/yr) and low storage prospectivity

### The Republic of Korea and Chinese Taipei

- ◆ Both the Republic of Korea and Chinese Taipei have limited sedimentary basins within their boundaries and consequently little option for saline reservoir, hydrocarbon field or coal bed storage.

# Technical Summary

The positions of counties depicted in Figures 2 and 3 were determined using technical information. Some of the main technical points are shown on Figure 3. Further details are below.

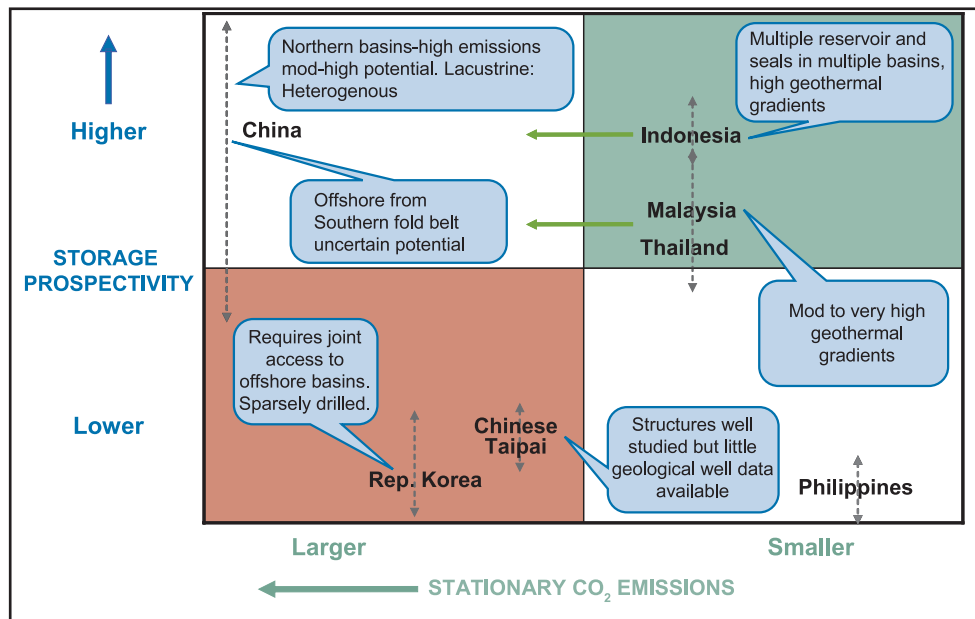


**Figure 3.** Stationary source CO<sub>2</sub> emissions vs prospectivity with geological notes.

## 1. Very high emissions (10<sup>3</sup> Mt/yr) and moderate to high prospectivity for storage

### China

Stationary emissions are estimated at 2970 Mt CO<sub>2</sub>/yr (IEA, 2000), on par with the emissions of the USA. China's emissions are 9 to 66 times larger than the other member economies in this study. Most of the CO<sub>2</sub> is generated in northern China in the region of the well-explored Bohai, Subei and Songliao basins. The Tarim Basin and other western basins were not considered in this study as they are considered to be too remote (thousands of kilometres) from the major CO<sub>2</sub> emission sources. China has many potential storage opportunities but significant uncertainty exists regarding the degree of prospectivity. This can be addressed by initiating specific geological studies in this region.

The annual stationary source CO<sub>2</sub> emissions in China are of the same order of magnitude as China's ultimate hydrocarbon field CO<sub>2</sub> storage capacity. Storage in depleted fields would be a favourable place to start using Carbon Capture and Storage (CCS) technology, but their potential cannot match the scale of China's longer term emissions.

Fluvial-lacustrine depositional environments dominate Cenozoic (and in some cases Jurassic) sequences in China's sedimentary basins. This includes Bohai, Subei, Songliao Hefei, Jiangnan and Nanpanjiang basins which underlie the most concentrated CO<sub>2</sub> emission sources. The facies assemblages of such basins vary on short time scales with high heterogeneity driven by local tectonics and climatic variation. Experience at Sleipner and recent modelling shows that a degree of heterogeneity is positive for CO<sub>2</sub> storage capacity (Hovorka et al., 2004; Doughty et al., 2001).

In general, the main challenge of lacustrine environments is finding reservoir formations with a good thickness of high porosity and permeability for the actual points of injection. The higher energy braid plain, fluvial and delta facies within lake systems will be the best reservoir for injection. These are fluvial systems that extend along structural strike from the basin edge into the basin as deltas. The seal for these systems becomes a risk near the basin edge (up the depositional dip). However the degree of risk depends on the injection and migration rate of CO<sub>2</sub> in a given area.

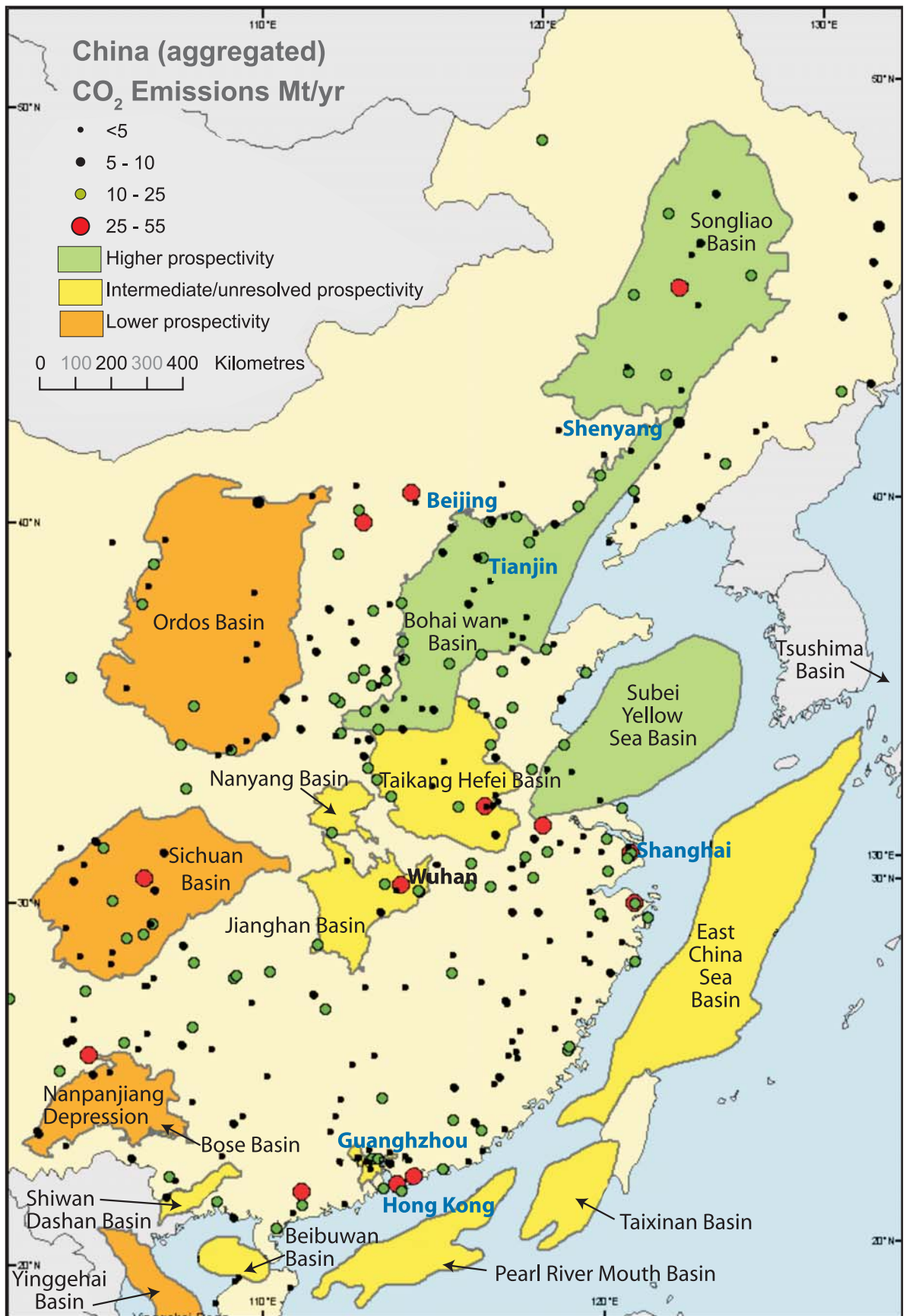


Figure 4. A tentative ranking of the CO<sub>2</sub> storage prospectivity of sedimentary basins in eastern China together with stationary CO<sub>2</sub> emissions.

The Bohai, Subei and Songliao basins appear to have good prospectivity. The basins in the Dabieshan region (Hefei and Nanpanjiang basins) are more complicated poly-phase basins with multiple fault sets and major angular unconformities.

Significant and rapidly growing emissions are found in the Southern province of Guangdong. Guangdong province lies in the southern fold belt area of China. This region is challenged by the absence of major onshore sedimentary basins. The prospectivity of the offshore Pearl River Mouth Basin has some encouraging aspects. Information on minor basins in the southern fold belt is difficult to locate. Shanghai is at the northern tip of the southern fold belt but is also in the region of the Subei, southern Bohai and Dabieshan basins. Natural gas is piped from the offshore East China Sea Basin to Shanghai. The storage CO<sub>2</sub> prospectivity of the East China Sea Basin is unclear due to sparse drilling across most of the basin.

Lesser CO<sub>2</sub> emissions occur in the vicinity of the western Sichuan and Ordos basins. Palaeozoic carbonates occur in the Sichuan and Ordos basins. The Sichuan Basin has generally very poor permeability and porosity carbonate rocks with nearly all porosity and permeability due to fractures. Such formations are not likely to be useful for storage. This is in contrast to the enhanced porosity due to weathering of Cretaceous basement carbonates of the Bohai and Subei basins (i.e. “buried hill” oil play). The Ordos Basin has Ordovician carbonate reservoirs enhanced by weathering but porosity and permeability are poor. Sandstone reservoirs with effective seals are in the Upper Permian, Upper Triassic and Lower Jurassic of the Ordos Basin. All have poor to modest permeability and porosity.

Many formations in China’s fluvial-lacustrine successions are red due to a high content of red coloured iron oxide minerals (mainly haematite). Divalent cations of Ca, Mg and Fe can facilitate mineral trapping in the right physical and chemical conditions (Baines and Worden, 2004). However, the highly oxidised nature of these formations means that the Fe present is in a trivalent state, providing no inherent Fe mineral trapping advantage.

There is a wide range of published geothermal gradients for China’s basins. Gradients range from 30 to 50°C/km and most basins fit in the 30 to 40°C/km range. This range is average to above average for geothermal gradients.

The basin with the best prospectivity for coal storage is the Ordos Basin and the adjacent eastern areas. The coal is very plentiful and shallow lying over large areas. This seems to be the area with most prospectivity for coal bed storage and/or Enhanced Coal Bed Methane (ECBM).

A tentative ranking of the storage potential of China’s basins is illustrated in Figure 4.

## 2. Moderate emissions (10<sup>2</sup> Mt/yr) and moderate storage prospectivity

### Indonesia

Indonesia’s five major hydrocarbon basins have multiple good quality reservoir-seal pairs. However, high geothermal gradients are a negative factor for the basins off Java and Sumatra. The Kutei Basin of Borneo has an average geothermal gradient. Higher geothermal gradients mean higher reservoir temperatures. Higher reservoir temperatures will result in a lower density for stored CO<sub>2</sub>. Therefore, the storage efficiency of a cubic metre of a warm reservoir is lower than a cubic metre of a cool reservoir.

Lacustrine depositional environments occurred during the early rift section in the Sumatra/Java basins, but lacustrine rocks do not dominate the basin fill, as they do in China. Marine conditions occurred from the Miocene resulting in reef and marine/deltaic sand reservoirs and marine seals. Carbonate reservoirs in Indonesian basins are Tertiary reef carbonates with preserved primary porosity.

Emissions are concentrated in the Jakarta region. The onshore NW Java Basin is the nearest storage option and has several reservoir-seal pairs and numerous, but very small hydrocarbon fields. A second major source of CO<sub>2</sub> results from hydrocarbon refining in the Kutei Basin. This CO<sub>2</sub> could be returned to the Kutei Basin, which has numerous deltaic reservoirs and a moderate geothermal gradient, unlike the Java and Sumatra basins.

Indonesia's deep saline reservoir prospectivity is encouraging in terms of reservoir-seal pairs. However a high geothermal gradient will present a negative aspect for CO<sub>2</sub> storage capacity due to reduced storage density.

Indonesia's main coal resources occur in sedimentary basins in south Sumatra and east Kalimantan, which are remote from Jakarta. There may be some smaller localised coal bed storage and/or ECBM opportunities in these areas.

### **Thailand and Malaysia**

These member economies have moderate storage prospectivity. Prospectivity probably has a reasonable match with their current CO<sub>2</sub> emissions. High geothermal gradients will be a limiting factor. These countries may face a challenge as their emissions increase.

Malaysia and Thailand have significant hydrocarbon resources. These volumes can be converted to a theoretical stored CO<sub>2</sub> mass that is tens of times greater than annual CO<sub>2</sub> production. Malaysia still has very large reserves of gas. In practice only a fraction of this pore space will be actually available for storage use in the near term.

The Thai Gulf and Malay basins are in a region of elevated geothermal gradient. The geothermal gradient increases from south to north in the Malay Basin from 35 to 55°C/km. The geothermal gradient in Thai Gulf Basin is around 55°C/km. These higher gradients will have a negative impact on storage density in saline reservoirs and hydrocarbon fields.

## **3. Low emissions (10<sup>1</sup> Mt/yr) and low storage prospectivity**

### **Philippines**

Philippines' emissions are the lowest in this study but its prospectivity for CO<sub>2</sub> storage is very low. As emissions grow, locating viable storage sites might be a challenge.

## **4. High emissions (10<sup>2</sup> Mt/yr) and low storage prospectivity**

### **Republic of Korea and Chinese Taipei**

The Republic of Korea, and Chinese Taipei have limited development of sedimentary basins and consequently little option for saline reservoirs, hydrocarbon fields or coal seam storage.

Korea's options are restricted to minor opportunities onshore and limited areas offshore.

## **Conclusion**

This report deals with selected APEC member economies in the northern and south-eastern Asia regions. Prospectivity for CO<sub>2</sub> storage within the studied group is varied. Some regions have few choices for geological sinks and may have to plan to place new sources near a viable sink. Other member economies potentially have a number of choices that will require considerable internal planning to manage CO<sub>2</sub> storage. CO<sub>2</sub> storage space is a resource and trade and/or cooperation regarding CO<sub>2</sub> storage strategies between members (and non-members) will be an important aspect of a future in which energy use is likely to be integrated with large scale geological storage of CO<sub>2</sub>. For this future to be effectively managed, studies must progress from prospectivity studies to the search for actual storage locations for specific source emitters. If uncertainty around storage capacity is to be reduced site specific conditions must be determined by the detailed evaluation of geological, geophysical, geochemical and reservoir engineering data. Such focused practical efforts will greatly increase understanding and reduce uncertainty regarding the capacity of specific project sites and the target sedimentary basins.

# 1. Introduction

The work reported here was initiated in 2001 by the APEC Expert Group on Clean Fossil Energy (EGCFE) as the first phase of a multi-phase program on carbon dioxide capture and geological storage in the APEC region. The EGCFE operates under the APEC Energy Working Group (EWG), one of whose key roles is to promote sustainable energy development within the APEC community. Innovative Carbon Technologies Pty Ltd (ICTPL), the commercial arm of the Cooperative Research Centre for Greenhouse Gas Technologies (CO2CRC), was awarded a tender for *Assessment of Geological Storage Potential of Carbon Dioxide in the APEC Region - Phase 1: CO<sub>2</sub> Storage Prospectivity of Selected Sedimentary Basins in the Region of China and South East Asia* (APEC project number: EWG 06/2003). The objective of the study is to establish a sound understanding of the relationship between the key emission sources and the prospective sedimentary basins that may contain potential storage sites, and to derive a qualitative assessment of whether the storage prospectivity in a specific member economy will match its storage requirements through the foreseeable future. Phase 2 of the program is related to providing contacts, outreach and technology transfer.

Developed countries in the APEC region are Australia, Canada, Japan, New Zealand and United States. These countries have vigorous programs in Carbon Capture and Storage (CCS), a strong research program, and roadmaps for CCS implementation. These countries, by and large, have completed or have under way, the initial steps of an inventory of CO<sub>2</sub> sources and estimation of CO<sub>2</sub> capacity, and are at various stages of source-sink matching. APEC member economies considered in this study include: China, Indonesia, South Korea, Malaysia, Philippines, Chinese Taipei and Thailand (Figure 5).

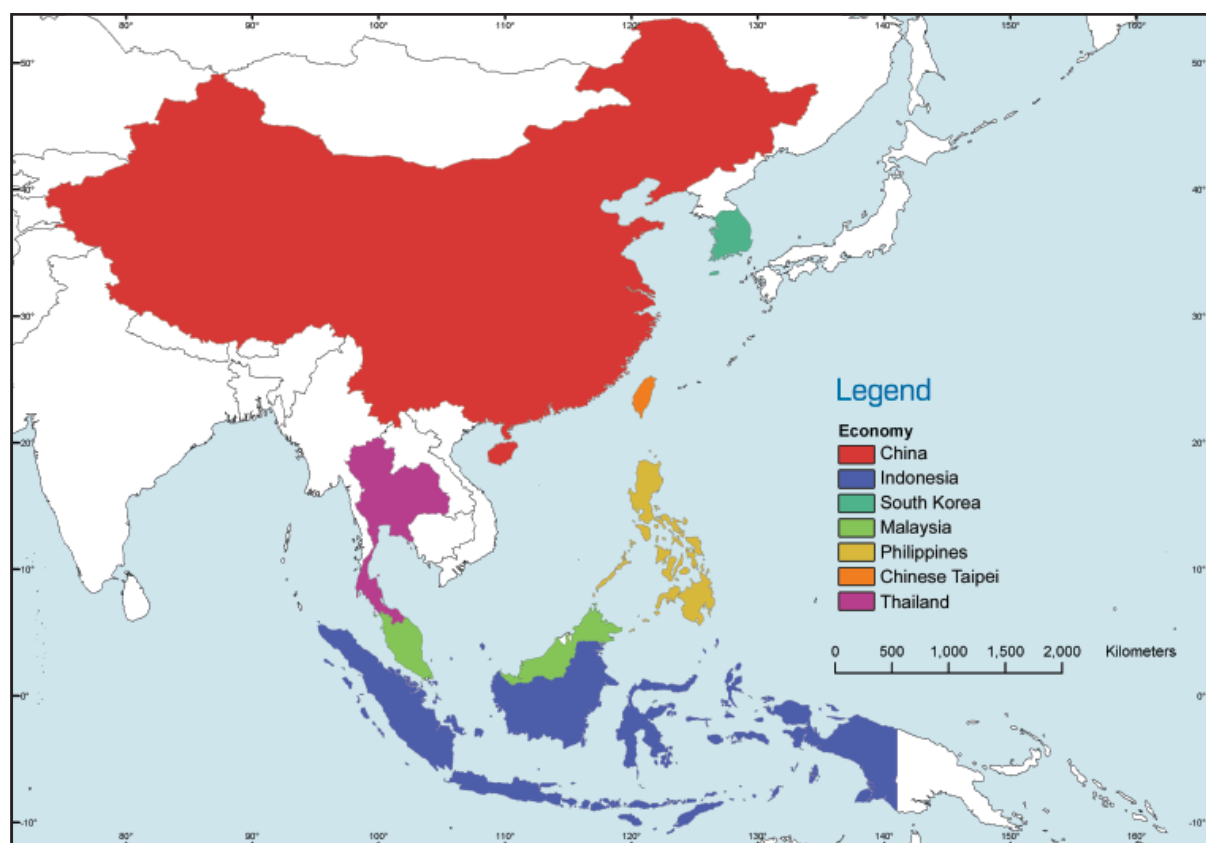


**Figure 5. APEC economies that are a focus of this report.**

The prospectivity for geological storage of CO<sub>2</sub> in selected basins was assessed by reviewing published literature. This report has several levels of detail. The body of the report is a moderately detailed technical discussion of each

member economy and its basins. Appendix A is included for readers requiring additional technical information, diagrams and references on each basin. A table summarising basin attributes is also included.

The capture of CO<sub>2</sub> is not considered in this report. Sources of anthropogenic CO<sub>2</sub> have been spatially summarised and matched to basins. All source-sink matching studies to date (i.e. cost-curves for CO<sub>2</sub> capture and storage) have used a radius of 300 km around a CO<sub>2</sub> node, on the assumption that this is a 'significant' length of pipeline. If this limit of 300 km is used, then the sedimentary basins of interest in the study area in east and south-east Asia are essentially reduced to Cretaceous-Tertiary extensional basins. These basins are dominated by lacustrine sequences, rift sequences, and post-rift non-marine and marine sediments. Potential storage sites within these sequences include lacustrine fan, fluvio-deltaic, mass flow deposits, or 'buried hill' plays sealed by thick mud-rich lake sequences. Due to the 300 km limit and the relatively small emissions, the basins of western China (e.g. Tarim) were not included in the assessment.

Economic calculations for CCS are not included in this report as the economics of a full cycle capture and storage project are very sensitive to all project specific details, most of which are not available from the publicly available literature. Monitoring issues are not discussed.

## 2. Definition

### 2.1 Geological Storage

Several monographs containing many contributions are available to explain the principles of geological storage; these include Holloway et al., 1996 and Gerhard et al., 2001. A special report from the Intergovernmental Panel for Climate Change (IPCC) on carbon dioxide capture and storage will be released in late 2005. This report includes a concise summary of the various aspects of geological storage. Bachu (2001, 2003) provides an overview of the major geological storage issues.

“Geological media have both the space (porosity) and injectivity (permeability) necessary for CO<sub>2</sub> injection, and, by and large, have the ability to either prevent or delay for geologically significant periods of time the CO<sub>2</sub> returns to the atmosphere. Crystalline and metamorphic rocks, such as granite, on continental shields, are not suitable for CO<sub>2</sub> storage because they lack the porosity and permeability needed for CO<sub>2</sub> injection, and because of their fractured nature. Volcanic areas and orogenic belts (mountains) are also unsuitable mainly because they lack capacity and are unsafe. Fortunately and serendipitously, sedimentary basins are also where fossil energy resources are found and produced, by and large.”(Bachu, 2003).

Most knowledge of deep formations (> 800 m) is due to hydrocarbon exploration and development. For the reasons outlined above this study will primarily deal with sedimentary basin sequences. The total storage prospectivity of any basin can be considered as having three significant options; deep saline reservoirs, depleted oil and gas field storage and coal bed storage as shown in Figure 6.

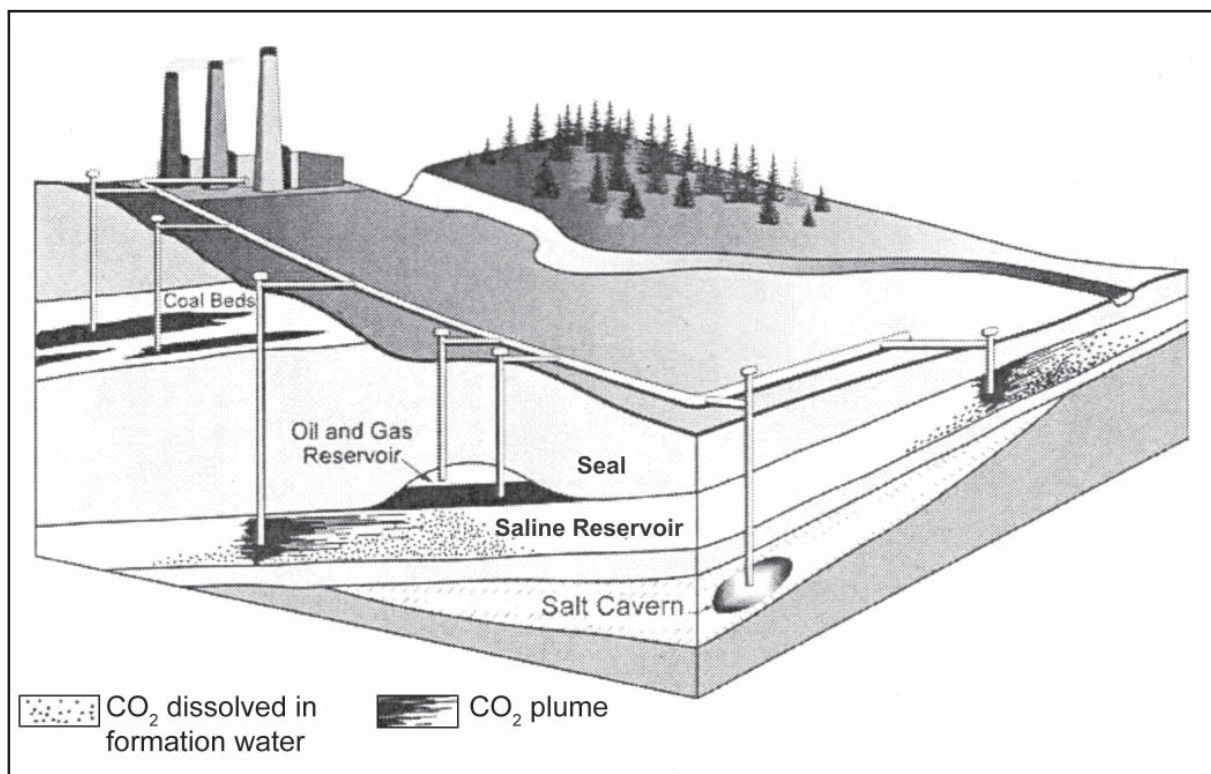


**Figure 6. Diagrammatic representation of various means of CO<sub>2</sub> storage in geologic media (modified after Bachu, 2003).**

## Deep sandstone and carbonate reservoirs (Trapping mechanisms: solubility, residual phase, mineral and hydrodynamic flow)

This concept requires a fairly extensive reservoir formation with a matching top seal formation. This idea is fundamental to petroleum geology where the term “reservoir-seal pair” may be used. However for the purposes of CO<sub>2</sub> storage a closed structure or “trap” is not essential. This mode of storage relies on the utilisation of the pore space in the reservoir and solubility of CO<sub>2</sub> in the pore water. Some CO<sub>2</sub> will ultimately be trapped by precipitation of minerals. To initially contain the buoyant CO<sub>2</sub> some form of top seal is required, ideally a claystone or evaporite with proven seal properties. Thick sequences of lithologies such as siltstone might still be effective if the path of the CO<sub>2</sub> through the formation is sufficiently long and tortuous for all migrating CO<sub>2</sub> to be trapped in the pore waters. The reservoir (reservoir) should have high permeability to allow injection at acceptable rates. Storage of CO<sub>2</sub> in deep saline reservoirs requires consideration of many factors. Some of them are outlined in Table 1.

**Table 1. Factors for consideration for CO<sub>2</sub> storage in deep saline reservoirs.**

Factor	Description
Area of Seal	This mode of storage assumes a contiguous seal with an extent of at least tens of kms. That is, a semi-regional or regional seal.
Dip of the top seal and reservoir	CO <sub>2</sub> will in most situations rise toward the surface due to buoyancy. Very low dips will result in very limited upward progress during lateral migration (see also <i>Area of Seal</i> ) (Doughty et al., 2001).
Reservoir heterogeneity	Heterogeneity will create a more tortuous migration path which may enhance solution and mineral trapping. Assessment of heterogeneity is dependant on the scale of investigation (e.g. seismic, log, core). (Doughty et al., 2001; Hovorka et al., 2003)
Porosity and permeability	Rate of injection depends on permeability. Porosity determines capacity.
Temperature & pressure and storage density of CO <sub>2</sub>	Temperature & pressure are normally proportional to depth. The relationship between temperature, pressure and CO <sub>2</sub> density stored is depicted in Figure 7 (Bachu, 2003).
Salinity	High salinity results in lower solubility of CO <sub>2</sub> (Bachu, 2001).
Mineralogy	Mineral trapping will depend on mineralogy along with temperature, pressure and rate of injection. Carbonate minerals are reactive with CO <sub>2</sub> in days and weeks. Interaction of CO <sub>2</sub> with reactive minerals in silicate rocks can result in mineral trapping of CO <sub>2</sub> after tens of thousands to millions of years, depending on conditions. (Baines and Worden, 2004).

These items are very site specific and this report can not cover them in any detail. The published literature can only provide a general description of the geology. Most of the report will identify potential reservoir-seal pairs.

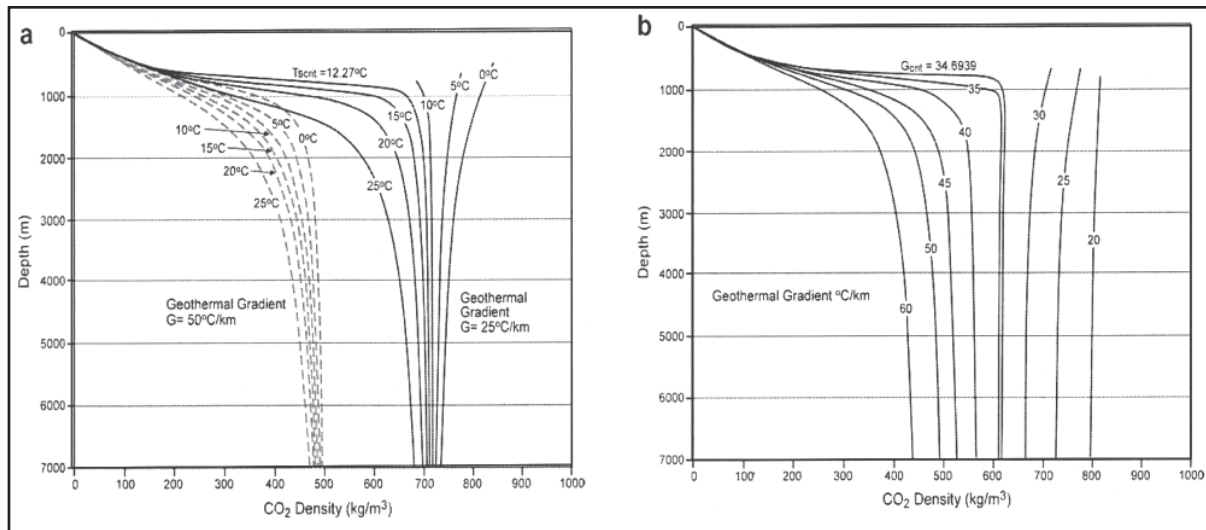


**Figure 7. Variation of CO<sub>2</sub> density with depth in sedimentary basins: (a) assuming hydrostatic pressures and various surface temperatures ( $T_s$  and geothermal gradients representative of “cold and warm” basins); and (b) for surface temperature  $T_s + 5$  degrees Celcius and a range of possible geothermal gradients (from Bachu, 2003).**

### Oil and gas reservoir storage (Trapping mechanisms: Structurally contained, solubility and mineral trapping)

This may take the form of storage in depleted oil or gas fields or in association with EOR (enhanced oil recovery). EOR is primarily a means to increase oil recovery. Depleted field storage capacity can be estimated by converting known hydrocarbon pore space (past production plus remaining reserves) to CO<sub>2</sub> equivalent. This assumes that the reservoir can be returned to its pre-production pressure.

The storage capacity of depleted fields can be estimated with less uncertainty than other modes of geological storage. By applying the calculations in Holloway et al., (1996) hydrocarbon production and reserves volumes can be converted to stored CO<sub>2</sub> mass.

### Coal bed Storage (Trapping mechanism: adsorption)

Deep unmineable coal beds represent another potential geologic storage method for CO<sub>2</sub> and in some instances will provide a value-added benefit of enhanced methane production. Coal bed methane (CBM) is a naturally occurring gas often found in coal seams and is becoming an important energy source. To exploit CBM reserves, production wells are drilled and the gas produced is processed for sale to a commercial pipeline.

Methane production from coal beds can be enhanced by injecting CO<sub>2</sub> into coal formations, a process known as enhanced coal bed methane recovery (ECBM). At least two to three molecules of CO<sub>2</sub> are stored for each molecule of methane produced depending on the rank of the coal. The CO<sub>2</sub> can be stored permanently, provided the coal is never mined. Unlike in oil and gas reservoirs, the methane and CO<sub>2</sub> in coal seams is retained by adsorption rather than by trapping. The methane adsorbed in the coal desorbs, diffuses, and flows with the water to the production wells.

ECBM is an immature technology and favourable geology and stress field are the key technical criteria for successful application. The coal seams must be saturated with gas, located at suitable depths and in simple structures, and have sufficient permeability. Other factors that impact production include the quality and concentration of the gas as well as porosity of the coal. Revenue from ECBM can offset the costs of CO<sub>2</sub> capture and transport (Gale & Freund, 2001).

# 2.2 Methodology and assumptions

## Overview

This report seeks to characterise the source and sinks in areas of most opportunity within APEC member economies. Focus economies were identified and basins and sources were matched at a regional level.

## Focus Economies

APEC has 21 member economies. It was decided to divide the economies into three groups on the basis of opportunities to progress geological storage of CO<sub>2</sub>. A number of economies have relatively small emissions (Figure 8 & Figure 9). Another group have considerable emissions but have completed quite detailed surveys of geological storage similar to the GEODISC project in Australia (Rigg et al., 2001). The middle group is the focus of this report. Nearly all of these member economies are within North and SE Asia and it was decided to limit the study to this region.

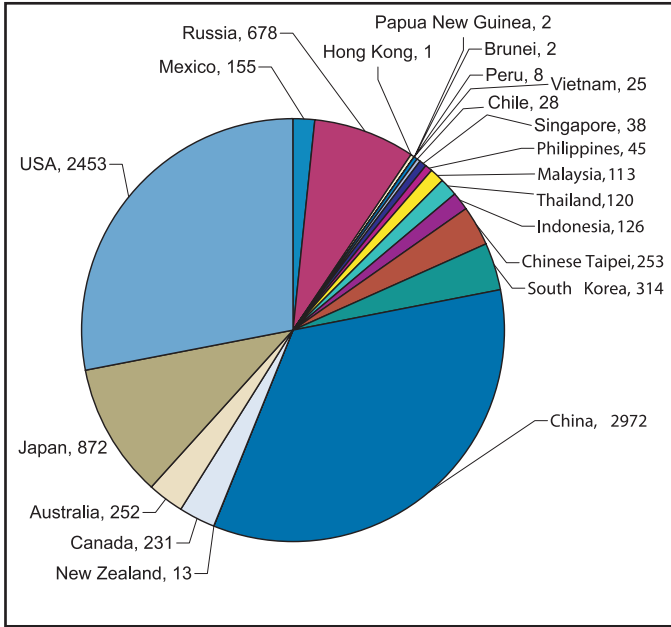


Figure 8. APEC stationary source CO<sub>2</sub> emissions, Mt/year (data from IEA, 2000).

Selected Economies		
Investigating CCS (10 <sup>2</sup> to 10 <sup>3</sup> Mt/Yr)	Selected/Focus (10 <sup>2</sup> to 10 <sup>3</sup> Mt/Yr)	Smaller Emissions (10 <sup>0</sup> to 10 <sup>1</sup> Mt/Yr)
Australia	China	Brunei
Canada	S. Korea	Chile
Japan	Indonesia	HKG
USA	Malaysia	NZ
	Philippines (10 <sup>1</sup> )	Peru
	Chinese Taipei	PNG
	Thailand	Singapore
	Mexico	Vietnam
	East Russia	

Figure 9. APEC geological storage groups.

## Regional Source and Basin matching

The dataset of world emissions published by the International Energy Agency (IEA, 2000) is the primary source for emission point sources used in this study. It is regarded as representative of regional emissions, although there are some inadequacies in precise locations of some major sources, particularly in the Asian region. Where possible, sources with no location details (latitude and longitude) were updated from public information sources. APEC member economies emit 64% of the world’s total CO<sub>2</sub> emissions (Figure 10). Figure 8 shows the emission distribution of the member economies.

The US Geological Survey (2000) identifies hundreds of sedimentary basins in the APEC region. Terranes other than deep sedimentary basins were filtered out (Figure 11). The numerous point sources within the focus economies (Figure 12) were represented by a number of arbitrary nodes, usually centred near cities (Figure 13). A limit of 300 km from source to sink is arbitrarily set as a “significant” pipeline length. Figure 14 shows the intersection of a 300 km radius with sedimentary basins. Offshore basins were included. The final set of basins selected for study is shown in Figure 15.

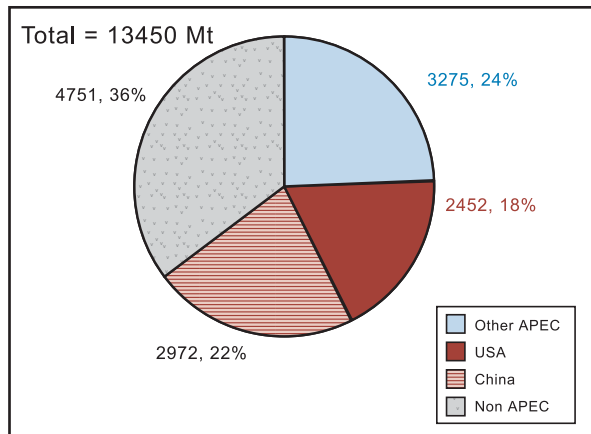


Figure 10. Global point source emissions - APEC contributions.

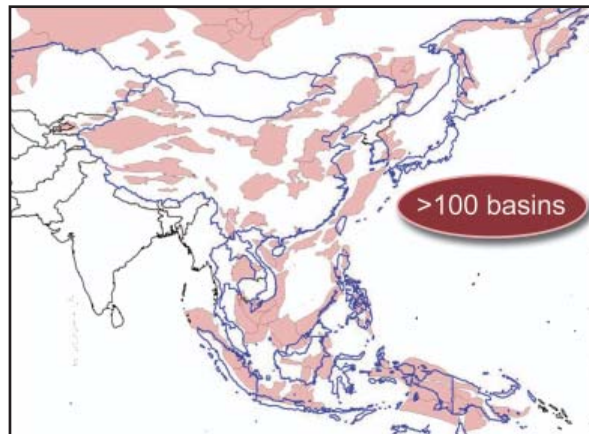


Figure 11. APEC - East and South East Asia significant sedimentary basins.

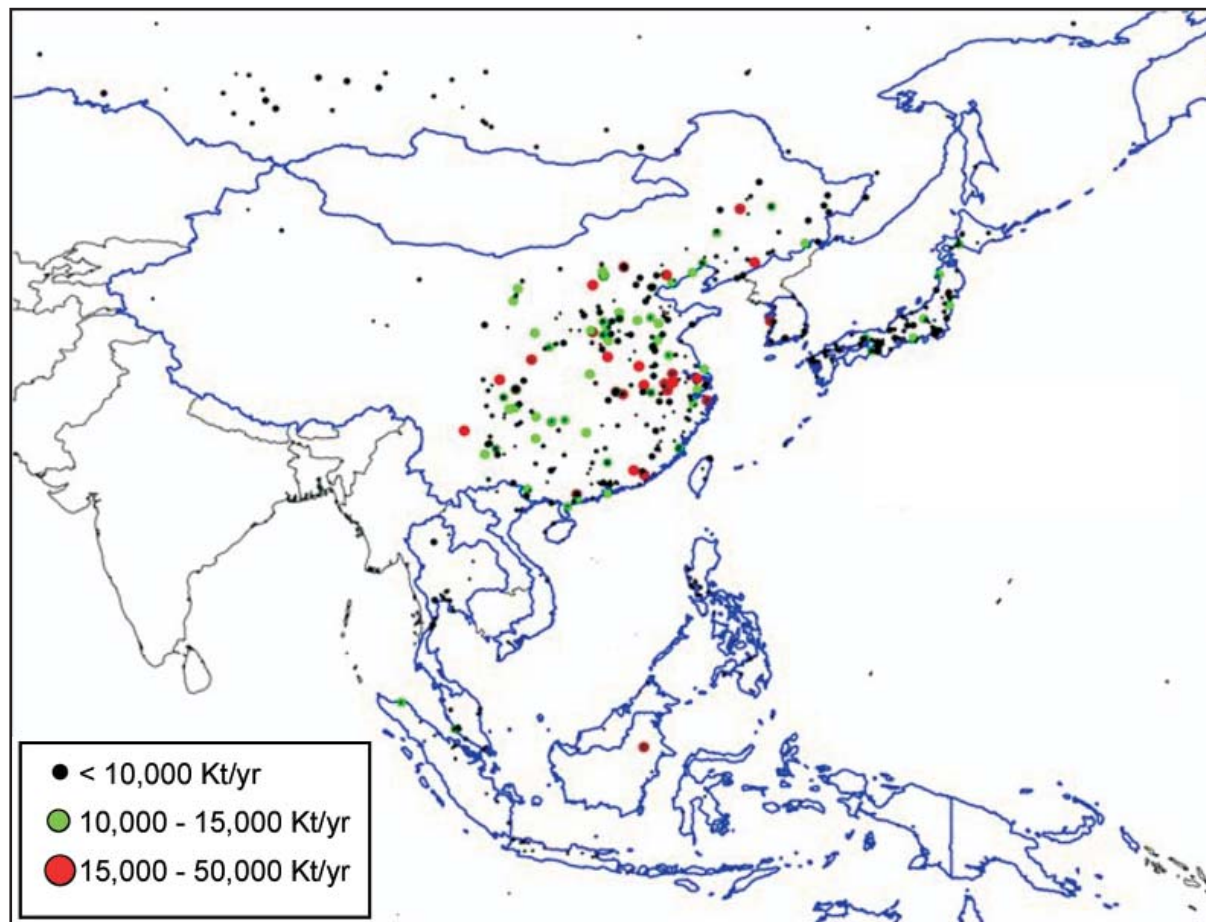


Figure 12. CO<sub>2</sub> emissions from stationary sources. Note: IEA data, 20% of points are without location data.

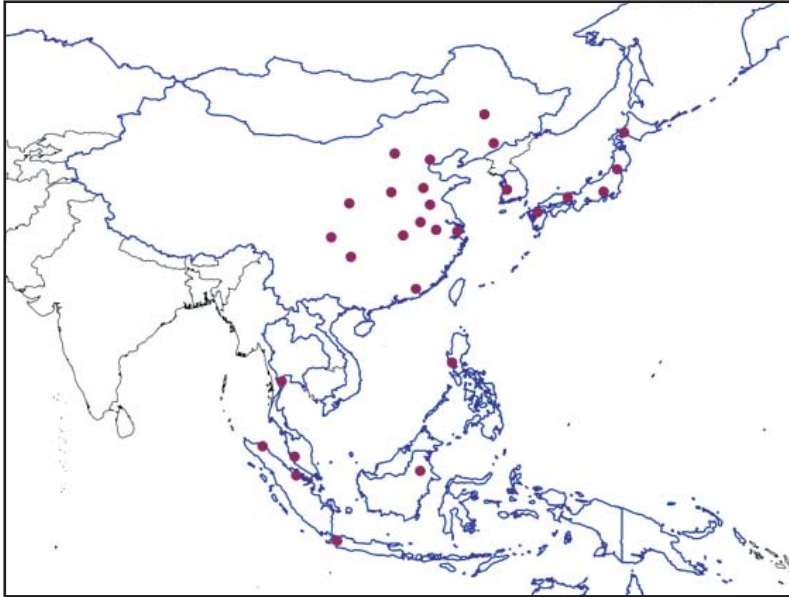


Figure 13. Stationary source CO<sub>2</sub> emissions and arbitrary nodes.

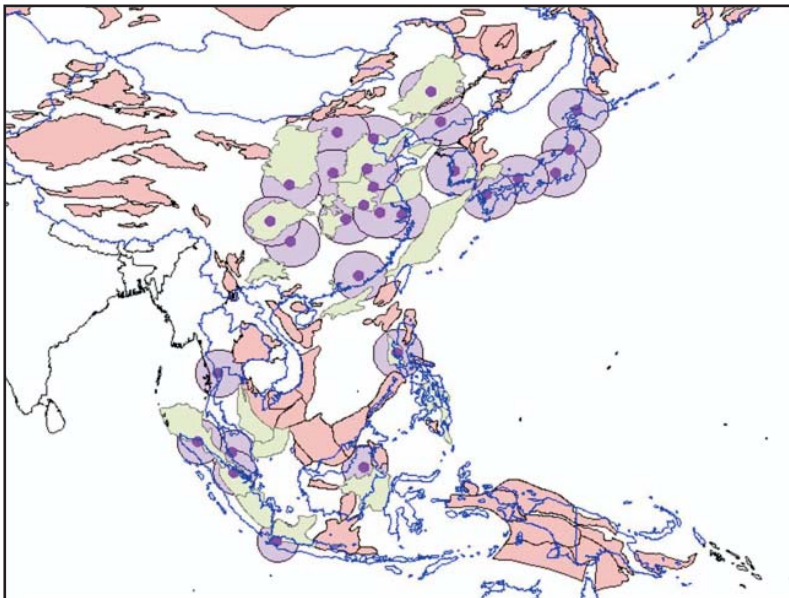


Figure 14. Sedimentary basins which fall within 300 kms of nodes.

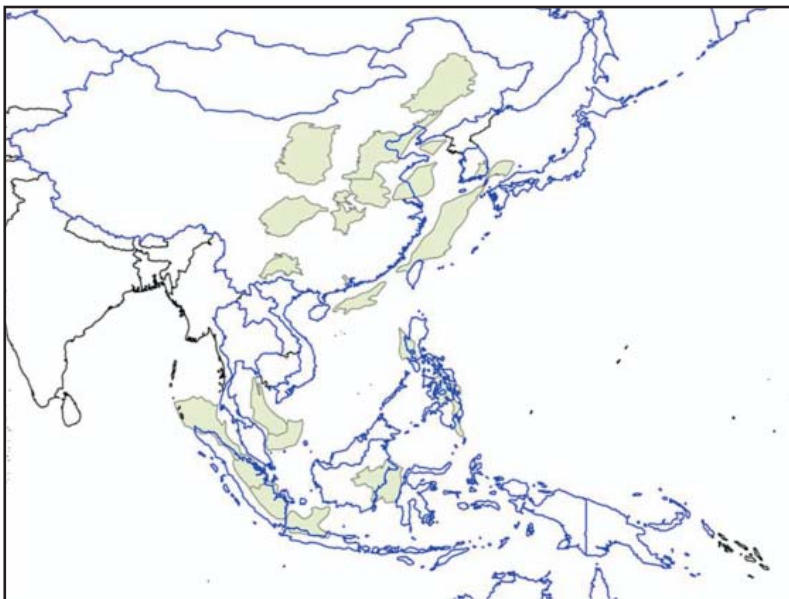
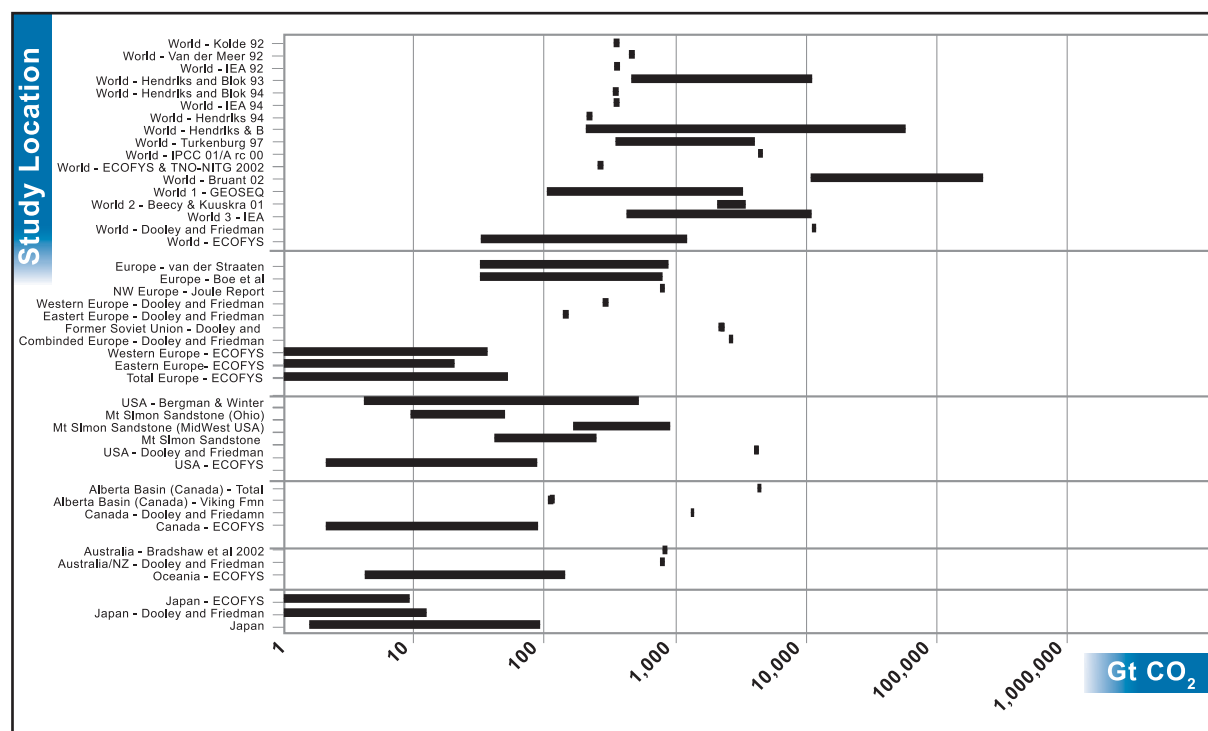


Figure 15. Selected basin set.

## Scope and limitations of this report

In the body of the report each focus economy is examined in turn. A brief characterisation of CO<sub>2</sub> emissions is provided. The geological characteristics of each basin are summarised from publicly available information in Appendix A. Some tentative opinions on prospectivity are offered. The source of geological information is published literature in English. This literature only provides a very general description of the geology. The main facts regarding each basin (area, depth, etc) are summarised in a table included in Appendix A.

The behaviour of CO<sub>2</sub> in any host formation will be site specific (Holloway et al., 1996). There is no attempt to calculate saline reservoir or coal bed storage capacity in this report. There are already numerous and wide ranging estimates in the literature (Figure 16). This study used published literature, and is not a detailed study using seismic and well data. It is considered by the authors that there is little value in producing another capacity estimate with very high level of uncertainty.



**Figure 16. World and regional storage capacity estimates (almost all estimates based on using surface area calculation).**

Estimates of the CO<sub>2</sub> storage capacity of depleted hydrocarbon fields are included based on calculations from reserves and production data. Generally production and reserves data represents pore space that will be available for CO<sub>2</sub> storage at “some time in the future”. In any basin the majority of the hydrocarbon pore space is contained a few large fields. Giant fields in China and SE Asia are still in production and are likely to stay in production for tens of years. In practice, a detailed economic assessment matching CO<sub>2</sub> source facility to an appropriate sized depleted field will be required.

### Note regarding location data for CO<sub>2</sub> emission sources:

Estimated annual emissions used in the text of this report or annotated on maps are calculated from a spreadsheet containing the full IEA data set. When using the GIS project associated with this report, the user should be aware that not all of the data from the full IEA database is geospatially referenced (i.e. has latitude and longitude). For the counties of interest to this study, location data was reviewed and updated. Most of the sources over 1 Mt CO<sub>2</sub>/yr were given a location. For the focus countries around 90% of the emissions by volume are located.

A second unrelated point should be noted regarding maps generated with the GIS: there was a need to produce less cluttered emissions maps. As a result the GIS project contains two emission files/layers. One layer will plot all located point sources (in general all those over 1 Mt CO<sub>2</sub>/yr) separately. A second layer was created which plots an aggregated representation of all of these located point sources. This aggregation was made by adding together emissions from sources with coincident latitude and longitude.

## 2.3 Current CO<sub>2</sub> Storage Pilot Sites

Four pilot CO<sub>2</sub> storage sites are currently active in Asia (Figure 17). An Enhanced Oil Recovery pilot in the third largest oilfield in China, the Liaohe Oilfield, is injecting steam and/or flue gases with ~12% CO<sub>2</sub>. With steam alone, oil recovery increases of 20-30% were achieved. However, using the combination, levels increased by 50-60%.

An Enhanced Coal Bed Methane micro-pilot using varying flue gas compositions (CO<sub>2</sub>+N<sub>2</sub>+O<sub>2</sub>) is underway in the southern Qinshui Basin, south of Beijing. This pilot project is a joint Canadian and Chinese operation. A 6.33 m thick anthracite seam at a depth of ~475 m was injected with 193t CO<sub>2</sub>. Preliminary results indicate there is a direct relationship between the volume of gas, the CH<sub>4</sub> desorption ratio and CO<sub>2</sub> adsorption ratio per unit pressure.



In Japan, an Enhanced Coal Bed Methane pilot project in the Tertiary Ishikari Coal field in Hokkaido is injecting CO<sub>2</sub> in a 5.6 m coal seam, dipping at 20 degrees at a depth of 980 m. A deep reservoir storage pilot (at 1100 m) in the Niigata Basin has been suspended following an earthquake on 23 October 2004. No damage was reported on the surface equipment and no unusual data was observed. The pilot test started in July 2003 and is scheduled to run for 18 months. CO<sub>2</sub> has been injected at a rate of about 20 t CO<sub>2</sub>/day to a total of approximately 10,000 t CO<sub>2</sub>.

The East Natuna Basin gas project in the South China Sea is one of the largest natural gas accumulations in the world, containing 28% methane (72 Tcf), and 72% CO<sub>2</sub> (168 Tcf). It is proposed that the methane will be produced for Liquid Natural Gas (LNG) and the CO<sub>2</sub> will be injected into Miocene age carbonate reservoir.

Figure 17. Some of the CO<sub>2</sub> storage pilot projects in the study region.

# 3. China

## 3.1 Source Characterisation

- ◆ The IEA (2000) estimated that China produced around 2970 Mt/yr of CO<sub>2</sub> from all stationary sources This amount is expected to increase to 4600 Mt/yr by the year 2010.
- ◆ China has the six largest point source emissions in the world (all are power stations with 3600 MW or more capacity). The estimated contribution of these is 227 Mt (6% of China's stationary emissions). This is double the entire stationary emissions contribution of Malaysia.
- ◆ The power sector is responsible for approximately 93% of stationary CO<sub>2</sub> emissions. Other sources include iron and steel, ammonia, refineries, cement, ethylene, and ethylene oxide.
- ◆ 73% of power generation emissions are from coal fired power stations.
- ◆ There are 77 pure CO<sub>2</sub> sources. Some of these can be found in the Sanshui, Beibuwan, Sichuan, Taikang Heifei, Bohaiwan, Ordos, and Songliao basins.

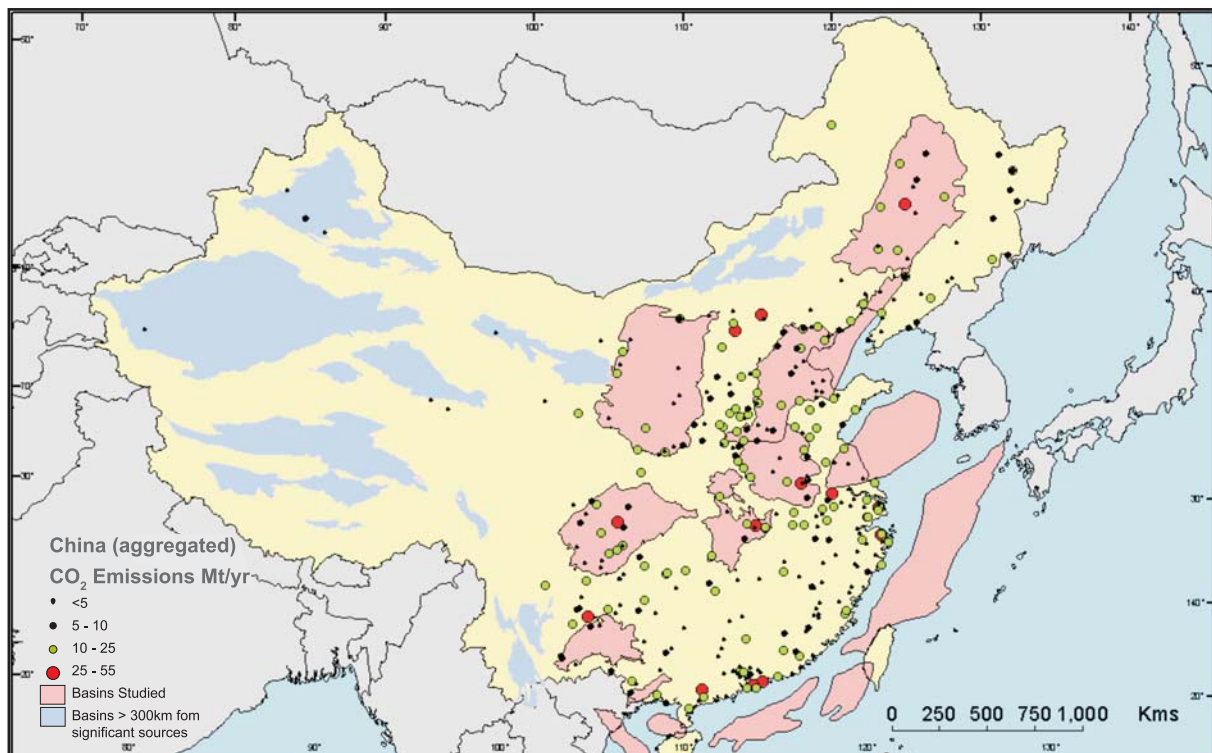


Figure 18. China aggregated CO<sub>2</sub> sources and basins in proximity to concentrated emissions.

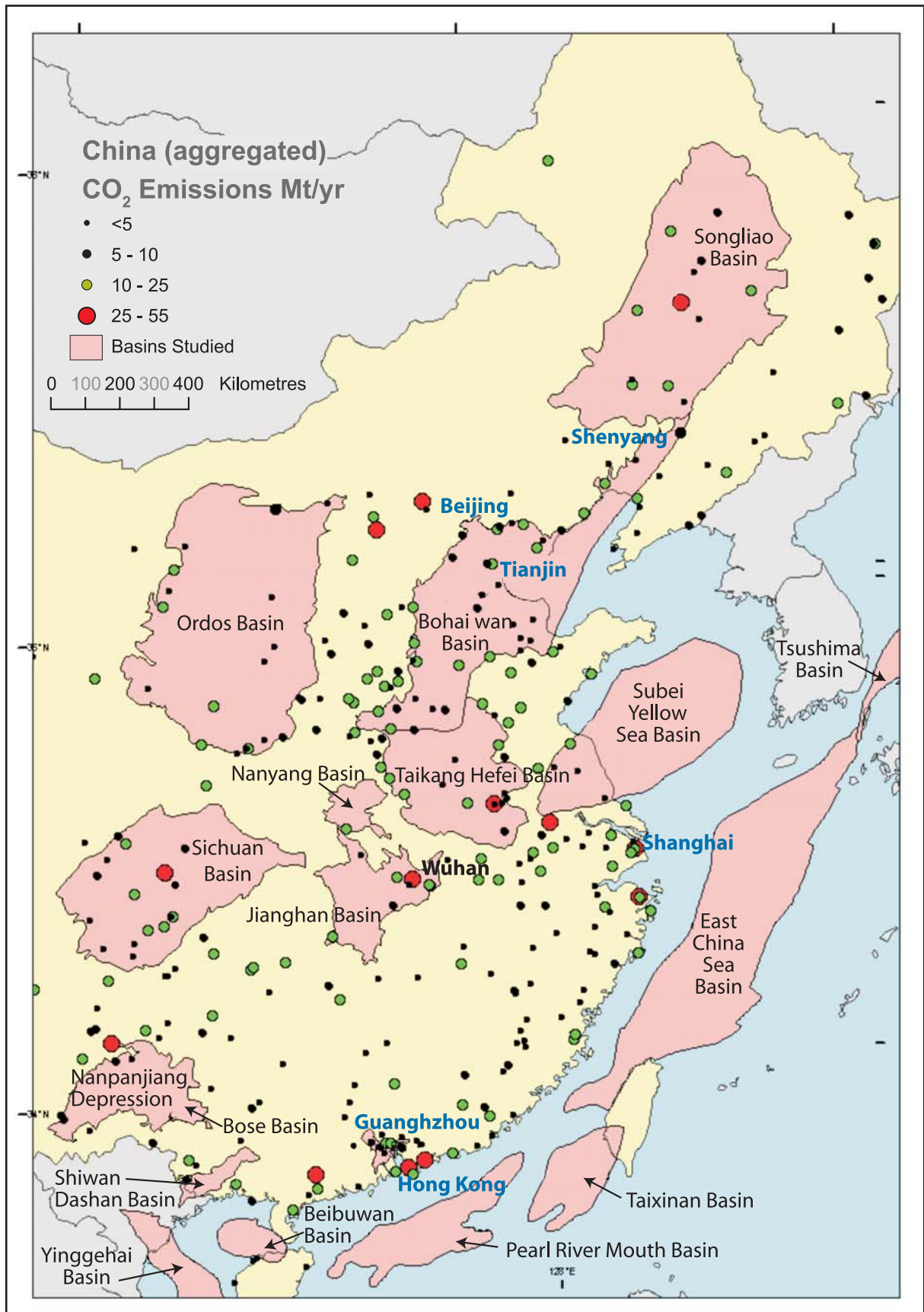


Figure 19. Eastern China aggregated CO<sub>2</sub> sources and basins in proximity to emissions.

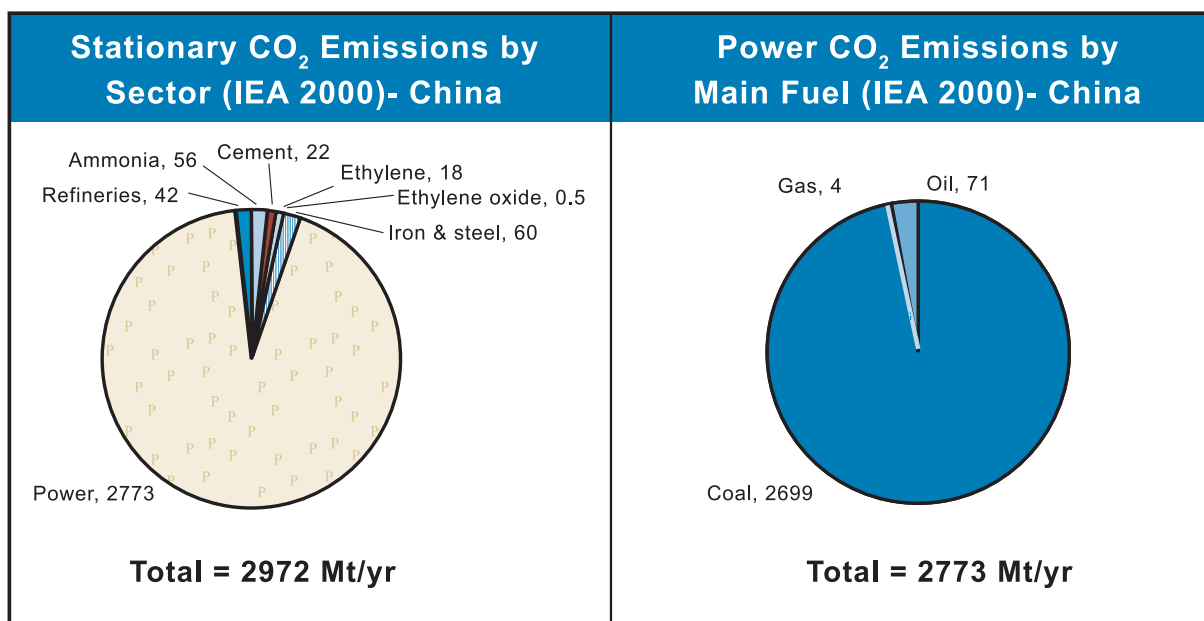


Figure 20. China CO<sub>2</sub> Emissions.

## 3.2 Geological Storage Summary

China is a complex, composite “sub continent” formed by the accretion of geological terranes from the Late Palaeozoic to the Early Tertiary, when India collided with central Asia. These terranes include continental blocks that are bound by fault systems and volcanic arcs and accretionary complexes that form suture zones between the major continental blocks (Figure 21).

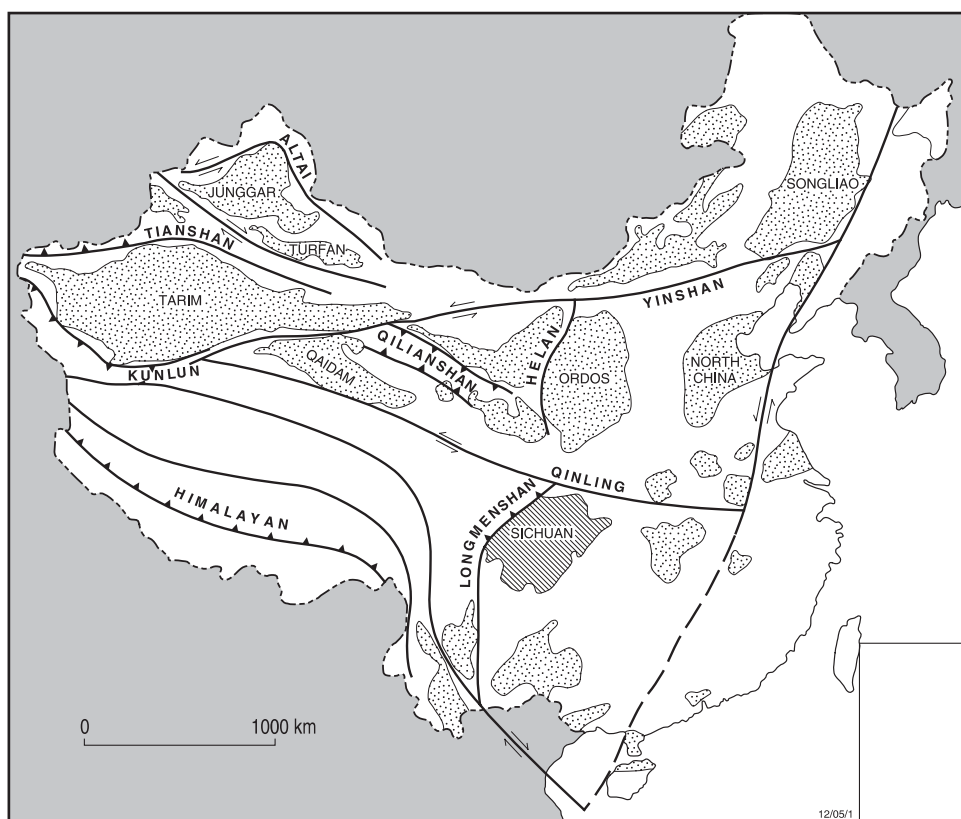


Figure 21. Structural elements of China (from Korsh et al., 1991).

Numerous sedimentary basins were formed during the accretion of these terranes and as a result of tectonic activity associated with the circum-Pacific margin. A basin classification scheme by Watson et al., (1987) depicts the various types of sedimentary basins in China and their associated basin-forming mechanisms (Figure 22).

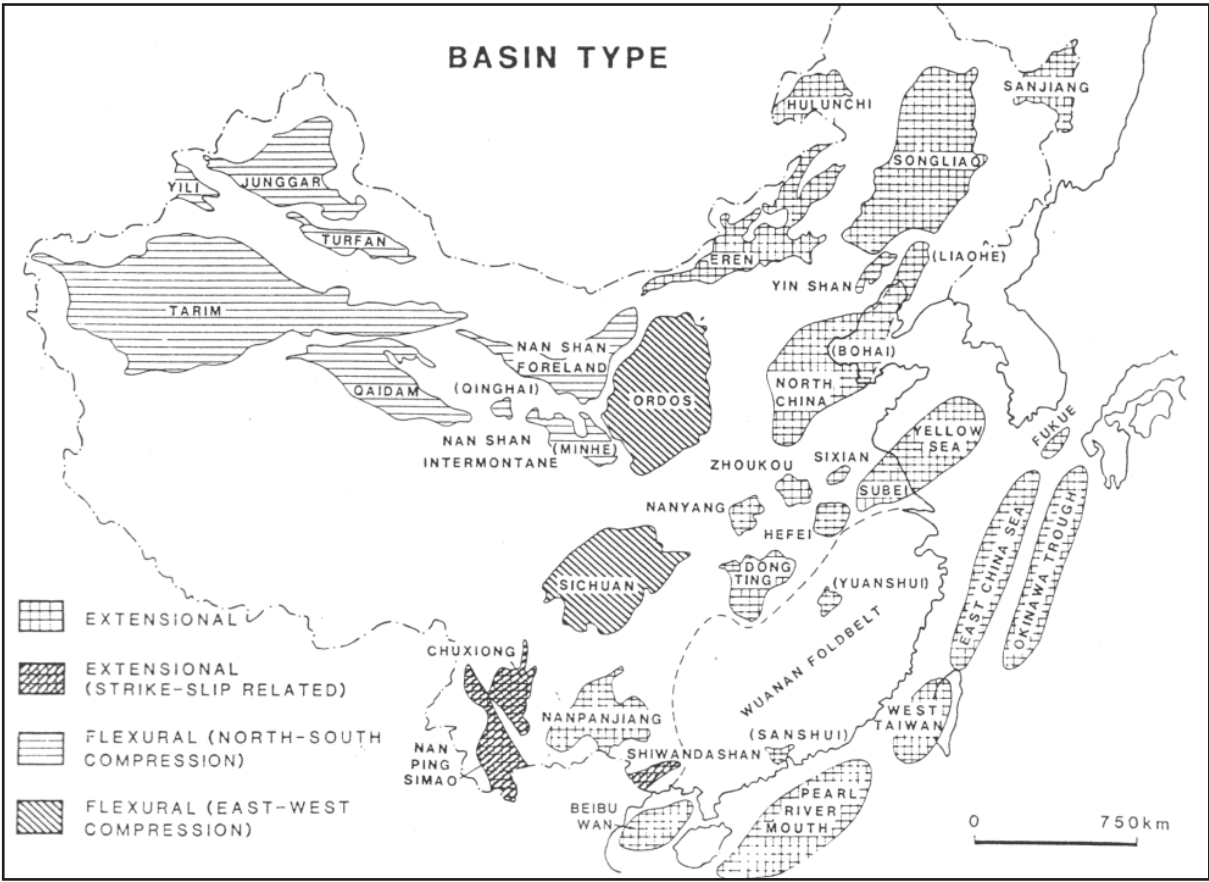


Figure 22. Classification of China’s sedimentary basins (from Watson et al., 1987)

### 3.2.1 Basin Fill

China has numerous extensional basins (Figure 22) and the best known of these are proximal to major CO<sub>2</sub> emissions (Figure 19). The Bohai, Songliao, Subei-Yellow Sea, Jianghan, and the Hefei region basins are matched with around two thirds of the CO<sub>2</sub> sources in China (Figure 23). The offshore East China Sea and Pearl River basins are also extensional. These basins are up to 300 km from CO<sub>2</sub> sources but have been included as there are no obvious geological storage options onshore in the South China Fold belt and Yangtze block for the considerable emissions of the east and south China coast. (Figure 24)

Most of the available information used in this assessment is from oil and gas exploration. Thus most of the information on storage prospectivity is biased towards the Mesozoic and Cenozoic sequences which hold so much of China’s hydrocarbon resources. China has fair to good prospectivity for storage in saline reservoirs. Most of the basins selected for study have one or two potential saline reservoir storage options consisting of lacustrine mudstones sealing fluvial or lacustrine delta sandstones. Deposition in lake environments is very sensitive to the interaction of tectonic events and climate. Lake facies are highly variable on short time scales leading to highly heterogeneous basin fill. However there appear to be one or two laterally continuous mudstone formations in most basins resulting from persistent deep lake environments. Given the overall lower depositional energy of a lacustrine system compared to a marine environment, the identification of a good quality reservoir over an extensive area may be the main challenge. Axial fluvio-deltaic systems should offer the best potential for good reservoirs in lacustrine settings.

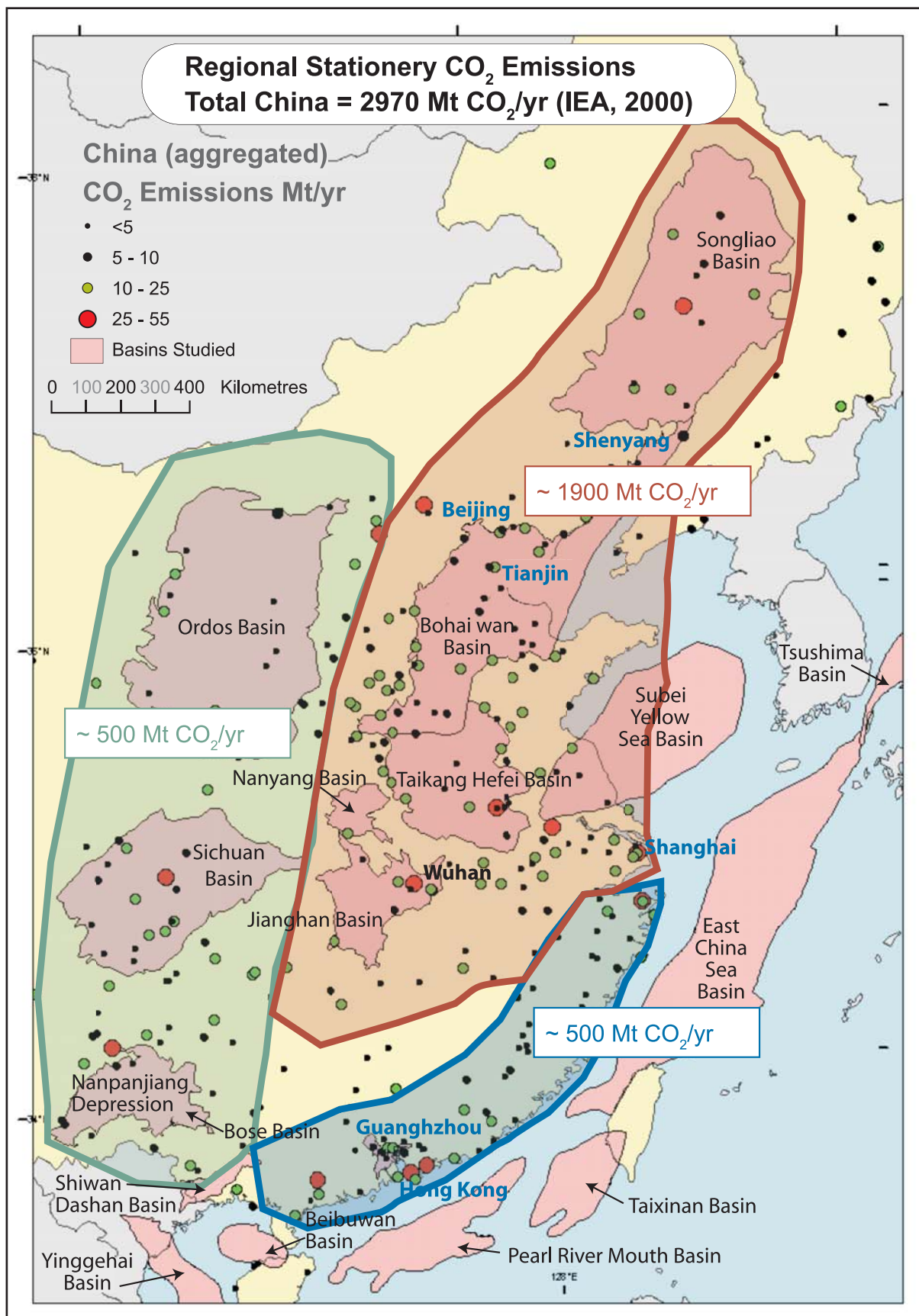


Figure 23. Eastern China approximate totals for annual stationary source CO<sub>2</sub> emissions in generalised 'geological' regions.

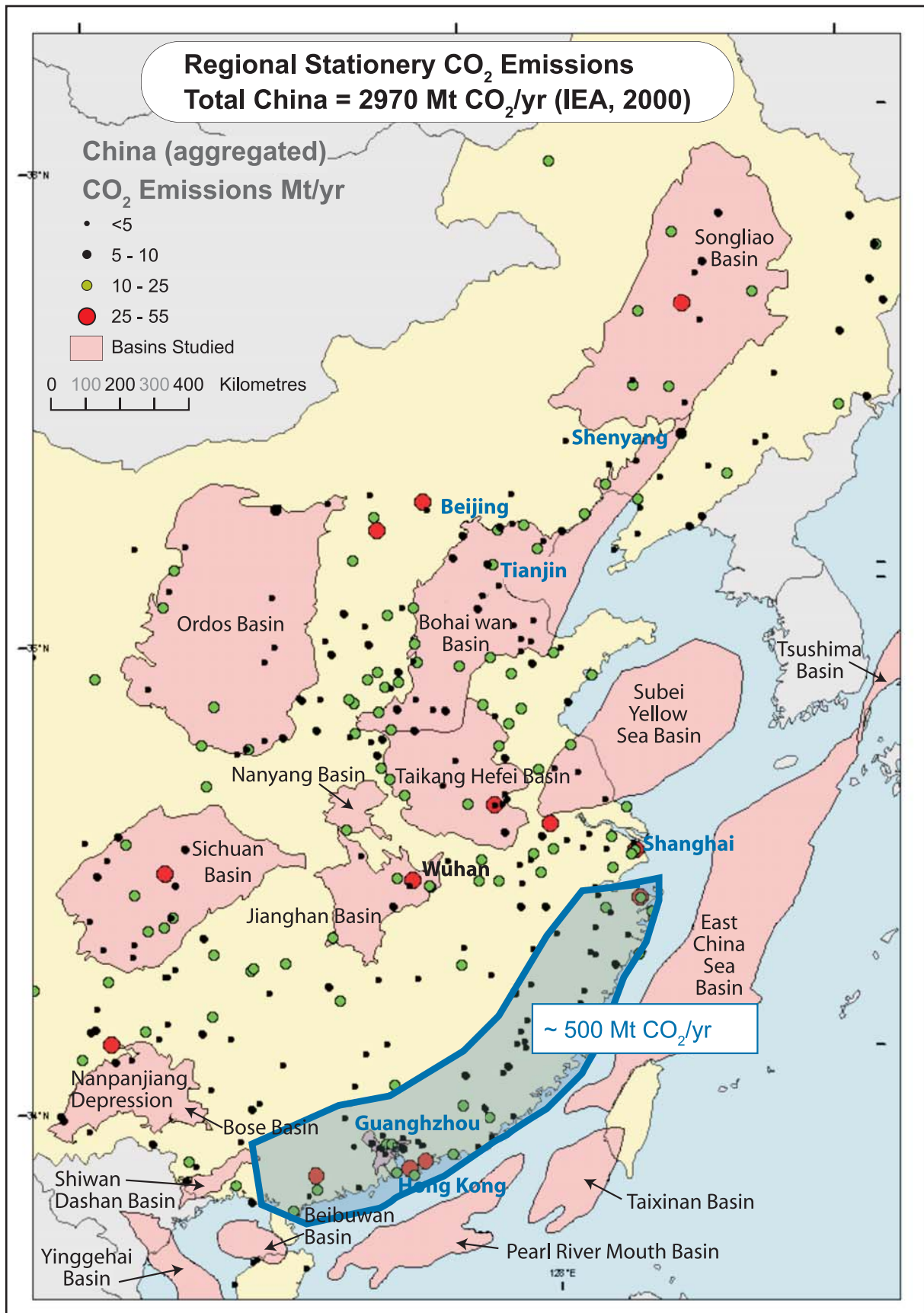
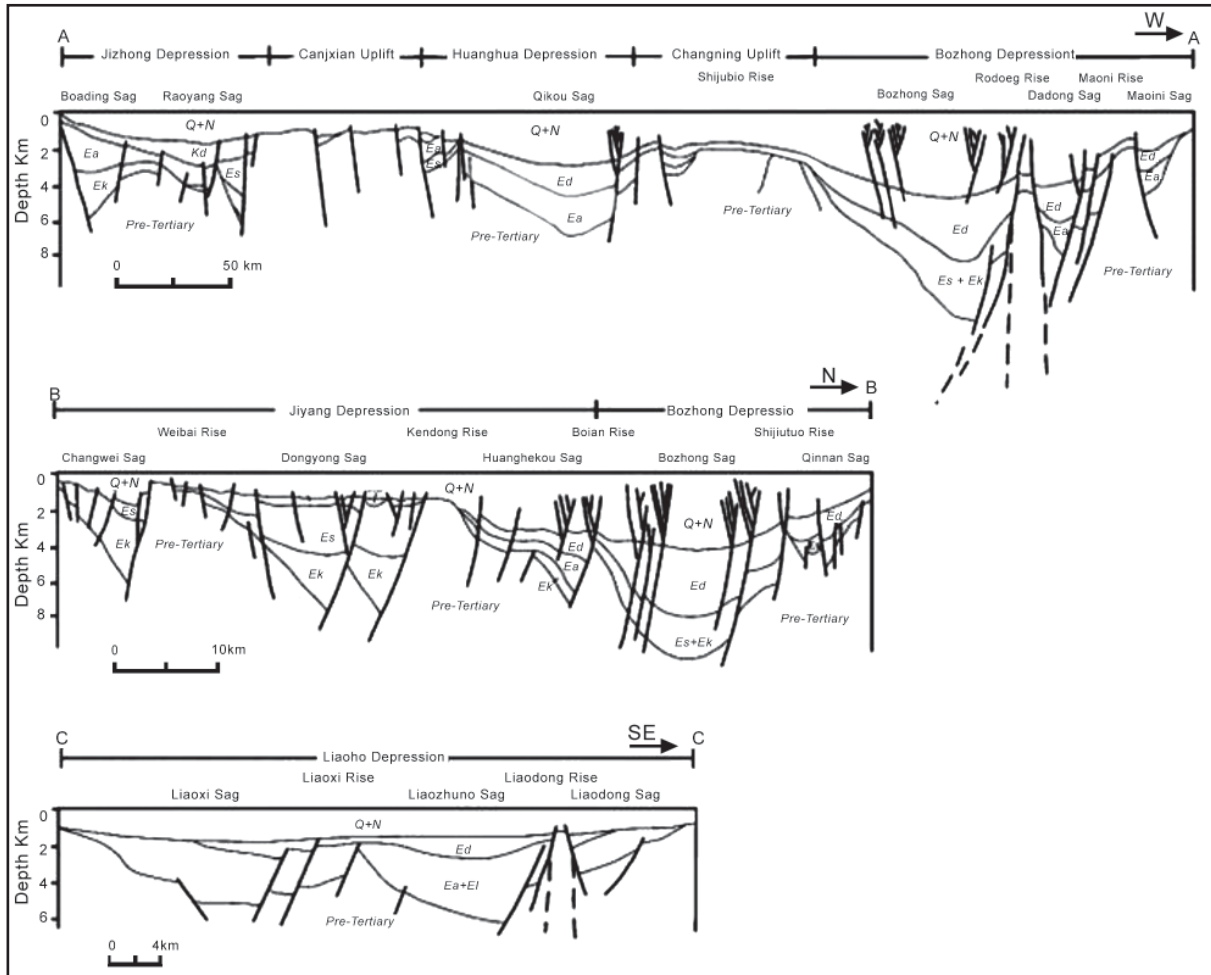


Figure 24. The southern coastal region of the southern fold belt. No major sedimentary basins except offshore.

The half grabens (10 km wide and 30 km long) which make up the early history of the Cenozoic basins may contain strata with dips of up to 10 degrees. The cross-sections in Figure 25 suggest that relatively high dips occur in the earlier phase of rift basins. This will allow CO<sub>2</sub> to have a greater vertical buoyancy vector (Figure 26). Most target reservoirs (saline reservoirs) will be within the gentler dipping syn-rift section of China's lacustrine basins. Heterogeneity may also reduce buoyancy effects (Figure 26) (Doughty et al., 2001 see also Hovorka et al., 2004). This has the effect of “smearing” the CO<sub>2</sub> through the pore space increasing the relative storage efficiency of a reservoir (Figure 27) (Hovorka et al., 2004).



**Figure 25. Cross-sections of the Bohai Basin illustrating the early, syn and late phases of rift base evolution (from Yang and Xu, 2004).**

Basins such as Bohai, Subei and Songliao are collections of half grabens which merged during the sag phase of their evolution. Typically the strata of the sag phase exhibit low angles of dip over large areas (Figure 25). Sag phase formations are more favourable due to dip, area and potential continuity of seal and reservoir facies.

There is also potential to inject into the basement of the Cretaceous rift basins. The Bohai Basin in particular is formed from tilted fault blocks of weathered carbonate which are unconformably covered by a mudstone seal (often a hydrocarbon source rock) deposited during early rifting. Such carbonates with secondary porosity are often oil fields. Such fields are known in China petroleum exploration as the “buried hill” play. This play may also be applicable in the Jiangsu/Subei Basin. The Bohai Bay area of the Bohai Basin may have a high potential reservoir-seal pair. The Guantao Formation is homogenous braided river sandstone with good reservoir qualities and consistent thickness. It is known to be overlain by good sealing formations in several hydrocarbon fields.

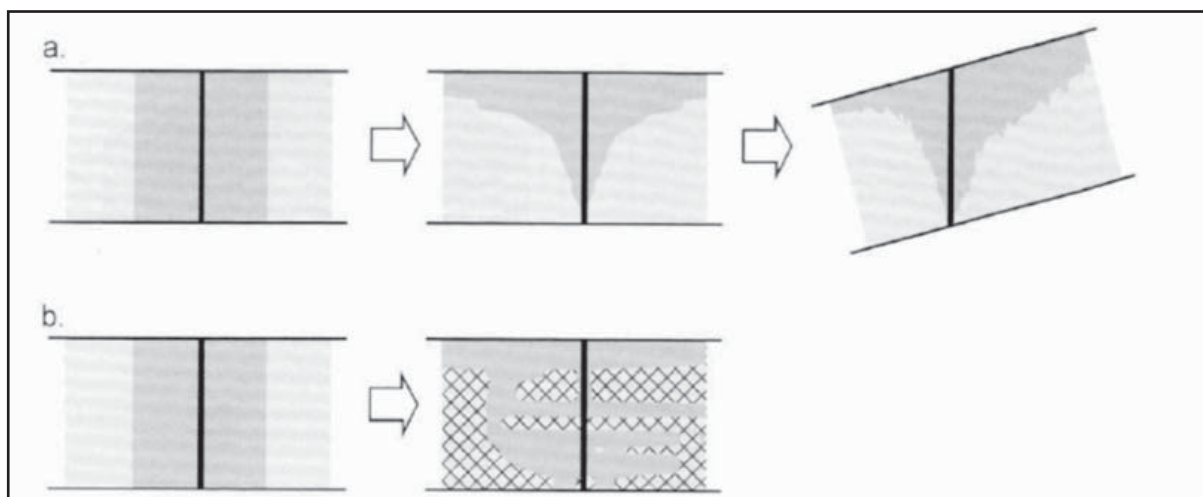


**Figure 26. (a) Strongly dipping homogenous formation causes CO<sub>2</sub> to migrate up dip as shown. (b) The model of heterogeneous low dip media is analogous to low dip syn-rift lacustrine sediments of China's rift basins. Heterogeneity will neutralise buoyancy effects to some degree. (Figure and text from Doughty et al., 2001)**

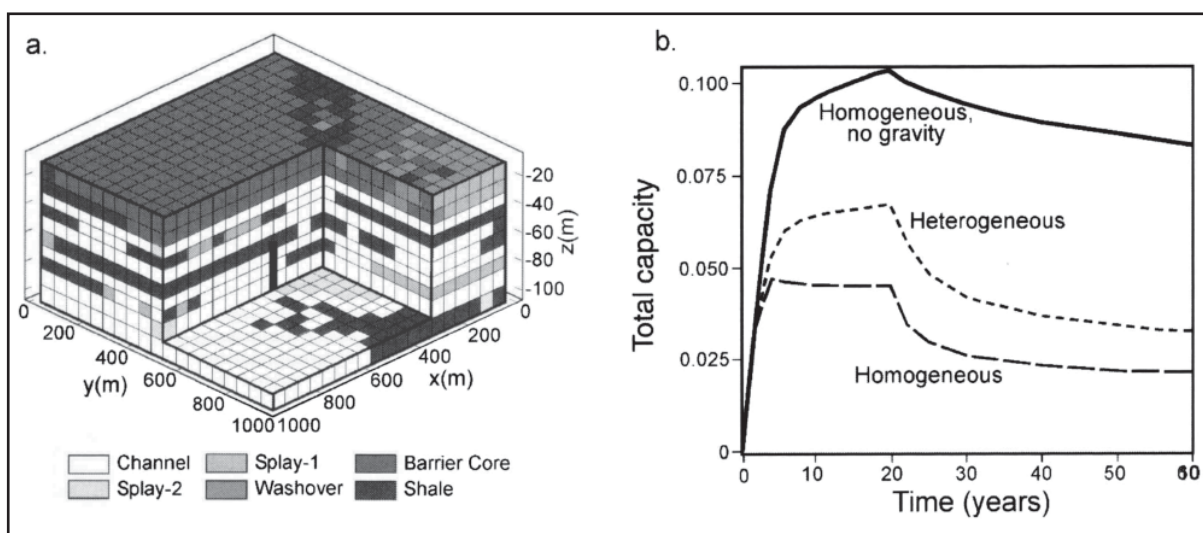


**Figure 27. The effect of CO<sub>2</sub> buoyancy and heterogeneity on the efficiency of CO<sub>2</sub> geological storage as indicated by numerical simulation of 20 years of CO<sub>2</sub> injection into a heterogeneous aquifer (a) simulation grid showing the heterogeneous nature of the subsurface: and (b) storage efficiency (as defined by capacity) (From Hovoroka et al., 2003 after Doughty et al., 2001).**

The Songliao Basin has a number of strong points. The Songliao Basin began forming in the Late Jurassic, earlier than the Bohai or Subei basins. In the Cretaceous a very large, deep lake formed. Persistent deep water resulted in regional deposition of mudstone seals such as the Qingshankou /Nenjiang Formations which seal the Daqing field. Parts of the Daqing complex may have depleted storage or EOR opportunities. Regional scale basinward ground water flows may occur in the Songliao Basin. For these reasons the Songliao is ranked first in terms of CO<sub>2</sub> storage prospectivity for China. A map indicating the relative ranking of basins is provided in Figure 28.

Relative sea level changes in marine environments of deposition offers the potential for large scale high energy clastic reservoirs sealed by extensive shale deposition events. The East China Sea and Pearl River basins are offshore basins. The Subei-Yellow Sea and Bohai basins are on/offshore basins. The marine environments within these basins only date from the Pleistocene. These basins essentially have fluvio-lacustrine fill.

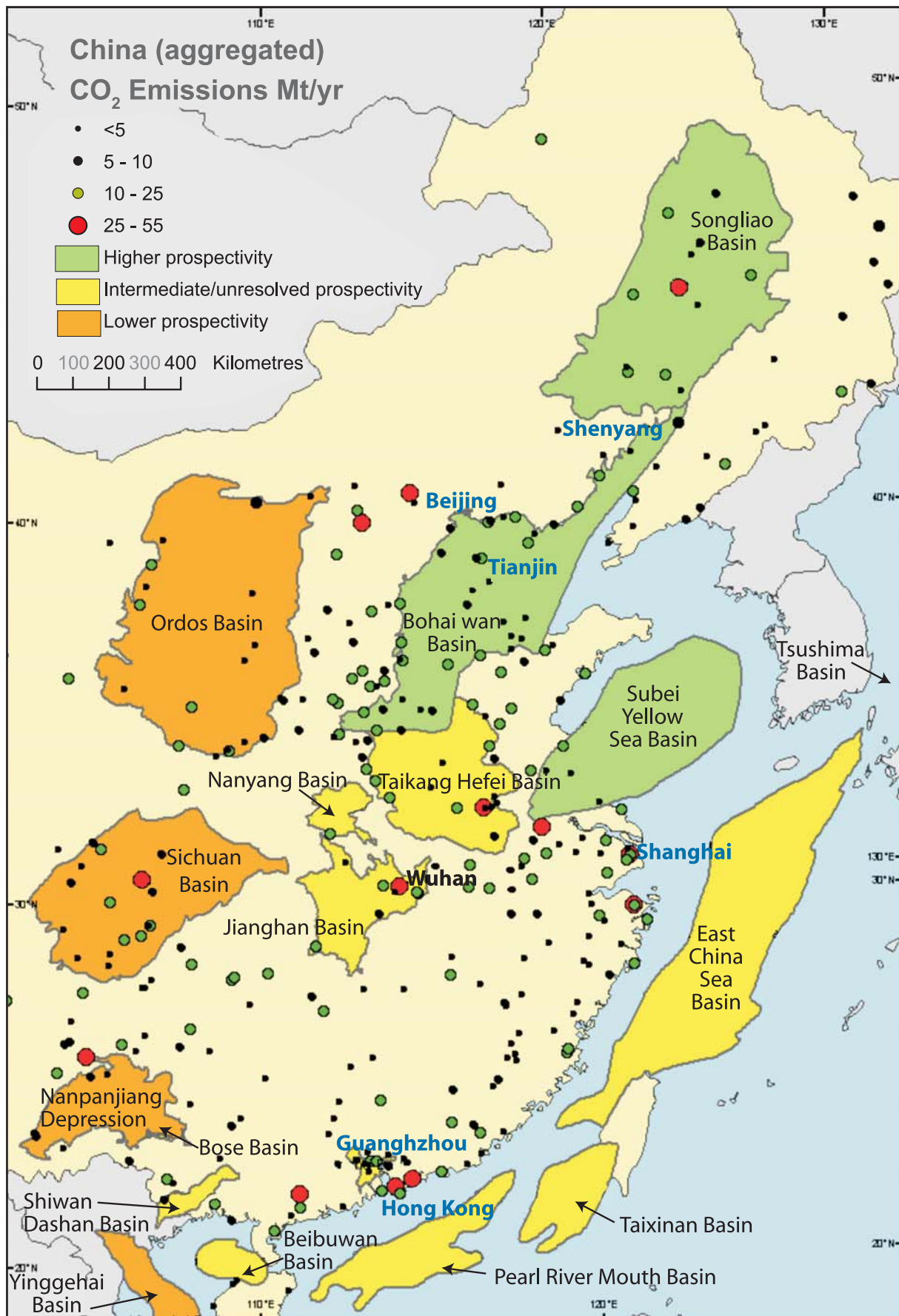


Figure 28. China: relative prospectivity of the basins studied with aggregated CO<sub>2</sub> emissions.

The southern East China Sea had a marine influence from the Late Cretaceous called the “Taibei Gulf”. This area may contain marine claystone seals over marine delta formations. Due to poor hydrocarbon drilling results, information on the area is limited as the main hydrocarbon finds have been in the Xihu trough.

The Pearl River Mouth Basin (PRMB) has sequences with fluvial-lacustrine to fluvial-deltaic environments of deposition. The sediment input kept pace with subsidence and displays an apparently aggradational pattern with a steady overall marine transgression from the Miocene to present. It is likely that most of the seals in the PRMB are localised fluvial and delta mudstones.

The Palaeozoic to Tertiary Ordos and Sichuan basins represent complex polycyclic basins. These basins are almost certainly strongly faulted in a number of orientations due to a geological history that includes extension and two phases of compression along their western margin, associated with thrust-belt loading. At a basin scale, the sedimentary sequences have low westward dip with an angular unconformity developed during the Cretaceous. The Ordos and Sichuan basins developed as foreland basins for most of their history, driven by adjacent mountain belt loading. As a result, subsidence can be irregular and rapid and basin depocentres have migrated to different locations within the basin. This may have created some large scale plays, particularly in the Ordos Basin.

The Sichuan Basin has low prospectivity due to poor porosity and permeability. Overpressure is often present. Large poorly defined quantities of gas sit in continuous columns within generally Palaeozoic carbonate formations. This gas can not be easily produced due to poor permeability; most of the permeability present is due to fractures. Given the solubility of carbonate in the presence of CO<sub>2</sub> there may be potential to inject into these areas if the geochemical conditions are right. Opportunities may also exist for Enhanced Gas Recovery (EGR) using CO<sub>2</sub> to improve permeability and assist gas production. The upper 3000 to 7000 m of sediment in the Sichuan Basin is highly oxidized arid climate sediments i.e. ‘red beds’ (Wang 1989). Red mudstone regional seals are observed in the Jurassic and Cretaceous (USGS, 2000). In summary; low permeability Palaeozoic to Upper Jurassic fill capped by red beds. The Ordos Basin is also characterised by low porosity and permeability through out the section (Sun et al., 1989).

### 3.2.2 Hydrocarbon fields

There are likely to be depleted hydrocarbon field options. Depleted fields will be a solution for a small fraction of China’s CO<sub>2</sub>. China’s stationary source CO<sub>2</sub> emissions are 2972 Mt/year (IEA 2000). According to BP (2004), China’s “known” gas reserves are 82 Tcf and 54 billion bbls (Total equivalent CO<sub>2</sub> stored 13761 Mt). China’s known hydrocarbon pore space storage capacity is about four and a half times the annual CO<sub>2</sub> emissions of 1998 (Figure 29). This is a simplistic ratio with a number of sources of error however the small magnitude of the ratio is significant. Other economies in the SE Asia region have hydrocarbon pore space tens to a hundred times larger than their emissions. The reason that the magnitude of the ratio is lower is due to the very large volume of emissions. Some economies have similar “known” hydrocarbon pore space to China (Figure 30). However China’s CO<sub>2</sub> emissions (like the USA) are an order of magnitude greater than the other economies in this study. Deep saline reservoir pore space must be utilised if geological storage is to cut emissions deeply on a multi-decade time scale.

Consider also a localised example. A 2000 MW coal fired power station can produce ~15 Mt of CO<sub>2</sub>/yr. The 30 year output of CO<sub>2</sub> for this one plant is 450 Mt. This is equivalent to the pore space occupied by 5.6 Tcf of gas or 3 billion barrels of oil. China’s known hydrocarbons are 82 Tcf of gas and 54 billion barrels of oil (BP, 2004). It is apparent that hydrocarbon pore space is not a large resource when faced with high rates of CO<sub>2</sub> production and a 30 year time frame. China has a least 20 plants with >2000 MW capacity (IEA, 2000).

**a.**

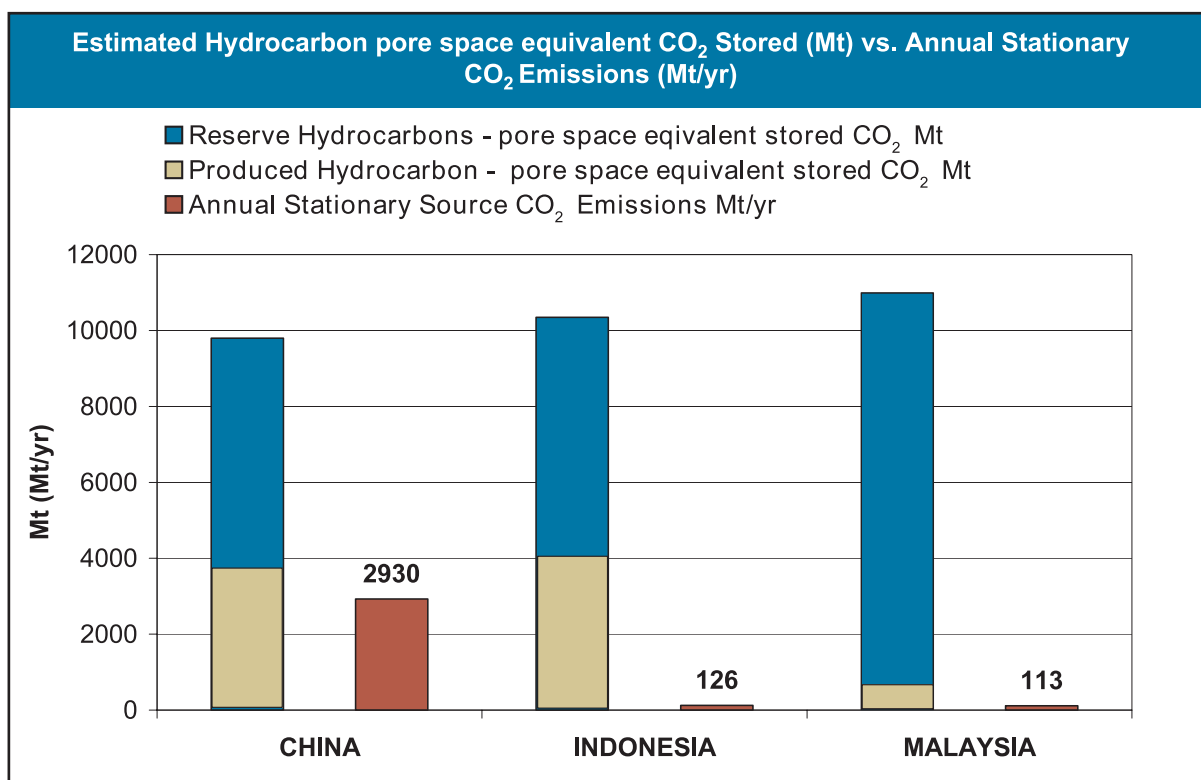
ECONOMY	Oil cum. production to 2000	Oil Reserve	Known oil	Produced	Gas cum. production to 2000	Gas Reserve	Known gas	Produced
	10 <sup>9</sup> bbl	10 <sup>9</sup> bbl	10 <sup>9</sup> bbl	%	Tcf	Tcf	Tcf	%
CHINA	23.9	24.5	48.4	49.4	9.9	33.9	43.8	22.6
INDONESIA	14.4	7.9	22.3	64.6	27.7	65.4	93.1	29.8
MALAYSIA	1.686	2.7	4.4	38.1	4.2	126	130.2	3.2

**b.**

ECONOMY	Known oil	Oil Fields eq CO <sub>2</sub> Storage	Known gas	Gas fields eq CO <sub>2</sub> Storage	Hydrocarbon fields eq CO <sub>2</sub> Storage	Emissions IEA	Emissions/storage ratio
	10 <sup>9</sup> bbl	Mt	Tcf	Mt	Mt	Mt/yr	
CHINA	48.4	6292	43.8	3504	9796	2930	3
INDONESIA	22.3	2899	93.1	7448	10347	126	82
MALAYSIA	4.425	575	130.2	10416	10991	113	97

**Figure 29. (a) Hydrocarbon reserves and production data (hydrocarbon data - USGS world hydrocarbon assessment, 2000) Please note that Korea, Thailand, Phillipines and Chinese Taipei have relatively small hydrocarbon reserves and are not included here. (b) Known hydrocarbon volumes (produced and reserves) converted to equivalent stored CO<sub>2</sub> mass, the conversions from hydrocarbon volume to stored CO<sub>2</sub> mass are in Appendix B.**



**Figure 30. Comparison of the magnitude of hydrocarbon space equivalent CO<sub>2</sub> stored with annual CO<sub>2</sub> emissions (Hydrocarbon data - USGS World Hydrocarbon Assessment 2000, Emissions - IEA).**

### 3.2.3 Coal

China's coal resources are estimated to be about 1000 Gt, with proven recoverable reserves accounting for 114 Gt (BP, 2004). Since 1985, China has been the largest producer and consumer of coal in the world. In 2002, China produced 1.37 Gt of coal and consumed about 1.28 Gt of coal (USDOE/EIA website.). The distribution of coal-bearing areas in China and surrounding regions is shown in Figure 31. Two thirds (76 Gt) of proven coal reserves occur in or adjacent to the Ordos Basin in Shaanxi, Shanxi and Inner Mongolia provinces.

The most economically important coal measures in China occur within Carboniferous, Permian, Jurassic and Cenozoic-age sediments. Underground mines produce over 95 percent of the coal production in China. Coal reserves suitable for surface mining are comparatively small (7 percent of total) and 70 percent of these reserves are lignite (USEPA, 1996).

Important Permo-Carboniferous coal-bearing sequences in North China are dominated by clastic sediments, and coal seams are generally thick, and laterally continuous. In South China, where marine influence and tectonic activity prevailed, the major Permian coal sequences contain carbonates and volcanic rocks, and the coals tend to be more numerous, but thinner, structurally deformed and laterally discontinuous (Liu, 1990).

In northeast China, predominantly Jurassic and to a lesser extent Early Tertiary age coal measures occur in a series of rift basins. These coal measures range from lignite to bituminous and form economically important coal deposits. Late Triassic to Early Jurassic coal measures also occur in southern China. However, many of these coal measures contain high rank (anthracite), thin seams that are often high deformed and amenable to small scale mines (USEPA, 1996).

The coal industry of China is currently undergoing a major reform and restructuring. China has three principal types of coal mines, State-run (central government), Locally-controlled, and Township and Private mines. Although most production is from State-run mines, there are estimated to be over 79,000 Township mines (USEPA, 1996).



**Figure 31. China coal map (modified from Podwysocki and Lovern, 2000). Note that China has  $114 \times 10^9$  tonnes recoverable reserves. Shaanxi, Shanxi and Inner Mongolia have  $76 \times 10^9$  tonnes recoverable reserves.**

## Coal Mine Methane

Coal bed methane is detrimental to the environment if vented to the atmosphere, but is a remarkably clean fuel when burned. Coal bed methane combustion produces no sulphur dioxide or particulates, and only half of the CO<sub>2</sub> associated with coal combustion. In many countries, methane produced by coal mines has historically been vented and become a wasted resource.

China has one of the longest histories of using coal bed methane recovered from its mines. Methane can be recovered before, during, or after coal mining and used as a fuel for power generation or consumed directly for industrial and residential energy needs.

In addition to its value as an energy source, drainage and use of methane from coal mines increases mine safety and productivity, due to the explosive nature of methane in relatively low concentrations (5-15 percent in air). As coal mines deplete shallower coal reserves, there is a shift to mining deeper, gassier coal beds. Underground mines generally release more methane than surface mines, because methane storage capacity increases with greater depth and pressure. In China, half of the largest state-run mines are considered highly gassy or prone to outburst; mine ventilation and methane drainage is critical for mine safety (USEPA, 1996).

According to the China Coal bed Methane Clearinghouse, Chinese mines liberate about 9 billion cubic meters (bcm) of methane (more than 127 million metric tons of CO<sub>2</sub> equivalent) annually. Since Chinese mines recover and use less than 0.5 bcm of this methane, (Figure 32) there is a enormous potential for coal mine methane development projects. (China Coal bed Methane Clearinghouse, [http://www.coalinfo.net.cn/coal bed/r01.htm](http://www.coalinfo.net.cn/coal%20bed/r01.htm)).

## Enhanced Coal Bed Methane (ECBM)

China has had three stages of exploration and development of coal bed methane resources. The first during the 1950-60s, which involved drilling methane drainage wells from underground mines and venting the methane directly to the atmosphere. The second stage (1970s-90s) saw the beginning of exploration and development of pilot wells. From the 1990s to the present day there has been broadened exploration and an increase in modern drilling and development technology and involvement by foreign companies.

Estimates of gas-in-place resources for coal bed methane in China shallower than 2000 m range from 30 to 35 trillion m<sup>3</sup> (Sun & Huang, 1995); PetroChina recently estimated a 22.5 trillion m<sup>3</sup> resources. Most coalfields suitable for ECBM are located in the eastern and central provinces, especially in the Ordos Basin and Qinshui Basin in Shanxi province (Su et al., 2005). The first commercial CBM field is located in the southern Qinshui Basin (Liu et al., 2004).

More than 200 wells have been drilled throughout China, and 11 pilot projects have commenced. Figure 33 shows the location of coal bed methane projects in China in 1996. The main obstacles in developing the coal bed methane industry has been the low permeability of many of the coal measures (often below 1 mD), complex reservoirs, high cost and uptake of exploration, drilling and production technology, and the limited nature of a coal bed methane database (Liu et al., 2004).

ECBM opportunities may in the future provide a net benefit as carbon sinks in China. All types of geological storage are strongly dependant the local conditions at the site of injection. Unfortunately, the factors that are important to the process of carbon storage during ECBM operations are more poorly understood, and more uncertain than for other types of CO<sub>2</sub> storage.



Figure 32. Location of coal mines in China practicing methane drainage (USEPA, 1996).



Figure 32. Location of coal bed methane projects in China.

### 3.2.4 Summary

A provisional, qualitative geology ranking of the relative suitability of basins for geological storage is presented in Figure 28. Storage in an offshore basin is intrinsically more costly. However factors influencing the relative economy of capturing and transporting from source to sink are not considered. These issues are assumed equal and the basins are ranked on the basis of their perceived geological storage prospectivity (porosity, permeability, seals etc).

# 4. Indonesia

## 4.1 Source Characterisation

- ◆ Total emissions of Indonesia are approximately 126 Mt CO<sub>2</sub> /yr according to IEA (2000) data.
- ◆ Power generation is 38.6% of emissions. Main emission centres are associated with coal-fired power stations near Jakarta in west Java, and near Surabaya in eastern Java. Sources on Sumatra are very widely spread, and related to gas processing in the north and coal and oil-fired power stations in southern Sumatra.
- ◆ Indonesia is planning to construct two nuclear power stations, one in central Java and another on Madura Island off the east Java coast (Adelaide Advertiser 23/3/05).
- ◆ Gas processing accounts for 33.5% of emissions. A highly localised and significant gas processing centre lies in the Kutei Basin in eastern Kalimantan.
- ◆ Indonesia has major sedimentary basins adjacent to all significant emissions areas (Figure 34).
- ◆ The Jakarta region has the most concentrated and largest volume of CO<sub>2</sub> emissions.

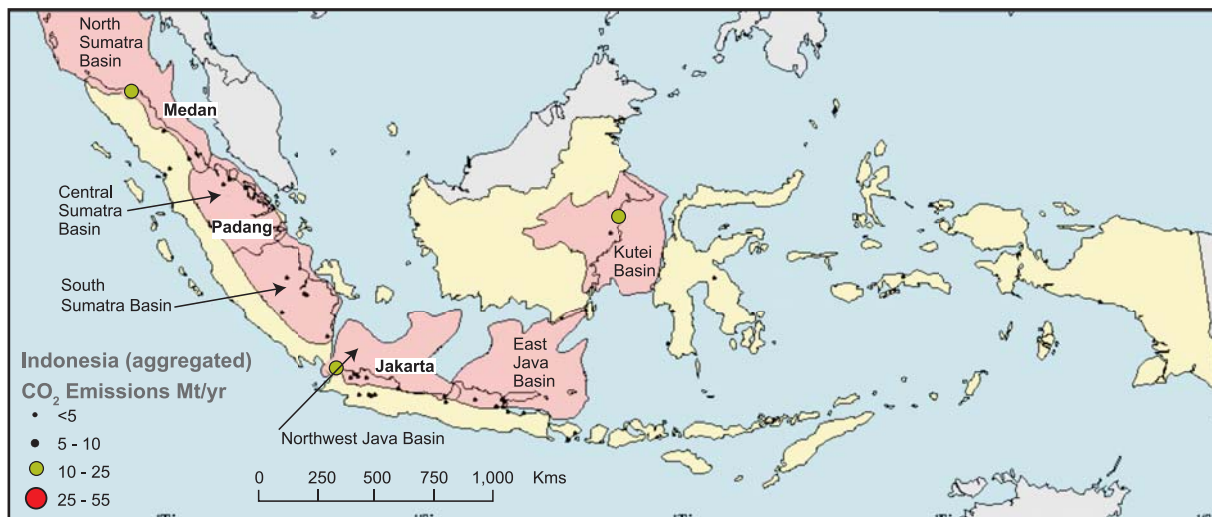


Figure 34. Indonesia stationary CO<sub>2</sub> emissions and basins studied.

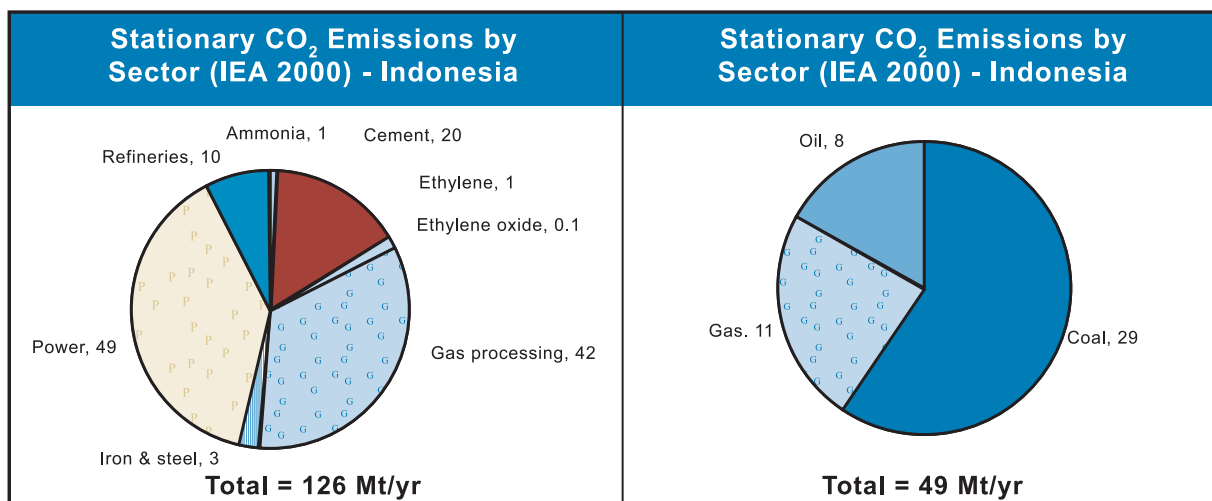


Figure 35. Indonesia stationary CO<sub>2</sub> emissions.

## 4.2 Geological Storage Summary

Indonesia has a chain of back-arc basins that lie onshore and offshore of the two main islands of Sumatra and Java. As noted above, the majority of emissions are produced on the Island of Java. The main basins of interest are the Northern, Central and Southern Sumatra basins, Northwest and East Java basins and the Kutei Basin, which is the major source of hydrocarbons in Kalimantan.

Due to their common regional tectonic setting, the Sumatran and Java basins have general similarities. They all offer a range of reservoir-seal pair options. The presence of regionally extensive Miocene shales puts a very effective ultimate seal over large areas (Figure 36). A major negative factor throughout the Sumatra and Java basins is high geothermal gradients ranging from 45°C/km to 60°C/km. This will reduce the subsurface density of stored CO<sub>2</sub>.

Given its proximity to the large emissions of the Jakarta region the NW Java Basin is of interest for further investigation. The NW Java Basin has two sub basins, the Arjuna and Sunda basins that offer good quality marine clastic reservoirs and carbonate bioherm reservoirs. As noted above, the Gumai Shale is a seal on the entire petroleum system and is considered to add greatly to the prospectivity of this basin and the Sumatra basins.

The northern most Sumatra Basin has high porosity carbonate reservoirs known from oil exploration. There are also clastic reservoirs to the south. Marine Oligocene to Early Miocene claystone provides a regional seal.

Notably, the Central Sumatra Basin lacks carbonate reservoirs unlike the North and South Sumatra basins (Williams and Eubank, 1995). The Early Miocene Sihapas Group post-rift marine sandstones are the principal reservoir units in the Central Sumatra Basin for hydrocarbon production. Similarly the Northern Sumatra Basin, a regional seal is provided by the lower and middle Miocene Telisa Shale of the Sihapas Group which represents the maximum transgression in the basin. This shale is equivalent to Gumai Fm of the offshore NW Java Basin. It should be noted the onshore area of the basin is only a small fraction of the basin. It appears that the Middle to late Miocene marine sandstones may offer opportunities, particularly in the shelfal sands, which may form larger bodies. The debris-flow facies tend to be more constrained in size, occurring as fans or channels. The Kujung Formation provides carbonate saline reservoir targets for CO<sub>2</sub> storage. The extent of these reef facies in the basin is unclear.

The shelfal siliciclastic reservoirs of the Ngrayong Sandstone of the onshore East Java Basin appears to be the best early target for CO<sub>2</sub> storage in the East Java Basin.

The majority of CO<sub>2</sub> emissions on Kalimantan are the result of hydrocarbon refining/processing operations. The Miocene to present day fluvial-deltaic system has high prospectivity for extensive good reservoir quality sandstones with extensive transgressive seals. There is some evidence for fresh pore water down to 1830 m. The risk of CO<sub>2</sub> injection impacting on the extraction of hydrocarbons would need to be carefully assessed. Depleted fields (if such exist) within the Samarinda anticlines would provide high confidence storage sites. There are obvious technological synergies that favour storage in saline reservoirs and/or depleted fields on Kalimantan.

Indonesia has considerable, but declining, reserves of hydrocarbon, and the largest fields are in Central Sumatra Basin. Hydrocarbon fields in the East Java Basin are relatively small. Depleted field storage may be a viable option for Indonesia, with many of the hydrocarbon fields being onshore. Unfortunately most of the hydrocarbon fields of the NW Java Basin (nearest to Jakarta) are in the offshore portion of the basin. However the distribution of depleted fields is unknown.

Using USGS (2000) data the “known” oil and gas (past production plus remaining reserves) of the major basins of Indonesia is 22 billion bbls of oil and 93 Tcf of gas. (Note: The reserves used in the BP Statistical Review of World Energy Worksheet are similar to those of the USGS (2000)). The USGS (2000) estimate of known oil and gas is equivalent to ~10 300 Mt of stored CO<sub>2</sub>. This is 80 times the estimated annual emissions of 126 Mt CO<sub>2</sub> /yr.

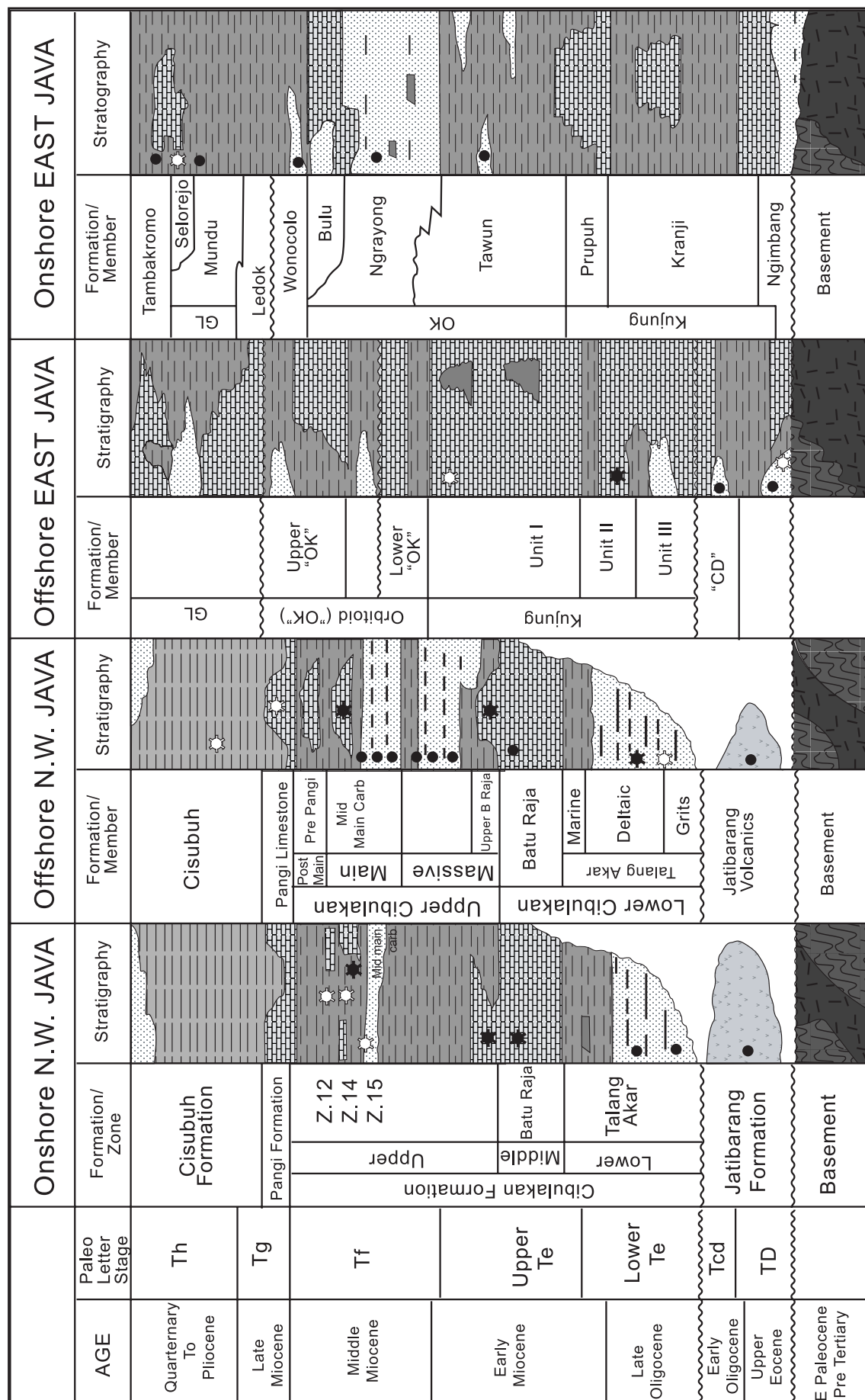


Figure 36. The geology and hydrocarbon potential of the Island of Java and its adjoining offshore areas (from Indonesian Petroleum Association Oil and Gas Field Atlas IV, publication date unknown).

The depleted field storage potential of the Jakarta region and the nearby NW Java Basin should be considered. Total emissions in the Jakarta region are about 25 Mt CO<sub>2</sub>/yr. The NW Java Basin has a “known” hydrocarbon volume (USGS, 2000) equivalent to 1000 Mt stored CO<sub>2</sub>, this is 40 times the annual emissions.

The coal bed methane (CBM) resource in Indonesia may be substantial. A recent CBM study identified a potential resource of 337 Tcf of coal bed methane from eleven sedimentary basins in Indonesia (Scott et al., 2001). This resource estimate is probably optimistic due to the lack of actual reserve data. Although most coal seams currently exploited in Indonesia are of low rank and low methane content, many of these coals increase rank rapidly with depth (Figure 37).

Currently there are no commercial CBM projects in Indonesia, although exploration activity has commenced. Consequently, niche opportunities for ECBM could be generated probably within the South Sumatra Basin, the Barito and Kutei basins in Kalimantan and in onshore basins on Java.

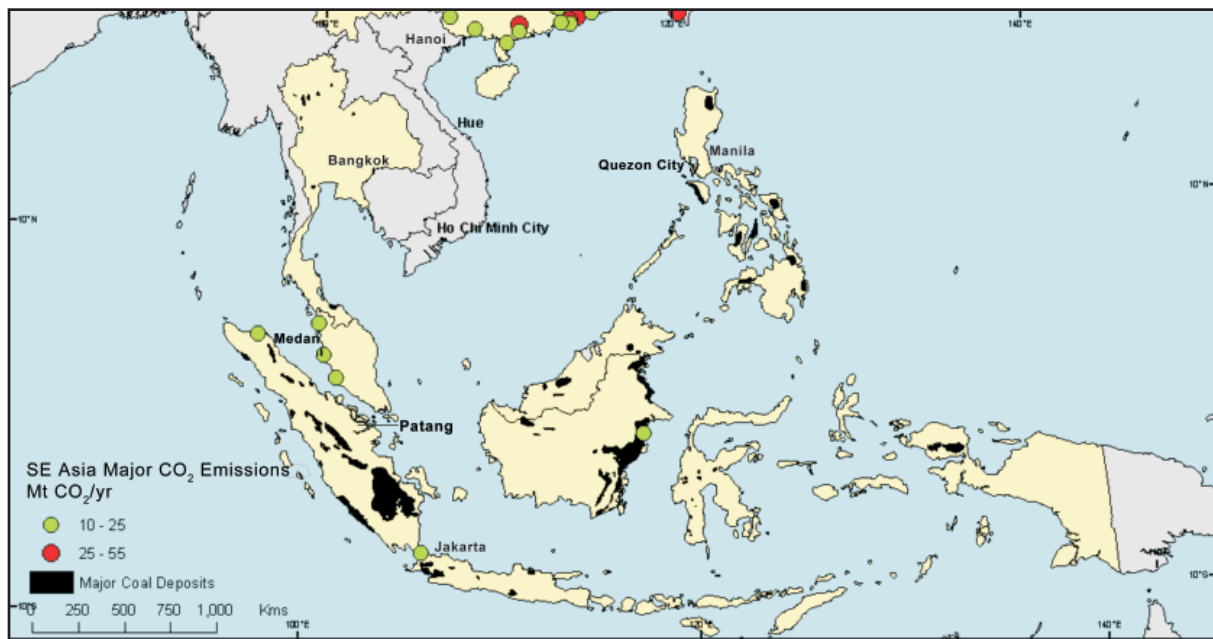


Figure 37. South East Asia major stationary CO<sub>2</sub> emissions (aggregated) and coal deposits.

# 5. South Korea

## 5.1 Source Characterisation

- ◆ The IEA (2000) estimated that South Korea produces around 314 Mt/yr of CO<sub>2</sub>. This is expected to increase to 421 Mt by the year 2010.
- ◆ Point-source emissions are concentrated along the southern and north-west coasts.
- ◆ The largest source of CO<sub>2</sub> emissions is in the south, which produces 29.5 Mt CO<sub>2</sub>/yr.
- ◆ The power generation sector is responsible for approximately 71% of CO<sub>2</sub> emissions.
- ◆ Coal-fired power stations produces 84% of stationary CO<sub>2</sub> emissions, followed by gas 11% and oil 5%.
- ◆ There are seven sources in South Korea with a pure CO<sub>2</sub> concentration. Most of these are located on the southern coast.

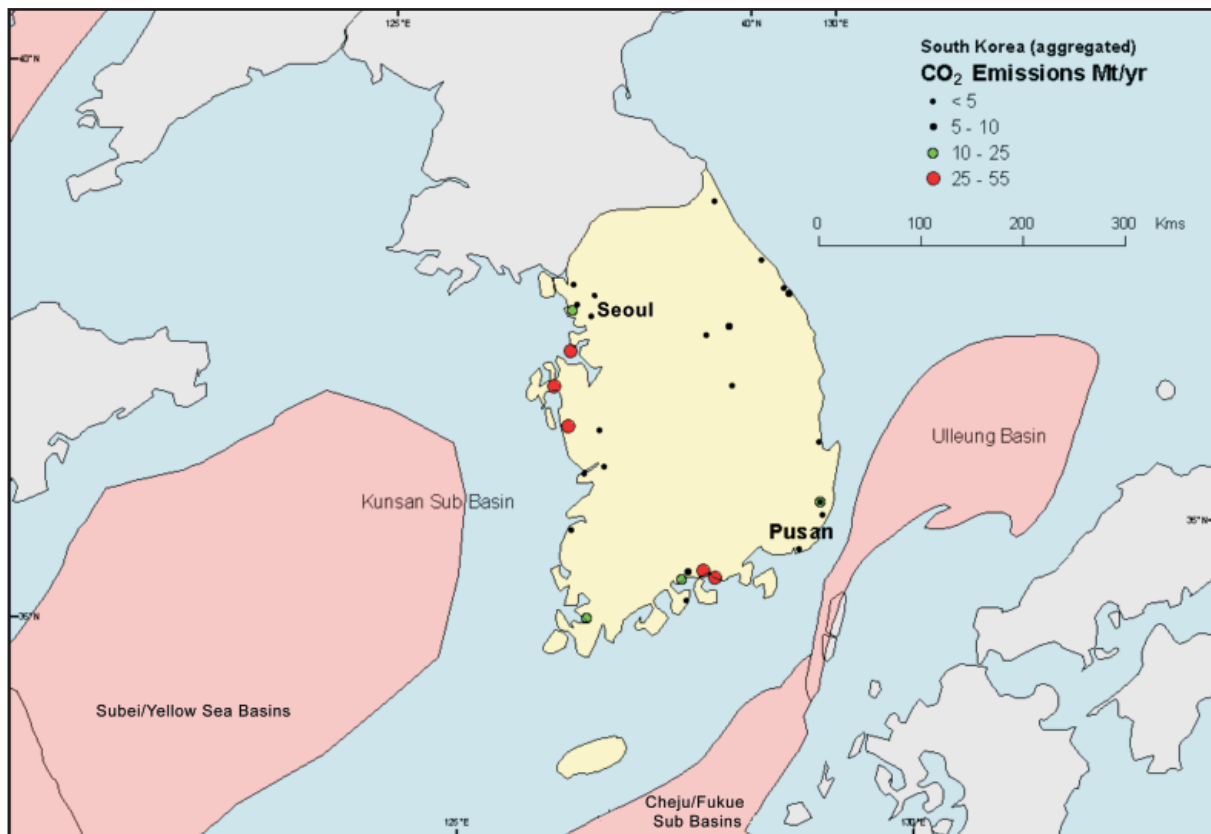


Figure 38. South Korea stationary CO<sub>2</sub> emissions and study basins.

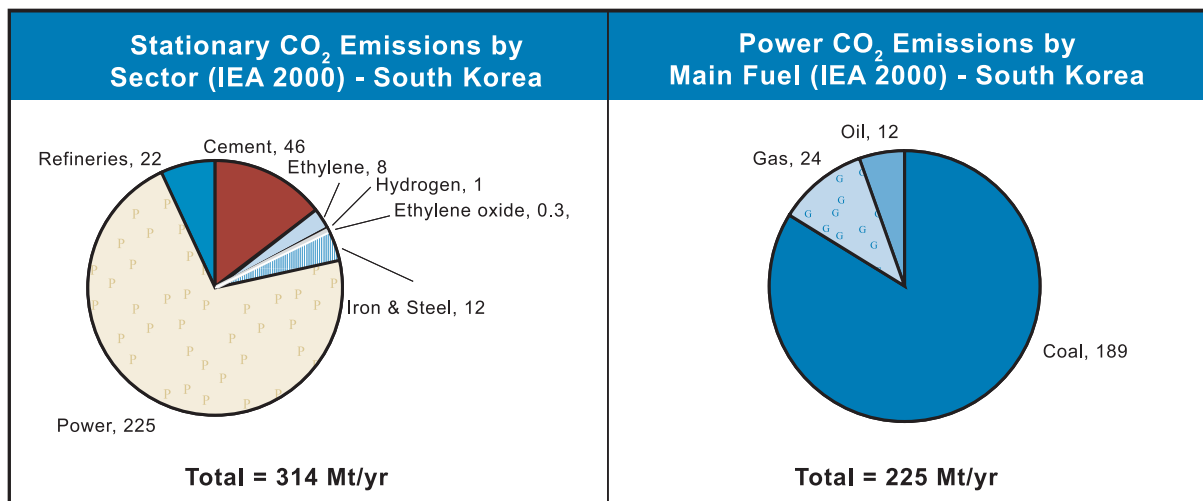


Figure 38. South Korea stationary CO<sub>2</sub> emissions.

## 5.2 Geological Storage Summary

South Korea's prospective geological sinks for CO<sub>2</sub> are limited to offshore sedimentary basins, as most of the onshore area consists of granitic basement or Precambrian metamorphic rocks. The three main basins considered as possible storage basins are the Ulleung Basin, the northern extremity of the East China Sea Basin, and the eastern edge of the North Yellow Sea Basin (Kunsan Basin).

The Ulleung Basin is essentially a slope basin dominated by debris flow deposits. Although a large proportion of this basin lies in over 1000 m of water, the shelfal part of the basin may be more accessible, but seal presence may be a problem. South Korea's only gas field occurs in this basin and contains 210 Bcf of reserves. In 2005, the Korea National Oil Corporation signed a one year joint study agreement with a foreign exploration company to investigate the further hydrocarbon potential of the Ulleung Basin.

The Chedju (Fukue) Basin forms the northern extremity of the East China Sea Basin. This area is a joint development zone administered by South Korea and Japan. This basin appears to contain good extensive seals and reservoirs and shows of hydrocarbon but no apparent commercial discoveries. The area appears have prospectivity as a geological storage area.

The Kunsan Basin is in the South Korean sector of the Yellow Sea Basin and lies off the west coast of South Korea. Emission sources on the west coast emit 50% of South Korea's CO<sub>2</sub> total emissions. Information is limited on the Kunsan Basin. No indication of reservoir quality was located in the literature. From stratigraphic columns and logs provided in Yi et al., (2003) it appears likely to have acceptable reservoir and seal characteristics similar to the fluvial-deltaic sandstones in the Cenozoic rift basins of onshore China.

Depleted hydrocarbon field storage is not applicable due to South Korea's very small hydrocarbon reserves. Coal resources are limited to thin (generally less than 2 m thick), low-quality anthracite seams in the central and western part of South Korea. These coal deposits may have potential for coal bed methane (Kumar and Kim, 1997), although due to the highly deformed nature of the coal measures, this potential is probably very limited. Coal supplies about 69% of South Korea's total power requirements (while producing 84% of all power sector CO<sub>2</sub> emissions). Most of this coal is imported, as indigenous coal resources are used in home heating and small boilers.

# 6. Malaysia

## 6.1 Source Characterisation

- ◆ According to the IEA (2000) Malaysia has annual CO<sub>2</sub> emissions of 113 Mt/yr.
- ◆ The majority of Malaysia's stationary CO<sub>2</sub> emissions are generated along the west coast of Peninsular Malaysia (West Malaysia). Given the distribution of Malaysia's CO<sub>2</sub> emissions the main basin of interest is the Malay Basin.
- ◆ Malaysia's power generation is predominantly fuelled with offshore gas and oil resources.
- ◆ Malaysian coal reserves are mainly located in East Malaysia remote from stationary emission sources in Peninsula Malaysia.
- ◆ Currently Malaysia's gas and renewable resources provide the opportunity for a relatively low CO<sub>2</sub> emission profile. As gas reserves are depleted, it is expected that CO<sub>2</sub> emissions will grow as coal is utilised for power generation.
- ◆ The large and prolific Greater Sarawak-East Natuna Basin system of East Malaysia is not adjacent to significant stationary CO<sub>2</sub> sources according to IEA (2000) data. The natural gas field named Natuna is in this area, it contains 70% CO<sub>2</sub> and is only a proposed development project.

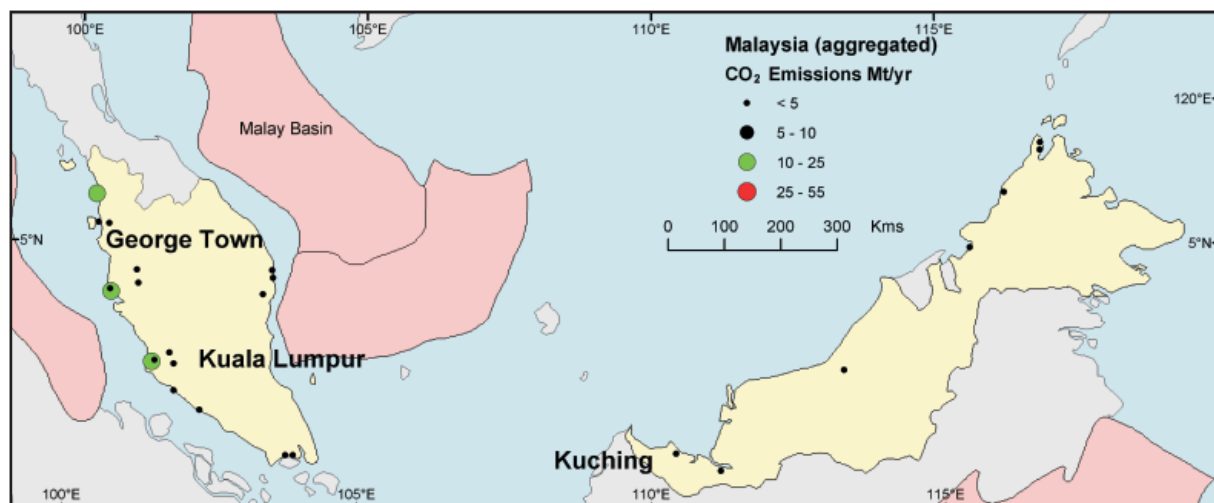


Figure 40. Malaysia stationary CO<sub>2</sub> emissions and study basins.

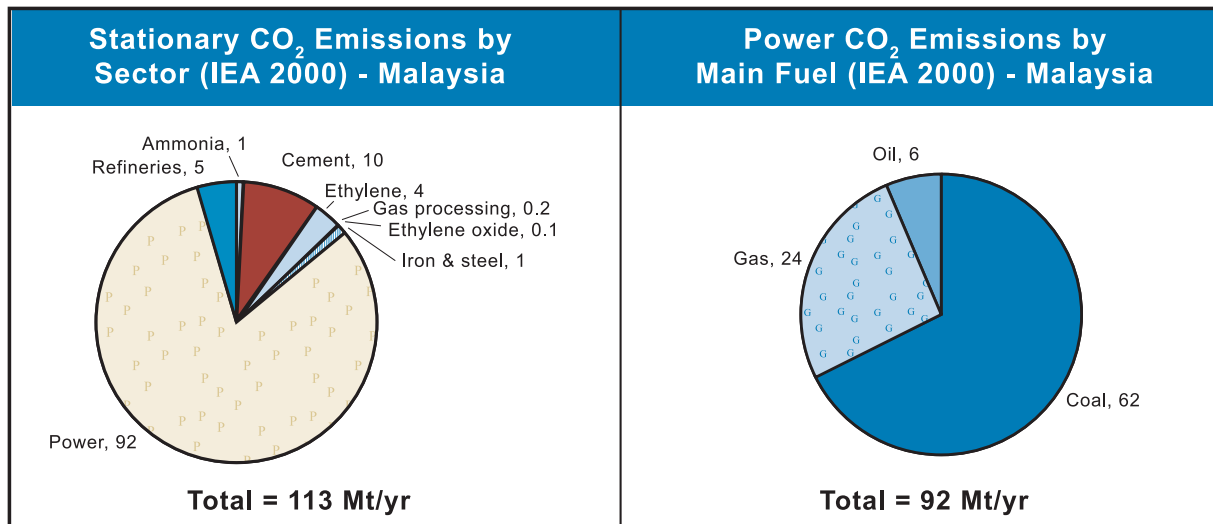


Figure 41. Malaysia stationary CO<sub>2</sub> emissions.

## 6.2 Geological Storage Summary

The Malay Basin (Figure 42) contains compressional structures resulting from Miocene structural inversion. Anticlinal structures would have high confidence for storage, whether they are depleted hydrocarbon fields or saline reservoirs.

The high geothermal gradients 35°C/km to 55°C/km will reduce the CO<sub>2</sub> sub surface storage density.

Data compiled by the USGS (2000) suggests there are good porosities and permeability in the Malay Basin, indicating good quality reservoirs in the Malay basin. The major Miocene transgression formed a claystone dominated sequence, which is a possibly a regional seal in the basin.

There is a large known hydrocarbon pore space. It is apparent that reserves are far from depleted and the access to depleted gas fields may not occur for some time.

Being an offshore basin may be a disadvantage from an economic viewpoint.

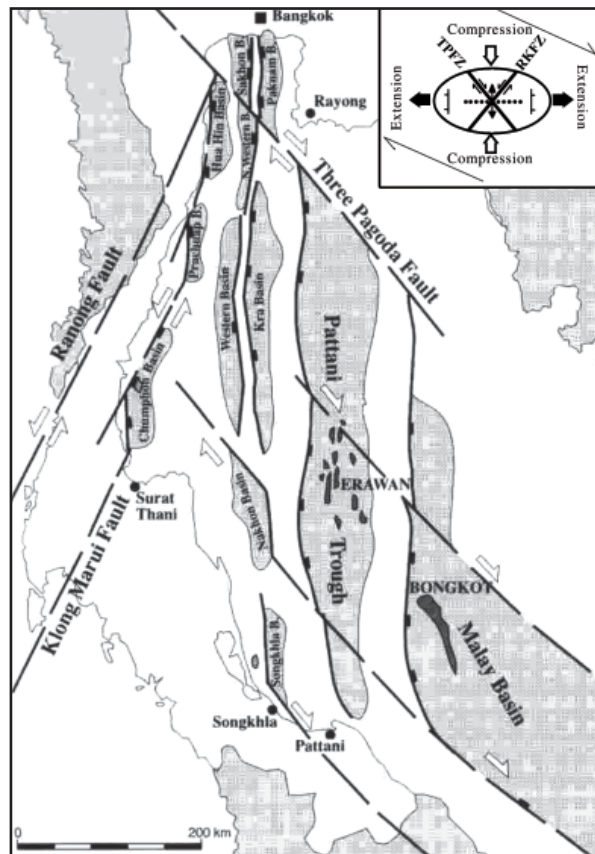


Figure 42. Simplified structural map of the Gulf of Thailand and Malay basins (from Leo, 1997).

# 7. Philippines

## 7.1 Source Characterisation

- ◆ The Philippines have total stationary emissions of 44.8 Mt/yr.
- ◆ The majority of emissions; 30 Mt/yr (67%) are the result of power generation.
- ◆ Most power generation is fuelled by coal (~65%) followed by oil (~ 35%).
- ◆ Geographically most of the emissions; 24 Mt/yr (75%) are produced by power generation near to Manila on Luzon Island. Manila lies in the Luzon Central Valley fore-arc basin



**Figure 43. Philippines stationary CO<sub>2</sub> emissions and study basins.**

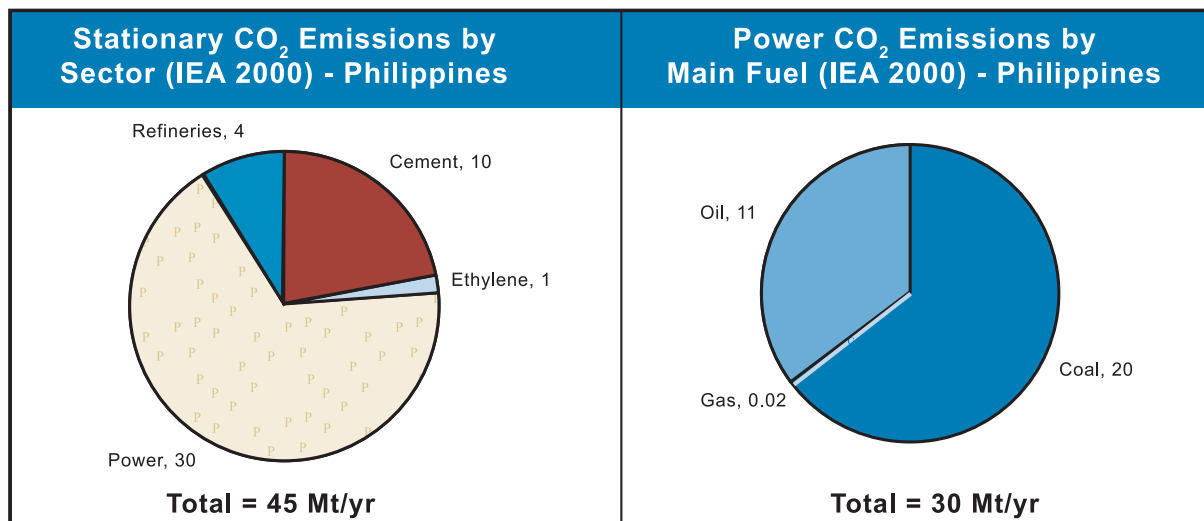


Figure 44. Philippines stationary CO<sub>2</sub> emissions.

## 7. 2 Geological Storage Summary

The Luzon Basin is a fore-arc basin located on the western margin of Luzon Island, the northern-most island in the Philippines archipelago. The basin covers an area of 20,000 km<sup>2</sup>. The basin forms a north-south structural terrace on the landward side of the West Luzon Trench. It contains about 14 km of Cenozoic sediments and the geothermal gradient is 16-24°C/km (Hutchison, 1987). The basins of the Philippines archipelago have a range of geothermal gradients: Visayan (31°C/km), Ragay-Samar (41°C/km ) (Hutchison, 1987).

The Philippines has proven oil reserves of 178 mmbbls and 3.7 Tcf of gas, which occur mainly in the Palawan Basin, offshore NW Borneo Oil and Gas Journal, 2001). This equates to an estimated 319 Mt of CO<sub>2</sub> storage potential. This is less than ten times the annual emissions of 44.8 Mt/yr. This does not represent a large storage opportunity.

Recoverable coal reserves in the Philippines are estimated at 322 Mt and these coal reserves are generally of low to medium rank. In 2002, coal production was limited to 1.7 Mt (EIA US DOE website). Coal related storage is not considered to be a high potential solution for storage as coal deposits are remote from major emission centres.

The Philippines tectonic location near a subduction boundary indicates it is in a complex geologic province. The Luzon Basin underlies Manila and is near other major CO<sub>2</sub> sources. Poor reservoir quality is expected through most of the basin stratigraphy. The shelfal sandstones deposited from the Middle Miocene to Pliocene and the non-marine deposition from the Pliocene present possibilities for better quality clastic reservoirs. The low geothermal gradient is a positive factor and folding on the eastern flank of the basin may create structurally closed areas for storage.

# 8. Chinese Taipei

## 8.1 Source Characterisation

- ◆ Chinese Taipei produces around 253 Mt/yr of CO<sub>2</sub>, which is estimated to increase to 366 Mt/yr by the year 2010.
- ◆ The largest source of emissions is in the city of Tai-Chung which produced an estimated 48 Mt/yr.
- ◆ The largest source of emissions is the power sector, which is responsible for approximately 80% of CO<sub>2</sub> emissions.
- ◆ There are six pure CO<sub>2</sub> sources and all are located in western Chinese Taipei.



Figure 45. Chinese Taipei stationary CO<sub>2</sub> emissions and study basins.

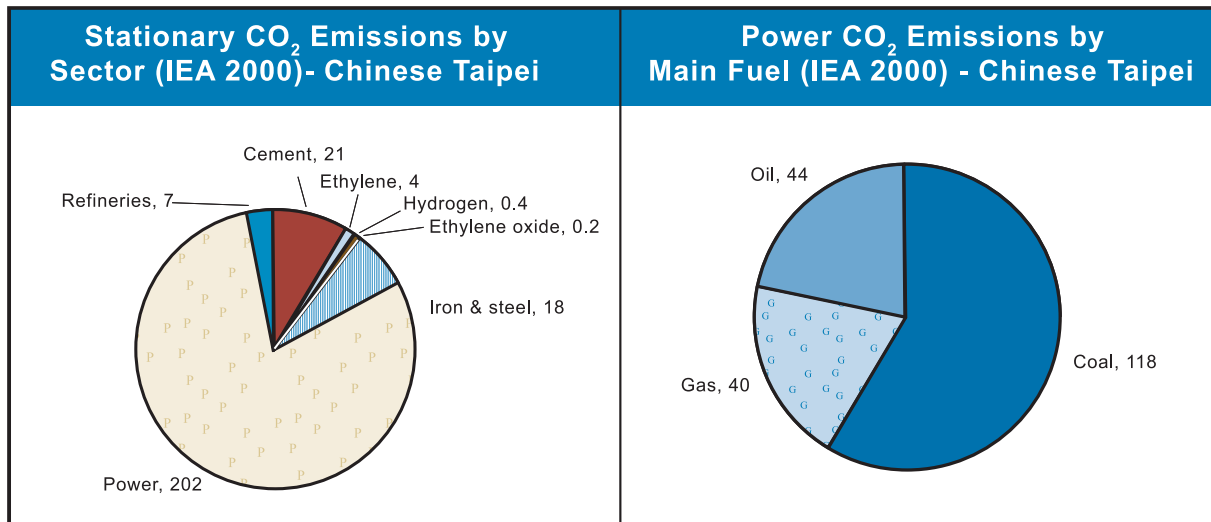


Figure 46. Chinese Taipei stationary CO<sub>2</sub> emissions.

## 8.2 Geological Storage Summary

Three Cenozoic sub basins lie to the west and south-west of Chinese Taipei. These are the Penghu, Taihsi and Tainan basins (Figure 47). The Taihsi and Tainan basins partly underlie Chinese Taipei. The Taihsi and Tainan have both a rift and foreland basin phases. The Tainan Basin appears to have reservoir-seal pairings in the rift and foreland phases. The Pengu Basin appears to be quite sand prone and lacking in seal formations.

Due to Chinese Taipei's minor hydrocarbon reserves the depleted hydrocarbon field storage option has little practical application.

The island of Chinese Taipei is located in a major tectonic collision zone. The island consists of an accretionary wedge formed by a subduction associated transfer zone. The foreland basin began to develop during the Pliocene.

Chinese Taipei ceased coal production in 2000. Deep uneconomic coal seams may be present. Whether they could be economically used for methane production and/or CO<sub>2</sub> storage is a matter for site specific evaluation.

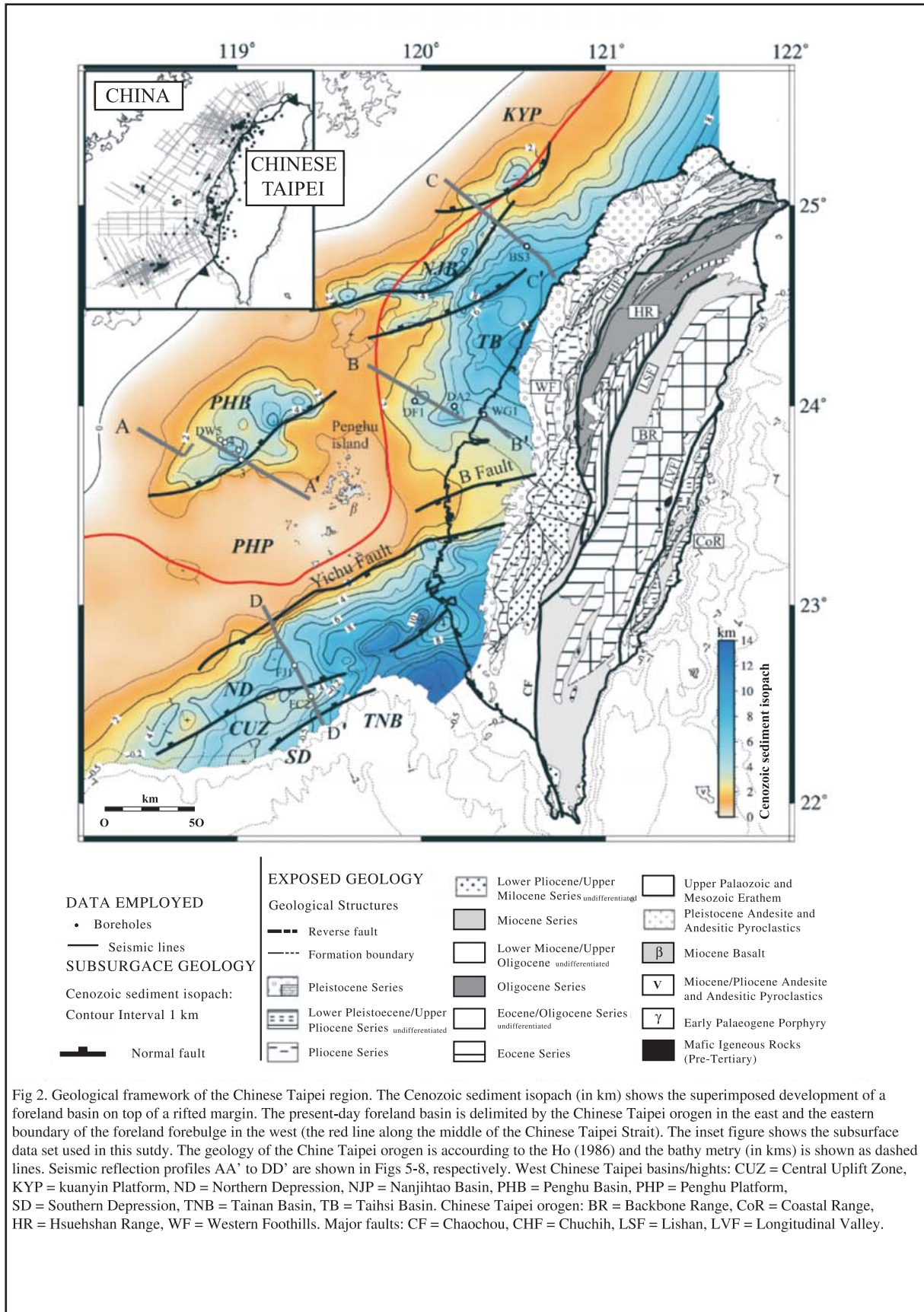


Figure 47. Basins in the Chinese Taipei region (from Lin et al., 2003).

# 9. Thailand

## 9.1 Source Characterisation

- ◆ According to IEA figures (2000) Thailand produces 120 Mt of CO<sub>2</sub> per year. Around 54 Mt/yr is produced at the head of the Gulf of Thailand in the region of Bangkok.
- ◆ 60% of Thailand's electricity production is fuelled by gas, 24% by coal and 16% by oil.
- ◆ 43% of Thailand's power generation emissions result from burning gas. An equal amount of CO<sub>2</sub> results (43%) from burning coal, however coal-fired power stations generate less than half the electricity.
- ◆ Coal fired facilities generate power for localities remote from Bangkok.
- ◆ Cement production is an unusually high proportion of emissions at 34.8 Mt/yr (29% of total stationary emissions). This may be a statistical/reporting artefact. Taking the data on face value, the cement industry presents a major opportunity for CO<sub>2</sub> reduction.
- ◆ Thailand's energy resources are dominated by gas and coal. Thailand's gas resources are an advantage to minimising growth in emissions as power generation increases.

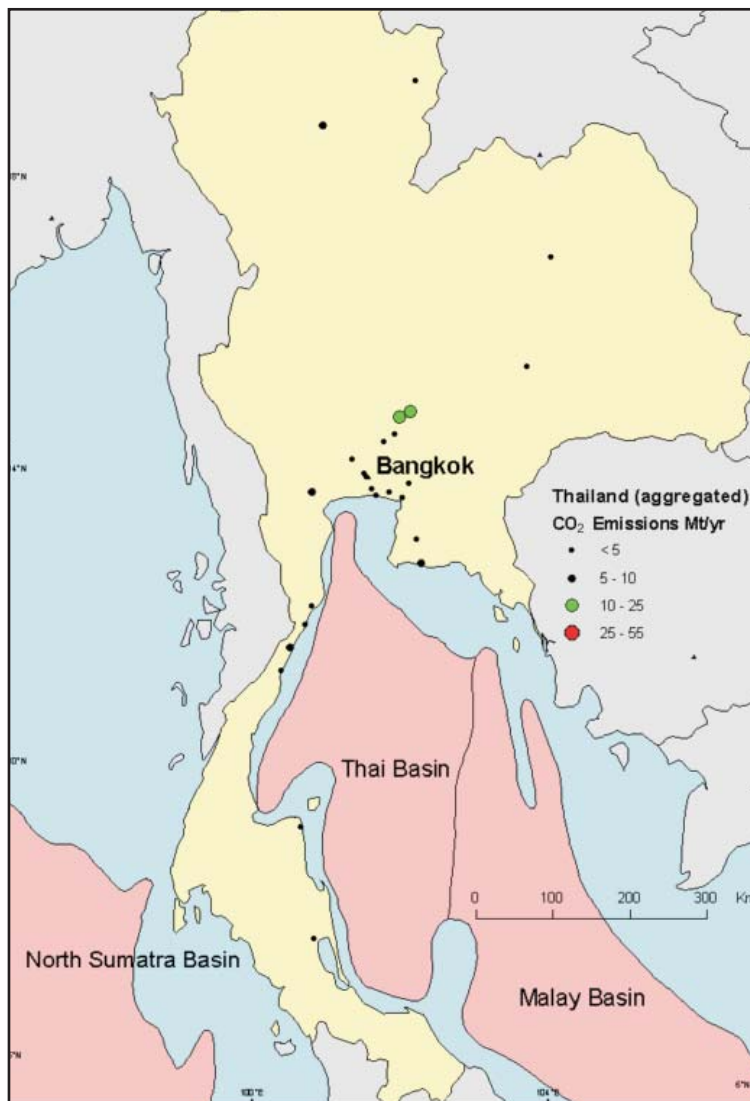


Figure 48. Thailand stationary CO<sub>2</sub> emissions and study basins.

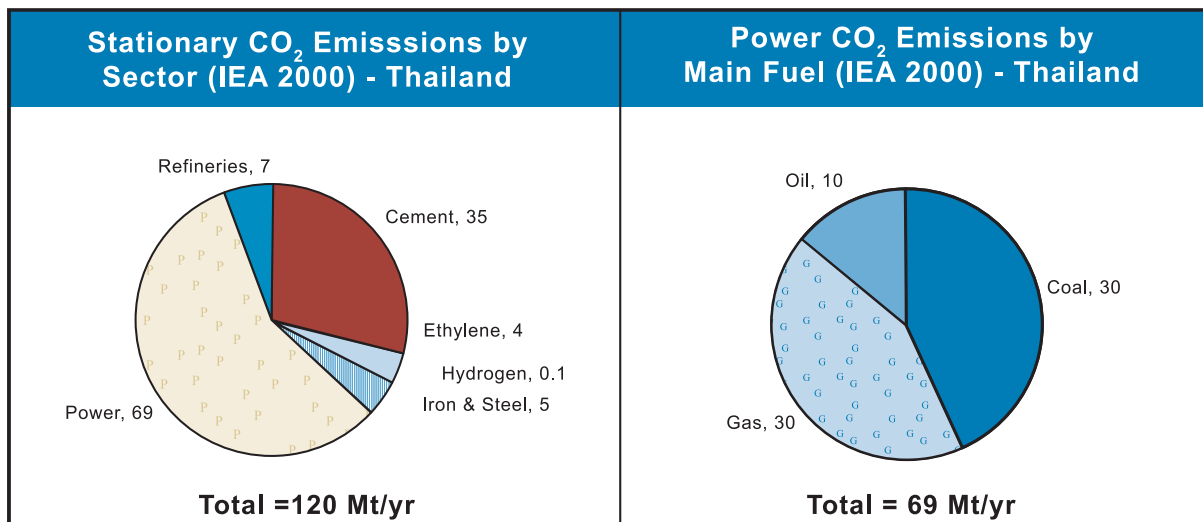


Figure 49. Thailand stationary CO<sub>2</sub> emissions.

## 9.2 Geological Storage Summary

Thailand has access to one sedimentary basin of note, the Thai Basin (Figure 50). The offshore Gulf of Thailand Basin contains gas reserves within poorly interconnected fluvial sands. Gas is extracted from this area using statistical well positioning to insect as many reservoirs as possible. The discontinuity of these sands is a large disadvantage.

To access better connected sandstones in the search for CO<sub>2</sub> storage sites, exploration should be focused up depositional dip north west of the gas producing area.

Minor coal deposits are currently mined in the northern part of Thailand, distant from Bangkok. Lignite to sub-bituminous coal is used for local power generation at Mae Moh in the north, and for cement production. ECBM as a CO<sub>2</sub> storage option appears to have little application.

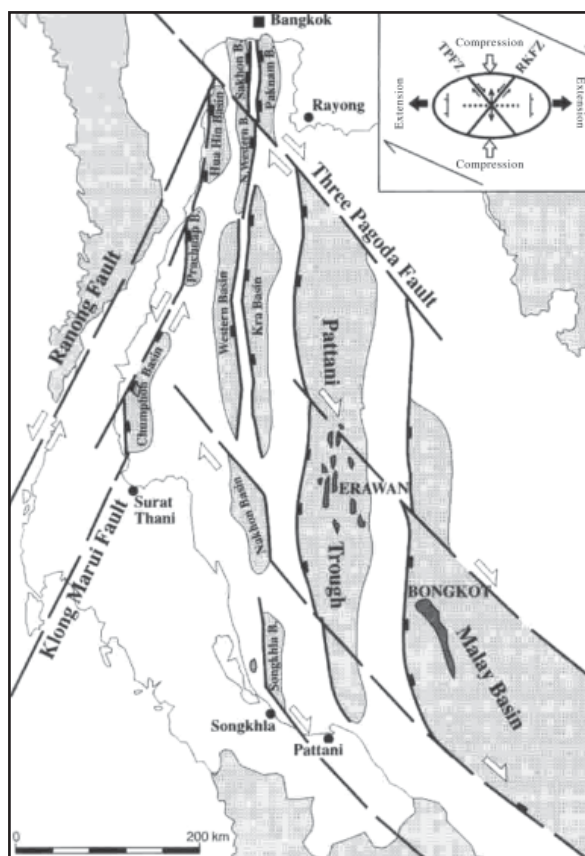


Figure 50. Simplified structural map of the Gulf of Thailand and Malay basins (from Leo, 1997).



# 10. References

- Bachu, S. Geological Sequestration of Anthropogenic Carbon Dioxide: Applicability and Current Issues. In: Gerhard, L.C., Harrison, W. E. and Hanson, B. M. (eds.), *Geological Perspectives of Global Climate Change*, 285-303. 2001.
- Bachu, S. Screening and ranking of sedimentary basins for sequestration of CO<sub>2</sub> in geological media in response to climate change. *Environmental Geology (Berlin)* 44, 277-289. 2003.
- Baines, S.J. and Worden R.H. The long term fate of CO<sub>2</sub> in the subsurface; natural analogues for CO<sub>2</sub> storage. In: Baines, S.J. and Worden, R.H. (eds.), *Geological Storage of Carbon Dioxide*, Geological Society Special Publications, Geological Society of London, 233, 59-85. 2004.
- British Petroleum Limited. Statistical Review of World Energy Worksheet 2004. <http://www.bp.com/subsection.do?categoryId=95&contentId=2006480>. 2004.
- Doughty, C., Pruess, K., Benson, K., Hovorka, S.D., Knox, P.R., and Green, C. Capacity investigation of brine bearing sands on the Frio Formation for geological sequestration of CO<sub>2</sub>. In: *First National Conference on Carbon Sequestration*, May 14-17, Washington DC, United States Department of Energy National Energy Technology Laboratory. 2001.
- EIA Country Analysis Briefs Website: China. U. S. Department of Energy, Energy Information Administration, Washington, DC. 2002 <http://www.eia.doe.gov/emeu/cabs/china.html>.
- Gale, J. and Freund, P. Coal bed methane enhancement with CO<sub>2</sub> sequestration worldwide potential. *Environmental Geoscience* 8[3], 210-217. 2001.
- Gunter, W.D., Bachu, S., and Benson, S. The role of hydrogeological and geochemical trapping in sedimentary basins for secure geological storage of carbon dioxide. In: Baines, S.J. & Worden, R.H. (eds.), *Geological Storage of Carbon Dioxide*, Geological Society Special Publications, Geological Society of London 233, 129-145. 2004.
- Holloway, S., Heederik, J.P., Van Der Meer, L.G.H., Czernichowski-Lauriol, I., Harrison, R., Lindeberg, E., Summerfield, I.R., Rochelle, C., Schwarzkopf, T., Kaarstad, O., and Berger, B. The underground disposal of carbon dioxide. Joule II Project number CT92-0031, Final report. British Geological Survey, Nottingham, UK. 1996.
- Hovorka, S.D., Doughty, C., Benson, S.M., Pruess, K., and Knox, P.R. The impact of geological heterogeneity on CO<sub>2</sub> storage in brine formations: A case study from the Texas Gulf Coast. In: Baines, S.J. & Worden, R.H. (eds.), *Geological Storage of Carbon Dioxide*, Geological Society Special Publications, Geological Society of London 233, 147-163. 2004.
- IEA GHG (International Energy Agency Greenhouse Gas R & D programme). *Greenhouse Gas Emissions from Major Industrial Sources*. 2000.
- Korsch, R.J., Mai, H., Sun, Z., and Gorter, J.D. Evolution and subsidence history the Sichuan Basin, Southwest China. Lui, Baojun & Li, Sitan (eds) In: *Proceedings of the 30th International Geological Congress; Basin Analysis, Global Sedimentary Geology and Sedimentology*. Vol. 8, 208-221. 1997.
- Lee, K.Y. and Masters, C.D. Geologic framework, petroleum potential and field locations of the sedimentary basins in China. *Miscellaneous Investigations Series - U. S. Geological Survey I-1952*, 2 sheets. 1988.
- Liu G. Permo-Carboniferous paleogeography and coal accumulation and their tectonic control in the North and

South China Plates: *International Journal of Coal Geology*, 16, 73-117. 1990.

Liu, H., Liu, H. and Wang, H. China has good CBM prospects but few commercial projects. *Oil and Gas Journal*, Dec. 13. 2004.

Podwysocki, S.M. and Lovern, V.S. Coal-bearing regions and structural sedimentary basins of China and adjacent seas. Open-File Report - U. S. Geological Survey OF 00-0047, 1 disc. 2000.

Rigg, A.J., Allinson, J., Bradshaw, J., Ennis-King, J., Gibson-Poole, C.M., Hillis, R.R., Lang, S.C., and Streit, J.E. The search for sites for geological sequestration of CO<sub>2</sub> in Australia: A progress report on GEODISC. *Australian Petroleum Production and Exploration Association Journal*, 711-725. 2001.

Su, X., Lin, X., Zhao, M., Song, Y and Liu, S. The upper Paleozoic coal bed methane system in the Qinshui basin, China. *AAPG Bulletin* 89[1] 81-100. 2005.

Sun M. and Huang S. Important aspects of coal bed methane development in China: p. 6-9 In *China Coal bed Methane* No. 1, May 1995, *China Coal bed Methane Clearinghouse*, 54 p. 1995.

United States Environmental Protection Agency, 1996. Reducing Methane Emissions From Coal Mines in China: The Potential for Coal bed Methane Development. EPA 430-R-96-005, July, 1996.

USGS World Energy Assessment Team. World Petroleum Assessment 2000. United States Department of the Interior, U.S.Geological Survey, Digital data series DDS-60[4 discs]. 2000.

Williams, H.H. and Eubank, R.T. Hydrocarbon habitat in the rift graben of the Central Sumatra Basin, Indonesia. In: Lambiase, J J (eds.), *Hydrocarbon habitat in rift basins*, Geological Society Special Publications, Geological Society of London 80, 331-371. 1995.

(Note: Appendix A contains more detailed information with further references on individual basins)

# Appendices



# Appendix A: Additional Basin Discussion

## A1. China

### A1.1 Bohai (North China) Basin

#### A1.1.1 CO<sub>2</sub> Sources

CO<sub>2</sub> emissions in the region directly overlying the Bohai Basin contributed approximately 248 Mt CO<sub>2</sub> /yr to China's estimated total stationary source CO<sub>2</sub> emissions of 2970 Mt/yr (IEA, 2000).

The Bohai Basin lies in the most industrialised area of China. In a 300 km radius from the basin there are combined emission sources of approximately 882 Mt CO<sub>2</sub>/yr.

Note: The total of sources within 300 km of a basin is a very crude indication of the magnitude of emissions which may be within reach of the basin. These “catchments” overlap for many basins and should not be summed.

#### A1.1.2 Basin Overview

The Bohai Basin is a 200,000 km<sup>2</sup> northeast-trending, Cenozoic back arc rift basin (Figure A1) made up of the Bozhong, Huanghua, Liaohe, Linqing/Dongpu, Jiyang and Jizhong depressions (Figure A2, Figure A3) each of which contains numerous “sags” or half grabens. The basin has 4 to 7 km of fill. The main environment of deposition is fluvial-lacustrine. There are 3 to 4 sequences of lacustrine deposition between the Early Eocene and Late Pliocene (Figure A4).

Structures containing hydrocarbons include tilted fault blocks (buried hill), anticlines and fault/stratigraphic traps. The Tan-Lu fault and other features are evidence of dextral trans-tension strike slip motion. Major structures such as the offshore 19-3 field are wrench anticlines. At least four reservoir-seal pairs provide opportunities for depleted hydrocarbon and/or saline reservoir storage.

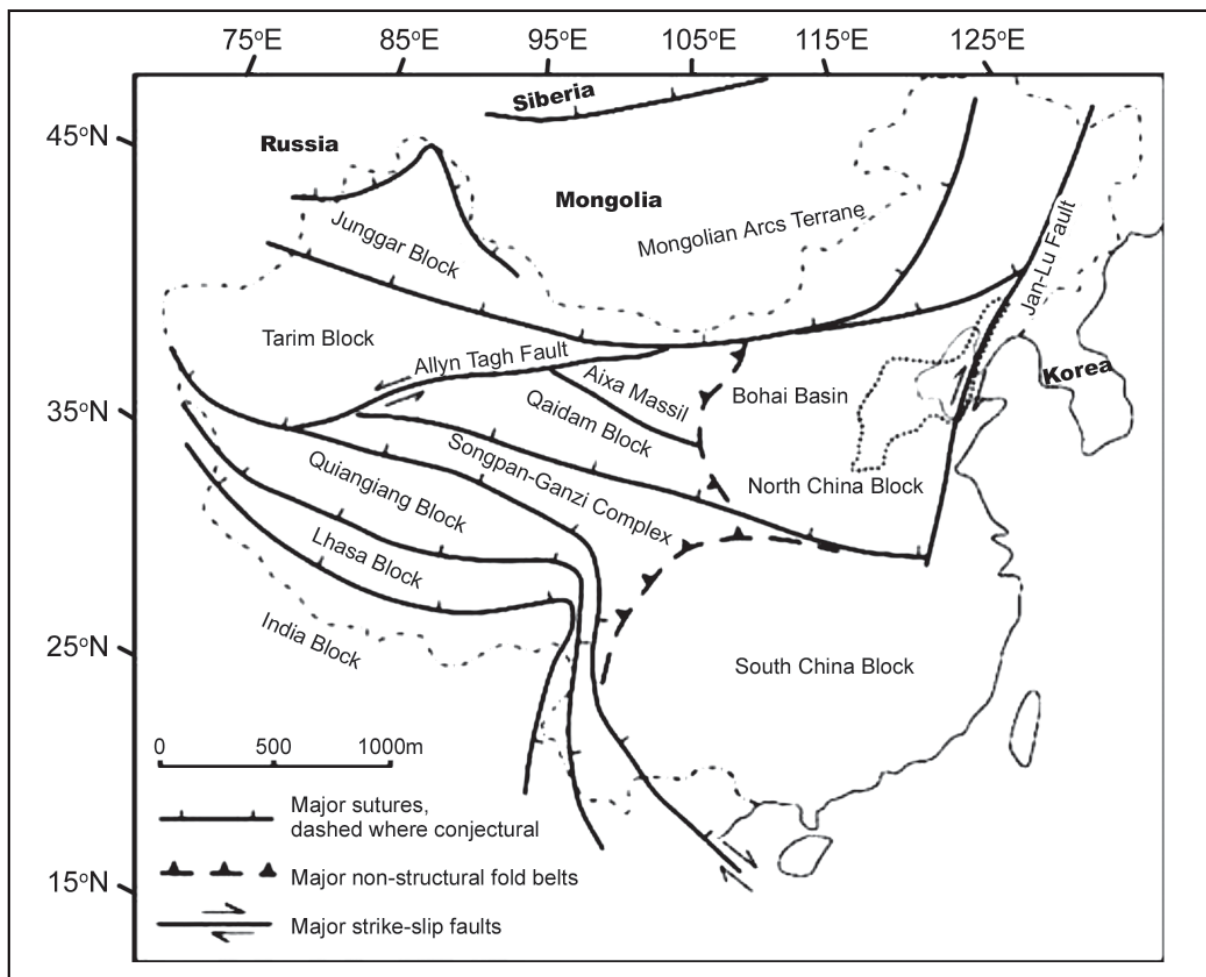


Figure A1. Bohai Basin location and structure map of China.

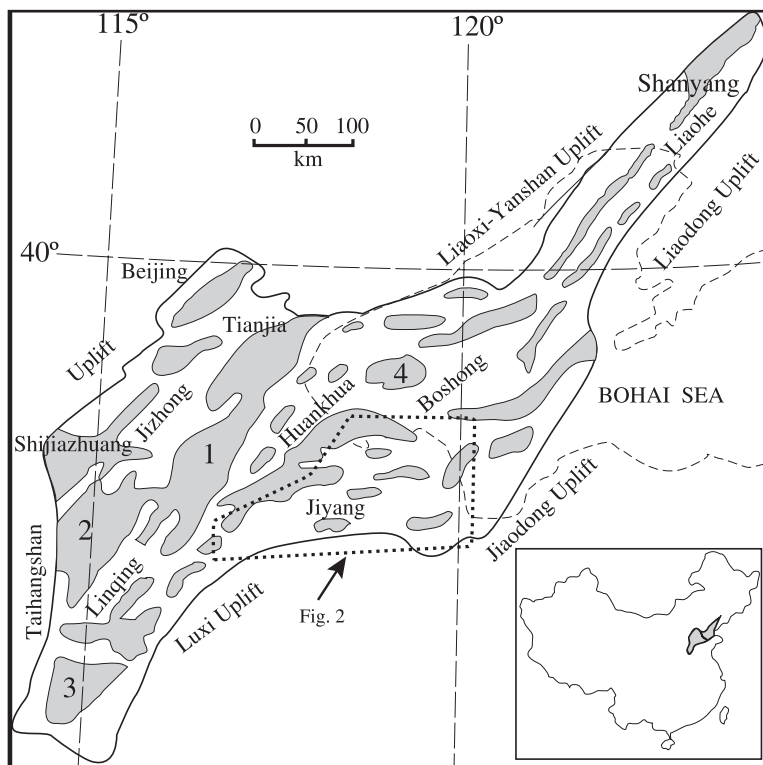


Figure A2. Regional structure setting of the Bohai Basin. Uplifts (shaded areas): 1= Cangdong, 2= Xingheng, 3+ Neihuang, 4= Shaletitian (Haizhong), 5= Chenging. The sub-basins are labelled, the Jiyang Sub-basin is in the SE of the Bohai Basin (from Yang and Xu, 2004).

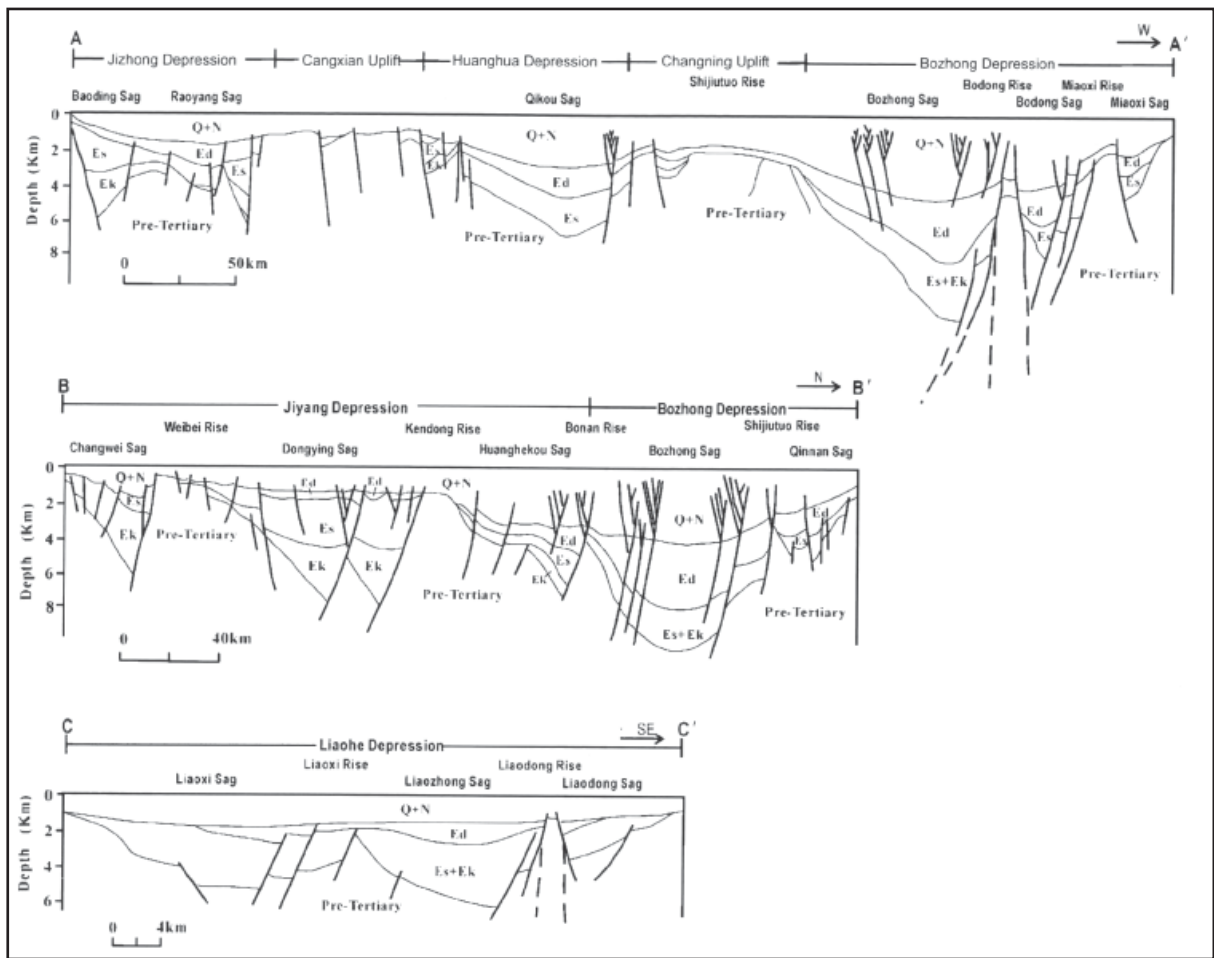


Figure A3. Bohai Basin cross-sections (Yang and Xu, 2004).

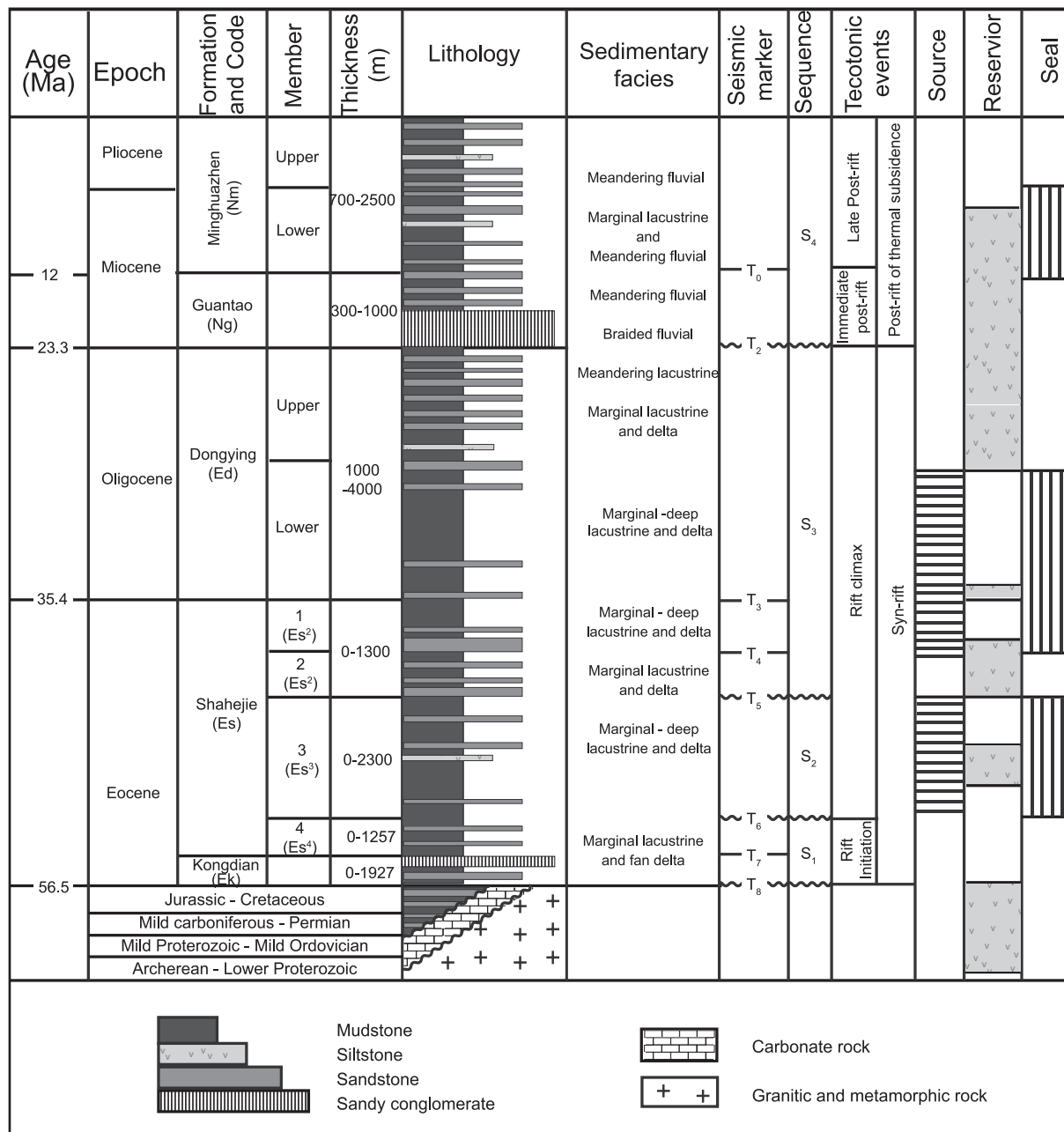


Figure A4. Bohai Basin stratigraphy (From Yang and Xu, 2004, after others.).

### A1.1.3 Basin Fill

There are four Deep Saline Reservoirs or reservoir-seal pairs known from petroleum exploration in the offshore Bohai Basin. (Yang and Xu, 2004). Most of these are also found onshore.

Maximum palaeo-water depth appears to occur in the Lower Oligocene when the basin becomes unified, with its primary depocentre in the Bozhong depression (offshore present day). Following the deep lacustrine/delta environment of the Lower Eocene, net accommodation space decreased and lacustrine facies gave way to meandering fluvial facies in the Upper Eocene. The Miocene Himalayan event is apparent as an unconformity which triggered the braided stream deposition of the next fluvial-lacustrine systems tract cycle. Accommodation space for this cycle was created by thermal subsidence phase of the basin. The Bozhong depression became open marine in the Pleistocene.

## Pre Tertiary

The best pre Tertiary reservoir rocks are shallow marine dolomite and limestone beds of Proterozoic, Cambrian, and Ordovician age that have been exposed to long periods of karstification processes. Solution-enlarged fractures, vugs and cavities are common features in the better reservoirs (USGS, 2000). The giant Renqui oil field has reservoirs of this type. Permeability is enhanced for oil production by acid treatment (Horn, 1990).

These reservoirs are in part the “buried hill” oil play in which seal and source is provided by unconformably overlying Eocene or Oligocene Lacustrine mudstones (e.g. Shahejie Member 3). This reservoir-seal pair appears to have a wide extent. An understanding of the distribution of enhanced porosity in the pre Tertiary will be important to the selection of possible injection sites. Several giant fields with long production histories are formed by this geology. Opportunities may exist for EOR, especially as the reservoirs are carbonates and/or full scale CO<sub>2</sub> storage.

## Eocene

The Kongdian to Shahejie 3 reservoirs are deltaic and lacustrine mass flow sandstones deposited in a deep lake setting. These formations have “relatively poor” reservoir characteristics due to the depth to which these sequences have been buried (Yang and Xu, 2004). Well BZ 25-1 intersected turbidites with porosities from 1 to 18% and permeability from 0.98 to 88.3 mD (Wang and Zhao, 1990). These facies are restricted to the fringes of uplifts or down thrown faults. The palaeogeography maps of Yang and Xu (2004) (Figure A5) reflect this restricted distribution. The mass flow sands may represent a closed pressure system. Injection of CO<sub>2</sub> could be limited by the entry pressure of the lacustrine mudstone seal rocks and failure strength of the reservoir rocks. Considering the previous factors listed above this seems to be a limited CO<sub>2</sub> storage option.

## Oligocene

A period of apparent maximum accommodation space in the lower Eocene resulted in deposition of lacustrine mudstones of the Dongying Formation which provide a seal for the delta and marginal lacustrine sandstones of the Shahejie 2 Member. The Lower Dongying also provides seal to the pre-Tertiary reservoirs.

The upper Dongying has good quality sandstone in the SZ 36-1 oil field with porosity of 28 to 35% and permeability 100 to 10,000 mD with an average of 2000 mD in an interval from 1286 to 1537 m (Liu and Chen, 1992). The Dongying Formation has intra-formational mudstone seals around 400 m thick. (Liu and Chen, 1992). This interval appears to offer a number of reservoir-seal pairs resulting from higher order deltaic/lacustrine cycles. Palaeogeography maps by Yang and Xu (2004) suggest a quite heterogeneous section (Figure A5). However if there are very substantial “intra-formational” mudstones at the top of the Dongying Formation it seems possible that there are options for CO<sub>2</sub> storage.

## Pliocene-Miocene

In the offshore area (Bozhong Depression) the Minghuazhen and Guantao formations are hydrocarbon reservoirs. Across the onshore and offshore areas the Lower Guantao Formation was deposited in a braided river environment. It appears that the lower Guantao is a homogeneous and extensive good quality reservoir with 60% to 90% net sandstone, average porosity of 21% and average permeability of 253 mD (Yang and Xu, 2004). The upper Guantao was deposited in a meandering river environment. Zhang et al., (2004) draw attention to the high reservoir connectivity of the lower Guantao versus the lower connectivity of the upper Guantao in the onshore Jiyang depression (Figure A6, Figure A7). In the offshore area the Lower Minghuazhen consists of lacustrine mudstones which seal the Guantao reservoirs. In a paper describing the offshore 19-3 field Kuykendall et al., (2003) state, “The lower portion of the Minghuazhen Formation has sand net-to-gross ratio of 25-30% and contains the regional to sub regional top seal, which consists of intra-formational mudstones”. These seals are flood plain and lacustrine mudstones. Yang and Xu (2004) observed that this seal interval is not present in the Jiyang onshore area “where mudstones are not present due to a braided river depositional system”.

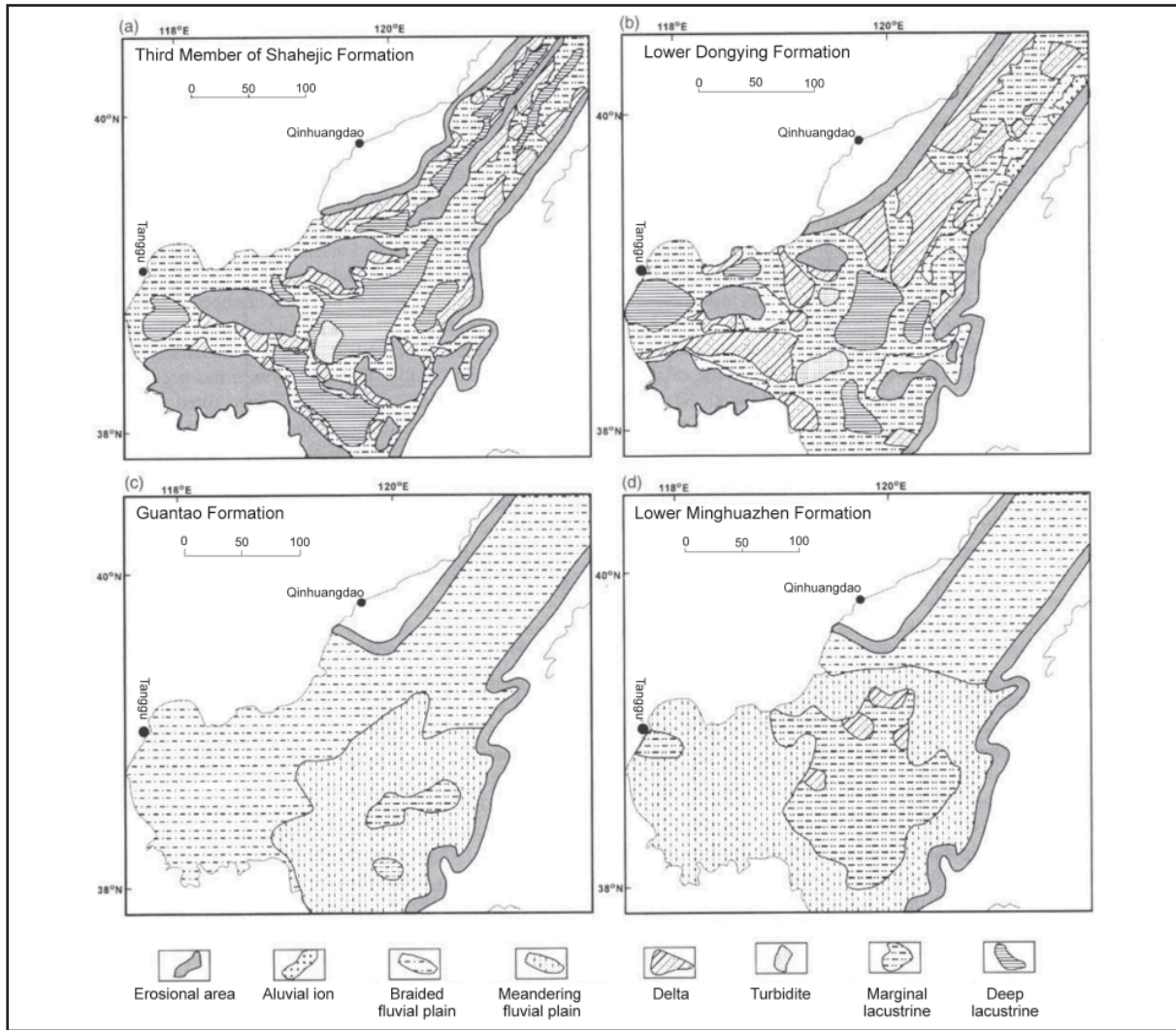


Figure A5. Sedimentary facies maps in the offshore Bohai Basin, (a) Middle Eocene; (b) Early Oligocene; (c) Early Miocene; (d) Late Miocene. (Yang and Xu, 2004)

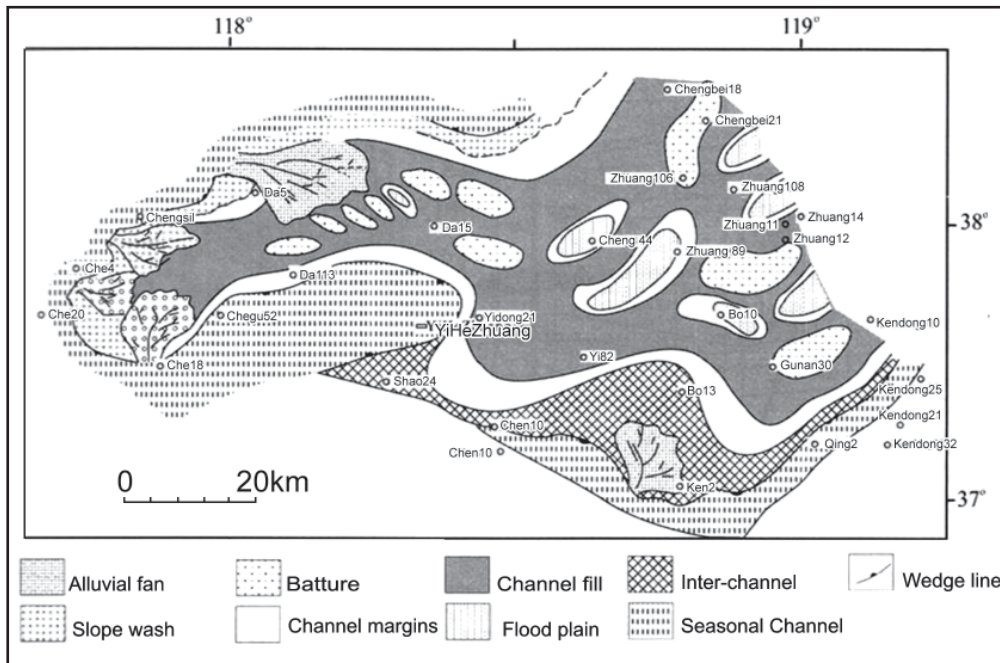
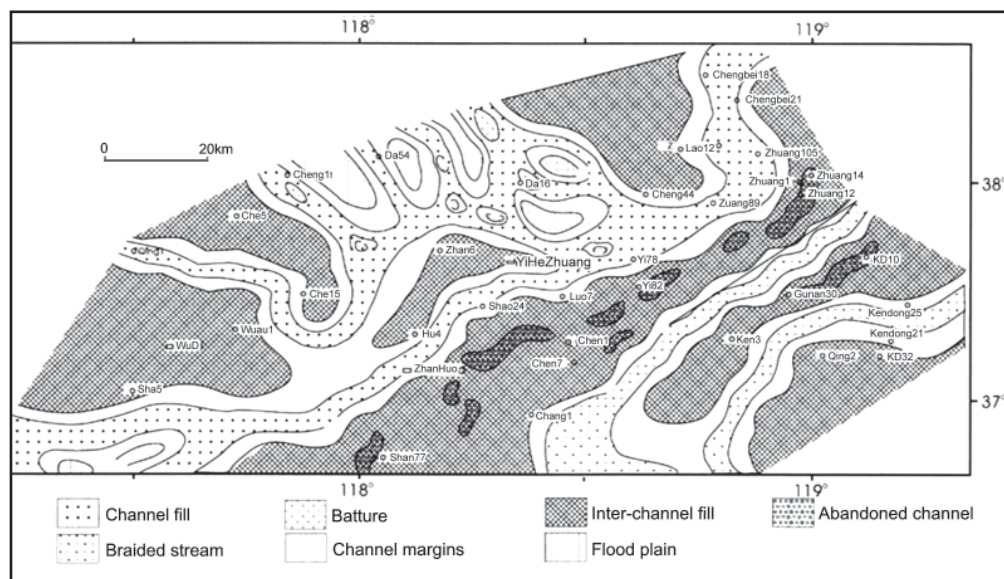


Figure A6. Facies variation for the low stand sediments of the lower Guantao member in the Chezheng-Zhanhua depressions (Zhang et al., 2004)

Hydrocarbon occurrences appear to show that the Minghuazhen Formation is ultimately an effective seal resulting from a low net to gross section in which intra-formational seals are “stacked” to form an effective regional seal. The Guantao Formation is potentially a high injection rate formation due to high permeability and good connectivity.



**Figure A7.** Facies variation for the high stand sediments of the lower Guantao member in the Chezheng-Zhanhua depressions (Zhang et al., 2004)

### Offshore example 19-3 field

This description is included to provide an example of the character of one of the fluvial-lacustrine reservoirs that exist in the Bohai Basin. Quite comprehensive data is available in Kuykendall et al., (2003) on the 19-3 field, offshore Bohai Basin. The Minghuazhen/Guantao reservoirs have an average porosity of 27% and permeability of 750 mD. The net to gross sand in the section is 43%, which is to be expected in a fluvial to lacustrine depositional setting. Sand beds range in thickness from 1-3 m to 15 m (Kuykendall et al., 2003). The reservoir sandstones are classified under the Folk system as, arkose sandstones (feldspathic sandstones). Clay content is 2 to 25% averaging 6%. Mostly the clay is kaolinite but also illite, mixed layer illite-smectite and smectite. There is very minor calcite cement in some sands. Some sands contain appreciable amounts of detrital clay matrix. The primary diagenetic factor is compaction. (Kuykendall et al., 2003). The calcite present may dissolve in weeks or months, enhancing porosity and permeability.

### A1.1.4 Hydrocarbon fields

Hydrocarbon accumulations occur though-out the Bohai Basin, both onshore and offshore. The Bohai Basin has an estimated “known” hydrocarbon endowment (produced plus reserves) of 24.5 billion bbls of oil and 15.6 Tcf of gas (USGS, 2000). This is equivalent to a potential storage for 4.5 Gt of CO<sub>2</sub>.

The five largest discovered fields in the Bohai have a total volume of 12 billion barrels (USGS, 2000). This equates to potential storage for approximately 1.6 Gt of CO<sub>2</sub>. The available data does not indicate to what extent individual fields are depleted. Data on the size distribution of gas fields was not available in the USGS report, however there are 15.6 Tcf of gas known with 3 Tcf produced and 12.6 Tcf in reserves (USGS, 2000). This known gas volume is equivalent to storage potential 1.25 Gt CO<sub>2</sub>.

Liaohoe field is the third largest oil field in China. Results of experiments with EOR using flue gas were reported in 2001. The flue gas consisted of 10-14% CO<sub>2</sub> with ~80% N<sub>2</sub>. In the trials a total of 2500 tonnes of steam and flue gas was injected. The results appear to have been encouraging for oil recovery. It is not clear which oil-bearing formation was targeted. The efficiency of CO<sub>2</sub> storage was not specifically reported. There are plans to investigate further using higher concentrations of CO<sub>2</sub>.

## A1.1.5 Coal Occurrence

Coal occurs in large volumes in the Shanxi province which lies to the west of the Bohai Basin. See section 3.2.3 of the main report for a discussion of Coal and ECBM.

## A1.1.6 Potential CO<sub>2</sub> Storage Options

Hydrocarbon fields have a considerable potential CO<sub>2</sub> storage volume, though the number of currently depleted fields is unknown. It can be assumed some of the early discovery billion barrel sized fields are nearing depletion and could offer early candidates for CO<sub>2</sub> storage projects. The 4.5 Gt of depleted hydrocarbon field storage that may ultimately be available is 15 times the estimated CO<sub>2</sub> emissions for the Bohai Basin region (300 km radius of the basin edge).

The Bohai Basin appears to offer a number of reservoir-seal pairs. The reservoirs generally have good porosity and permeability despite containing up to 25% feldspars (eg Minghuazhen/Guantao Formations of the 19-3 field). Lacustrine mudstones with proven seal properties are present through the succession. The Pre-Tertiary, Oligocene and Eocene reservoir-seal pairs are restricted to the half grabens in the onshore area. The offshore Bozhong depression is a graben of larger extent and may have larger areas of contiguous seal rock. The Pliocene-Miocene is thin in the onshore area and appears to contain better reservoir-seal pairs offshore.

The Guantao Formation stands out as homogenous braided river sandstone with good reservoir qualities and consistent thickness. It is known to be overlain by good sealing formations in several hydrocarbon fields. The formation should be at sufficient depth (> 800 m below sea bed) in the offshore Bozhong depression. Unfortunately this formation and its matching seal formation are best developed in the offshore section of the basin.

## A1.1.7 References

Chang, C. Geological characteristics and distribution patterns of hydrocarbon deposits in the Bohai Bay basin, East China. *Marine and Petroleum Geology* 8[1], 98-106. 1991.

Horn M K. Renqiu Field. In: *Structural traps; II. AAPG Treatise of Petroleum Geology, Atlas of Oil and Gas Fields*, 227-252. 1990.

Kukendall, M.D., O'Reilly, J.B., Patton, B.D., Mott, R.P., Yang-Logan, J., Qian Gui, M., Ying, L., Hua, S., Li Xin, T., and Peng Fei, Z. Petroleum Geology of the Peng Lai 19-3 Field, Bohai Bay, People's Republic of China. In: Halbouty, M. T. (ed), *Giant oil and gas fields of the decade 1990-1999*, AAPG Memoir 78, 321-331. 2004.

Yang, Y. and Xu, T. Hydrocarbon habitat of the offshore Bohai Basin, China. *Marine and Petroleum Geology* 21[6], 691-708. 2004.

Zhang, S., Wang, Y., Shi, D., Xu, H., Pang, X., and Li, M. Fault-fracture mesh petroleum plays in the Jiyang Super depression of the Bohai Bay Basin, eastern China. *Marine and Petroleum Geology* 21[6], 651-668. 2004.

## A1.2 East China Sea Basin

### A1.2.1 CO<sub>2</sub> Sources

CO<sub>2</sub> emissions in the coastal region within 300 km of the East China Sea Basin contributed approximately 314 Mt CO<sub>2</sub>/yr to China's estimated total stationary source CO<sub>2</sub> emissions of 2970 Mt/yr (IEA, 2000). This area includes Shanghai.

Note: The total of sources within 300 km of a basin is a very crude indication of the magnitude of emissions which may be within reach of the basin. These "catchments" overlap for many basins and should not be summed.

### A1.2.2 Basin Overview

The East China Sea lies in the convergence zone between the Eurasian plate, the Pacific plate and the Philippine Sea plate. This zone consists of, from west to east, the Min-Zhe Uplift belt, the East China Sea Shelf Basin, the Diaoyudao Folded Uplift belt, the Okinawa Trough, the Ryukyu Arc and Ryukyu Trench (Figure A8). The Diaoyudao Folded Uplift belt is often referred to as the Diaoyudao Island Uplift or the Chinese Taipei-Sinzi Folded Zone (Yang 2004).

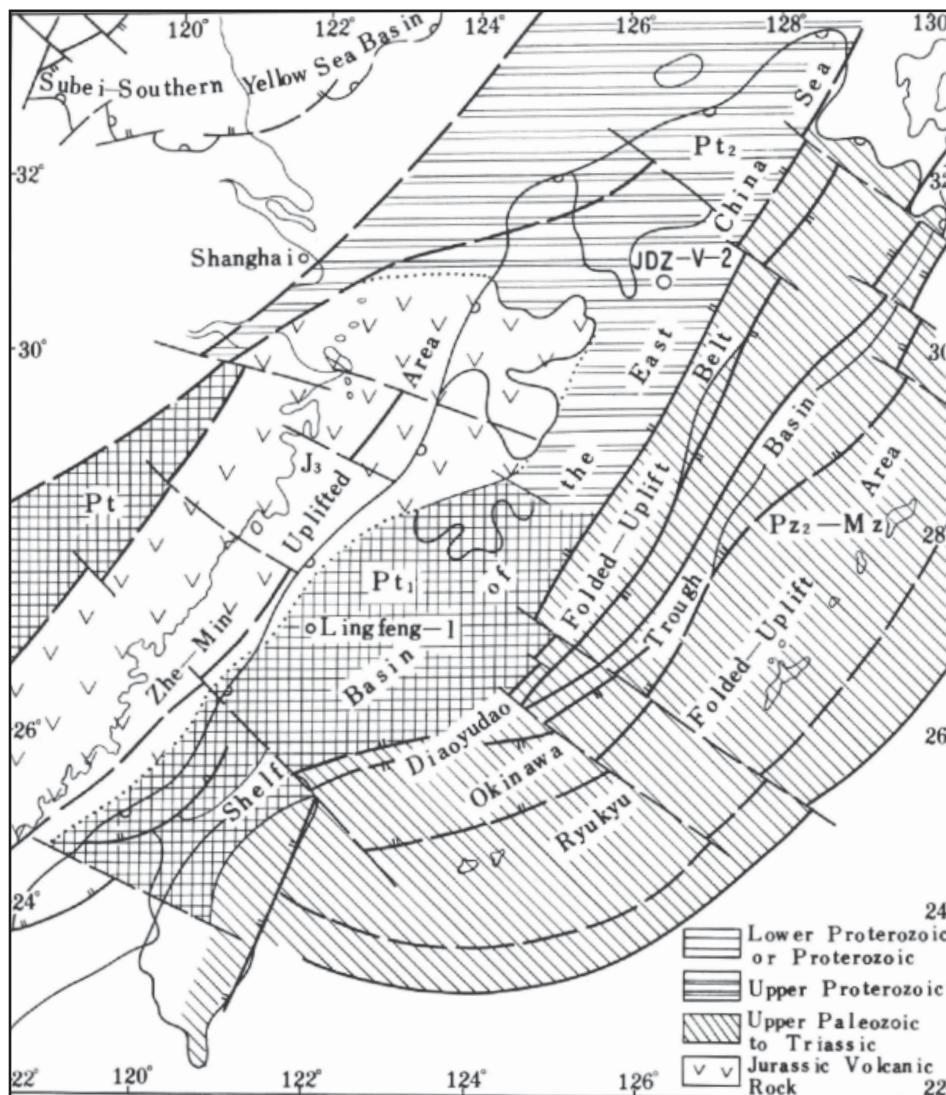


Figure A8. The character of the basement of the East China Sea (from Zhou et al., 1989).

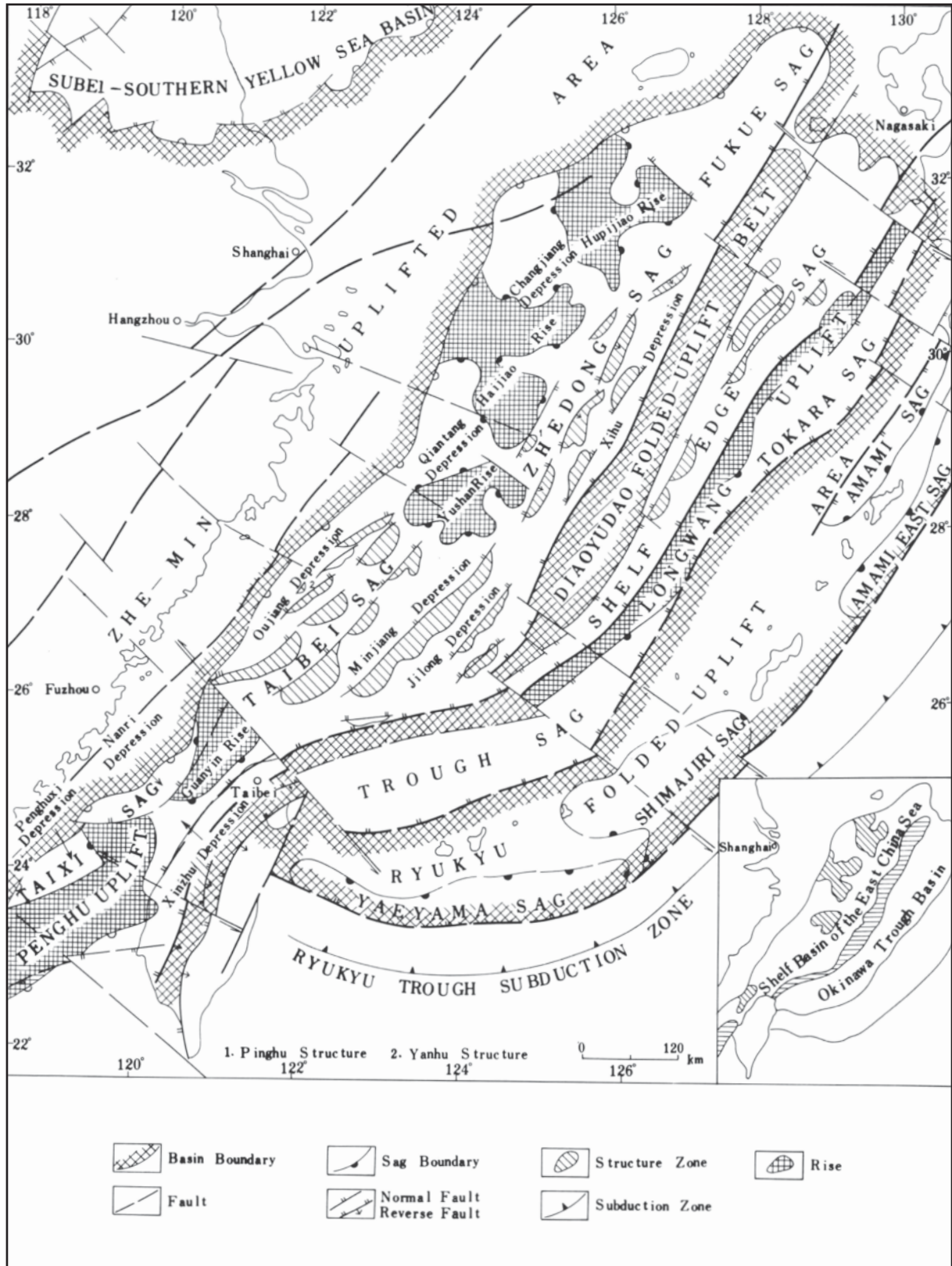


Figure A9. The structural divisions of the East China Sea (from Zhou et al., 1989).

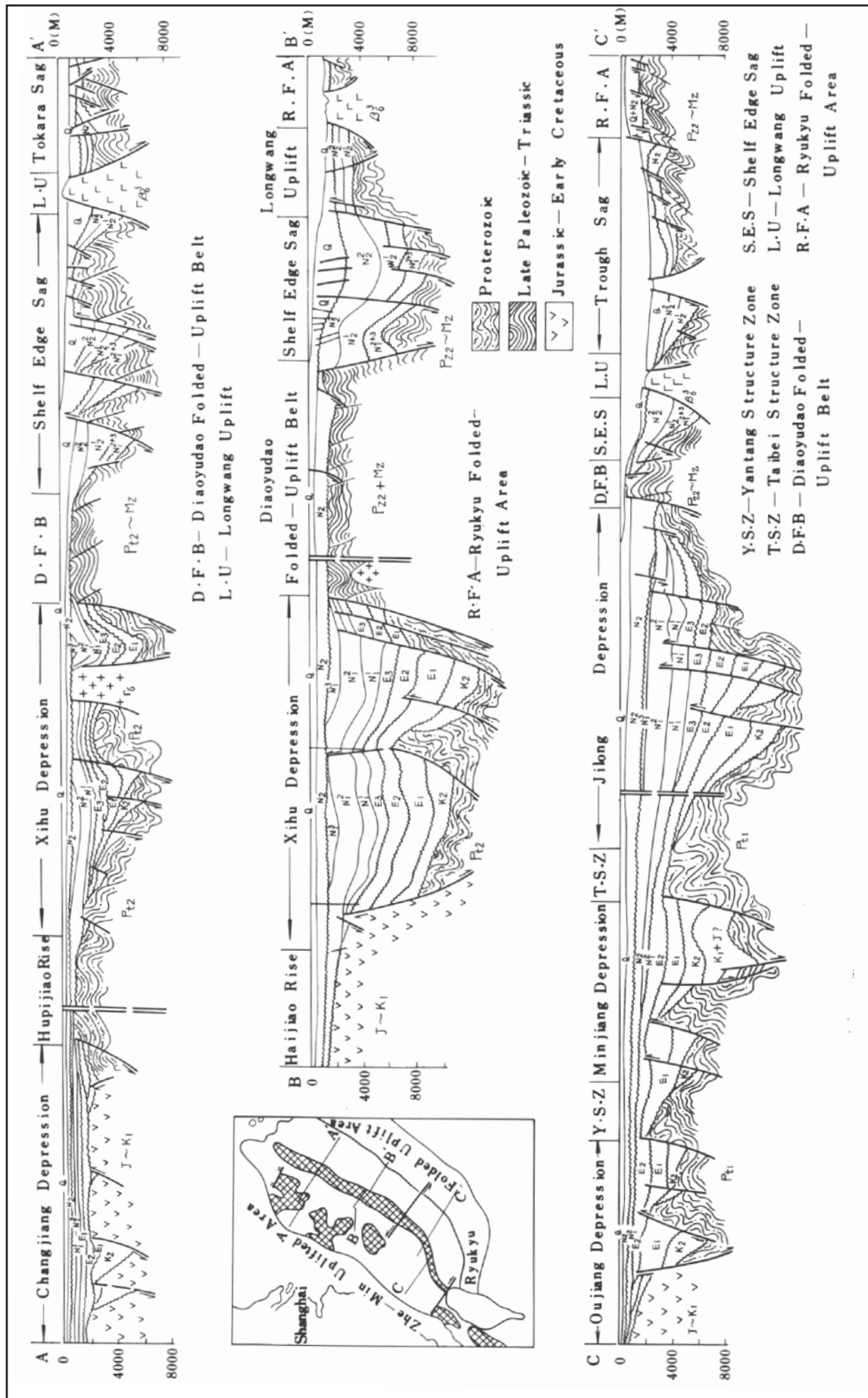
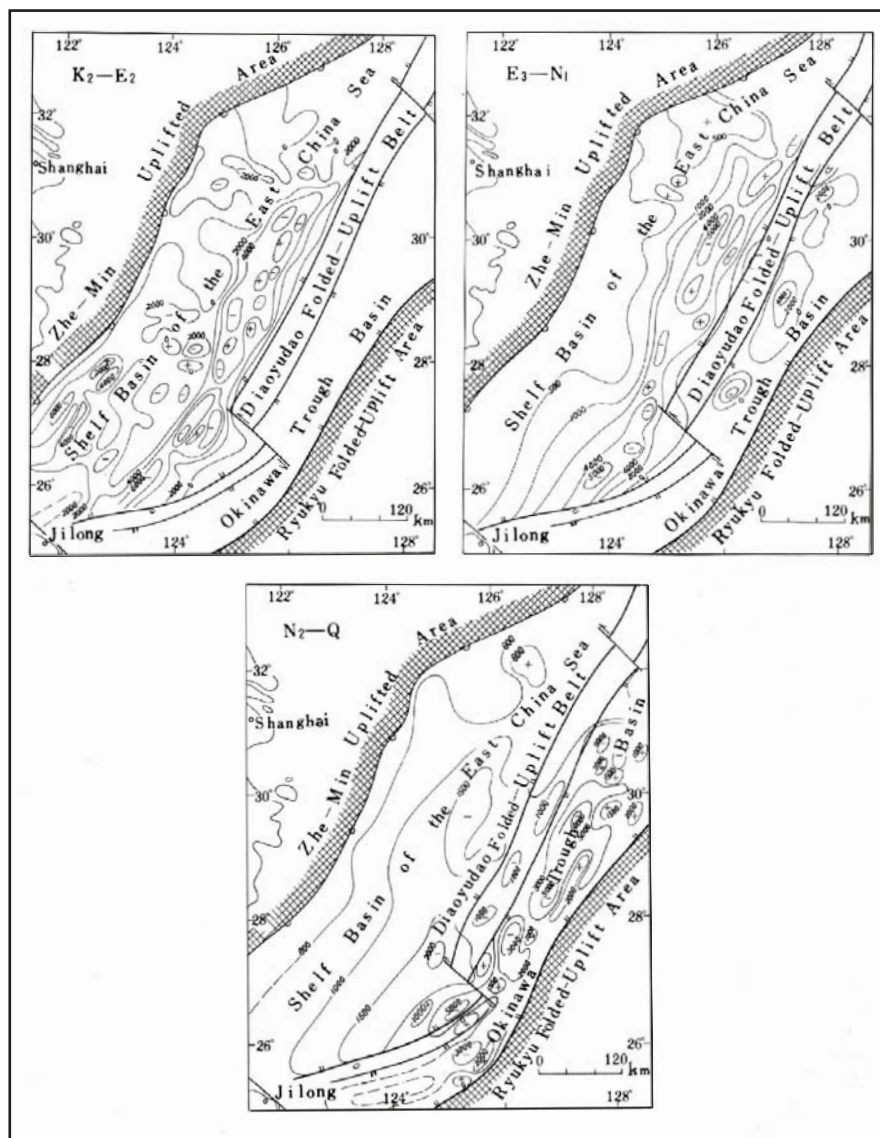


Figure A10. Structural cross-section of the East China Sea (from Zhou et al., 1989)

The East China Sea Basin (ECSB) is essentially two NE trending rift complexes, the East China Sea Basin and the Okinawa Trough. The total area is 770,000 km<sup>2</sup> with water depths from 100 m to 2334 m (Zhou, 1989). The East China Sea Basin (ECSB) began in the Late Cretaceous like other eastern Chinese rift basins, in response to the subduction of the Pacific plate. It is divided by NE striking faults into a number of parallel basins and basement highs. The component nearest to shore (average water depth 100 m) and of most interest to this study is the East China Sea Shelf Basin. The Shelf Basin includes the Taibei and Zhedong sags (Figure A9). The western portion of the northern end of the East China Sea Shelf Basin has 4 km of sediments. Immediately to the east, the Xihu Trough (Figure A9) contains around 10 km of Cretaceous to Quaternary sediments. The central and southern parts of the Shelf Basin have up to 9 km of Tertiary-Quaternary sediments (Yang et al., 2004, Zhou et al., 1989). (Figure A10, Figure A11, Figure A12)



**Figure A11. Isopach maps of the Cenozoic sediments in the East China Sea (from Zhou et al., 1989).**

The geothermal gradient of the Shelf Basin is an average of 32.7°C/km and present day heat flow averages 70.8 mW/m<sup>2</sup> using data from the Xihu Trough (Yang et al., 2004). Temperature and heat flow data from the Taibei Trough has similar average values (Yang et al., 2004).

The other major component of the East China Sea Basin is the Okinawa Trough Basin (OTB), which is separated from the Xihu Depression by the Diaoyudao Folded uplift belt (DFB). This is an active back arc trench basin also related to the subduction of the Pacific plate under the Eurasian plate (Yang et al., 2004). (Figure A9)

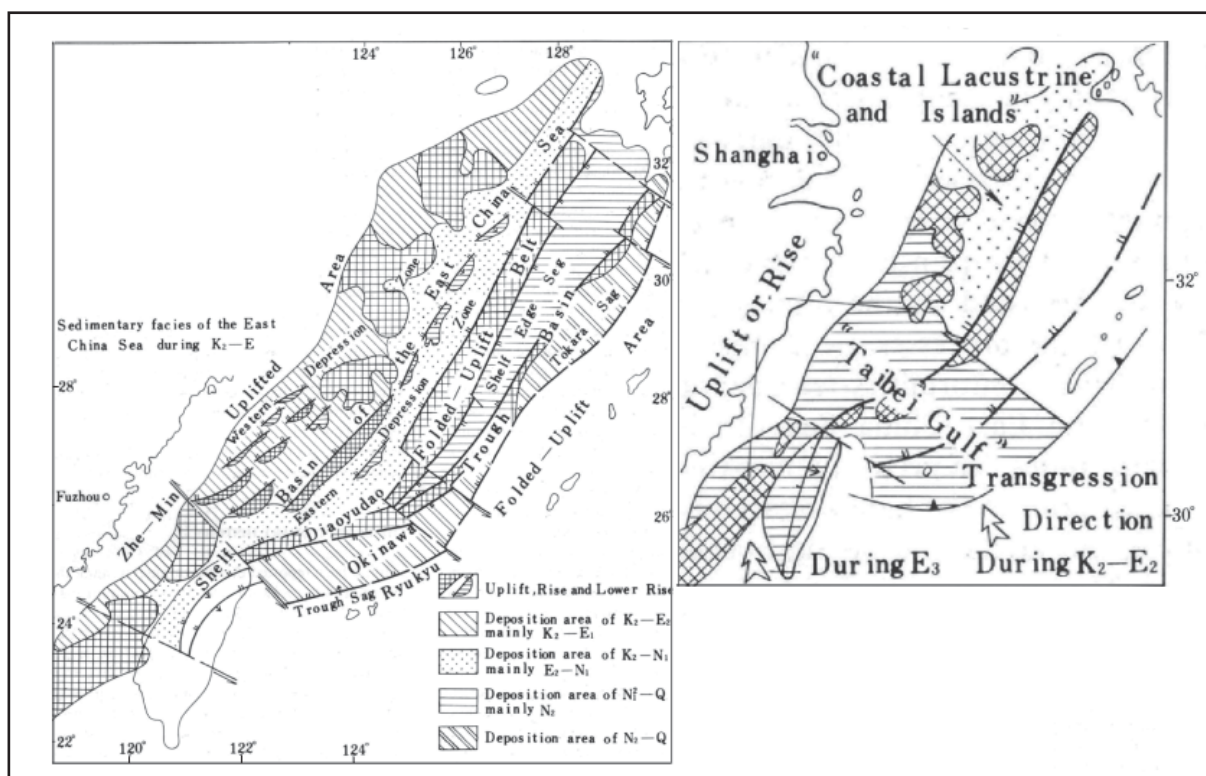


Figure A12. Distribution of Cenozoic sediments of the East China Sea (from Zhou et al., 1989).

### A1.2.3 Basin Fill

The main area of interest is the Shelf Basin. The Shelf Basin is divided into two main sags, Zhedong and Taibei. It is adjoined by the Taixi Basin (near Chinese Taipei). The structural framework of this northern Zhedong sag is defined by the Hupijiao and Hiajiao rises and bordered by the Diaoyudao folded uplift (Figure A9). Throughout the Palaeocene-Miocene the Shelf Basin environment of deposition is divided into a northern terrestrial environment of deposition (Zhedong Sag) and a marine southern environment (Taibei) (Figure A13). Mainly terrestrial to lacustrine and swamp environments occurred north of the Yushan rise. This area has occasional intercalations of marine sediments (Zhou et al., 1989).

The marine influenced area in the Taibei sag is known as the "Taibei Gulf" and persisted from the Late Cretaceous to the Eocene (Figure A13). In contrast the northern or "Coastal Lacustrine Islands Area" (Figure A12-inset, Figure A13) was predominantly fluvial- lacustrine environments with minor marine beds. Sandstones and mudstones were deposited. Marine beds indicate occasional marine transgressions from the "Taibei Gulf". These intervals are termed "minor" whether they represent potential seal intervals is not clear. No descriptive stratigraphy column was available. Basic stratigraphy is set out in Figure A14 and Figure A15. A reservoir-seal pair may have occurred when the northern area was completely flooded in the Pliocene (Figure A13). However it is apparent the sediment is quite thin in the western part of the Zhedong sag (Figure A10, Figure A11). This was due to inversion in the Oligocene-Miocene (Figure A15). The main depocentre is the Xihu Trough through most of the Eocene and Miocene.

During the Middle to Late Miocene, subduction of the Pacific plate intensified resulting in the formation of a new trench back arc system to the northwest of the current Okinawa Trough. This rifting caused compressive stress on the Shelf Basin, which formed anticlines at the end of the Miocene (Zhou et al., 1989).

In the Pliocene to Quaternary, the East China Sea Shelf Basin subsided and the Okinawa Trough developed. A marginal marine environment developed across the whole East China Sea Basin. The Okinawa Trough is still in an early rift stage today, with recent volcanic activity, high heat flow and earthquake activity (Zhou et al., 1989).

Quantitative reservoir quality data was not located. Kwon and Boggs (2002) studied sandstone samples of Oligocene to Quaternary age from wells in the Cheju sub Basin (northern most ECSB). Kwon and Boggs (2002) classified the samples as subfeldsarenites or sublitharenites using Folk's classification, i.e. feldspar content <25% of sediments. No data on porosity or permeability is available.

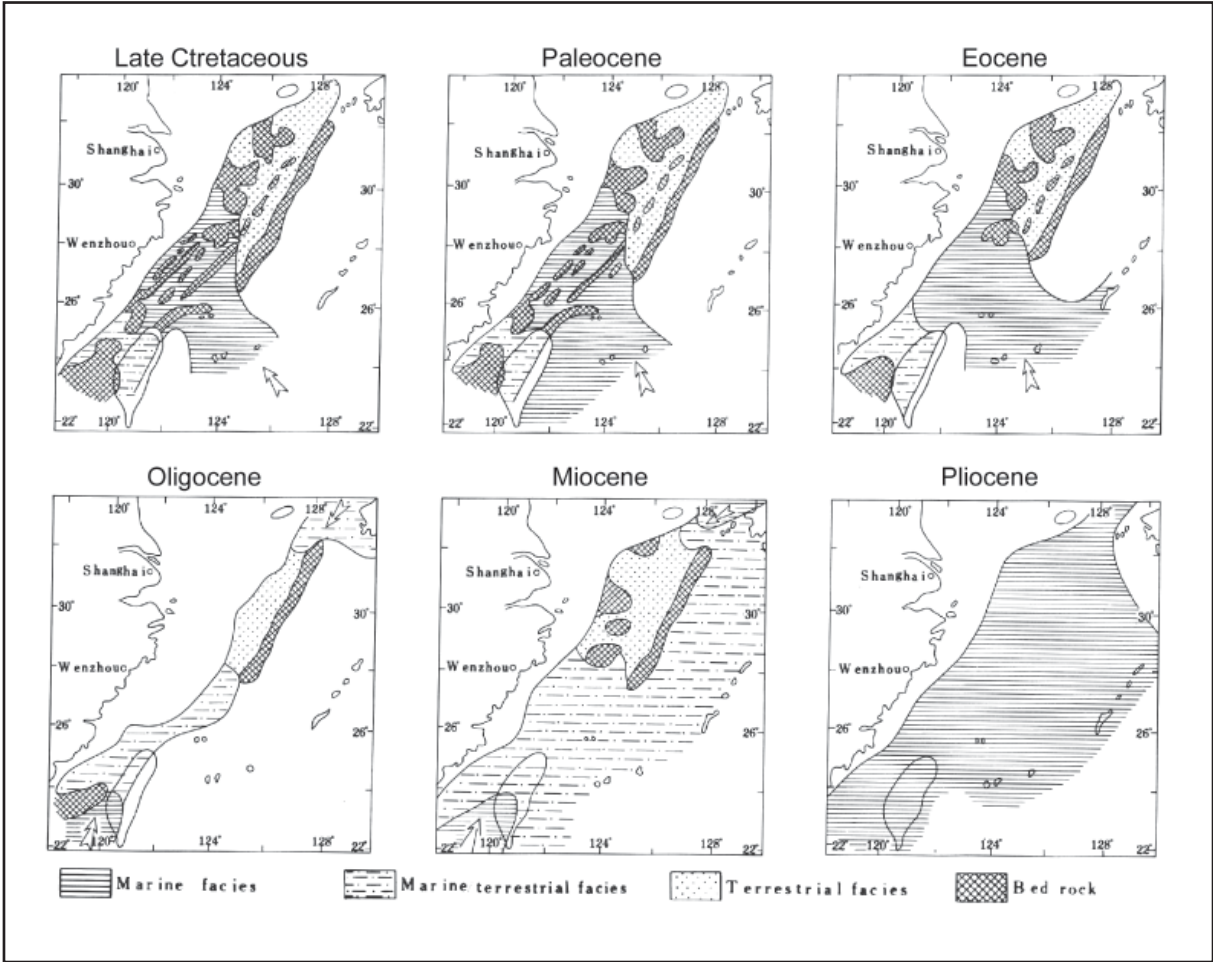


Figure A13. The paleogeography of the Cenozoic sediments (from Zhou et al., 1989).

Stratigraphy/age	Stratigraphy division	Contact	Tectonic movement		Evolutional characteristics			
			Taiwan	East China Sea	Shelf		Okinawa Trough	
QUATERNARY	Donghai Group (Qd)	disconformity or unconformity	Taiwan Movement	Okinawa Trough Movement	west	east	west	east
NEOGENE Pliocene	Santan Formation (N <sub>2</sub> s)	unconformity	Coastal Range Movement	Longjing Movement	regional subsidence	regional subsidence	depression	faulted depression
<i>Miocene:</i> Upper Miocene	Liulang Formation (N <sub>1</sub> <sup>l</sup> L)	local unconformity			depression	depression	faulted depression	
Middle Miocene	Yuquan Formation (N <sub>1</sub> <sup>l</sup> Y)	local unconformity						
Lower Miocene	Longjing Formation (N <sub>1</sub> <sup>l</sup> L)	local unconformity			depression			
PALEOGENE Oligocene	Huangang Formation (E <sub>3</sub> h)	unconformity	Puli Movement	Yuquan Movement				
Eocene	Pinghu Formation (E <sub>2</sub> p) / Oujiang Formation (E <sub>2</sub> o)	unconformity						
Paleocene	Lingfeng Formation (E <sub>1</sub> L)	unconformity or unconformity	Taiping Movement	Oujiang Movement Yandang Movement	faulted depression			
Upper Cretaceous		unconformity	Nanao Movement	Jilong Movement	faulted depression			

Figure A14. Cenozoic stratigraphy of the East China Sea (from Zhou et al., 1989)

Stratigraphy/age	East China Sea Shelf Basin		Okinawa Trough Basin	
	western part	eastern part	shelf edge sag	trough sag
Quaternary		Donghai Group	Donghai Group	Donghai Group
Pliocene	Qd	Santan Formation	Santan Formation	Santan Formation
	N <sub>2s</sub>		Liulang Formation	
Miocene	N <sub>1L</sub>			
	N <sub>1Y</sub>	Yuquan Formation	Yuquan Formation	
Oligocene	N <sub>1L</sub>		Longjing Formation	
	E <sub>3h</sub>		Huagang Formation	
Eocene	E <sub>2p</sub>	Oujiang Formation	Pinghu Formation	
	E <sub>2o</sub>			
Paleocene	E <sub>1L</sub>	Lingfeng Formation	Lingfeng Formation	
Late Cretaceous	K <sub>2</sub>	Upper Cretaceous	Upper Cretaceous	
	J <sub>3-K<sub>1</sub></sub>			

Figure A15. Stratigraphic correlation of the East China Sea (from Zhou et al., 1989)

## A1.2.4 Hydrocarbon Fields

Since the beginning of petroleum exploration in the East China Sea Basin in 1974, twelve oil and oil/gas fields such as Pinghu, Chunxiao, Tianwaitian, Wuyunting, Baoyunting and Yuquan have been discovered. (Sinopec website - <http://english.sinopec.com/en-company/en-subsidiaries/en-oilfieldbranch/en-offshore/1129.shtml>)

All hydrocarbon accumulations are in the Xihu trough on the eastern edge of the basin. This suggests source rocks are best developed in the Xihu trough. Pinghu field has been supplying gas through a 400 km pipeline to Shanghai since November 1998 (<http://www.cnooc.com.cn/english/business/index4.html>).

Most of the hydrocarbon accumulations are in drapes over these basement features (Figure A16). These drape plays and other stratigraphic traps seem to be of limited size, though no data was obtained on field sizes.

The resources of this area were not assessed by the USGS in 2000. No estimate of CO<sub>2</sub> storage in hydrocarbon fields was made.

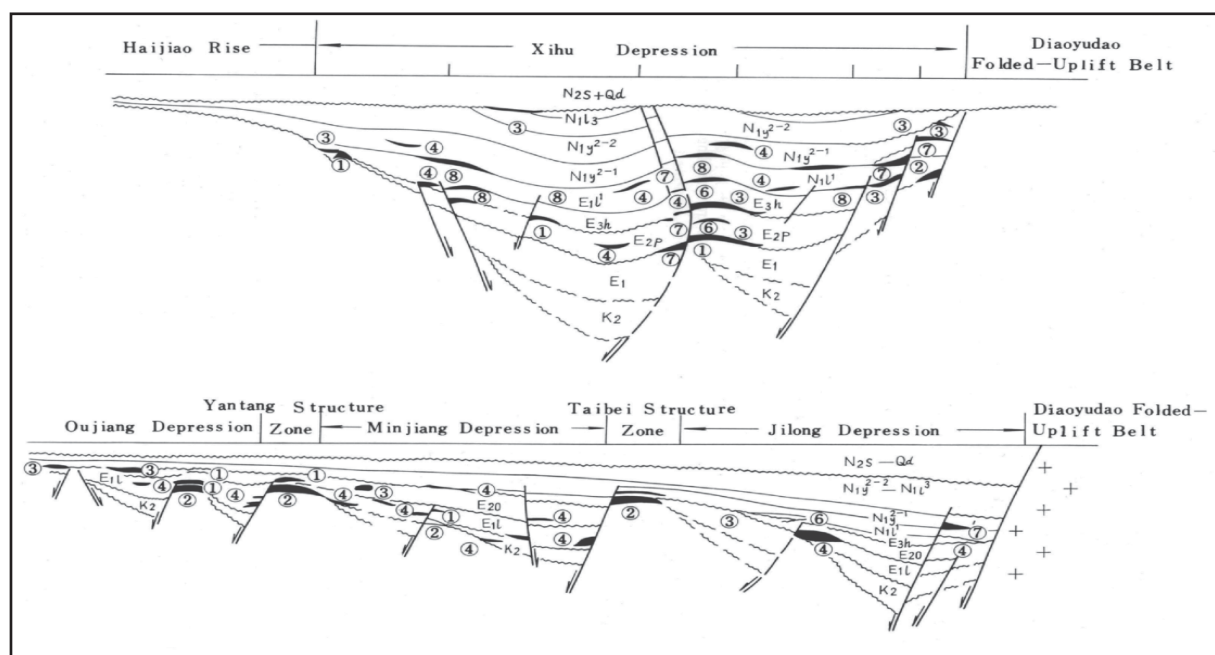


Figure A16. Schematic cross-section showing the predictive types of traps (1= draping structure; 2= buried hill; 3= unconformity; 4= onlapping litologic and stratigraphic trap; 5= reef; 6= compressional anticline; 8= roll-over anticline). From Zhou et al., 1989).

## A1.2.5 Coal Occurrence

Coal occurs interbedded in Cretaceous to Quaternary age terrestrial sequences. Coal appears to be best developed in the lower half of the widely distributed Yuquan Formation of Middle Miocene age. The formation is interpreted as a swamp- flood plain environment with marine intercalations (Zhou et al., 1989).

## A1.2.6 Potential CO<sub>2</sub> Storage Options

The offshore location adds an economic burden to CO<sub>2</sub> storage in the East China Sea Basins. The Shelf Basin is the region closest to shore. The northern section of the shelf basin (Zhedong Sag) appears to have high clastic sediment input and good potential for terrestrial clastic reservoirs. Possibilities for seals are brief marine transgressions, intraformational seals or a widespread Pliocene marine seal. The distribution of facies is only generally understood from the work of Zhou et al., (1989). Unfortunately the sediment thickness is very thin in the west of this area (Figure A13). The basement of the Shelf Basin and adjacent areas is Proterozoic metamorphic rocks. With no carbonate a tilted fault block (buried hill) weathered basement reservoir appears very unlikely.

The deeper depocentres such as the Xihu trough lie at 300 to 400 km offshore and contain hydrocarbon traps. There are hydrocarbon accumulations concentrated in the Xihu trough with shows in the Taibei Sag.

The East China Shelf is a large area and specific details of its stratigraphy and facies distribution have not been uncovered by this study. Investigation by drilling has not been as intensive as onshore. The western most edge of the basin is around 240 km offshore of Shanghai. This basin has been ranked as “intermediate” potential due to the uncertainty about the geology and unexplored economics of an offshore setting.

## A1.2.7 References

Kwon, Y.I. and Boggs, S. Provenance interpretation of Tertiary sandstones from the Cheju Basin (NE East China Sea); a comparison of conventional petrographic and scanning cathodoluminescence techniques. Abstracts with Programs - Geological Society of America 33[3], 44. 2000.

Yang, S., Hu, S., Cai, D., Feng, X., Chen, L., and Gao, L. Present-day heat flow, thermal history and tectonic subsidence of the East China Sea Basin. *Marine and Petroleum Geology* 21[9], 1095-1105. 2004.

Zhou, Z., Zhao, J., and Yin, P. Characteristics and Tectonic evolution of the East China Sea. In: Zhu, Xia (ed.), *Chinese sedimentary basins*. Elsevier Sci. Publ. Amsterdam, Netherlands, 165-179. 1989.

## A1.3 Hefei (Hehuai) Basin

### A1.3.1 CO<sub>2</sub> Sources

CO<sub>2</sub> emissions in the region directly overlying the Hefei Basin (also known as the Hehuai Basin) contributed approximately 104 Mt CO<sub>2</sub> /yr to China's estimated total stationary source CO<sub>2</sub> emissions of 2970 Mt/yr (IEA, 2000).

The Hefei basin lies south of the Bohai basin in the most industrialised area of China. In a 300 km radius from the basin there are sources totalling approximately 868 Mt CO<sub>2</sub>/yr.

Note: The total of sources within 300 km of a basin is a very crude indication of the magnitude of emissions which may be within reach of the basin. These “catchments” overlap for many basins and should not be summed.

### A1.3.2 Basin Overview

This basin lies at the junction of the Tan Lu fault and the Tongbai-Dabie suture zone formed by the collision of the North China Block and the South China Block. As seen in Figure A17 and Figure A18 the Tan Lu fault forms the eastern boundary of the Hefei Basin and the edge of the Bohai Basin. On some simple basin maps the Hefei may appear to be an extension of the Bohai Basin. However, the Hefei has a complex poly phase origin (Figure A19, Figure A20), including a foreland basin phase in the Lower and Middle Jurassic, followed by erosion until the Upper Cretaceous when a rift basin formed. The rift basin structure resulted mainly from the reactivation of existing east west thrust faults and does not have the obvious NNE trend of other extensional basins such as Bohai, Songliao and Subei (Liu et al., 2003). The area of the basin is approximately 1000,000 sq km (Han et al., 1989).

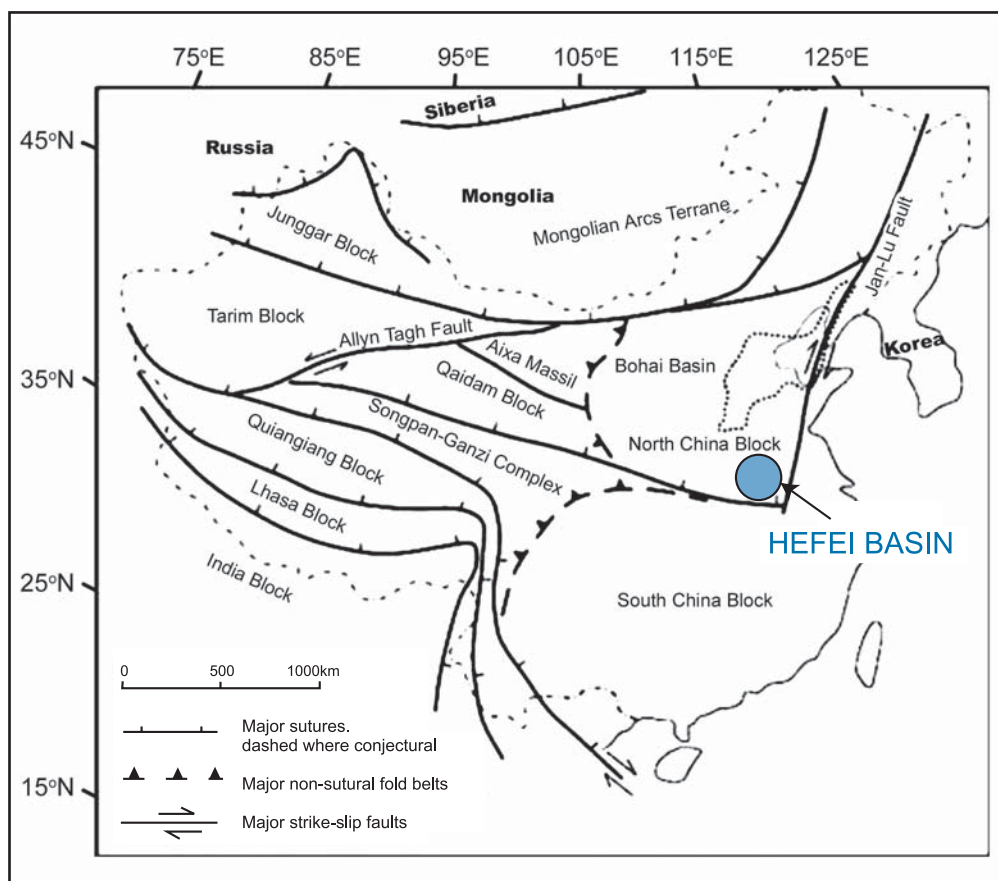


Figure A17.  
Hefei Basin  
location.

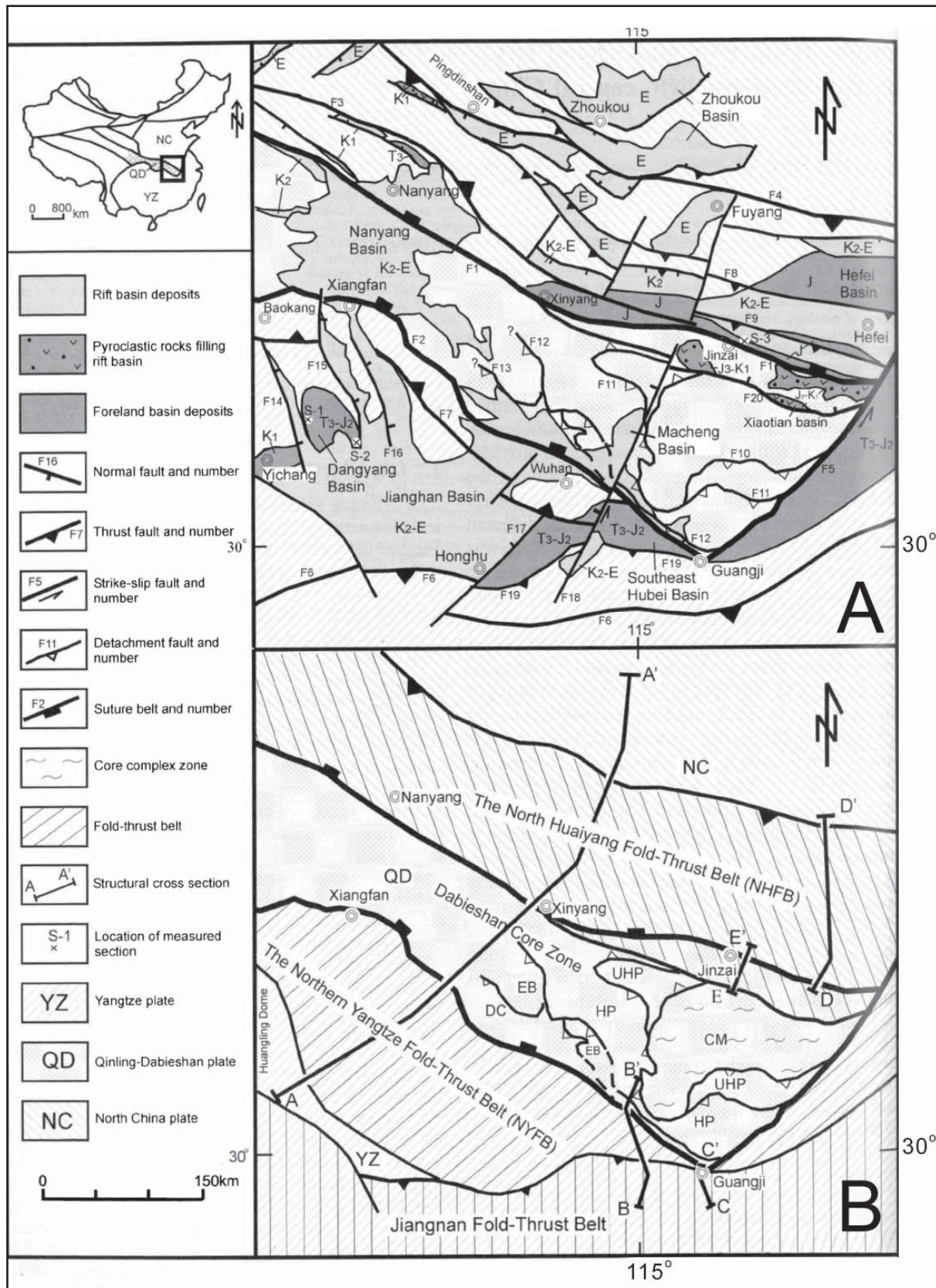
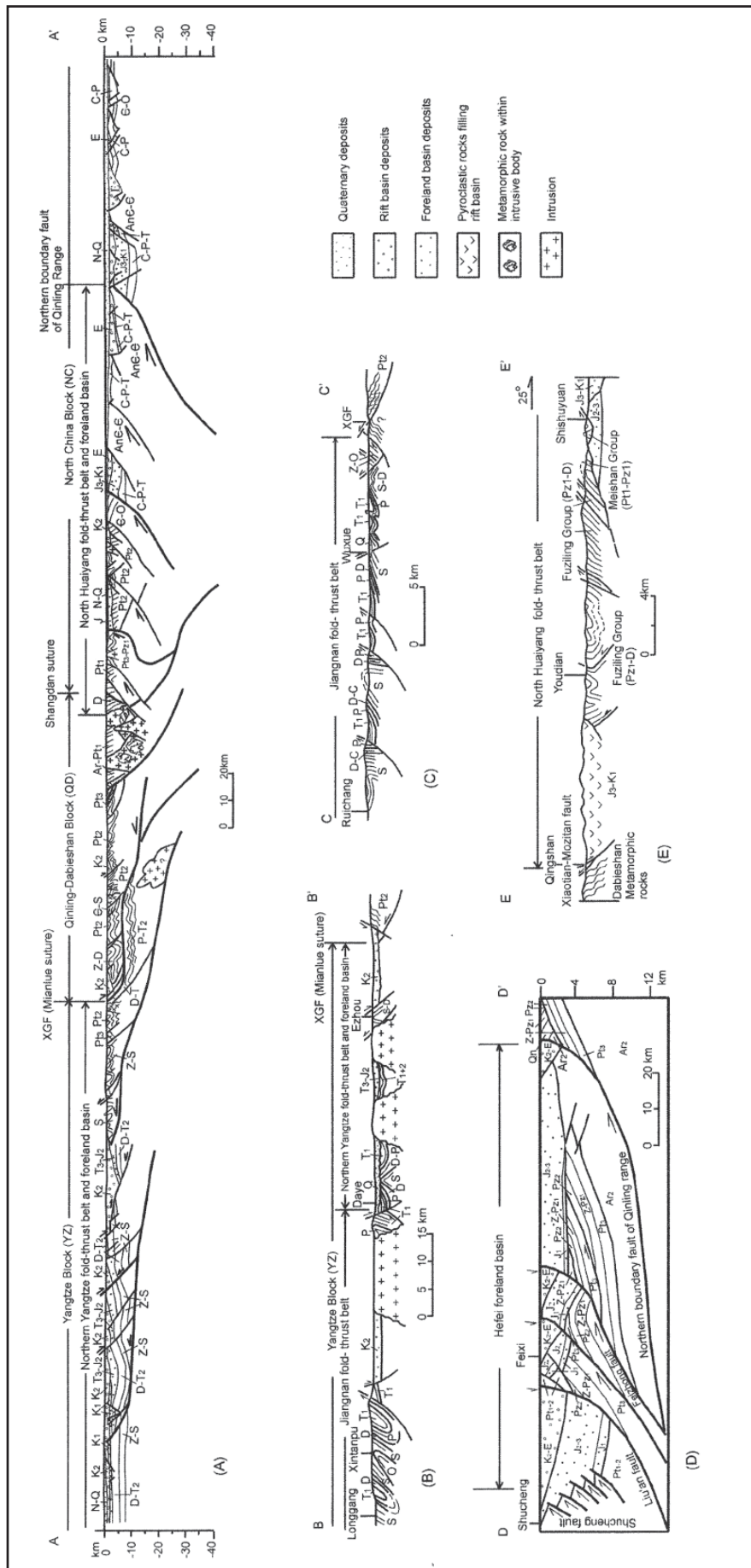
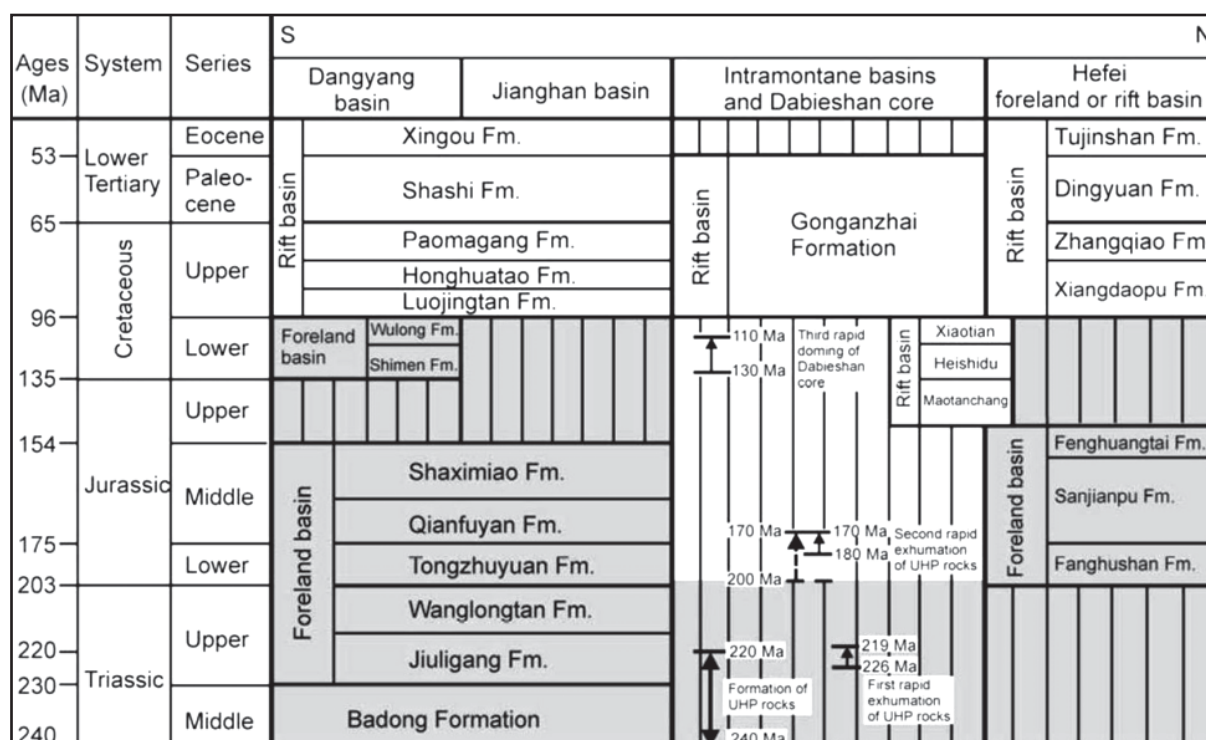


Figure A18. Structure map showing the locations of the basins including Hefei (from Liu et al., 2003)





**Figure A20. Upper Triassic through Lower Tertiary unit names for foreland and rift basins, age data for ultrahigh-pressure (UHP) rocks, and formation and rapid exhumation of UHP rocks and rapid doming episode of Dabieshan core. Ruled pattern represents hiatuses; dark shading highlights times of compressional deformation (from Liu et al., 2003).**

### A1.3.3 Basin Fill

Recent work by Lui et al., (2003) explains the complex evolution of the basins in Dabieshan. The Hefei Basin began with a Jurassic foreland basin phase which was characterised by alluvial to braid plain environments (Figure A20). The 6 km of foreland basin sediments are mainly conglomerate up to boulder sized. The area is proximal to the rapidly eroding Dabieshan complex. Lui et al., (2003) describe 12 to 50 m claystone beds in the Dangyang Triassic Jurassic foreland basin. These are apparently the result of periodic lake formation in a generally braided stream environment.

The Hefei Cretaceous to Tertiary rift basin phase is characterised by cycles of alluvial fan and deltaic deposits than fine up to lacustrine mudstones. There may be good porosity in the foreland basin but any ultimate top seal would be provided by the Cretaceous -Tertiary rift basin section. An event at the end of the Cretaceous relates to the change in motion on the Tan Lu fault that removed most of the Jurassic and Cretaceous sediments (Figure A21, Figure A22). As these are the best potential source intervals this severely limits the petroleum prospectivity. As source rock intervals are also good seals there are implications for CO<sub>2</sub> storage. Better lacustrine seal may occur where the Cretaceous-Tertiary is present and possibly more distal from the Dabieshan complex (northward in the case of Hefei Basin).

The dominant Eocene fill of the Tertiary rift basin is red fluvial-lacustrine sandstones and shales.

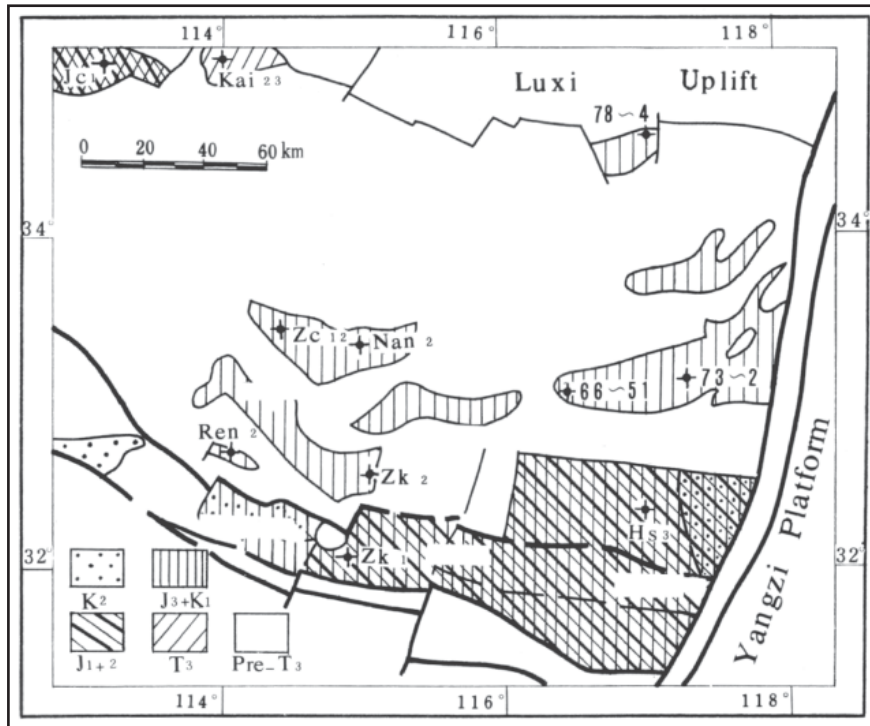


Figure A21. Distribution map of the residual Jurassic and Cretaceous formations, Hehuai Basin. From Han et al., 1989.

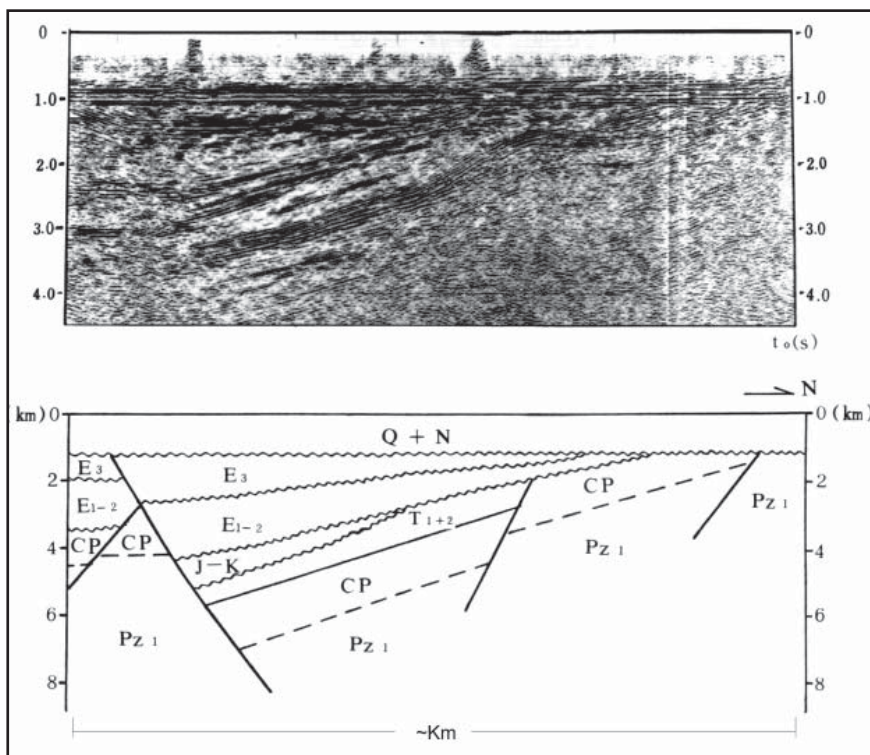


Figure A22. Seismic section and its interpretation along seismic line 840, Shenqui Depression (from Han et al., 2003).

### A1.3.4 Hydrocarbon Fields

There are only a few hydrocarbon shows in the basin (Han, 1989) and there is very limited source rock. From the information available it appears there are very few hydrocarbon fields.

### A1.3.5 Coal Occurrence

Coal is not expected in the very coarse clastic proximal foreland basin during the Jurassic. However Han (1989) notes briefly that coal occurs on the margins of this basin. It is assumed this coal developed in the north area of the rift basin during the Cretaceous - Tertiary. No information on this coal occurrence was located.

### A1.3.6 Potential CO<sub>2</sub> Storage Options

There is little coal or depleted hydrocarbon potential in this area. The basins of this area were fed by the erosion of the Dabieshan complex which has an E-W strike (Figure A17). In general the potential for lacustrine mudstone sealing formations will be greater further to the north or south of the Dabieshan core. There are significant thicknesses of coarse clastics in the Hefei foreland basin phase and other basins of the region such as Nanyang and Danyang. Good sealing formations appear to be generally absent. However lacustrine mudstones are reported in the Danyang Basin. The depositional cycles in the Hefei Basin rift phase are reported to have conglomerate bases that fine up through fluvial sandstones to lacustrine mudstones. These cycles may have potential for CO<sub>2</sub> storage. No data on porosity or permeability was located. Relatively steep dips ~10 degrees of dip will mean relatively rapid vertical progress of CO<sub>2</sub> migrating under a Cretaceous seal to the subcrop unconformity, beneath the Quaternary sequence. Because of this basin geometry, the seal potential of the Quaternary will also need to be understood (Figure A22).

### A1.3.7 References

Han, J., S. Zhu, and S. Xu. The generation and evolution of the Hehuai Basin. In: Zhu, Xia (ed.), Chinese sedimentary basins. Elsevier Sci. Publ.. Amsterdam, Netherlands , 125-134. 1989.

Liu, S., P. L. Heller, and G. Zhang. Mesozoic basin development and tectonic evolution of the Dabieshan orogenic belt, Central China. *Tectonics* 22[4], 12-1 - 12-21. 2003.

Liu, S., R. Steel, and G. Zhang. Mesozoic sedimentary basin development and tectonic implication, northern Yangtze Block, eastern China: record of continent-continent collision. *Journal of Asian Earth Sciences* In Press, Corrected Proof.

## A1.4 Jiangnan Basin

### A1.4.1 CO<sub>2</sub> Sources

CO<sub>2</sub> emissions in the region directly overlying the Jiangnan-Nanyang Basins contributed approximately 116 Mt CO<sub>2</sub>/yr to China's estimated total stationary source CO<sub>2</sub> emissions of 2970 Mt/yr (IEA, 2000).

In a 300 km radius from these basins there are sources totalling approximately 604 Mt CO<sub>2</sub>/yr.

Note: The total of sources within 300 km of a basin is a very crude indication of the magnitude of emissions which may be within reach of the basin. These "catchments" overlap for many basins and should not be summed.

### A1.4.2 Basin Overview

The Jiangnan Basin contains Late Cretaceous to Tertiary sediments up to 10 km thick. It is a 28,000 km<sup>2</sup> Cenozoic rift basin composed of eight depressions (Figure A23, Figure A24) Chen et al., (1989). The most notable feature of the Jiangnan Basin is the development of non-marine evaporite sequences (Figure A25, Figure A26). Mountain ranges in eastern China altered airflows and resulted in arid conditions during the Cretaceous and Palaeogene. Much of the available literature regarding Jiangnan Basin and the evaporite sequences in particular relates to the Qianjiang Depression (Figure A26).

The following is a summary of geology from Chen et al., (1989). The basement of the area consists of Early Proterozoic age rocks of metamorphic type. Sedimentary deposition began in the late Proterozoic with marine carbonate deposition which continued until the Triassic. These carbonates are up to 2000 m thick. This period of deposition was ended by the Indosinian orogeny, which resulted in a first order regression and the end of marine conditions. From the Upper Triassic till the Jurassic 1500 to 4000 m of marsh and lake sediments were deposited. The lithologies are mainly clastics and some coal seams.

In the Early Cretaceous extension initiated the rift basin phase of the Jiangnan. The sediments of this phase are around 10 km thick and range in age from the Early Cretaceous to the Tertiary. From the Upper Cretaceous to the Palaeogene the environment of deposition is essentially a salt lake. Lithologies are clastic and evaporite with interbedded volcanics. The geothermal gradient is 30 to 32°C/km (USGS, 1988).

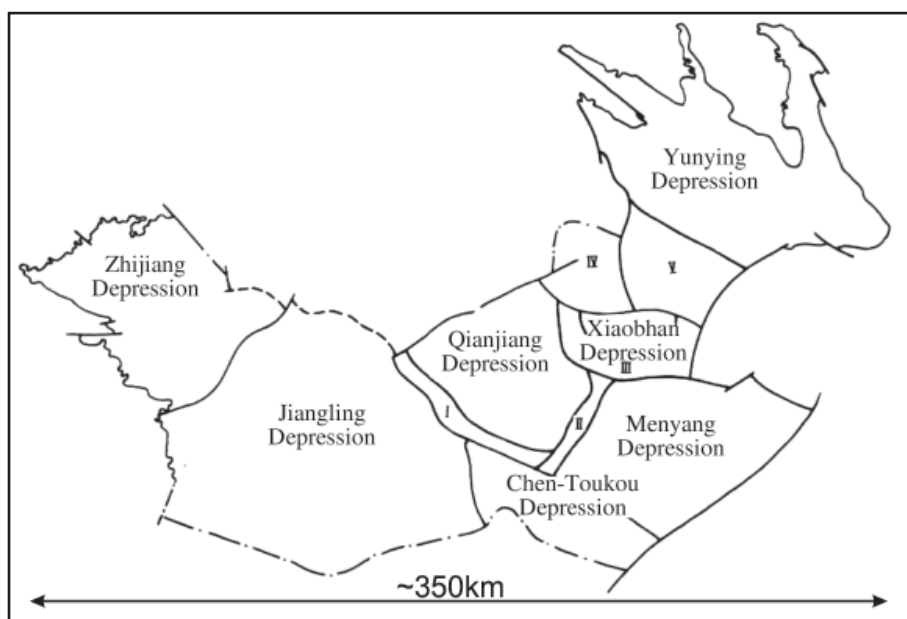


**Figure A23. Diagram of the tectonic elements in the Jiangnan Basin (I= Yajiao-Xingu low uplift; II= Tong Haikau Uplift; III= Chenhu; IV= Tiamen Uplift; V= Longsaihu Uplift) (from Chen et al., 1989)**

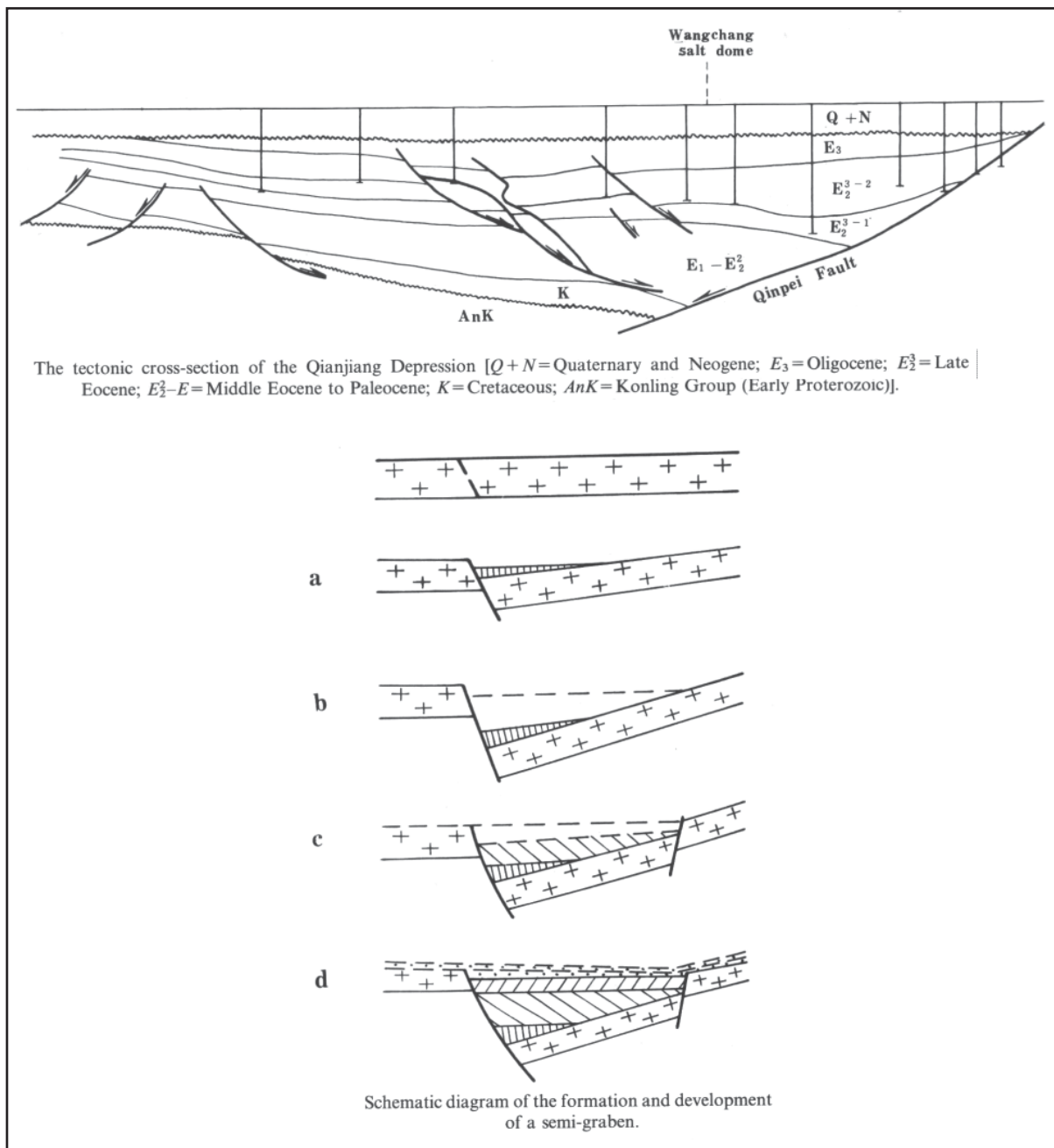


Figure A24. Jiangnan cross-section (from Chen et al., 1989).

Strata system	series	set	member	Lithologic character	Thickness (m)	Petroli-ferous sequence	Saline sequence
Quaternary	Recent	Pingyuan		clay, sand and gravel	50-150		
	Pleistocene	Guanghansi		variegated mudstone, clay and sandy conglomerate	300-900		
	Miocene	Jingsha		green-grey mudstone, sandstone with oil shale and glauberite-mudstone	0-1000		
Neogene	Oligocene		Qian 1	upper: dark mudstone, mud-gypsum rock and oil shale with salt rock middle: alternation of dark mudstone and sandstone lower: alternation of gypsum-halite sandstone and mudstones with limestone	120-450		
			Qian 2	cyclothem consists of halite/mud-gypsum, mirabilite-gypsum and mudstone	110-700	petroli-ferous sequence No. 2	saline sequence No. 2
Paleogene	Upper Eocene	Qianjiang*1	Qian 3	upper: dark mudstone, sandstone and marl with gypsum and halite lower: cyclothem consists of dark mudstone, mud-gypsum and halite with sandstone	150-640		
			Upper Qian 4	dark mudstone, glauberite	100-700		
			Lower Qian 4	alternation of dark mudstone, glauberite-mudstone and halite with sandstone	100-2200		
				red mudstone, gypsum-mudstone and siltstone	600-2000		
Cretaceous*2	Lower Eocene	Xingouzui	Yuyang	red-grey mudstone, mud-gypsum and sandstone	600-1000	petroli-ferous sequence No. 1	saline sequence No. 1
				grey-red mudstone, halite gypsum, gypsum-mudstone with sandstone	200-1900		
				red mudstone, mud-gypsum, halite gypsum, sandstone with conglomerate	1200-2800		
				upper: sandstone lower: conglomerate			

\*1The data for the Qianjiang set come from drilling in the Qianjiang Depression.

\*2The data for the Upper Cretaceous are based on drilling, and for the Lower Cretaceous on outcrops.

Figure A25. Stratigraphy in the Qianjiang depression of the Jiangnan Basin (from Chen et al., 1989)

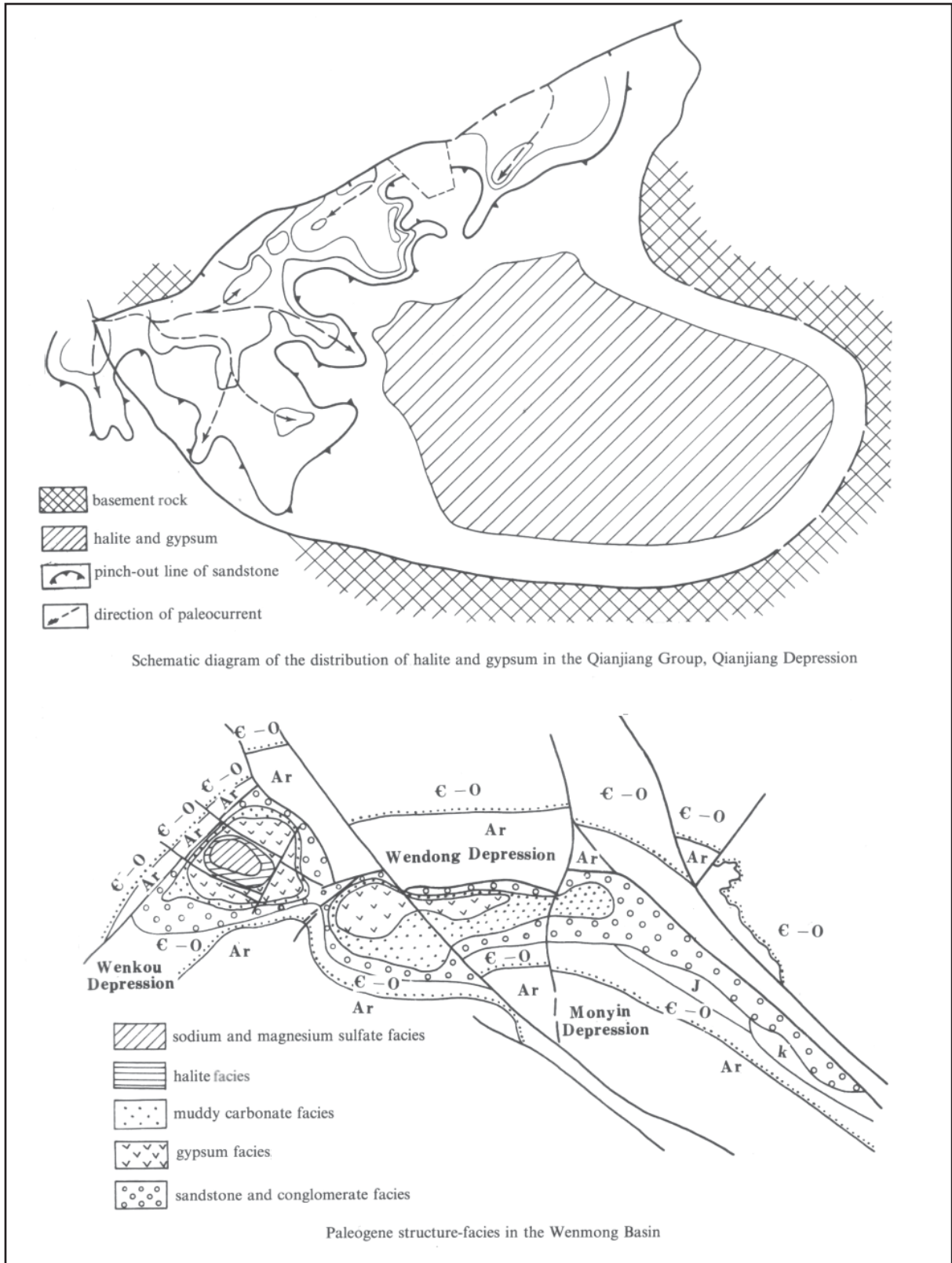


Figure A26. Salt bearing basins in eastern China (from Chen et al., 1989).

### A1.4.3 Basin Fill

There are two prominent evaporite deposition periods; the first in Upper Cretaceous the second in the Eocene. The Upper Cretaceous deposits are widespread, covering 10,000 km<sup>2</sup> and consisting dominantly of Gypsum with minor Halite. Thickness varies from a few metres to 400 m. Individual beds of evaporite are one to two metres thick (Chen 1989). The deposition in the basin became less marine in the Early Eocene. Later in the Eocene a second saline environment, resulted in 2,270 sq km of evaporite deposition. At the end of the Palaeogene the entire basin was uplifted and eroded. In the Neogene and Quaternary the basin developed into a tectonic sag phase and a floodplain environment was established.

Evaporite deposition is most pronounced in the Qianjiang depression. The Qianjiang Formation spans most of the Palaeogene. Typical evaporite deposition is rhythmic couplets consisting of a few meters of mudstone followed by a few meters of evaporite.

Fluvial/lacustrine-deltaic sandstone in the Palaeogene section is restricted to the margins of the Qianjiang depression. This is to be expected in an arid lake environment with very limited in flow of water and sediment and excellent source rock development. Cretaceous sandstone and conglomerate are reported from outcrops in Chen et al., (1989). The extent of this facies is not known, and reservoir qualities are unknown. The Cretaceous or perhaps Jurassic sandstones may be injection targets. The overlying evaporite and mudstone sequences could provide a good seal, as it is a working hydrocarbon play (Chen et al., 1989).

Chen 1989 reports pore water salinity of 200-330 g/l (Chen 1989). It should be noted that the solubility of CO<sub>2</sub> in pore waters is inversely proportional to salinity (Bachu, 2001). This salinity is quite high. Knowledge of the pore water salinity profile through the basin stratigraphy would be required in order to optimise storage capacity.

This basin contains gypsum, anhydrite and other evaporites. Anhydrite is reactive with CO<sub>2</sub> on a short time scales. However, Anhydrite forms a stable seal (caprock) for the Bravo Dome CO<sub>2</sub> field in New Mexico (Rochelle et al., 2004). Site specific conditions need to be assessed.

### A1.4.4 Hydrocarbon Fields

There are two petroleum source intervals which coincide with the saline events. The restriction resulting in saline conditions caused highly reducing conditions and thus excellent preservation of organic detritus. However the basin is not a major hydrocarbon province due to a lack of reservoir. Hence the USGS did not assess this basin in 2000. Reserves data specific to this basin could not be located.

Aside from the Cretaceous sandstone play the literature available does not suggest any reservoirs. It seems likely that Palaeogene reservoirs are non-existent or of poor reservoir quality given the conclusion of Xie et al., (1988) – “Fluvial Sandstone is not well developed, having a restricted distribution area in the basin; this condition is unfavourable to the migration of oil and gas”.

### A1.4.5 Coal Occurrence

Coal occurs in the pre-rift basin sequences, within Upper Triassic and Jurassic deposits. It is assumed these formations are known from outcrop where they are favourably folded and exposed. Generally these seams would lie very deep, i.e. over 10 km.

Due to the arid climate resulting in evaporite development it is clear that the Cretaceous to Palaeogene section lacks coal. It is also inferred from the brief description available that Neogene and Quaternary deposition was in a fluvial oxidizing environment.

## A1.4.6 Potential CO<sub>2</sub> Storage Options

Eocene evaporite sequences offer a very good ultimate top seal for saline reservoir storage in Cretaceous sandstones. Structuring by salt (e.g. anticlines) could form good traps. Little information was obtained on siliciclastic reservoirs. Xie et al., 1988 observe that, "Fluvial Sandstone is not well developed, having a restricted distribution area in the basin.". The presence of good quality, extensive siliciclastic reservoirs seems to be a problem given that saline environments develop in shallow water lakes with limited in flow of water and sediment.

Some of the pore waters of this basin are certainly highly saline (Chen et al., 1989). High salinity levels reduce pore water solubility trapping of CO<sub>2</sub>. The salinity and the presence of gypsum/anhydrite will have an influence on the nature and rate of mineral trapping. Geothermal gradient is moderate. Whether these influences are a net benefit or deficit for storage is a subject for site specific geochemical assessment.

## A1.4.7 References

Bachu, S. Geological Sequestration of Anthropogenic Carbon Dioxide: Applicability and Current Issues. In: Gerhard, LC, Harrison, W E & Hanson, B M (eds.), Geological Perspectives of global climate change, 285-303. 2001

Chen, Fajing; Dai, Shizhao, and Pan, Guoen. The Cretaceous-Paleogene Salt-Bearing Basins in Eastern China. In: Zhu, Xia (Ed.), Chinese Sedimentary Basins. Elsevier Sci. Publ.. Amsterdam, Netherlands. 1989; 137-146.

Lee, K. Y. and C. D. Masters. Geologic framework, petroleum potential, and field locations of the sedimentary basins in China. Miscellaneous Investigations Series - U. S. Geological Survey, 1988.

Rochelle, C.A., Czernichowski-Lauriol, I., and Milodowski, A.E. The impact of chemical reactions on CO<sub>2</sub> storage in geological formations: A brief review. In: Baines, S.J. and Worden, R.H. (eds.), Geological Storage of Carbon Dioxide, Geological Society Special Publications, Geological Society of London 233, 87-106. 2004.

Xie, Taijun; Wu, Lizhen, and Jiang, Jigang. Oil and Gas Fields in the Jiangnan Basin, Hubei Province, China. In: Wagner, H C, Wagner, L C, Wang, F F H & Wong, F L (Eds.), Petroleum Resources of China and Related Subjects. Circum-Pacific Council for Energy and Mineral Resources, Earth Science Series. 1988; 10; 345-358.

## A1.5 Nanpanjiang

### A1.5.1. CO<sub>2</sub> Sources

CO<sub>2</sub> emissions in the region directly overlying the Nanpanjiang Basin contributed approximately 45 Mt CO<sub>2</sub> /yr to China's estimated total stationary source CO<sub>2</sub> emissions of 2970 Mt/yr (IEA, 2000).

In a 300 km radius from the basin there are sources totalling approximately 203 Mt CO<sub>2</sub>/yr.

Note: The sum of sources within 300 km of a basin very crudely indicates the magnitude of emissions within reach of the basin. These “catchments” overlap for most basins and should not be summed.

### A1.5.2 Basin Overview

The basin is 100,000 sq km in area and contains essentially platform carbonates of Cambrian to Triassic age. Palaeozoic formations outcrop as a karst terrane. Little information was available. The information here comes from Halley et al., (1988).

### A1.5.3 Basin Fill

The Nanpanjiang Basin was a Palaeozoic to Triassic marine region with significant platform carbonate growth. At some time after the Triassic it was uplifted and has not subsided since. The Triassic reef platform sediments are apparently much studied by carbonate sedimentologists. It appears from the small amount of petroleum literature that there is no primary porosity but there is secondary porosity in much of the section due to various kinds of diagenesis (dolomitization ?). A maximum palaeo-temperature of 200°C is suggested for Triassic sediments (Halley et al., 1998). Halley et al., (1988) did not believe there was much petroleum potential but suggested there may be fractured reservoir gas plays in the basin.

### A1.5.4 Hydrocarbon Fields

There are seeps occur on the margins of the basin. Halley et al., (1988) observed only bitumen in their samples.

### A1.5.5 Coal Occurrence

No Specific information. Given the dominantly marine platform environment the presence of coal would be almost nil.

### A1.5.6 Potential CO<sub>2</sub> Storage Options

Halley et al., (1988) concluded that parts of the basin had been heated beyond the “level of hydrocarbon generation and retention”. This was particularly applicable to the western basin. The possibility of fractured carbonate gas plays in other parts of the basin was left open.

If there are sufficiently fractured Cambrian to Triassic carbonates in the basin injection of CO<sub>2</sub> may be possible. Such formations are likely to be quite low permeability and the efficacy of injection would need to be looked at carefully. The dissolution and re-crystallisation of carbonate minerals would be a factor affecting injection of CO<sub>2</sub> for storage.

## A1.5.7 References

Halley, R. B., J. T. Parrish, Z. Xie, W. Hu, P. A. Scolle, Z. Su, Y. Zhang, Y. Huang, and G. Li. Thermal and Cementation Histories of Permian Shelf-edge Carbonate rocks in the Nanpanjiang Basin, South China. In: Wagner, H C, Wagner, L C, Wang, F F H & Wong, F L (eds.), Petroleum resources of China and related subjects. Circum-Pacific Council for Energy and Mineral Resources, Earth Science Series 10, 627-635. 1988.

## A1.6 Nanyang

### A1.6.1 CO<sub>2</sub> Sources

CO<sub>2</sub> emissions in the region directly overlying the Jiangnan-Nanyang Basins contributed approximately 116 Mt CO<sub>2</sub>/yr to China's estimated total stationary source CO<sub>2</sub> emissions of 2970 Mt/yr (IEA, 2000).

In a 300 km radius from these basins there are sources totalling approximately 604 Mt CO<sub>2</sub>/yr.

Note: The sum of sources within 300 km of a basin very crudely indicates the magnitude of emissions within reach of the basin. These "catchments" overlap for most basins and should not be summed.

### A1.6.2 Basin Overview

The Nanyang Basin has a Cretaceous-Tertiary rift phase and contains up to 9000 m of fluvio-lacustrine sediments (Liu et al., 2003). The basin is located to the north of the Jiangnan Basin and overlies in the Dabieshan complex. The basin is similar to the Jiangnan Basin as it contains evaporite sequences, and like the Hefei Basin, the Nanyang Basin consists of a Mesozoic foreland phase sequence followed by a Tertiary rift phase.

### A1.6.3 Potential CO<sub>2</sub> Storage Options

There may be potential in this basin in the thick lacustrine section. There is not sufficient information to consider the potential of this basin.

## A1.7 Ordos Basin

### A1.7.1 CO<sub>2</sub> Sources

CO<sub>2</sub> emissions in the region directly overlying the Songliao Basin contributed approximately 91 Mt CO<sub>2</sub> /yr to China's estimated total stationary source CO<sub>2</sub> emissions of 2970 Mt/yr (IEA, 2000).

In a 300 km radius from the basin there are sources totalling approximately 487 Mt CO<sub>2</sub>/yr. The major coal reserves within the Ordos and the adjacent Shanxi province are the primary source of CO<sub>2</sub> produced by power stations in the area.

Note: The sum of sources within 300 km of a basin very crudely indicates the magnitude of emissions within reach of the basin. These “catchments” overlap for most basins and should not be summed.

### A1.7.2 Basin Overview

The Ordos Basin is a polycyclic basin with an average sediment thickness of 4 to 5 km and an maximum of 10 km on the western side. Strata are generally very flat lying to very gently folded. Around the basin margins the sequences are folded and outcrop in hill and mountain chains (Moore et al., 1986) (Figure A27, Figure A28). The Ordos Basin was foreland basin for most of its history with subsidence driven by adjacent mountain belt loading.

The early Palaeozoic deposition was in a carbonate platform setting on part of the Tarim-Sino-Korean plate (Moore et al., 1986). At this time the area subsided during extension (Sun et al., 1989). In the Late Permian – Early Triassic, the South China Block became completely sutured to the North China (Tarim-Sino-Korean) block (Figure A29). From this time the Ordos region was essentially a foreland basin. It is the stratigraphy of this basin phase that is depicted in Figure A30. By this time deposition was entirely fluvio-lacustrine across the Ordos and the rest of the North China Block (Watson et al., 1987). In the Late Triassic/Early Jurassic the western margin of the South China block became a major transcurrent or strike slip zone. This strike slip movement combined with oblique compression caused by the collision of the Qiantang block produced thrusting along the western margins of the Ordos and Sichuan basins (Watson et al., 1987). This deformation built mountain chains from the sediments to the west and south of the Ordos Basin. Erosion followed this uplift and generated incised valleys up to 300 m deep and kilometres wide that fed a basin wide drainage system flowing eastward. (Moore et al., 1986). The present day geothermal gradient is 22°C/km to 27°C/km (Zhao et al., 1995)

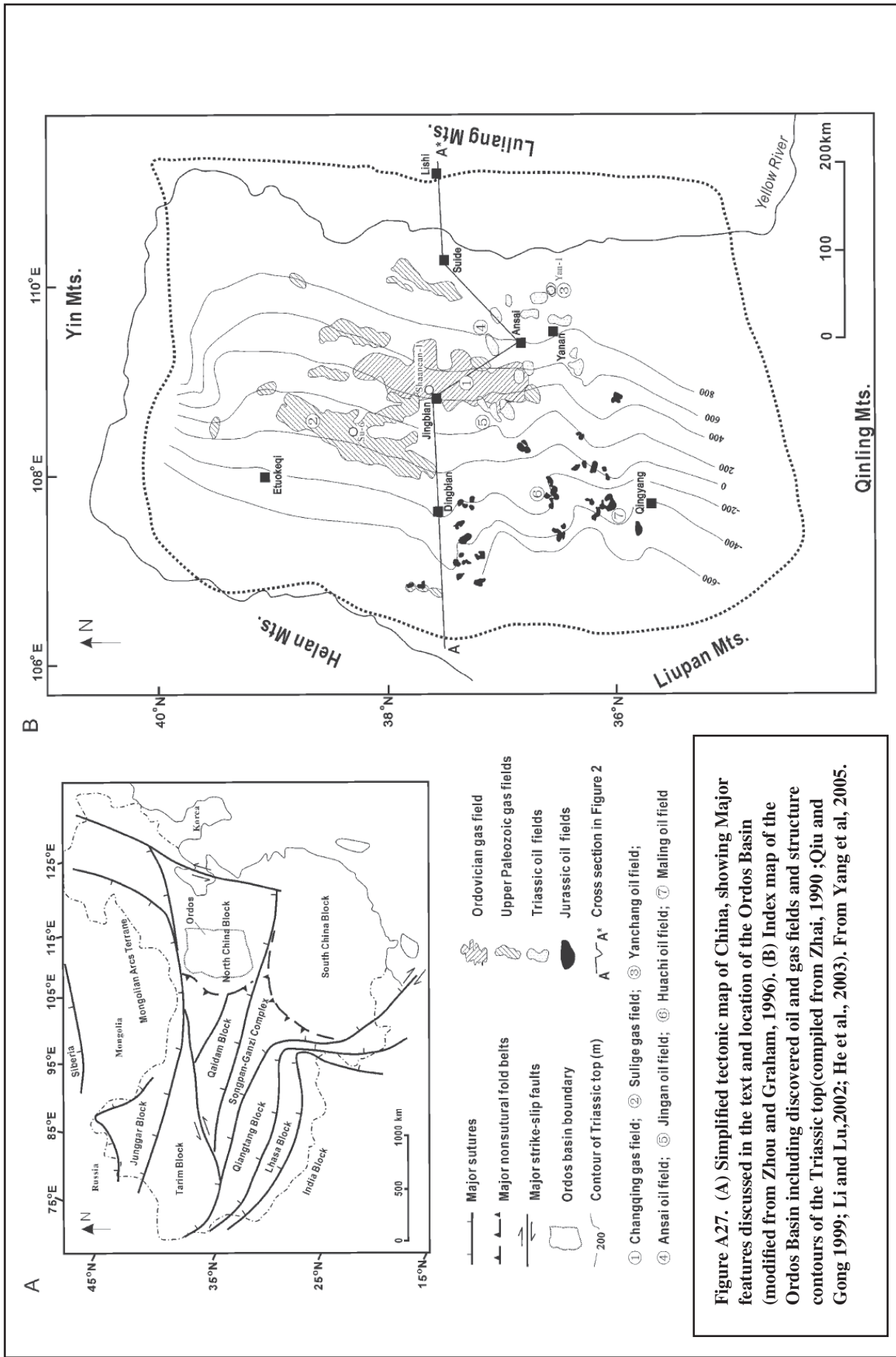


**Figure A27. (A)** Simplified tectonic map of China, showing Major features discussed in the text and location of the Ordos Basin (modified from Zhou and Graham, 1996). **(B)** Index map of the Ordos Basin including discovered oil and gas fields and structure contours of the Triassic top(compiled from Zhai, 1990 ;Qiu and Gong 1999; Li and Lu,2002; He et al., 2003). From Yang et al, 2005.

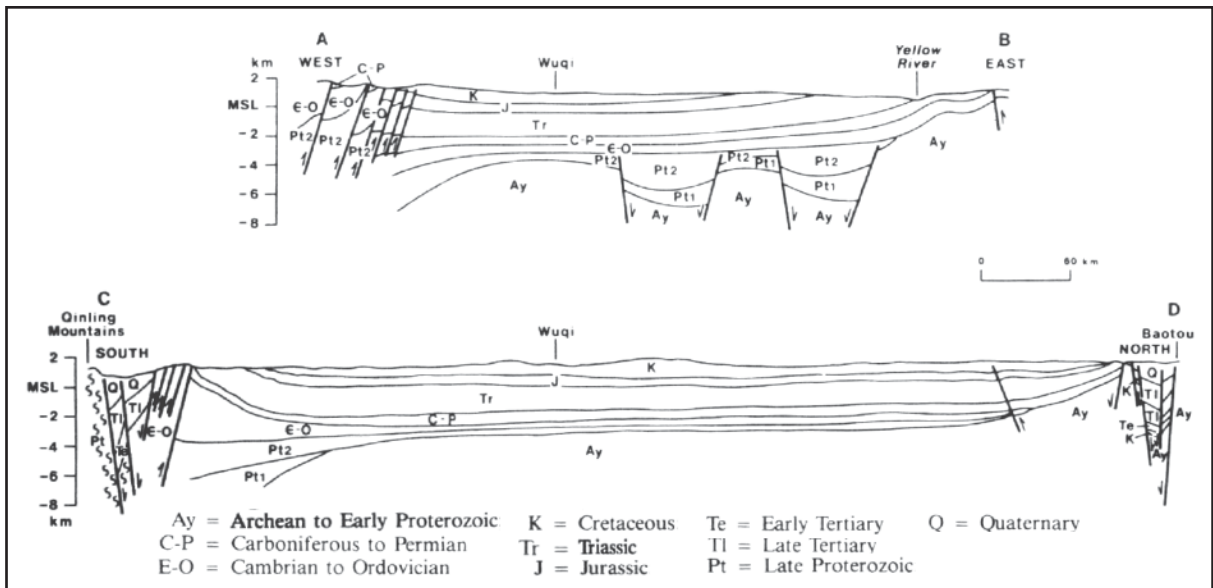


Figure A28. North-south and east-west cross-sections across the Ordos Basin (from Moore et al., 1986)

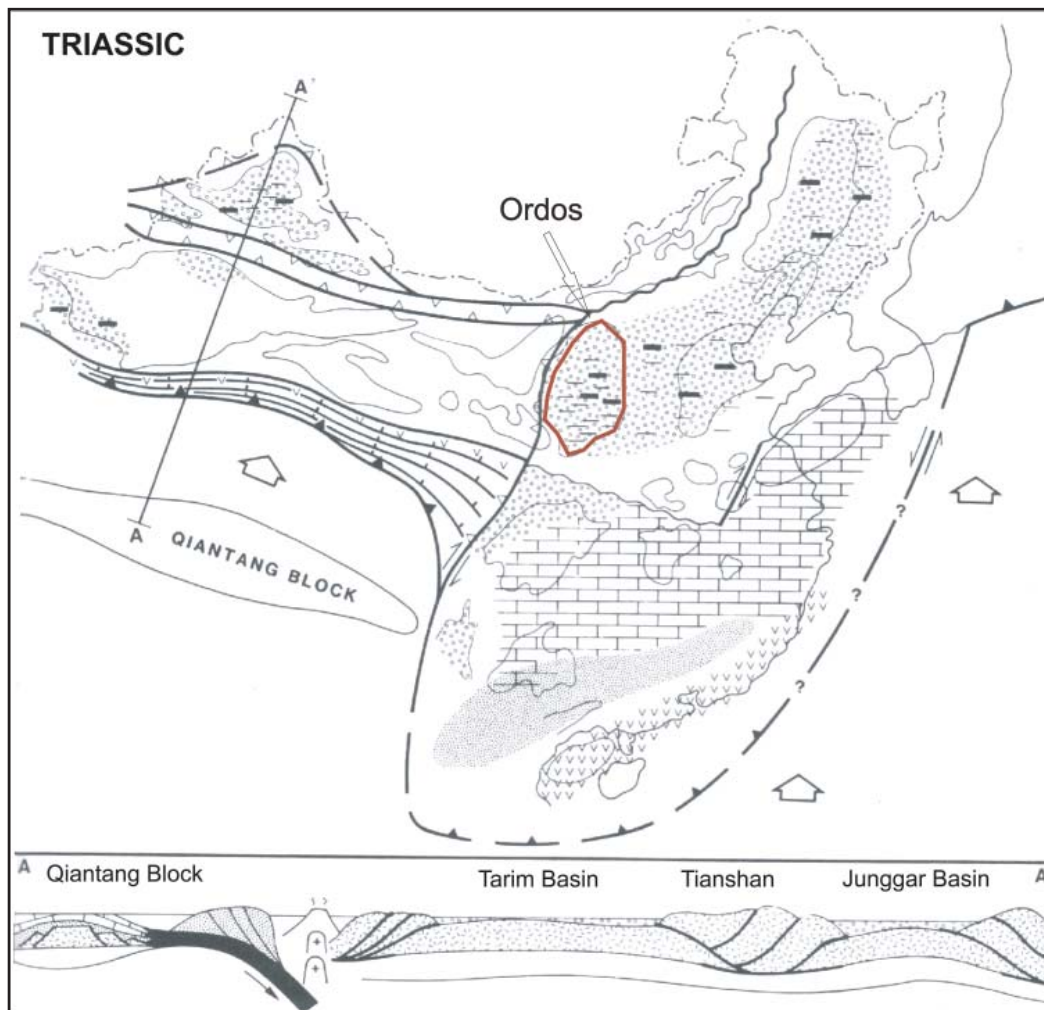


Figure A29. Plate tectonic reconstruction and sedimentary facies distribution for the Triassic (from Watson et al., 1987).

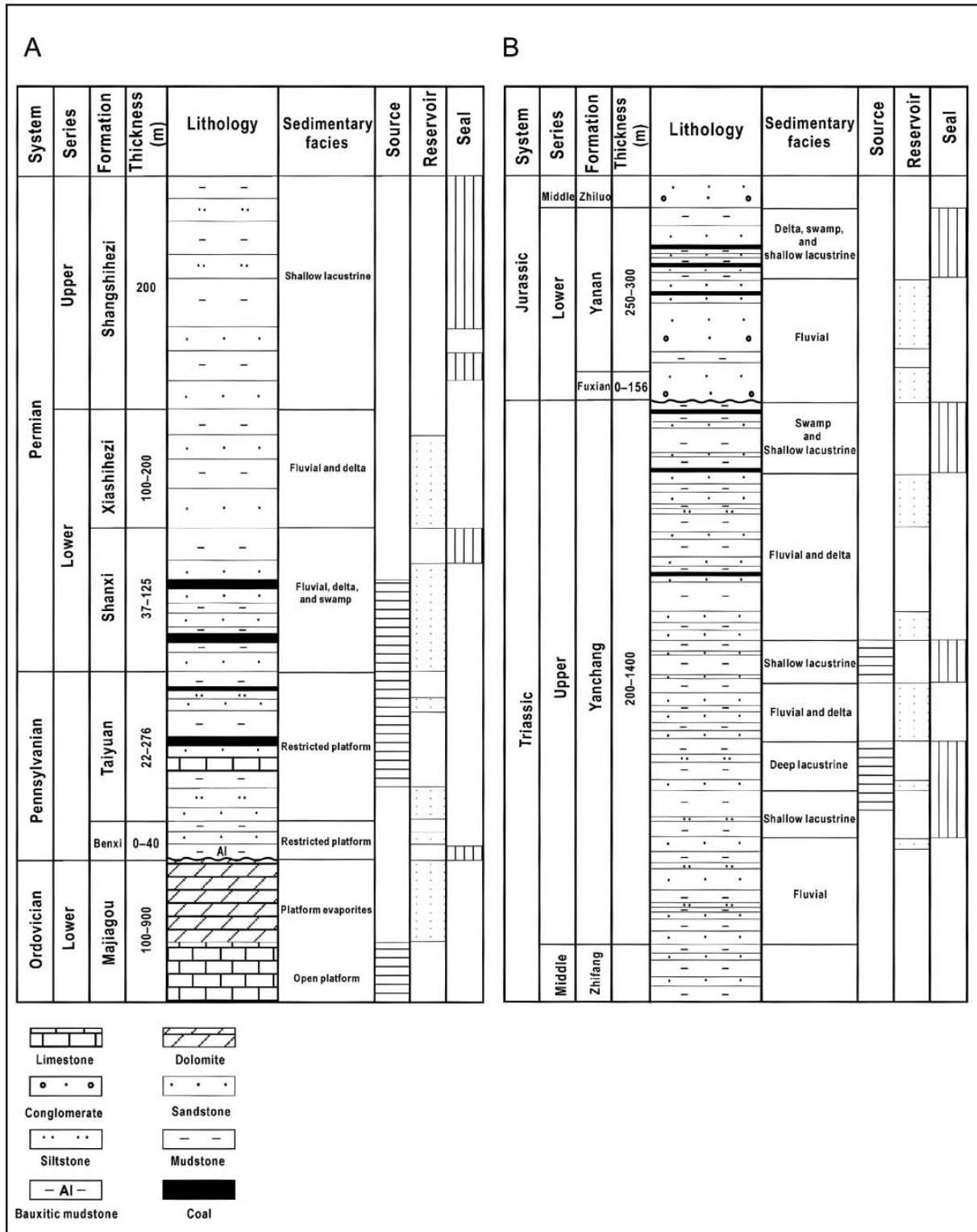


Figure A30. Stratigraphic columns, depositional environments, and source-reservoir-seal associations in the Ordos Basin (A) for the Lower Ordovician– Upper Permian (compiled from Zhai, 1990; Feng et al., 1998; Hong et al., 1998; He et al., 2003); (B) for the Upper Triassic–Lower Jurassic (compiled from Zhai, 1990; Wang 1998). This figure from Yang et al., 2005.

### A1.7.3 Basin Fill

Fluvio-lacustrine facies are persistent through the Late Permian to Cretaceous. Foreland subsidence driven by loading was spasmodic and rapid. This had a strong effect on the depositional patterns in the basin as palaeogeography maps in Figure A31 show. The change in depositional pattern between the Triassic and Jurassic may have created regional scale reservoir-seal pairs as the fluvial delta system of the Triassic gave way to a widespread silty floodplain facies. The locus of the Ordos depocentre through time is shown in Figure A32. It is apparent deep lake facies never occupied the north of the basin.

Upper Triassic and Lower Jurassic sandstone are reservoirs for hydrocarbons. The majority of reservoir rocks consist of sandstone and conglomeratic sandstone of fluvial origin in the Lower Jurassic Yanan and Fuxian Formations. Locally, where the sandstones are coarse grained and conglomeratic, the reservoir quality is good. However, most commonly the reservoir quality of the sandstone is fair to poor. Secondary reservoir rocks consist of fluvial, lacustrine delta and lacustrine turbidites sandstone in the Triassic Yanchang Formation. Typically these reservoirs have very low permeability values largely because of their fine to very-fine grain size and high feldspathic content (USGS, 2000).

“Thin, moderately continuous lacustrine shale and mudstone of the Upper Triassic and Lower and Middle Jurassic sequences are the best seal rocks.”(USGS, 2000).

Lacustrine shale and mudstone in the Upper Triassic Yanchang Formation is the dominant source rock. The composite thickness of the Yanchang source rock sequence is as much as several hundred meters. (USGS,2000). This formation should form a good ultimate seal for Lower Triassic fluvial-lacustrine sediments. Unfortunately the reservoir properties are poor.

Sun et al., (1989) provides the porosity and permeability data in Figure A33. Porosity and permeability are quite poor through-out the section. Injectivity appears to be a problem in this basin.

### A1.7.4 Hydrocarbon Fields

“Stratigraphic traps (facies-change and valley-fill varieties) and compaction anticlines formed over buried hills account for most of the traps for petroleum accumulations. Most of the fields are trapped on the gently westward-dipping homoclinal flank of the basin but several are trapped in anticlines along the thrust-faulted, western margin of the basin.”(USGS, 2000).

The estimated known oil reserve of the Ordos basin in 2000 was 602 mmbbls (USGS, 2000). This is equivalent to ~78 Mt of stored CO<sub>2</sub>. The largest oil field has 200 mmbbls ultimately recoverable. The modal size of known oil fields is 16-32 mmbbls (USGS, 2000). The small overall oil volume and small oil field sizes appear to have negative implications for the economics of depleted oil field storage.

Total known gas (produced plus reserve) was assessed as 5.6 Tcf (USGS, 2000). This is equivalent to 448 Mt of stored CO<sub>2</sub>. Figure A34 shows a large gas field called the Central gas field. The size of this field is unknown. It is assumed this field is a large very low permeability gas accumulation which currently has no economic value.

Details of gas field size could not be located. The USGS (2000) estimate of gas reserves for the Ordos Basin did not include size analysis.

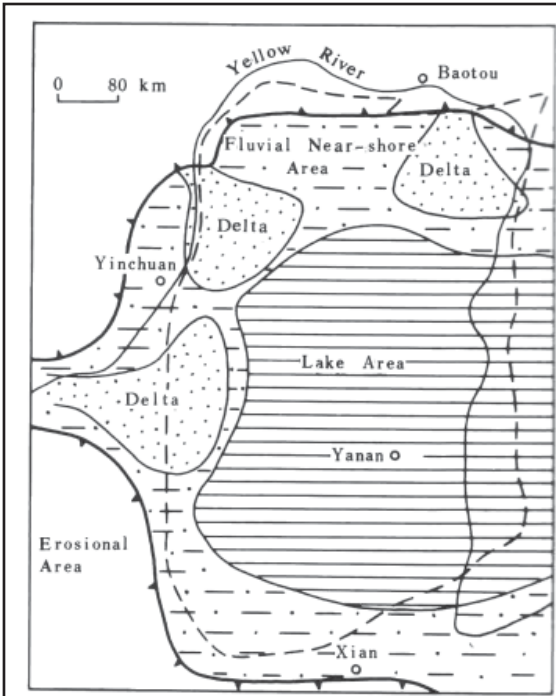


Fig. 7.8. The P<sub>1</sub>-P<sub>2</sub> paleogeography of the Ordos Basin (dotted line indicates the extent of the present-day basin).  
**PERMIAN**

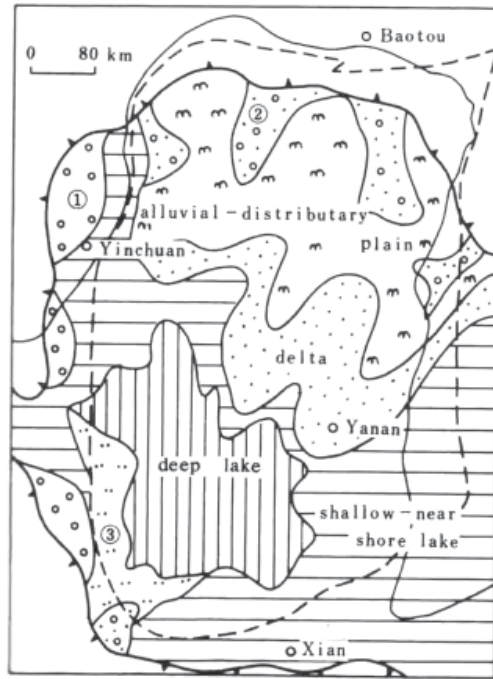


Fig. 7.10. The T<sub>3</sub> paleogeography of the Ordos Basin (1 = piedmont deposit; 2 = main course of river; 3 = sub-aqueous fan).  
**TRIASSIC**

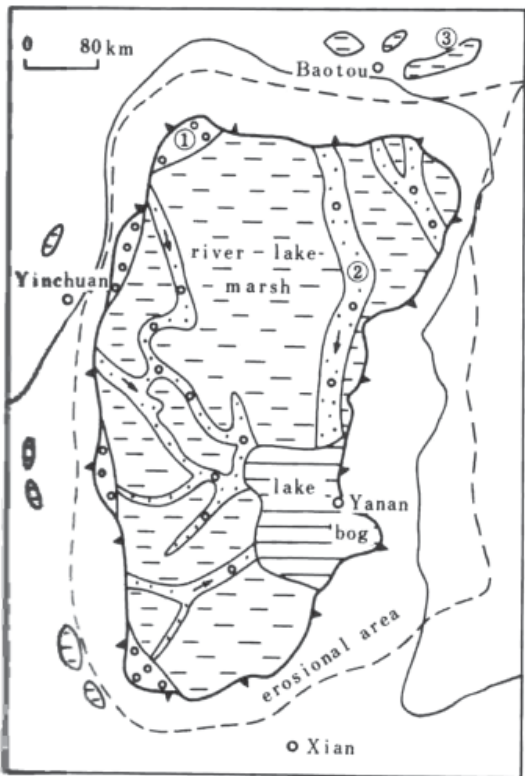


Fig 7.11 The J paleogeography of the Ordos Basin (1 = piedmont deposit; 2 = main course of river; 3 = sub-aqueous fan).  
**JURASSIC**

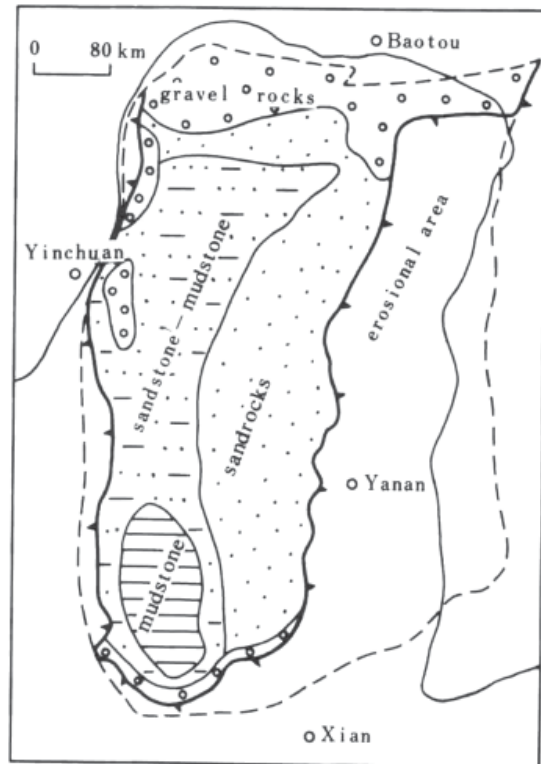


Fig. 7.12. The division of the K<sub>12</sub> sedimentation districts.  
**CRETACEOUS**

Figure A30. Paleogeography of the Ordos Basin from the Permian to cretaceous (from Sun et al., 1989).

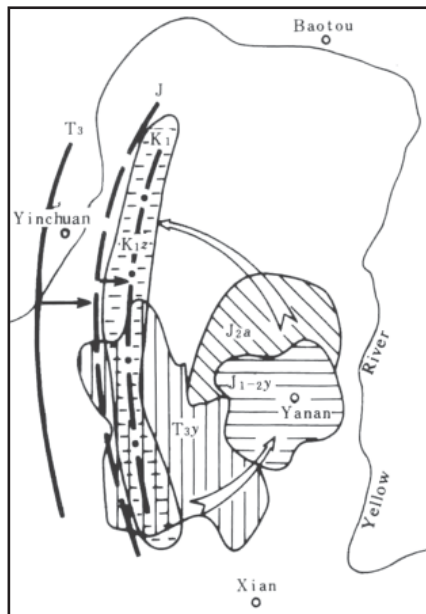


Figure A32. (above) Ordos Basin scheme showing the locus of the Mezoic depocenter (from Sun et al., 1989)

Figure A33. (right) Ordos Basin, porosity and permeability data.

Era	Sedimentary environment	Lithology	Porosity (%)	Permeability	Characteristics of pore texture	Distribution and thickness
N	fluvio-lacustrine	sandstone, conglomerate rocks				throughout the section
E	fluvio-lacustrine	sandstone, conglomerate rocks	12-18	0.43-3.76		several to tens of meters
K <sub>1</sub>	fluvio-lacustrine	sandstone, conglomerate rocks	7-12	2.6-4.9		
J <sub>2</sub>	lacustrine	marls	7-27	0.05		40 m
J <sub>1-2</sub>	fluvial	sandstone		10-50 (max. 6630)		several meters to 100 m
T <sub>3</sub>	fluvio-lacustrine	sandstone	10 (max. 20)	(max. 561)	micro-throat pore system dominated by intercrystalline pores, better in upper part	throughout the section
T <sub>1-2</sub>	fluvio-lacustrine	sandstone			intergranular, intercrystalline and intragranular pores with complicated textures of a wide range of variation	throughout the section
P <sub>2</sub>	shallow lacustrine	sandstone	10-20 (max. 25)	10 (max. 3688)		from a few meters to tens of meters; maximum thickness of 76 m for a single layer
P <sub>1</sub>	deltaic	sandstone				
O <sub>2-3</sub>	tidal flat	sandstone	~10(max. 18)	5 (max. 458)		throughout the section
O <sub>3</sub>	turbidite marine	dolomite	0.56	0.04	14 kinds of pores; the most important are intercrystalline and solution pores and fissures	throughout the basin; the dolomite is 650 m and the others near 1000 m in thickness
O <sub>1</sub>	marine	limestone	3.53	0.08		
e <sub>2-3</sub>	marine	limestone				
e <sub>1-2</sub>	marine	sandstone				
Z	marine	limestone, sandstone				> 1000 m

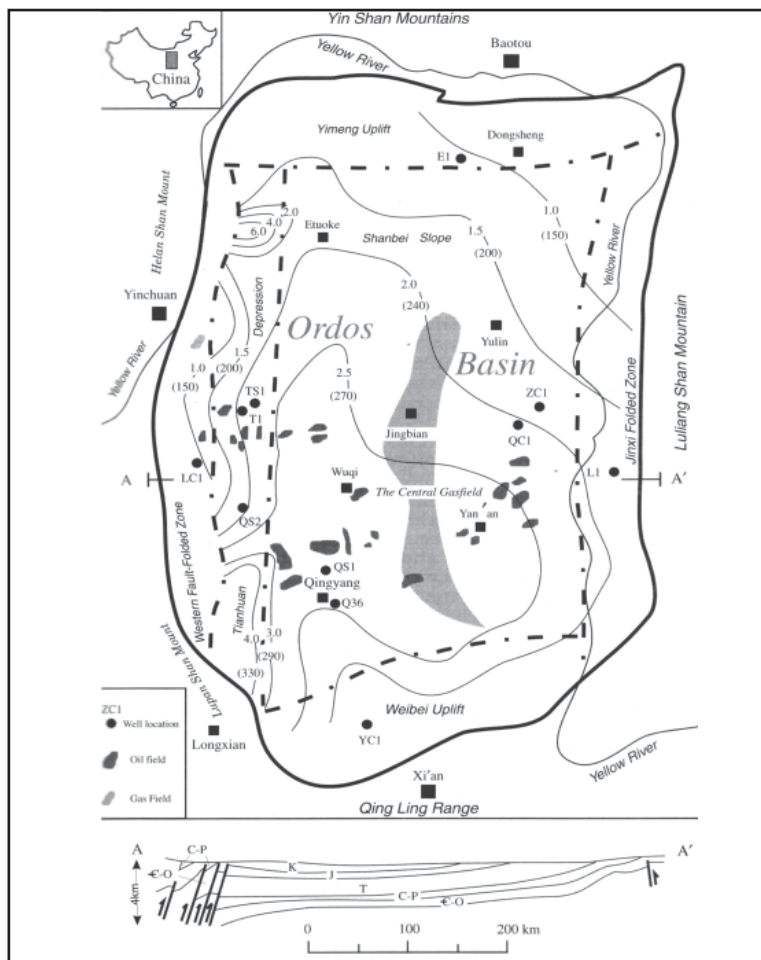


Figure A34. Location, cross-section and six structural units (separated by dashed line) of the Ordos Basin. Also shown are oil fields, gas fields, and locations of eleven wells from which experimental samples were obtained (from Zhao, 1996). This figure from Yaqng et al., 2005.

## A1.7.5 Coal Occurrence

Gas-bearing coal beds along the shallow eastern flank of the Ordos Basin are CBM and potential ECBM targets. These coal beds include the Upper Carboniferous Taiyuan Formation and Lower Permian Shanxi Formation source rocks that underlie large areas of the Ordos Basin. The net thickness of these predominately bituminous coal beds ranges from about 8 to 20 m. (USGS, 2000).

Most of the coal bed reservoirs are normally pressured but locally they may show either abnormally high or low pressures. It is unknown if the cleats provide the permeability necessary to produce the coal bed methane (USGS, 2000). The Permo-Carboniferous coal measures in the have been mature with respect to gas generation since about Early Cretaceous time. The coal bed methane is thermogenic. Typically, vitrinite reflectance (%Ro) values for the Permo-Carboniferous coal beds range from about 1.00 to 1.60.

Jurassic age coal measures within the Yanan Formation, although of low rank than the underlying Palaeozoic coals, are a potential ECBM target as many of the coal beds are thick and laterally continuous.

## A1.7.6 Potential CO<sub>2</sub> Storage Options

There appear to be several reservoir-seal pair options known from hydrocarbon exploration that might be exploited for deep reservoir storage of CO<sub>2</sub>. The shifts in the depocentre and the rearrangement of facies should create opportunity for reservoir-seal pairs. The Ordos is a shallow basin surrounded by mountains. Porosity and permeability is poor for all formations in the Mesozoic and Cenozoic. Fractured carbonates in the pre Triassic may provide an opportunity for storage. A cool geothermal gradient of 22 to 27°C/km will allow higher subsurface storage density.

The mean size of oil fields is relatively small at 16 to 32 million barrels and this may be a challenge to economic injection of CO<sub>2</sub> into depleted hydrocarbon traps. It is inferred from the data of Sun et al., 1989 (Figure A33) that the porosity and permeability of these fields is fair at best.

The large coal resources of the Ordos Basin could provide opportunities for ECBM or some form of CO<sub>2</sub> storage in coals seams.

## A1.7.7 References

Jenkins, C.D., Boyer, C.M., II, Fisher, R.D., Gobran, B.D., Shen J.B., and Zhang S., 1999, Reservoir characterization of the Hedong coal bed methane prospect, China, in Coal bed methane symposium proceedings [Tuscaloosa, Alabama, May 1999]: 13 p., 27 figs.

Moore, P. S., Hobday, D. K., Mai H., and Sun Z. C., 1986, Comparison of selected non-marine petroleum-bearing basins in Australia and China: Australian Petroleum Exploration Association Journal, v. 26, p. 285-309.

Sun Z. C., Xie Q. Y., and Yang J. J., 1989, Ordos Basin—A typical example of an unstable cratonic interior super-imposed basin, in Zhu X., ed., Chinese sedimentary basins: Sedimentary basins of the world: Elsevier, p. 63-75.

United States Geological Survey World Petroleum Assessment 2000

Watson, M. P., A. B. Hayward, D. N. Parkinson, and M. Zh. Zhang. Plate tectonic history, basin development and petroleum source rock deposition onshore China. Marine and Petroleum Geology 4[Aug], 205-225. 1987.

Zhao M.-W., Behr, H.J., Ahrendt, H., Wemmer, K., Ren Z.-L., and Zhao Z.-Y., 1996, Thermal and tectonic history of the Ordos Basin, China—Evidence from fission track analysis, vitrinite reflectance, and K-Ar dating: American Association of Petroleum Geologists Bulletin, v. 80, p. 1110-1134.

Yang, Y., W. Li, and L. Ma. Tectonic and stratigraphic controls on hydrocarbon systems in the Ordos Basin: A multicycle cratonic basin in central China. AAPG Bulletin 89[2], 255-269. 2005

## A1.8 Pearl River Mouth Basin

### A1.8.1 CO<sub>2</sub> Sources

CO<sub>2</sub> emissions within 300 km in the coastal region adjacent to the Pearl River Mouth Basin contributed approximately 336 Mt CO<sub>2</sub> /yr to China's estimated total stationary source CO<sub>2</sub> emissions of 2970 Mt/yr (IEA, 2000). This area includes Guangzhou and Hong Kong.

Note: The sum of sources within 300 km of a basin very crudely indicates the magnitude of emissions within reach of the basin. These “catchments” overlap for most basins and should not be summed.

### A1.8.2 Basin Overview

The Pearl River Mouth Basin (PRM) is a Cenozoic NE striking rift basin of Eastern China. The PRM's tectonic evolution is linked directly to spreading of the South China Sea and indirectly to the motion of the Pacific plate. The basin is 800 km long and 100-300 km wide (Figure A35), forming a total area is 147 000 sq km. The maximum sediment thickness is 10 km.

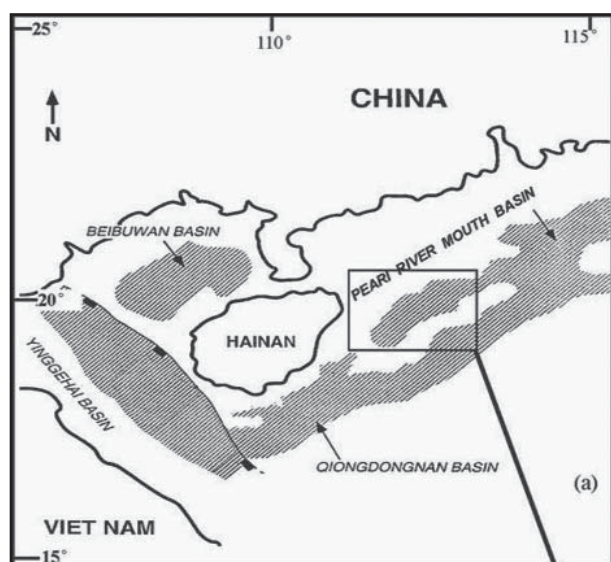


Figure A35. Location map of the Pearl River Basin and other South China Sea basins (Huang et al., 2003).

The basin is separated from the Tainan Basin by the Dongsha swell. The basin has six main structural elements, Zhu I, Zhu II, Zhu III sags, and the Dongsha, Shenhu and Panyu swells (Figure A36, Figure A37) (Guong et al., 1989) The geothermal gradient (in the Zhu III sag) is 33.7°C/km and 62.02 mW/m<sup>2</sup> (Zhu et al., 1999).

The PRM has the three developmental stages typical of rift basins;

- 1) Early rift - Late Cretaceous to Early Oligocene. In the late Cretaceous the beginning of sea floor spreading in the South China Sea initiated localised rift valleys. These were rapidly in filled as erosion occurred to balance tectonic and isostatic uplift. At the end of the Palaeocene crustal extension was manifested as graben formation.
- 2) “Syn” rift - Late Oligocene to Early Miocene. During this phase extension sag and faulting continued. Ultimately the individual rifts (lakes) of the early phase were united into the PRM Basin. Guong et al., (1989) concur with earlier workers that the 50-11 magnetic stripes in the South China sea are directly linked to this episode of the basins history. Marine transgression was ongoing in this phase.
- 3) Thermal sag - Mid Miocene to Quaternary. Basin wide subsidence occurred. Marine transgression continued.

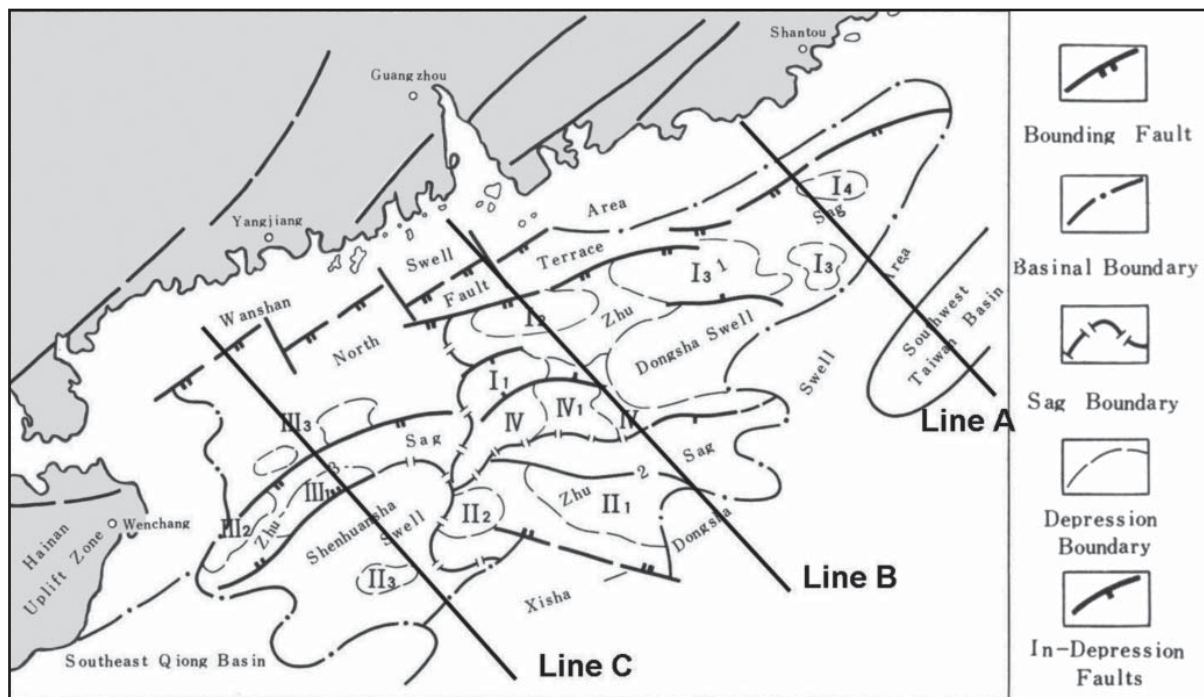


Figure A36. Location and tectonic element map of the Pearl River Mouth Basin (depressions: I<sub>1</sub> = Enping; I<sub>2</sub> = Xijiang; I<sub>3</sub> = Huizhou; I<sub>4</sub> = Lufeng; II<sub>1</sub> = Baiyun; II<sub>2</sub> = Kaiping; II<sub>3</sub> = Sunde; III<sub>1</sub> + Wenchang; III<sub>2</sub> = Qionghai; III<sub>3</sub> = Yangjiang; IV<sub>1</sub> = Panyu; lower-relief zone: Panyu low relief zone). Approximate location of cross-sections added (from Guong et al., 2003).

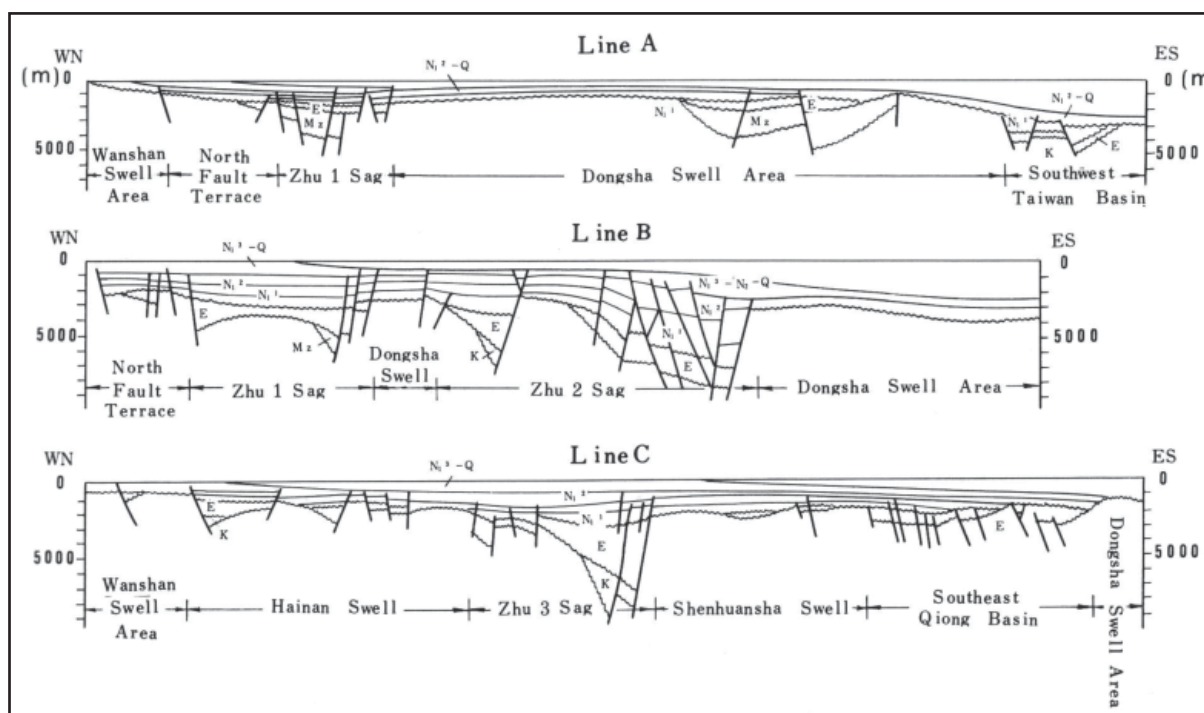
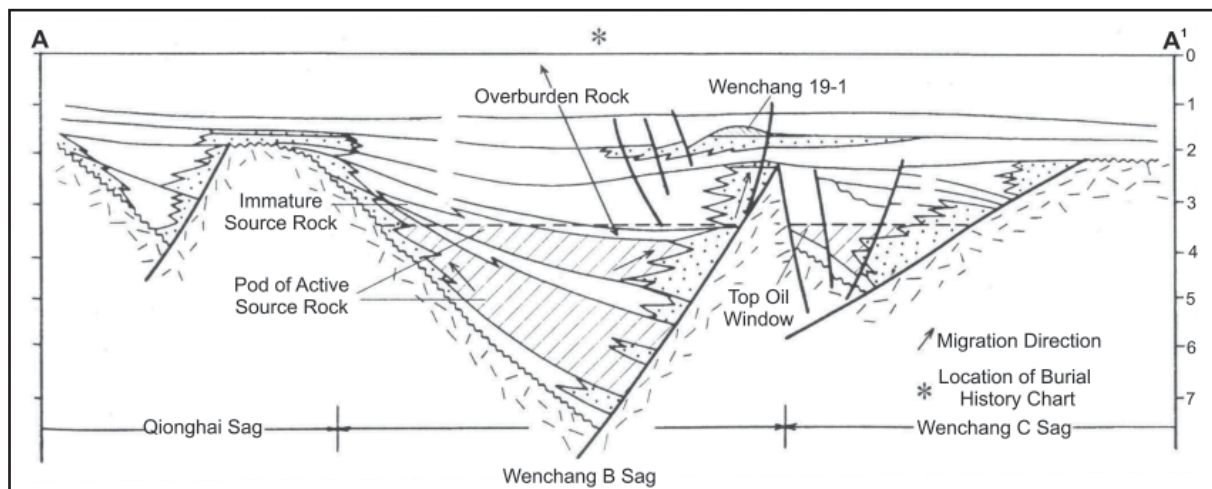


Figure A37. Structural profile of the Pearl River Mouth Basin (from Guong et al., 1989).

### A1.8.3 Basin Fill

An appreciation of the structure and fill of the PRM can be gained by matching the stratigraphy of Figure A36 with the detailed graben section in Figure A38.



**Figure A38. Cross-section through the Wenchang B sag showing the formation of oil accumulations in the Wenchang-Zhuhai Petroleum system (from Zhu et al., 1999).**

Wenchang and Enping (Eocene-Oligocene) formations developed during the early rift stage of the basin and consist of lacustrine facies. Shales in the Wenchang Formation are believed to be oil source rocks. Coal which developed in the more widespread Enping Formation is thought to contribute as a source rock for gas accumulations. A coarsening up sequence is observed in the Enping Formation, suggesting a “filling” phase in the lakes. The intensified faulting of the “syn” rift stage created an unconformity before increasing accommodation space and unifying the lake half grabens into one shallow marine basin system. (Figure A39, Figure A40, Figure A41)

The Zhuhai Formation was deposited in shallow water as a sandy, wave or fluvial dominated delta-shelf system (Chen et al., 1994). Sheet like sand sandstones are common, presumably due to periods of wave dominated deposition. The formation contains very little mudstone. Oil has been observed in the upper part of the formation where it is sealed by mudstone in the Zhujiang Formation (Chen et al., 1994). The Zhuhai has a maximum thickness of 1500 m. Lithology is mainly glauconitic quartzose sandstone and arkosic quartzose sandstone. Data from the Wenchang 19-1 oil field has a porosity range from 20 to 30%, averaging 25%, with permeability of 363 mD (Zhu et al., 1999). (Figure A42, Figure A43)

The overlying Zhujiang Formation was also deposited in a delta and shelf environment (Chen et al., 1994). Ongoing transgression resulted in somewhat deeper water environment of deposition than during the Zhuhai Formation deposition. Deeper water environment of deposition appear to have decreased the sandstone/mudstone ratio to 1:2. A maximum porosity and permeability measured in Wenchang 19-1 oil field was 36% porosity and 451 mD (Zhu et al., 1999). Carbonate platform reef facies developed on the Dongsha swell at this time (Figure A44, Figure A45).

In general the environment of deposition of the Hanjiang Formation is similar to that of the Zhujiang Formation occurring in a continuing overall transgression (Chen et al., 1994). The Upper Hanjiang has good seal potential, according to Chen et al., 1994, “the thick shelf mudstone, interbedded with offshore bar sandstones, would be one of the better regional seals in the study area” (Figure A46).



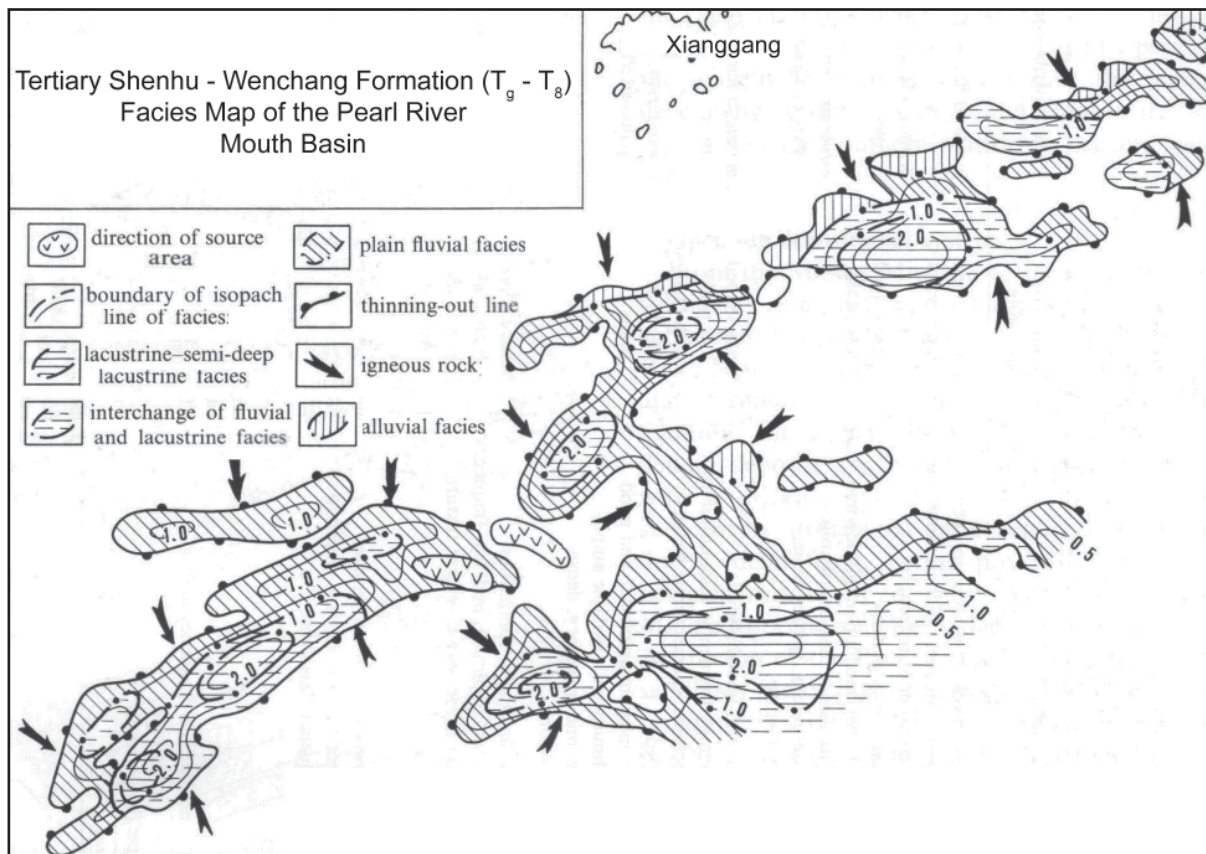


Figure A40. Tertiary Shenhu-Wenchang Formation ( $T_9-T_8$ ): facies map of the Peral River Mouth Basin (from Guong et al., 1989).

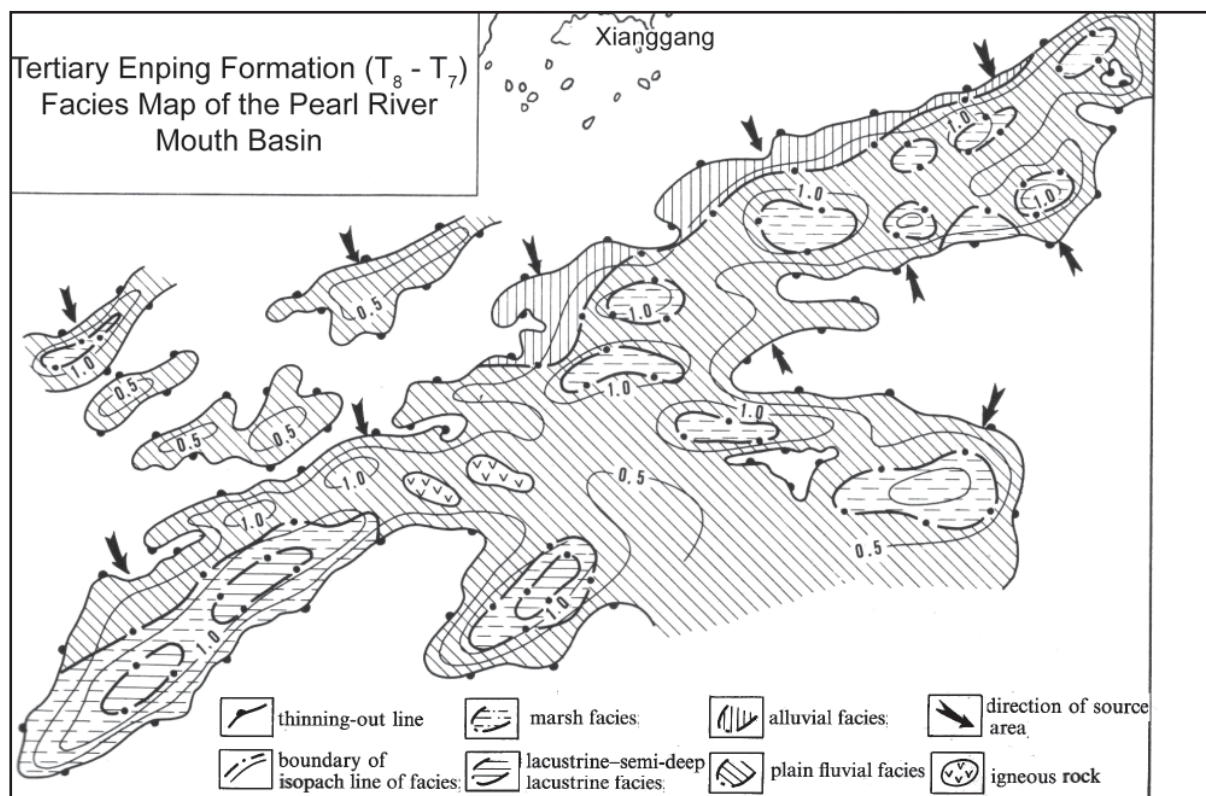


Figure A41. Tertiary Enping Formation ( $T_8-T_7$ ): facies map of the Peral River Mouth Basin (from Guong et al., 1989).

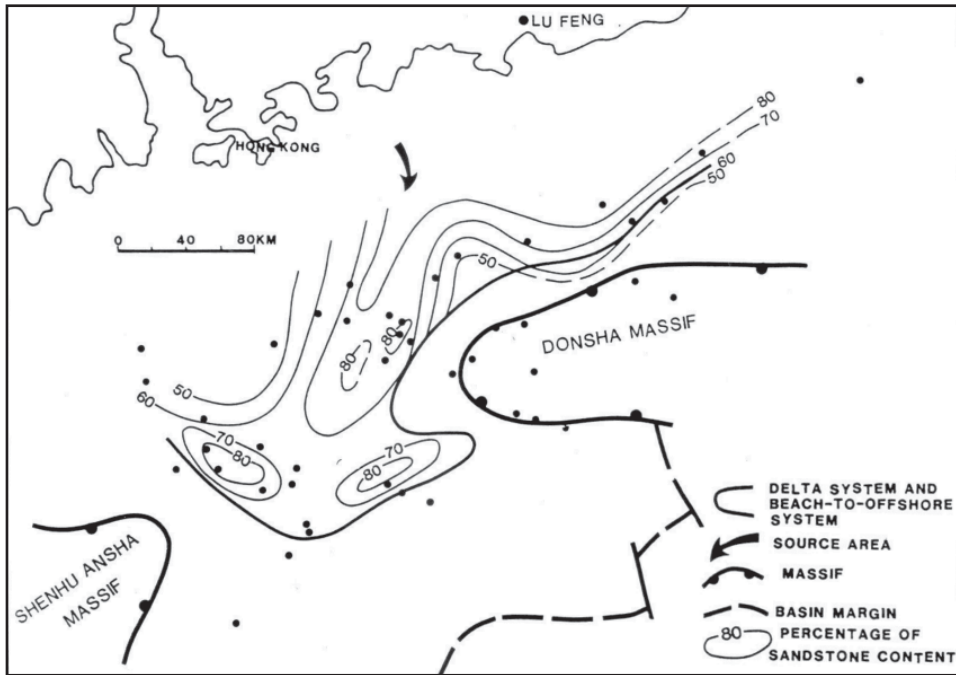


Figure A42. Delta systems in the Lower Zhuhai Formation (from Chen et al., 1994).

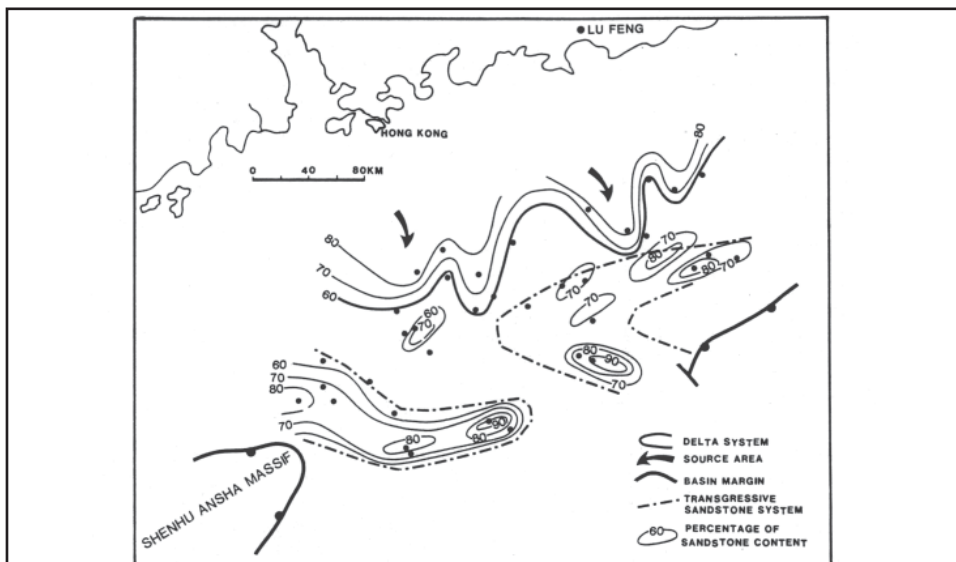
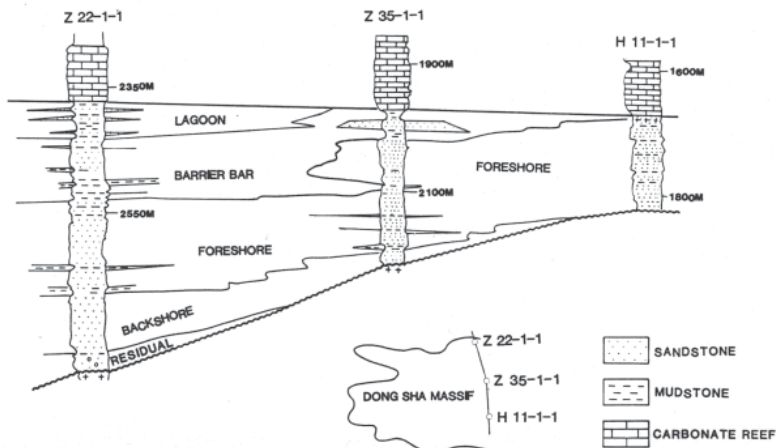


Figure A43. Sandstone distribution in the Upper Zhuhai Formation.

Destructive delta systems and transgressive sandstone sequences in Upper Zhuhai Formation.



Transgressive sandstone profiles across the Dong Sha Massif in the Upper Zhuhai Formation.

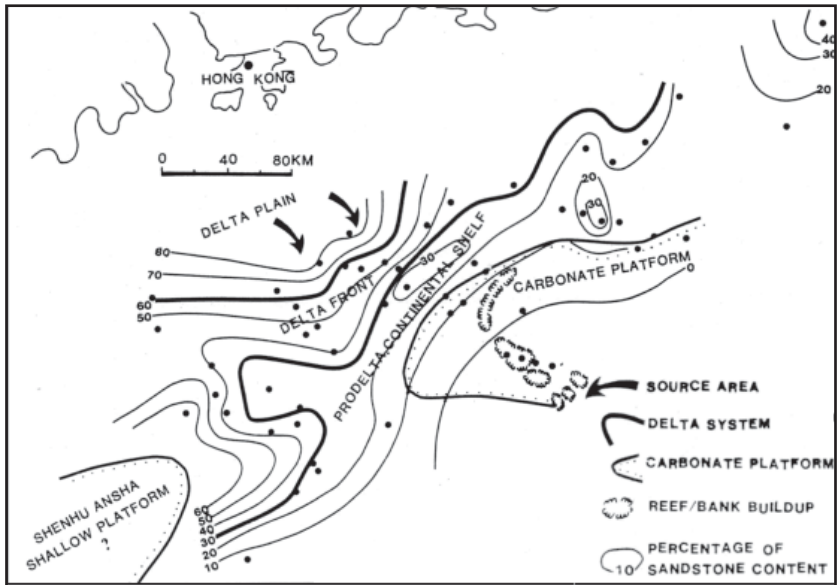


Figure A44. Sandstone distribution in the Middle Zhujiang Formation (from Chen et al., 1994).

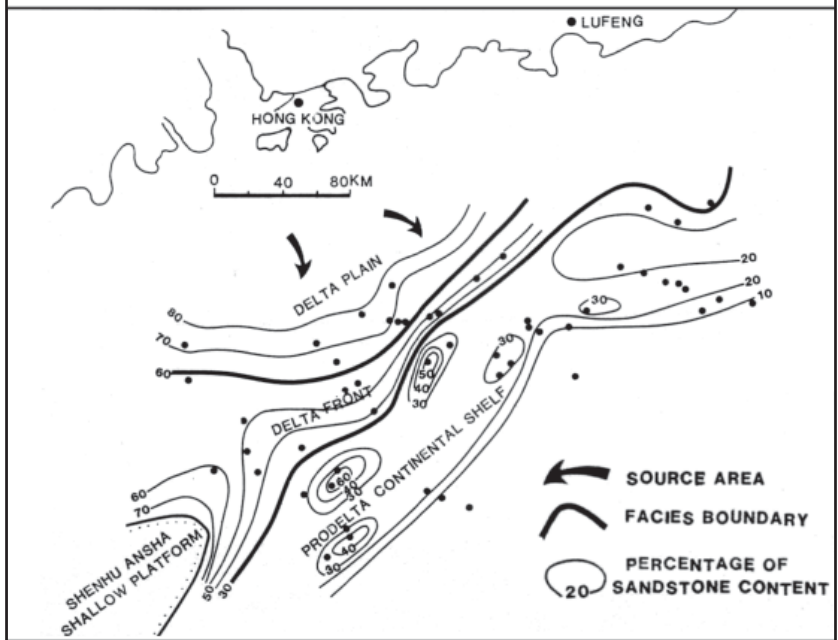
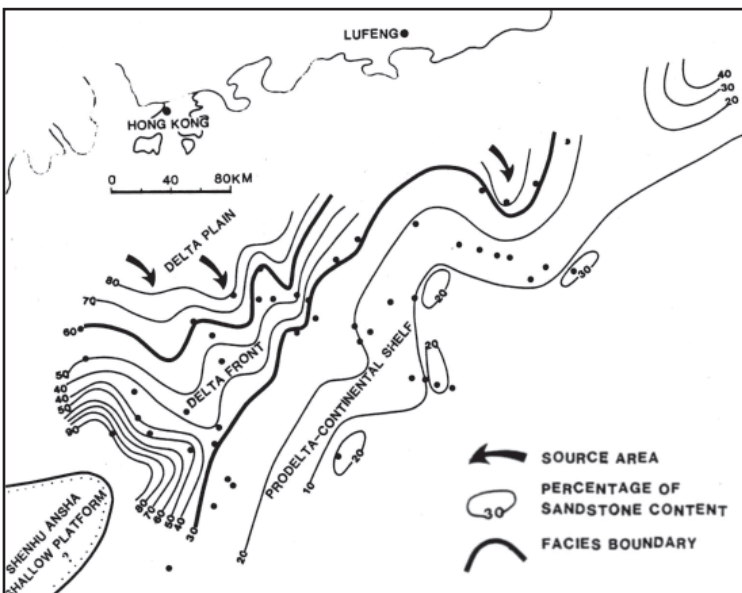


Figure A45. Sand distribution in the delta systems of the Upper Zhujiang Formation (from Chen et al., 1994).



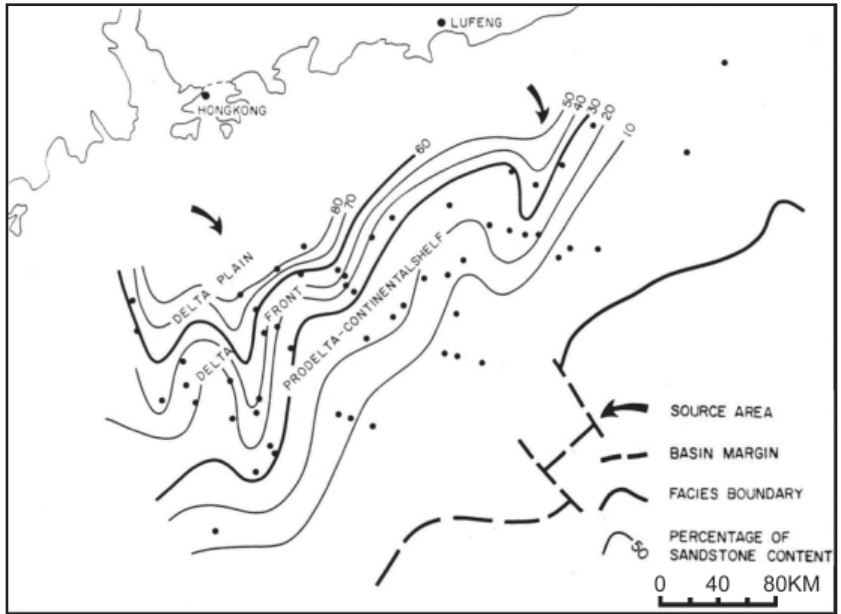


Figure A46. Sandstone distribution in the delta system of the Lower Hanjiang Formation (from Chen et al., 1994).

Landward migration of sequence onlaps from the Early Miocene to Quaternary is interpreted as an overall transgressive trend (Figure A47). Nie et al., (2000) sketched a migration of the shore line through the Tertiary (Figure A48) General transgression provides the opportunity for extensive seal areas however the actual presence of such seals seems doubtful. The basin changed from a fluvial-lacustrine setting to a semi closed marine (bay?) setting between the deposition of the Enping and Zhuhai Formations. Another major facies shift occurred between the Zhujiang to Hanjiang Formations as the basin became dominated by open marine environments.

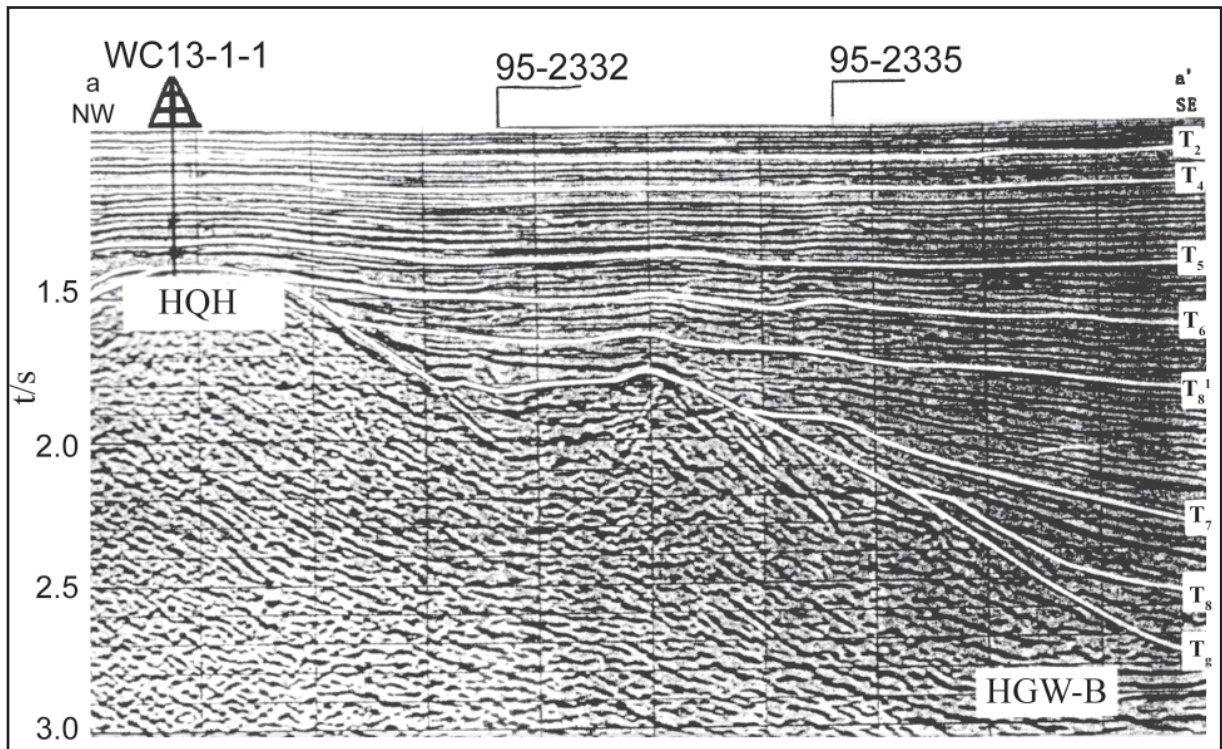


Figure A47. Zhuhai and Zhujiang Formations onlapping and draping the basement on horst Qionghai (a-a' from seismic line Zhu III depression. From Nie et al., 2000.

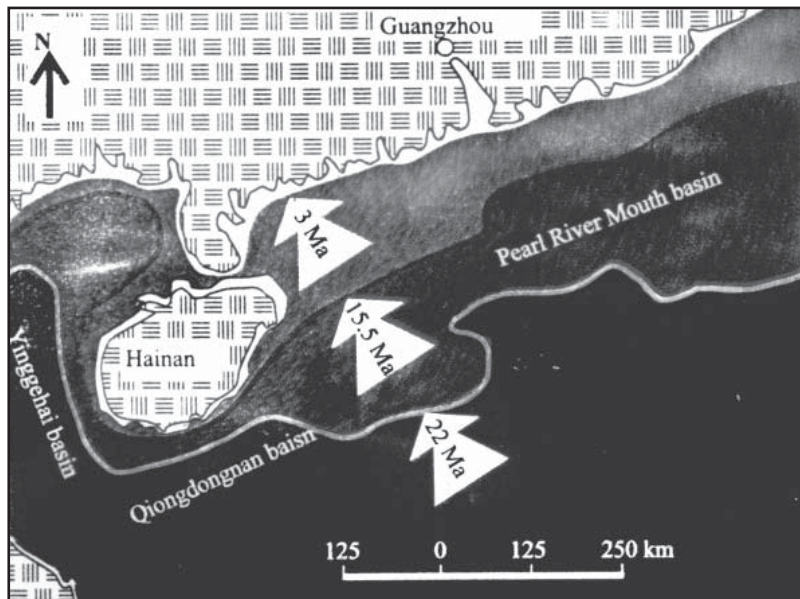


Figure A48. Sketch map showing shoreline migration as rise in sea level (from Nie et al., 2000)

### A1.8.4 Hydrocarbon Fields

The USGS did not assess this basin. No detail on fields in the PRM was located in the literature. It appears the Zhuhai delta sand bodies have good reservoir properties in the Wenchang 19-1 oil field (Zhu et al., 1999). Hydrocarbon potential appears to be limited mainly by charge.

From the limited data available the fields in the Pearl River Basin appear to be modest in size ranging from 3 to 64 mmboe. Chen et al., (1994) predicted that most of the hydrocarbon yet to be found would be located in subtle stratigraphic traps very close to active source rocks. There is not sufficient information to assess this prediction.

However it seems that this basin is not characterised by giant fields. It seems unlikely that depleted hydrocarbon trap space in the PRM will be a material factor in CO<sub>2</sub> storage.

### A 1.8.5 Coal Occurrence

Coal seams are present in the Early Tertiary Enping Formation.

### A1.8.6 Potential CO<sub>2</sub> Storage Options

There are several CO<sub>2</sub> storage options to consider: There may be the possibility to inject into enhanced porosity on the palaeo-crest of buried basement topography. Aside from the basement itself there are locations, such as the Dongsha swell, where platform reefs have formed. These might provide pore space. Seal could be provided either by sealing facies within reef build-ups or by draped prodelta shale (of the Hanjiang Formation for example).

In the grabens of the PRM Early Cretaceous alluvial deposits may have good injectivity. There is overpressure within these grabens, and while this preserves porosity, it will also complicate injection of CO<sub>2</sub> (Figure A38).

There are several reasons to infer that reservoir quality is generally good, particularly in the delta sections of the Zhuhai, Zhujiang and Hanjiang Formations. Palaeogeography interpretations by Guong et al., (1989) and Chen et al., (1994) suggest sandstone is wide spread. Average porosity and permeability from Wenchang field shows reservoir quality can be good. Reworking of sands is expected in a delta environment with marine wave action and a generally transgressive nature. The presence of wide spread potential mudstone seal rocks can also be interpreted from the palaeogeography.

Unfortunately the quality of these potential seal rocks may be poor. Chen et al., (1994) terms transgressive events as “destructive” delta systems and notes “They provide more sandstones and less mudstones. The thick and extensive shelfal mudstones in each formation are generally silty, hard and fragile. Ductile mudstones are poor in all three formations” (i.e. Zhuhai Formation to Hanjiang Formation).

However work by Zhu et al., (1999) suggests part of the Hanjiang Formation may provide a regional ultimate seal over the delta sandstones of the Zhuhai and Zhujiang Formations (Figure A39). The base of the Hanjiang Formation is near 1 km in depth.

Large scale fault bound structures do not appear to be a feature of the basin. Most hydrocarbons are trapped in structures draped over basement.

There are apparently no giant fields in the basin. The known hydrocarbon trap pore space is assumed to be low in relation to stationary CO<sub>2</sub> emissions.

Coal is present, however the sub sea location means it is very unlikely to be useful as a storage resource.

Overall the basin appears to have a great deal of reservoir potential but seal quality may be poor prior to the Hanjiang Formation. Large effective hydrocarbon traps are not a feature. Geothermal gradient is not high. Overpressure occurs only in the deeper rift sections. As in many areas a base regional seal map will be important in assessing CO<sub>2</sub> storage potential and risks.

## A1.8.7 References

Chen, J., S. Xu, and J. Sang. The depositional characteristics and oil potential of paleo Pearl River delta systems in the Pearl River mouth Basin, South China Sea. *Tectonophysics* 235[1-2], 1-11. 1994.

Nie, F., Li, S., Xie, X., Wang, H., Zhu, Wu, K., and Jiang, M. Lateral migration pathways of petroleum in the Zhu III subbasin, Pearl River Mouth Basin, South China Sea. *Marine and Petroleum Geology* 18[5], 561-575. 2001.

Guong, Z., Jin, Q, Qiu, Z., Wang, S. and Meng, J. Geology tectonics and evolution of the Pearl River mouth Basin. In: Zhu, Xia (ed.), *Chinese sedimentary basins*. Elsevier Sci. Publ.. Amsterdam, Netherlands , 181-196. 1989.

Huang, B., X. Xiao, and M. Zhang. Geochemistry, grouping and origins of crude oils in the Western Pearl River Mouth Basin, offshore South China Sea. *Organic Geochemistry* 34[7], 993-1008. 2003.

Li, P. and C. Rao. Tectonic characteristics and evolution history of the Pearl River Mouth Basin. *Tectonophysics* 235[1-2], 13-25. 1994.

Li, S., X. Xie, H. Wang, W. Zhu, and K. Wu. Study on basin-filling and reservoir sedimentology of Zhu III Depression of Pearl River Mouth Basin, South China Sea. *Journal of China University of Geosciences* 11[1], 37-46. 2000.

Zhang, C., S. Li, J. Yang, S. Yang, and J. Wang. Petroleum migration and mixing in the Pearl River Mouth Basin, South China Sea. *Marine and Petroleum Geology* 21[2], 215-224. 2004.

Zhang, S., D. Liang, Z. Gong, K. Wu, M. Li, F. Song, Z. Song, D. Zhang, and P. Wang. Geochemistry of petroleum systems in the eastern Pearl River Mouth Basin: evidence for mixed oils. *Organic Geochemistry* 34[7], 971-991. 2003.

Zhu, W., M. Li, and P. Wu. Petroleum systems of the Zhu III Subbasin, Pearl River Mouth Basin, South China Sea. *AAPG Bulletin* 83[6 ], 990-1003. 1999.

## A1.9 Sanshui Basin

### A1.9.1 CO<sub>2</sub> Sources

The Sanshui Basin underlies the city of Guangzhou. CO<sub>2</sub> emissions in the region directly overlying the Sanshui Basin contributed approximately 15 Mt CO<sub>2</sub>/yr to China's estimated total stationary source CO<sub>2</sub> emissions of 2970 Mt/yr (IEA, 2000). While this number is relatively small there are sources totalling approximately 112 Mt CO<sub>2</sub>/yr within a 110 km radius of the basin. This area contains Guangzhou and Hong Kong.

Note: The sum of sources within a given radius of a basin very crudely indicates the magnitude of emissions within reach of the basin. These "catchments" overlap for most basins and should not be summed.

### A1.9.2 Basin Overview

The southern fold belt of China contains smaller basins such as the Sanshui, Boise and others. Little detail regarding these basins can be found in English language publications. Most of this information comes from the USGS (1988). The Sanshui Basin is 2600 sq km in area and is 2 to 3 km deep. The basin contains Palaeogene to Quaternary rocks that include sandstones, mudstones, evaporites and volcanics. A geothermal gradient of 31 to 45°C/km was reported by USGS (1988).

### A1.9.3 Basin Fill

No stratigraphic column of detailed discussion of stratigraphy was located. The Sanshui contains some salt bearing formations between the Cretaceous and the Palaeogene (Chen et al., 1989).

### A1.9.4 Hydrocarbon Fields

There are small accumulations of oil. Little is known about them. Naturally occurring CO<sub>2</sub> generated from igneous rocks is trapped in very pure accumulations (99.5%)

### A1.9.5 Coal Occurrence

No information was located regarding coal occurrence. The presence of salt bearing formations in the Cretaceous and Palaeogene would suggest a region that was too arid to produce coals.

### A1.9.6 Potential CO<sub>2</sub> Storage Options

Injection of CO<sub>2</sub> may well be possible in the Sanshui Basin. There are sandstone reservoirs and mudstone and evaporite seal rocks. Traps containing hydrocarbon and natural suggest the basin may have some potential for anthropogenic CO<sub>2</sub> storage. The basin is very close to large sources of CO<sub>2</sub>.

## A1.9.7 References

Chen, Fajing; Dai, Shizhao, and Pan , Guoen. The Cretaceous-Paleogene Salt-Bearing Basins in Eastern China. In: Zhu, Xia (Ed.), Chinese Sedimentary Basins. Elsevier Sci. Publ.. Amsterdam, Netherlands. 1989; 137-146.

Lee, K. Y. and C. D. Masters. Geologic framework, petroleum potential, and field locations of the sedimentary basins in China. Miscellaneous Investigations Series - U. S. Geological Survey, 1988.

## A1.10 Shiwan Dashan Basin

### A1.10.1 CO<sub>2</sub> Sources

CO<sub>2</sub> emissions in the region directly overlying the Shiwan Dashan Basin contributed approximately 5 Mt CO<sub>2</sub>/yr to China's estimated total stationary source CO<sub>2</sub> emissions of 2970 Mt/yr (IEA, 2000). In a 300 km radius from the basin there are sources totalling approximately 123 Mt CO<sub>2</sub>/yr.

Note: The sum of sources within 300 km of a basin very crudely indicates the magnitude of emissions within reach of the basin. These "catchments" overlap for most basins and should not be summed.

### A1.10.2 Basin Overview

Basin area is 11,600 sq km.

### A1.10.3 Basin Fill

Little stratigraphic information was available. The basin contains bitumen and oils (?) within Triassic carbonates.

"In the basin, the T1 stratum consisting of marine Carbonates carbonate rocks is the main source of hydrocarbon accumulations. It is characterized by a great thickness, wide distribution and high abundance of organic matter at a level of moderate maturity. There are many oil seepages and solid bitumens in the stratum at north margin of the basin, because of tectonic activities (Gao and Chen, 1998). In the Shiwan Dashan basin, the T1 stratum consists of 61 layers of gray and oolitic limestones with 250 m thickness. Above the stratum are the middle Triassic (T2) rocks consisting of green shale and shale-arenite with thickness >300 m, or in some part are the Jurassic rocks consisting of gray-green mudstone and interbeds of purplish red mudstone and siltstone (>60 m). Below the T1 stratum, there is upper Permian (P2) stratum consisting of gray mudstone, bioclastic limestone and sandy mudstone (>300 m)." (Gao et al., 2001)

### A1.10.4 Hydrocarbon Fields

It is unclear whether this basin is a commercial hydrocarbon basin. Bitumen and oil seeps are found in the basin (Gao et al., 2001).

### A1.10.5 Coal Occurrence

Unknown.

### A1.10.6 Potential CO<sub>2</sub> Storage Options

Unclear. Expected to be limited.

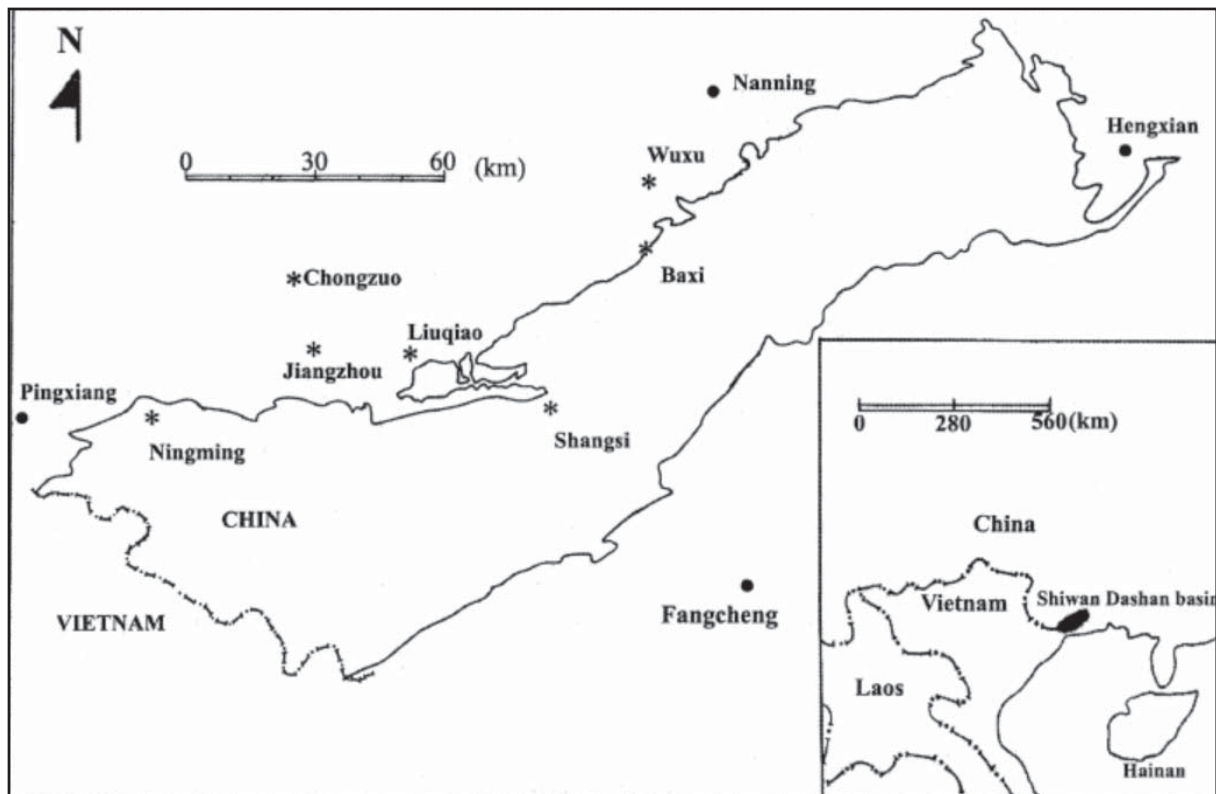


Figure A49. Location of the Shiwandashan Basin with towns and cities marked (from Gao et al., 2001).

### A1.10.7 References

Gao, Z.-N., Chen, Y.-Y., and Niu, F. Compressively matured solid bitumen and its geochemical significance. *Geochemical Journal* 35, 155-169. 2001.

## A1.11 Sichuan Basin

### A1.11.1 CO<sub>2</sub> Sources

CO<sub>2</sub> emissions in the region directly overlying the Sichuan Basin contributed approximately 127 Mt CO<sub>2</sub> /yr to China's estimated total stationary source CO<sub>2</sub> emissions of 2970 Mt/yr (IEA, 2000).

In a 300 km radius from the basin there are sources totalling approximately 431 Mt CO<sub>2</sub>/yr.

Note: The sum of sources within 300 km of a basin very crudely indicates the magnitude of emissions within reach of the basin. These "catchments" overlap for most basins and should not be summed.

### A1.11.2 Basin Overview

The Sichuan Basin has a polyphase history with a combined sedimentary thickness of 6 to 12 km (Wang et al., 1989) and an area of 230,000 sq km (Figure A50). Approximately 1 to 3 km of uplift and erosion has occurred in the Sichuan Basin since the early Palaeogene (USGS, 2000). An east-west section (Figure A51, Figure A52) shows a basin with a thrust/suture zone to the west and a folded eastern side. The Ordos and Sichuan basins were initiated as extensional basins and later compressed east to west and north to south becoming foreland settings. There was a shift from marine carbonate deposition to non-marine clastic deposition during the Late Triassic of the Sichuan Basin (Watson et al., 1987). From Wang et al., (1989) it appears there was a lacustrine depositional system from the Jurassic to Cretaceous. The present day geothermal gradient is 22 to 27°C/km (USGS, 1988).

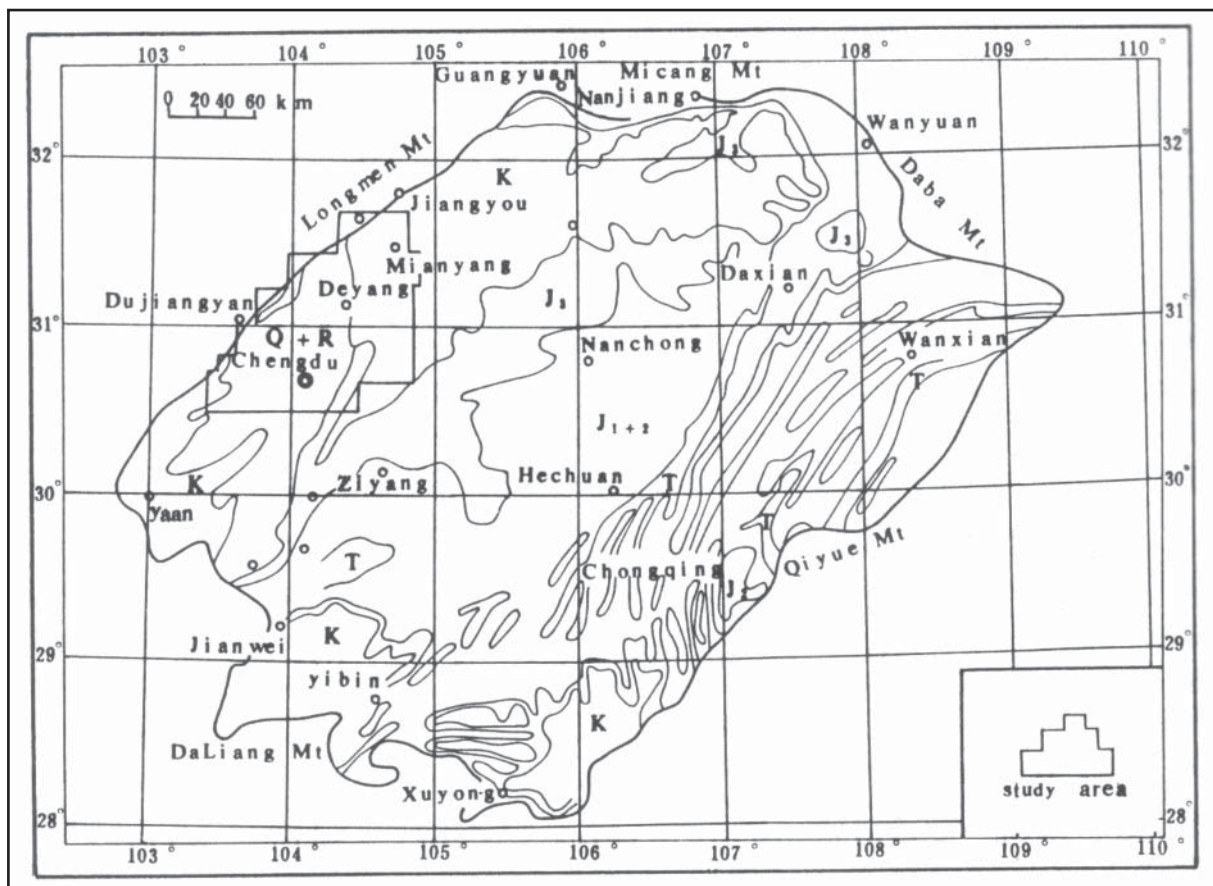
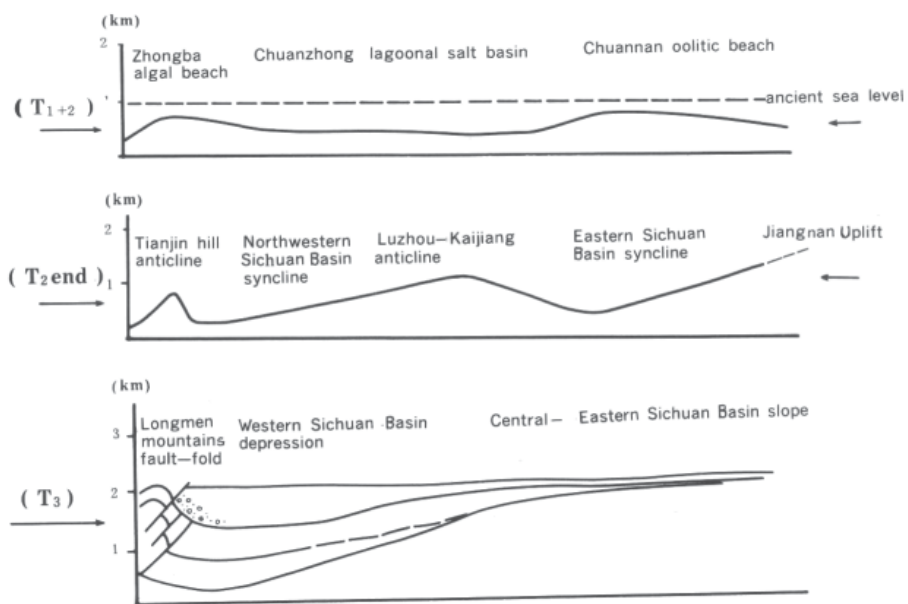
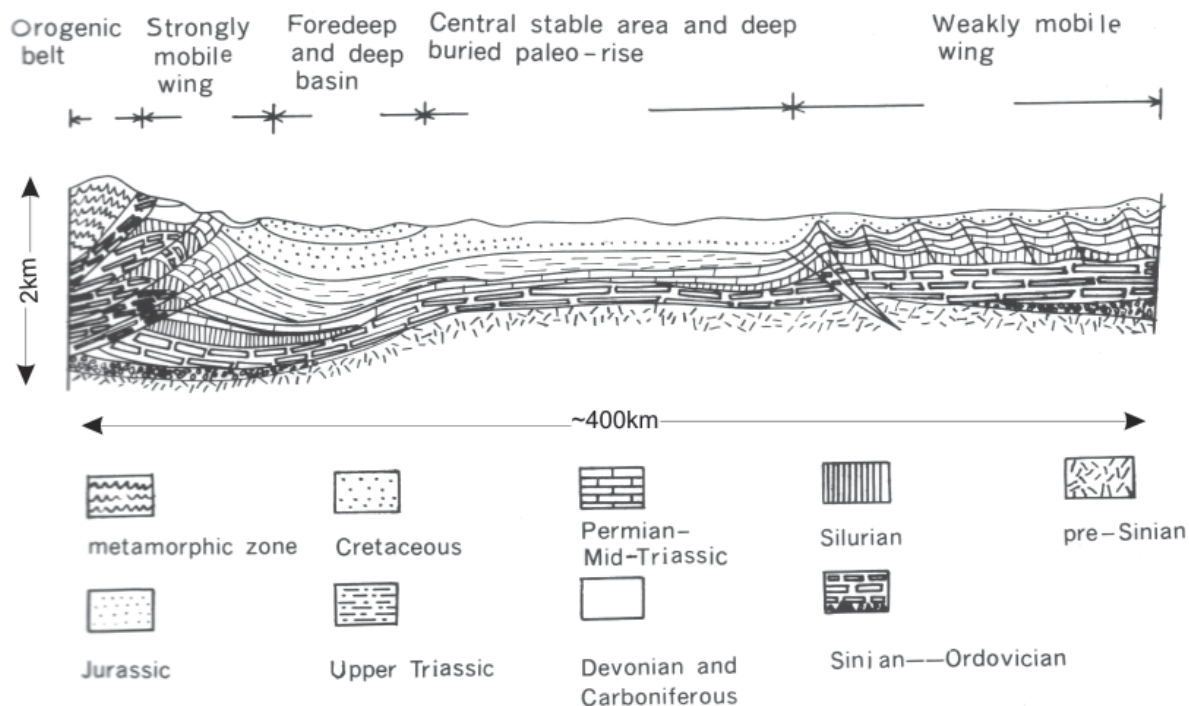


Figure A50. Oil and gas exploration and development block of Southwest Bureau of Petroleum Geology in Sichuan Basin (from Guo, 1997).



Sketch cross-section showing the craton compressed on both sides during different stages of the Triassic period.



Tectonic cross-section of the Sichuan Basin.

Figure A51. Formation of the Sichuan Basin (from Wang et al., 1989).

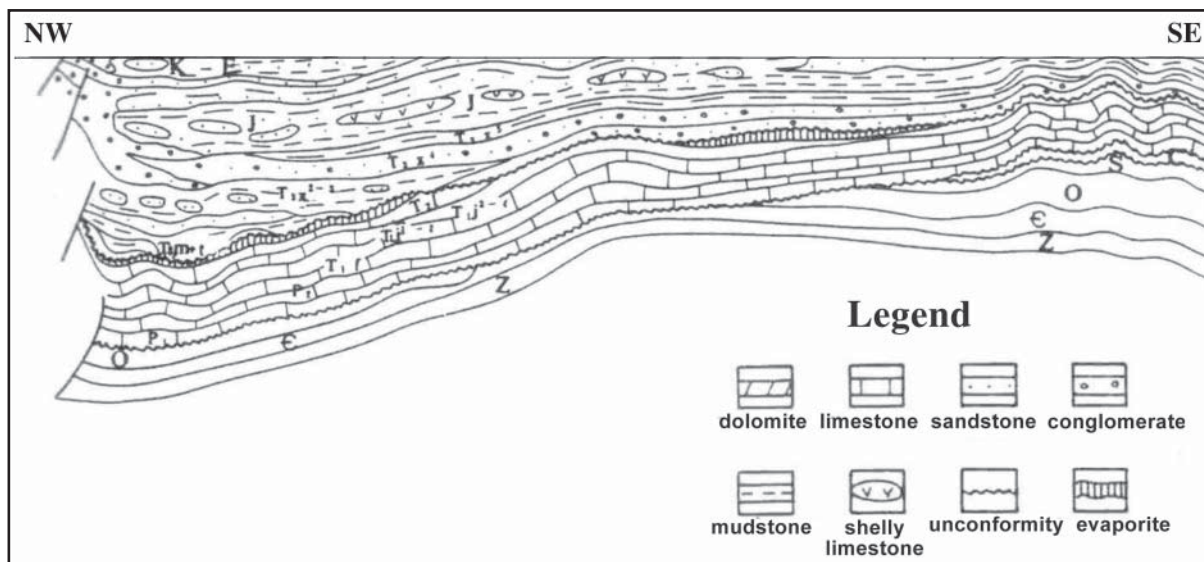


Figure A52. Sketch map of the sedimentation and structure in Sichuan Basin (from Guo, 1997).

### A1.11.3 Basin Fill

Much of the geology of the Sichuan is known through gas exploration and exploitation. The USGS (2000) divided the Sichuan into three assessment units for the purpose of hydrocarbon reserve estimation. These are the south-eastern, north-western and central uplift fold belts. All of these assessment units are characterised by structurally controlled gas fields in Carboniferous, Permian, and Triassic marine shelf carbonate reservoirs. Most gas accumulations are over pressured and have low porosity and permeability. Nearly all effective porosity is fracture porosity (Figure A53).

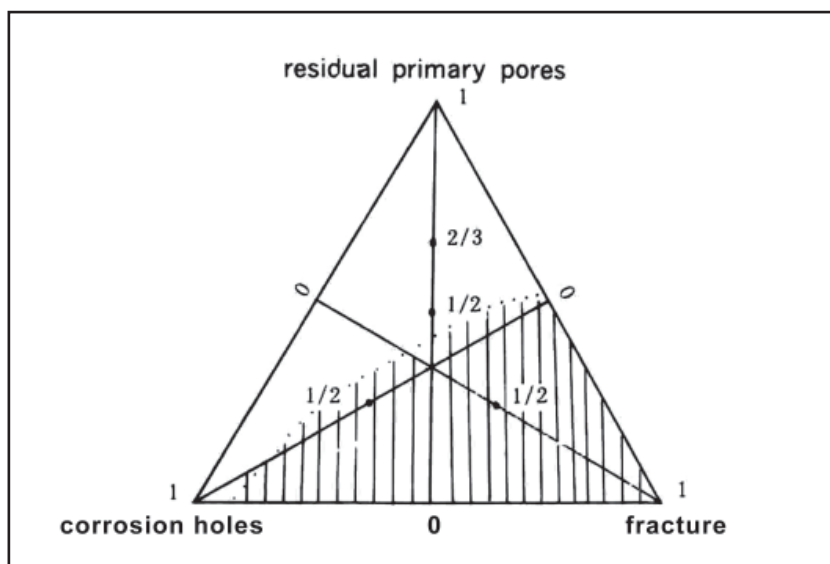


Figure A53. Triangle plot of the genetic types of reservoir pore space in the Sichuan Basin (ruled area denotes effective reservoir range) (Wang et al., 1989).

In a second petroleum system Lower Jurassic non-marine limestone and sandstone reservoirs are sourced from Lower Jurassic lacustrine shale. Other reservoirs occur in the Upper Triassic and middle Jurassic. These have porosity of 5-13% and permeability equal to or less than 1 mD (Guo, 1997).

In general all reservoir properties are poor. Primary porosity and permeability are poor and most reservoirs depend on fracture and/or dissolution porosity for deliverability (Figure A53). Hydrocarbon migration paths within

the Sichuan Basin are limited due to low permeability pathways in the Carboniferous to Jurassic formations. Overpressure is common in the basin and appears to have its upper limit in the Jurassic (Figure A54). The Early Cretaceous to Holocene is restricted to the western side of the basin. These formations are only 1000 m thick with localised areas up to 3000 m (Korsch et al., 1997). Wang et al., (1989) state that the upper 3000 to 7000 m of sediments in the Sichuan are dominated by red beds. Red mudstone units in the Middle Jurassic, Upper Jurassic and Lower Cretaceous are regional seals (USGS, 2000). This suggests the lacustrine environments proposed by Wang et al., (1989) were in a limited rainfall climate. Wang et al., (1989) sketched a facies map for the Jurassic to Eocene (Figure A55) that suggests relatively small shallow lake within a large expanse of often dry fluvial plains.

Details of reservoirs from USGS, 2000 follow:

“Primary reservoir rocks consist of limestone and dolomite of Carboniferous (Huanglong Formation), Early Permian (Maokou and Qixia Formations), Late Permian (Changxing Formation), Early Triassic (Jialingjiang Formation), and Middle Triassic (Leikoupo Formation) age. Reservoir quality is generally poor (porosity of 4 to 8 percent and permeability of ~0.1 mD). The best reservoirs (porosity of 10 to 15 percent and permeability of several tens of millidarcies) consist of grainstone, patch reefs (bioherms), and vuggy dolomite”. (USGS, 2000)

“In the north-western portion of the basin, Upper Triassic reservoir rocks consisting of the fluvial and fan deltaic sandstone of the Xujiache Formation are present. This sandstone was derived largely from the Longmenshan tectonic zone that flanks the north-western margin of the basin. Fluvial sandstone in the Middle Jurassic Shaximiao Formation, derived from the Longmenshan and uplifts along the northern margin of the basin, constitute additional reservoirs. The reservoir quality of the sandstones is generally poor (average porosity ~5 percent and average permeability no greater than 1 mD) and, thus, usually tectonic fractures are required to improve gas deliverability”. (USGS, 2000)

“The major traps are large faulted anticlines of thin-skin decollement origin. Combination anticlinal-stratigraphic traps (unconformity and facies-change varieties) may provide additional entrapment. Lower and Middle Triassic evaporite, Lower Triassic marine red mudstone, and Middle and Upper Jurassic non-marine red mudstone provide the best regional seals”. (USGS, 2000)

“Other reservoirs include the Lower Jurassic Daanzhai Formation a bioclastic limestone lacustrine origin and the Lower Jurassic Lianggaoshan Formation, a 20- to 30-m thick quartzose sandstone and siltstone of fluvial lacustrine origin. Generally, their quality is poor and they depend on secondary porosity provided by dissolution pores and vugs and open tectonic fractures for commercial production. Porosity in the better reservoirs ranges from 4 to 11 percent and averages about 8 percent and permeability ranges from 0.1 to several hundred millidarcies and averages about 10 mD”. (USGS, 2000)

“Major petroleum traps are broad, basement-involved anticlines, structural terraces, stratigraphic pinchouts, and combination structural-stratigraphic traps. Middle Jurassic, Upper Jurassic, and Lower Cretaceous non-marine red mudstone units provide regional seals”. (USGS, 2000)

#### A1.11.4 Hydrocarbon Fields

Hydrocarbon fields are largely unconventional continuous gas column accumulations in over pressured low permeability reservoirs. Because gas water contacts can not be defined the USGS preferred not to estimate the volume of these unconventional resources in 2000.

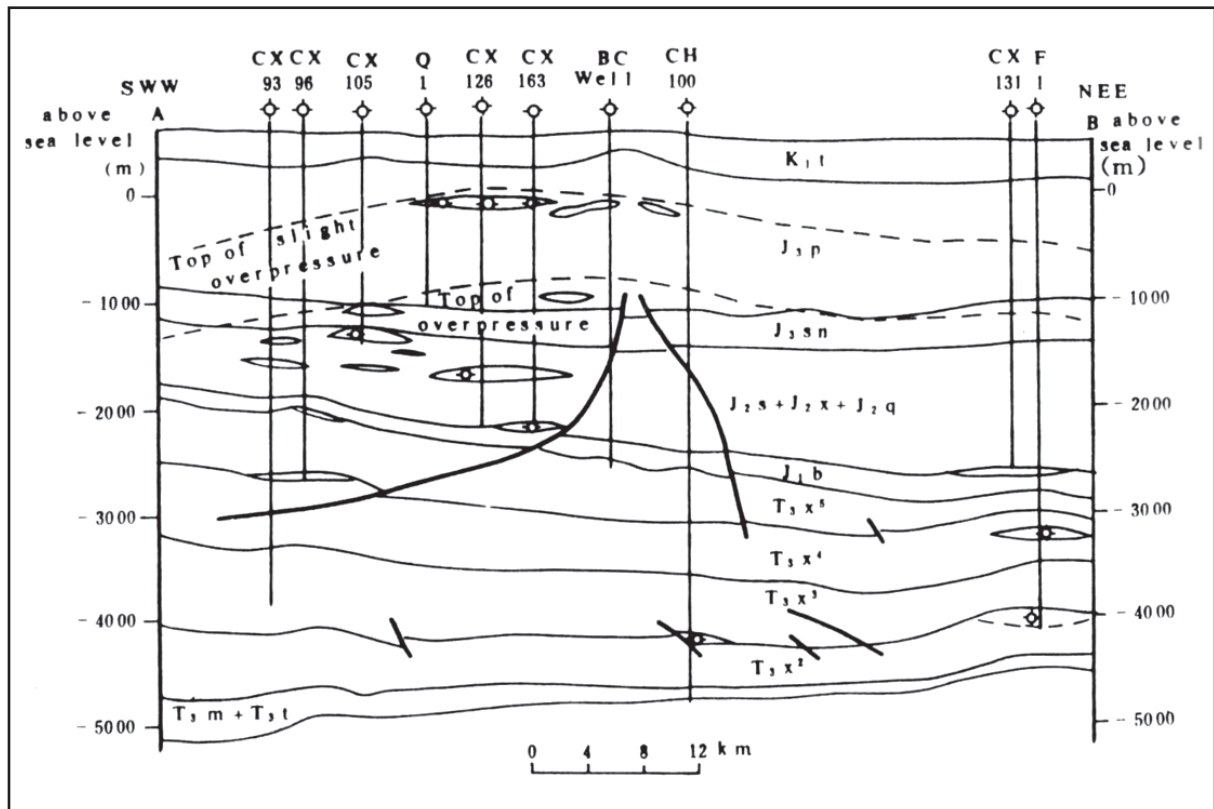


Figure A54. Gas pool section of Xiaoqan-Fenggu structural zone in western Sichuan depression (from Gou, 1997).

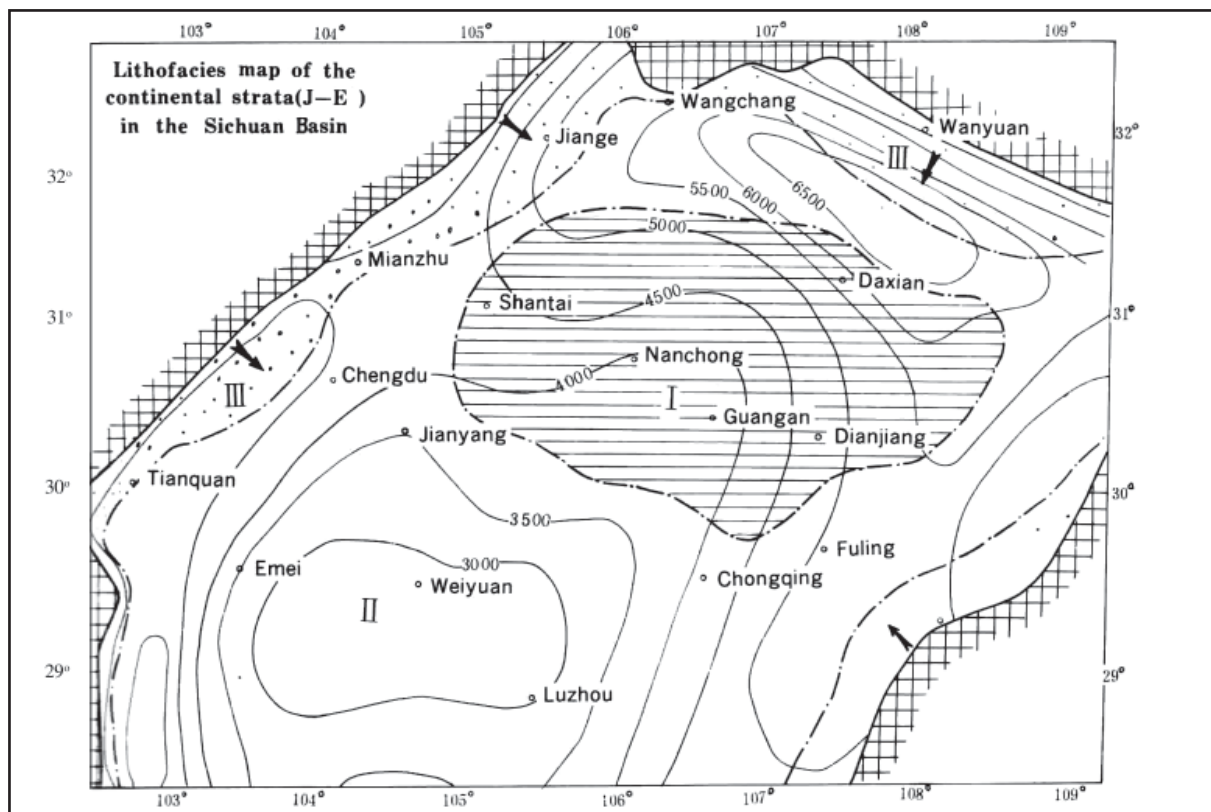


Figure A55. Lithofacies map of the continental strata (J-E) in the Sichuan Basin (I= lacustrine facies area; II= plain fluvial and shallow-lake facies areas; III= fluvial and diluvial facies areas) (from Wang, 1989).

### A1.11.5 Coal

Gas-prone coal beds occur in the Upper Permian Longtang Formation. The net thickness of coal beds in the Longtang Formation ranges from about 2 to 5 metres. These have current maturity of 1.5 to 2 VR (USGS, 2000).

### A1.11.6 Potential CO<sub>2</sub> Storage Options

The Sichuan Basin has large unconventional reserves of gas in very low porosity and permeability reservoirs aged from Carboniferous to Jurassic. Often these reserves are over pressured. Economic injection of CO<sub>2</sub> into such low permeability reservoirs seems extremely unlikely, especially if over pressured.

Better Jurassic reservoirs have 10 to 100 mD permeability. On face value this seems unlikely to allow an economic injection rate. However the pre Jurassic reservoirs are carbonates with fracture porosity. CO<sub>2</sub> injection may possibly induce dissolution and allow viable rates of injection. Depths of 3 or 4 km in most places and over pressure may hinder utilisation of these carbonate reservoirs.

Permian coals in the basin are thin and deeply buried with high rank and very likely highly fractured. If these coals are nearer to the surface in the east of the basin they might be a target for coal bed storage.

On the whole the Sichuan Basin appears to have limited storage potential unless fractured carbonates can be successfully injected.

### A1.11.7 References

Guo, Z. The gas resource in tight sandstone in Sichuan Basin. In: Proceedings of the 30th international geological congress; Geology of fossil fuels; oil and gas. Vol. 18A , 79-86. 1997.

Korsch, R. J., H. Mai, Z. Sun, and J. D. Gorter. Evolution and subsidence history the Sichuan Basin, Southwest China. Lui, Baojun & Li, Sitan (eds) In: Proceedings of the 30th international geological congress; Basin Analysis, Global Sedimentary Geology and Sedimentology. Vol. 8 , 208-221. 1997.

Tang, Z. and S. Zhan. Origin of Sinian (Upper Proterozoic) Gas Pools in the Sichuan Basin, China. In: Wagner, H C, Wagner, L C, Wang, F F H & Wong, F L (eds.), Petroleum resources of China and related subjects. Circum-Pacific Council for Energy and Mineral Resources, Earth Science Series 10 , 359-370. 1988.

USGS World Energy Assessment Team. World Petroleum Assessment 2000. United States Department of the Interior, U.S.Geological Survey, Digital data series DDS-60[4 discs]. 2000.

Wang, J., C. Bao, Z. Lou, and Z. Guo. Formation and development of the Sichuan Basin. In: Zhu, Xia (ed.), Chinese sedimentary basins. Elsevier Sci. Publ.. Amsterdam, Netherlands , 147-163. 1989.

Watson, M. P., A. B. Hayward, D. N. Parkinson, and M. Zh. Zhang. Plate tectonic history, basin development and petroleum source rock deposition onshore China. Marine and Petroleum Geology 4[Aug], 205-225. 1987.

## A1.12 Songliao Basin

### A1.12.1 CO<sub>2</sub> Sources

CO<sub>2</sub> emissions in the region directly overlying the Songliao Basin contributed approximately 128 Mt CO<sub>2</sub> /yr to China's estimated total stationary source CO<sub>2</sub> emissions of 2970 Mt/yr (IEA, 2000).

In a 300 km radius from Songliao Basin there are sources totalling approximately 283 Mt CO<sub>2</sub>/yr.

Note: The total of sources within 300 km of a basin is a very crude indication of the magnitude of emissions which may be within reach of the basin. These “catchments” overlap for many basins and should not be summed.

### A1.12.2 Basin Overview

The Songliao is a 260,000 km<sup>2</sup> back arc rift basin (Figure A56). It contains 3 to 7 km of Jurassic to Quaternary sediments (Figure A57). The depth to the Moho ranges from 34 to 29 km. The geothermal gradient is 37°C/km (Li, 1995), whilst USGS (2000) states 45°C/km. Earlier work (USGS, 1988) suggested 33°C/km to 50°C/km, which seems to be an appropriate range. Sediments were dominantly deposited in freshwater lacustrine and deltaic environments. In the Aptian and Albian the basin contained a fresh water lake with an area of 100,000 km<sup>2</sup> (Deshing, 1995). Cretaceous pore waters have a salinity of 6000-10,000 ppm (Li et al., 1989).

### A1.12.3 Basin Fill

The upper reservoirs are called the Saertou (Yaojia 2, 3 & Nenjiang Formations), Putaohua (Yaojia 1 Formation) and Gaotaizi (Qingshankou 2 & 3 Formation) (Li et al., 1989).

Reservoir rocks consist of very fine to fine-grained sandstone deposited in fluvial and deltaic systems on the margins of a large basin-centred lake. Typically, the reservoir sandstones are arkosic arenites. Six reservoirs of Early Cretaceous age are recognised as petroleum reservoirs. They are the Yangdachengzi, Fuyu, Gaotaizi, Putaohua, Saertou, and Heidimiao (Figure A58). These broadly defined reservoirs or pay zones are 200 to 500 m thick sandstone-bearing intervals that coincide with one or more formal stratigraphic units. The Putaohua and Saertou reservoirs are the primary reservoirs. The majority of the sandstone bodies in the six reservoirs were deposited in a fluvial-deltaic depositional system, located at the north end of the basin (USGS, 2000).

A palaeogeography map (Li et al., 1989) depicts the Qingshankou 2 & 3 as a delta environment in the Daqing field area (Figure A59). The depth to the Qingshankou Formation ranges from 200 m at the basin edge to 1800 m (Figure A60). Yang (1985) depicts a water flow vector into the basin from the western side within the Qingshankou (Member 2) Formation (Figure A61).

It can be inferred from the stratigraphic table by Huang (2004; after Li, 1995) that the upper reservoirs were also deposited in a delta environment. Li (1995) reports average porosity of 26.6 to 27.8% and permeability 552 to 973 mD for the Saertou reservoir group (Yaojia 2, 3 & Nenjiang Formations). Similar properties are recorded for the Putaohua reservoir group (Yaojia 1 Formations).

The regional seal rock consists of widespread lacustrine black shale and mudstone of Members 1 and 2 of the Nenjiang Formation and Member 1 and parts of Members 2 and 3 of the Qingshankou Formation (USGS, 2000).

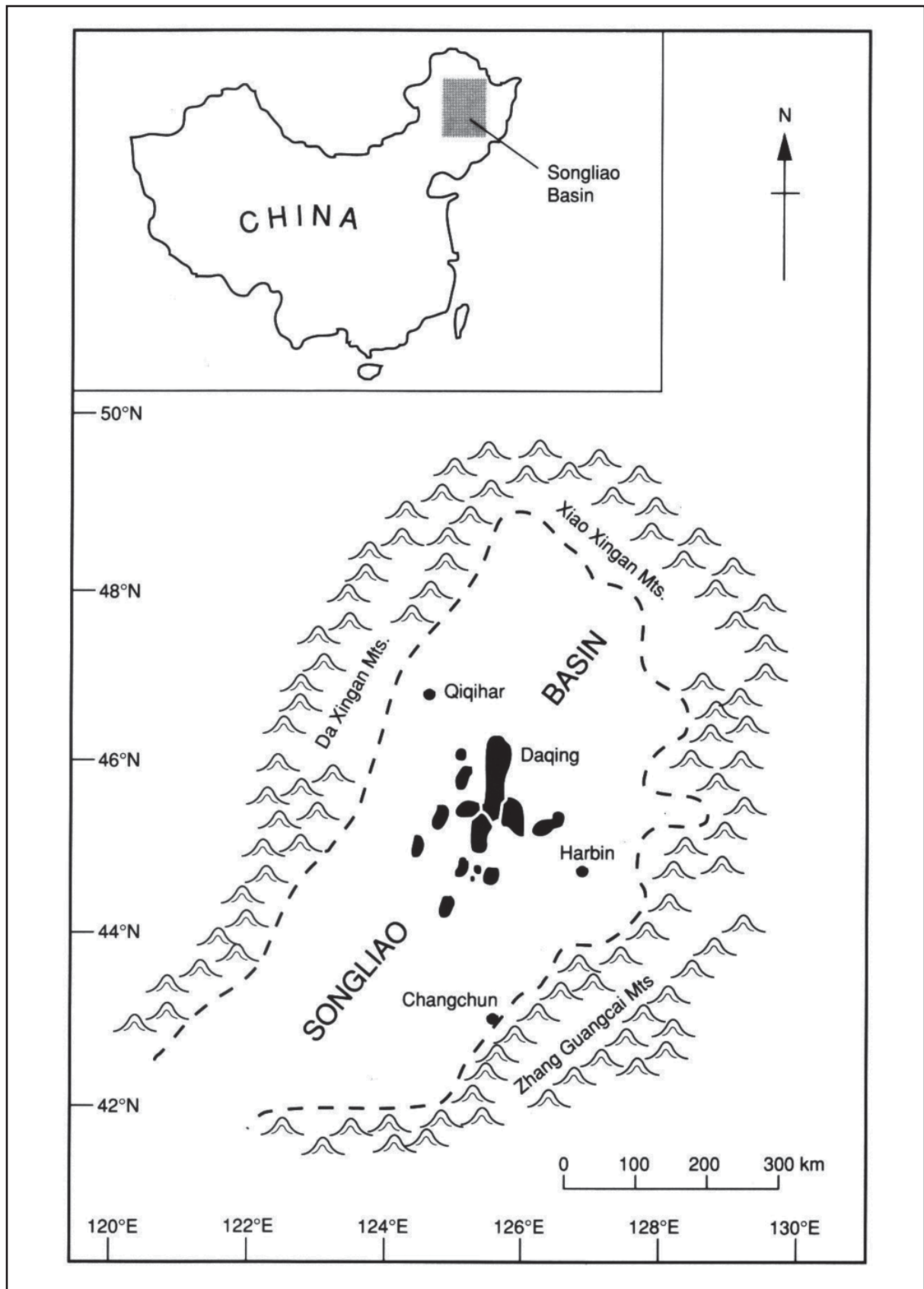


Figure A56. The location of the Songliao Basin (from Li, 1995).

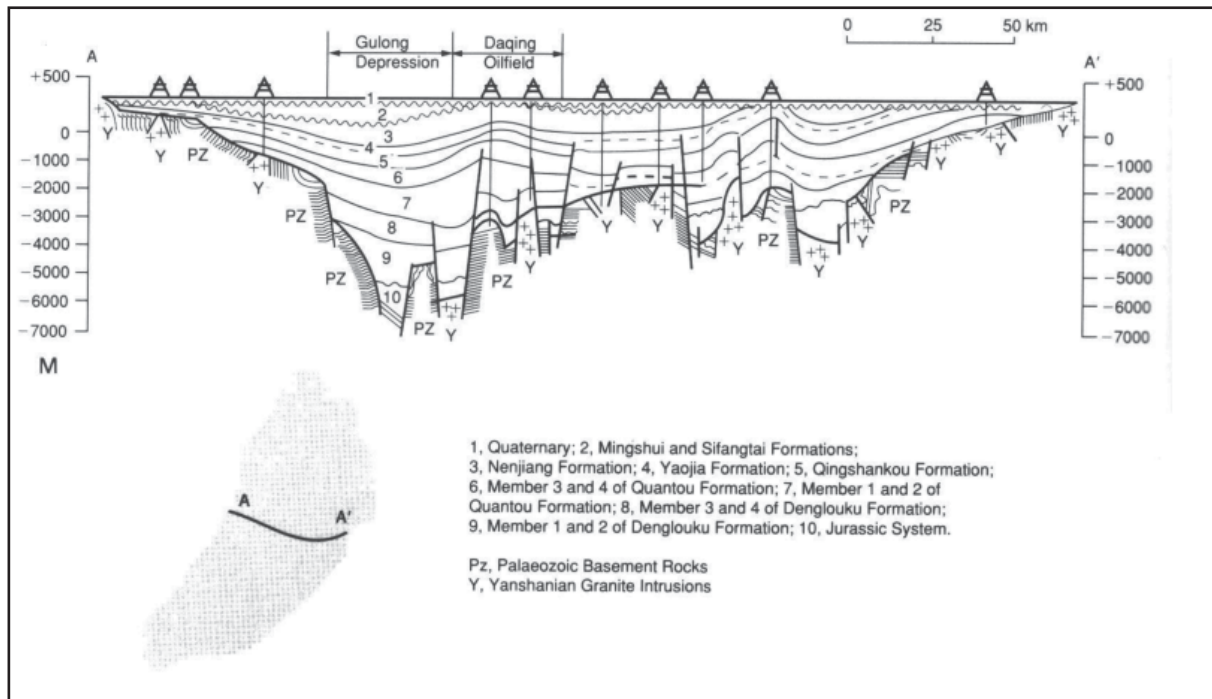


Figure A57. Structural cross-section of the Songliao Basin (from Li, 1995).

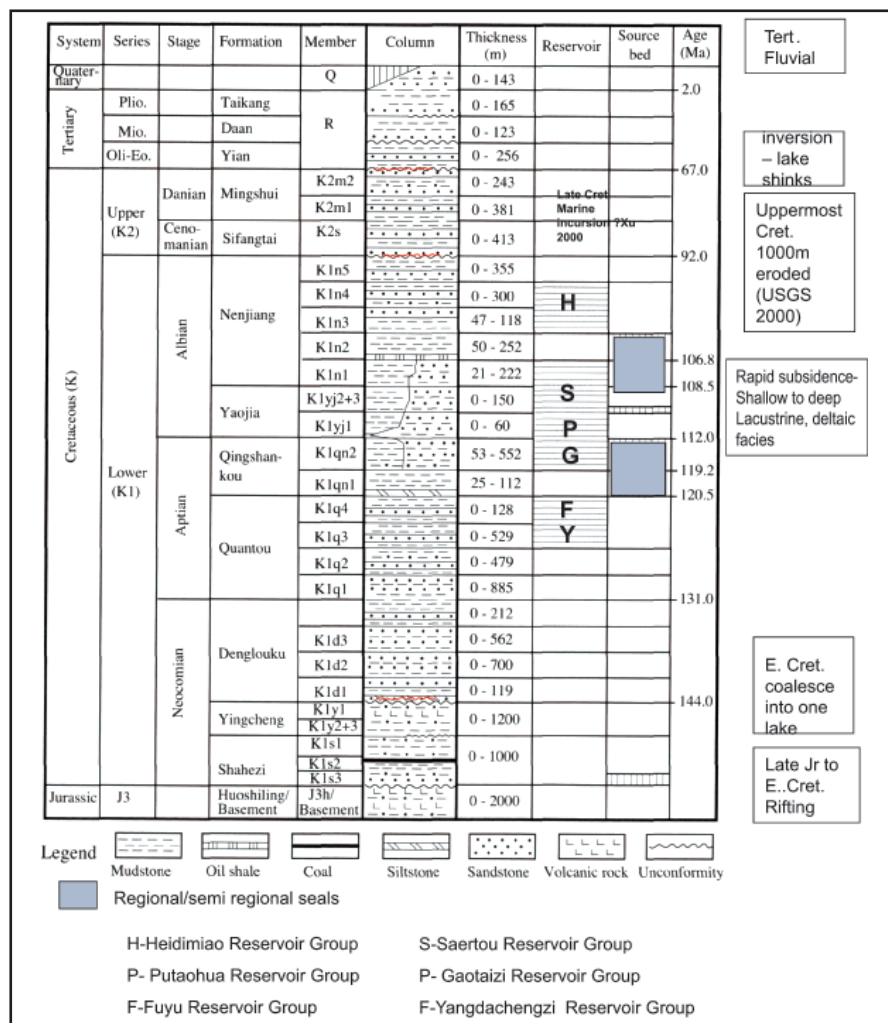


Figure A58. Mesozoic and Cenozoic stratigraphy of the Songliao Basin (modified from Huang et al., 2004).

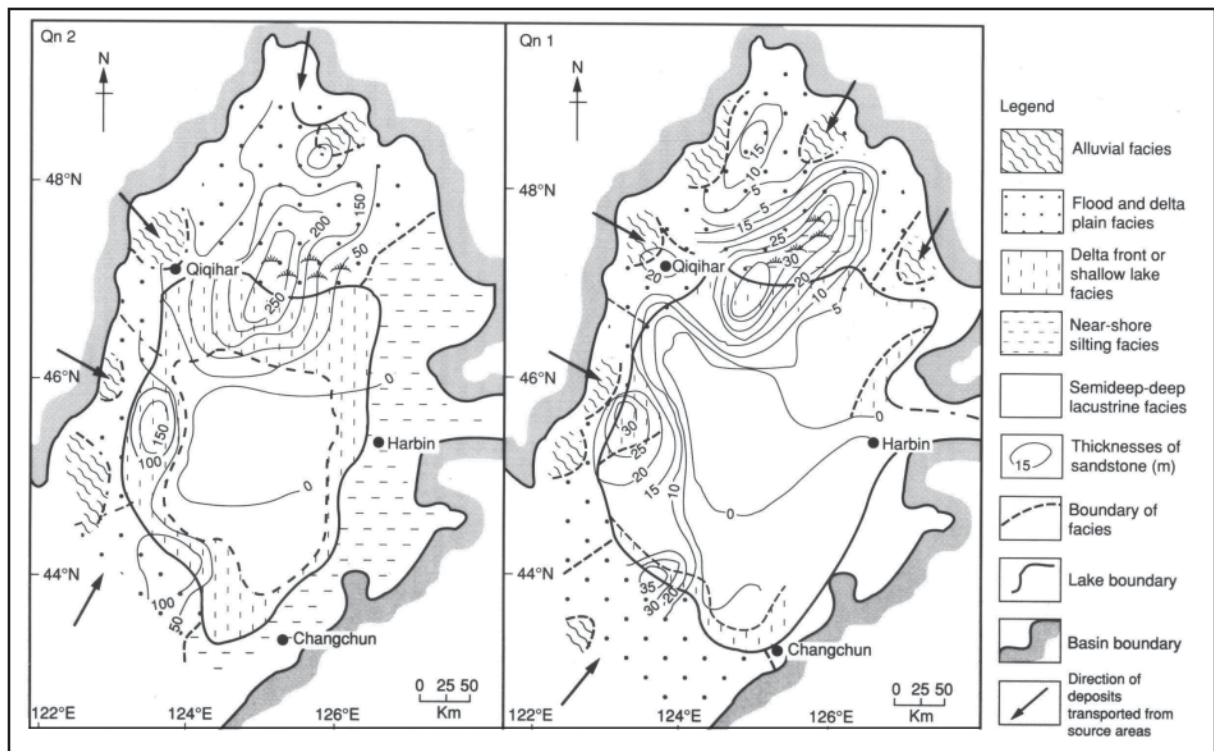


Figure A59. Facies distribution in the Qingshankou Formation during Qn1 and Qu2 time (from Li, 1995).

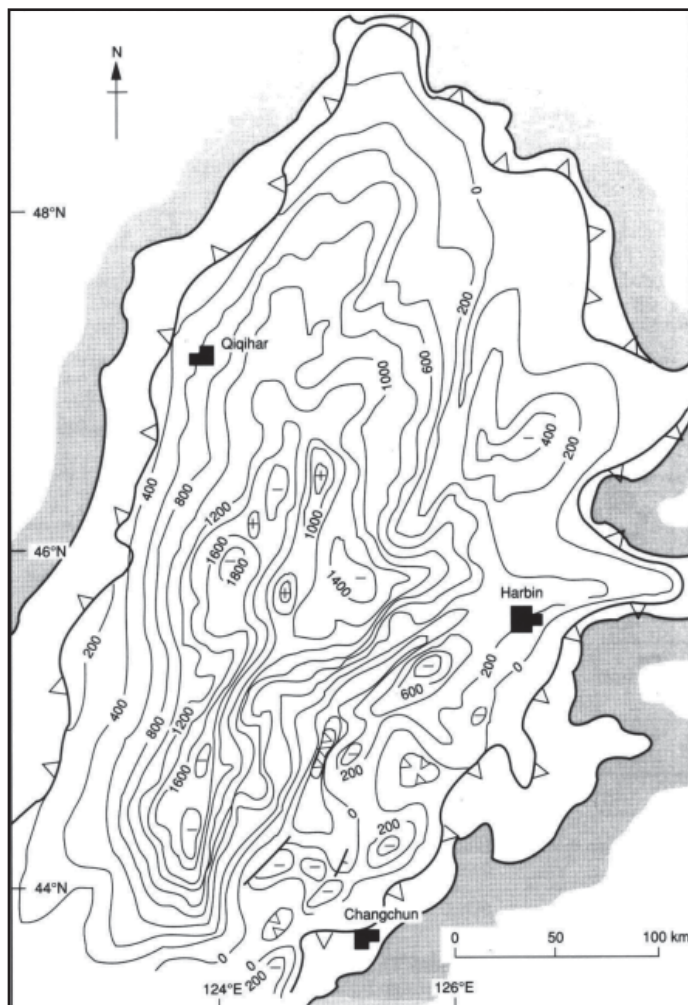
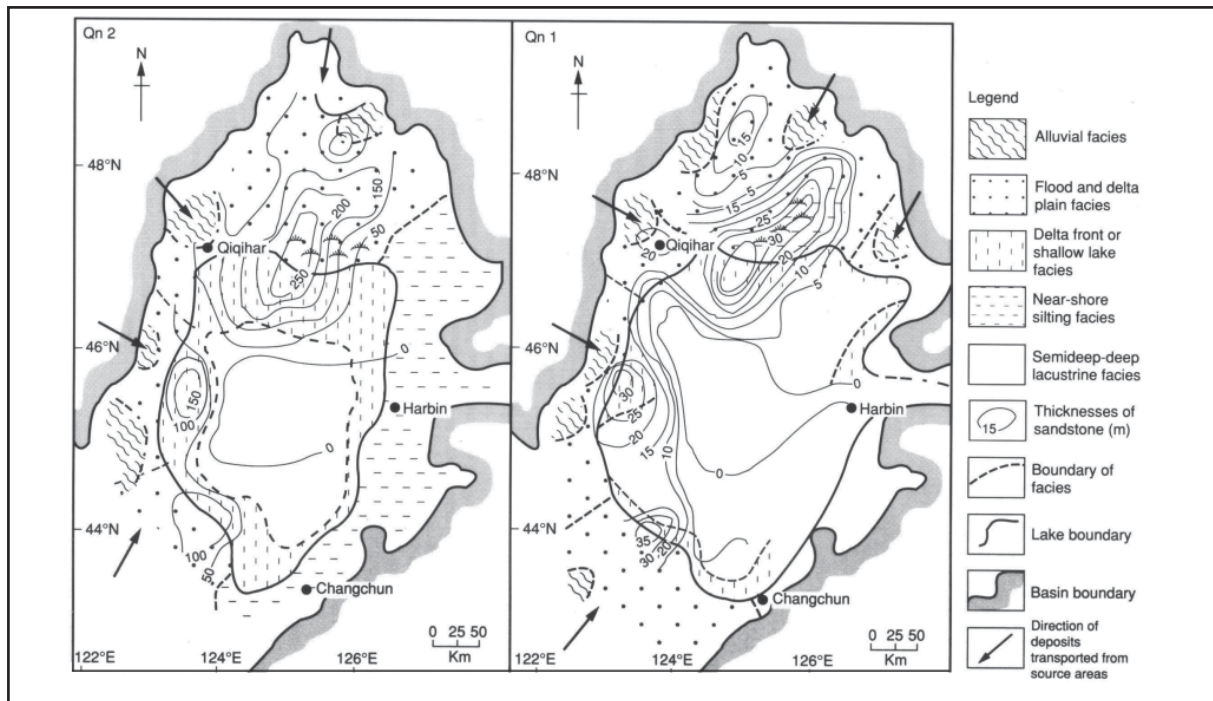


Figure A60. Burial depth (m) of the Qingshankou Formation (from Li, 1995).



**Figure A61. Cross-section of the Zhenlai to Shengping area showing source, carrier and reservoir rocks in the Songliao Basin.**

### A1.12.4 Hydrocarbon Fields

The Songliao Basin is the most important oil producing basin in China, accounting for one-third of petroleum production.

The major petroleum traps are large anticlines formed by compaction over extensional fault blocks, or by a Late Cretaceous to early Tertiary compressional event that led to partial structural inversion of the rift basin (USGS, 2000). Li (1995) attributes this compression to the opening of the Sea of Japan. Other important traps include large anticlinal noses and pinch-outs of near shore lacustrine and fluvial sandstones (USGS, 2000).

The giant Daqing field (Figure A56, Figure A62) contains most of the Songliao Basin's hydrocarbon resources. The Songliao Basin has estimated "known" oil of 15.5 billion barrels of which 12.4 billion barrels has been produced and 3.1 billion barrels is remaining reserves (USGS, 2000). This known hydrocarbon volume is equivalent to approximately 2 Gt of stored CO<sub>2</sub>. Daqing is a collection of seven anticline structures which seem to be related to a central basin high, enhanced by a late Cretaceous compressional event. The field is intensely faulted, numerous oil water contacts show the field is highly compartmentalised (Yang, 1985). The Coniacian Nenjiang 2 member is an extensive lacustrine mudstone/silt which apparently seals the Daqing field (Yang, 1985).

The Daqing production forecast for 2004 was 46.3 million tonnes (~342 million bbls (China Daily 6 January 2004). The field will produce for another 20 to 30 years depending on the adopted production policy (China Daily online 22 Sept 2003).

### A1.12.5 Coal Occurrence

Coal is present in the Upper Jurassic Shahezi and Yingcheng Formations. These formations are considered to be petroleum source rocks (USGS, 2000). There are several underground mines in the basin where Jurassic-age bituminous coals are mined. These coal seams are often gassy and range in depth from 30 to 1000 metres, the main mineable coal seam has an average thickness of 2-4 m (USEPA, 1996).

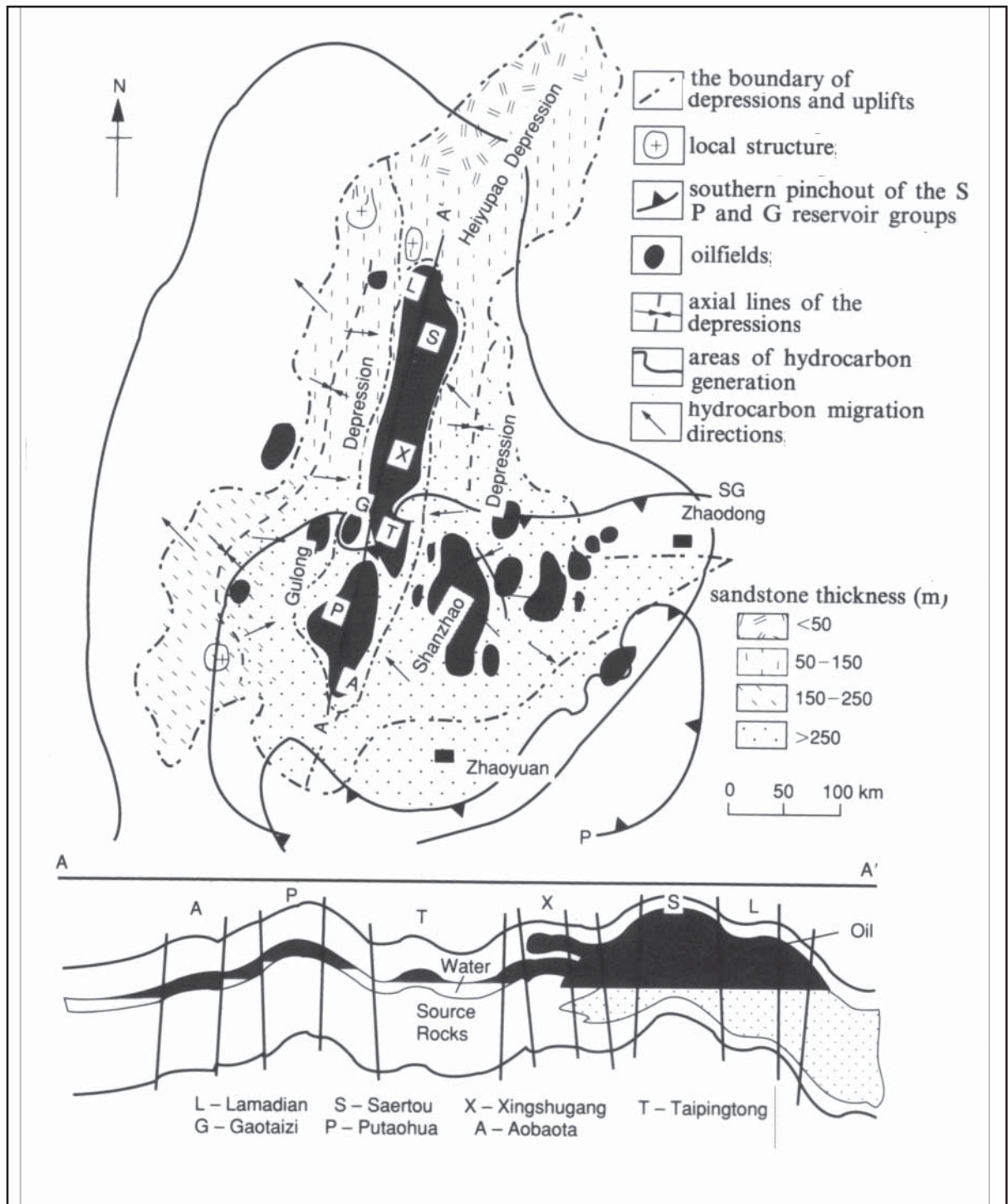


Figure A62. Geography of the super giant Daqing oilfield (from Li, 1995).

## A1.12.6 Potential CO<sub>2</sub> Storage Options

The Songliao Basin appears to offer a number of CO<sub>2</sub> storage options. While the Daqing field complex continues to produce ~340 million barrels per year there may be fully depleted sections of the field complex that are appropriate for CO<sub>2</sub> storage.

The Songliao Basin is a large graben formed by the unification of a number of Jurassic rifts during the early Cretaceous. This history can be contrasted to the Bohai Basin which only began in the Late Cretaceous and was not unified as a basin till the Oligocene. The opportunity for large scale contiguous sealed reservoirs appears greater in the Songliao due to its comparatively long history as a very large deep lake. The lacustrine shale facies in the Qingshankou Member 1 and the Coniacian Nenjiang Member 2 could provide good seals for saline reservoir storage options.

An “enhanced” deep saline reservoir trap (hydrodynamic flow trap) may be possible if the force of incoming ground water on the western flank is sufficient to force CO<sub>2</sub> within saline reservoir formations to down dip positions (Figure A61).

## A1.12.7 References

Hou, D., Li, M., and Huang, Q. Marine transgressional events in the gigantic freshwater lake Songliao: paleontological and geochemical evidence. *Organic Geochemistry* 31[7-8], 763-768. 2000.

Hu, W., Cai, C., Wu, Z., and Li, J. Structural style and its relation to hydrocarbon exploration in the Songliao basin, northeast China. *Marine and Petroleum Geology* 15[1], 41-42. 1998.

Huang, H., Yang, J., Yang, Y., and Du, X. Geochemistry of natural gases in deep strata of the Songliao Basin, NE China. *International Journal of Coal Geology* 58[4], 231-244. 2004.

Li, D. Hydrocarbon habitat in the Songliao rift basin, China. In: Lambiase, J J (eds.), *Hydrocarbon habitat in rift basins*. Geological Society Special Publications. :Geological Society of London 80, 317-329. 1995.

Ma, L., Yang, J., and Ding, Z. Songliao Basin; an intracratonic continental sedimentary basin of combination type. In: Zhu, Xia (ed.), *Chinese sedimentary basins*. Elsevier Sci. Publ.. Amsterdam, Netherlands , 77-87. 1989.

Ren, J., Tamaki, K., Li, S., and Junxia, Z. Late Mesozoic and Cenozoic rifting and its dynamic setting in Eastern China and adjacent area. *Tectonophysics* 344[3-4], 175-205. 2002.

Song, T. Inversion styles in the Songliao basin (northeast China) and estimation of the degree of inversion. *Tectonophysics* 283[1-4], 173-188. 1997.

USEPA United States Environmental Protection Agency.. *Reducing Methane Emissions From Coal Mines in China: The Potential for Coal bed Methane Development*. EPA 430-R-96-005, July, 1996.

USGS World Energy Assessment Team. *World Petroleum Assessment 2000*. United States Department of the Interior, U.S.Geological Survey, Digital data series DDS-60[4 discs]. 2000.

Xie, X.N., Jiao, J.J., and Cheng, J.M. Regional variation of formation water chemistry and diagenesis reaction in underpressured system: example from Shiwu depression of Songliao basin, NE China. *Journal of Geochemical Exploration* 78-79, 585-590. 2003.

Xu, M. Syn- and post-rift petroleum systems in the Songliao Basin, China. *AAPG Bulletin* 84[11], 1877. 2000.

Yang, W. Daqing oil field, People's Republic of China; a giant field with oil of nonmarine origin. *AAPG Bulletin* 69[7], 1101-1111. 1985.

Zhang, Y., Dong, S., and Shi, W. Cretaceous deformation history of the middle Tan-Lu fault zone in Shandong Province, eastern China. *Tectonophysics* 363[3-4], 243-258. 2003.

## A1.13 Subei (Jiangsu-Yellow Sea) Basins

### A1.13.1 CO<sub>2</sub> Sources

CO<sub>2</sub> emissions in the region directly overlying the Subei Basin contributed approximately 127 Mt CO<sub>2</sub>/yr to China's estimated total stationary source CO<sub>2</sub> emissions of 2970 Mt/yr (IEA, 2000).

In a 300 km radius from the basin there are sources totalling approximately 431 Mt CO<sub>2</sub>/yr.

Note: The sum of sources within 300 km of a basin very crudely indicates the magnitude of emissions within reach of the basin. These "catchments" overlap for most basins.

### A1.13.2 Basin Overview

The Subei/Yellow Sea Basin lies immediately to the north of Shanghai, eastern China (Figure A63, Figure A64). This discussion focuses primarily on the onshore portion known as Jiangsu Basin. Subei Basin is one of several NE-SW trending Cenozoic basins in eastern China (Songliao, Bohai, East China Sea Basins). The onshore area is around 35,000 sq km. (Moore et al., 1986). The total Subei/Yellow Sea Basin area is around 130 000 sq km (Zhang 1989). Geothermal gradient is 30 to 32°C/km (USGS,1989)

The Jiangsu Basin contains up to 6 km of fluvio-lacustrine sediment of Cenozoic age. The offshore Yellow sea portion has a similar thickness. The Jiangsu basin can be divided into three elements Yanhu sub Basin in the north, the Dongtai sub Basin to the south and the intervening Jianhu uplift. The Dongtai is the most prospective portion of the basin for oil and is composed of at least four major half grabens. (Moore, 1986).

The basin was initiated in the Palaeocene. The bulk of the extension occurred in the Eocene. During the Eocene sediments poured into the basin and were deposited in alluvial to deep lacustrine systems tracts typical of the North-eastern China basins. At the end of the Eocene local uplift and erosion occurred. Sedimentation resumed in the Oligocene, again with normal faulting and volcanism. (Moore et al., 1986). During the Late Tertiary and Quaternary deposition was controlled by regional sag rather than fault related subsidence (Moore et al., 1986).

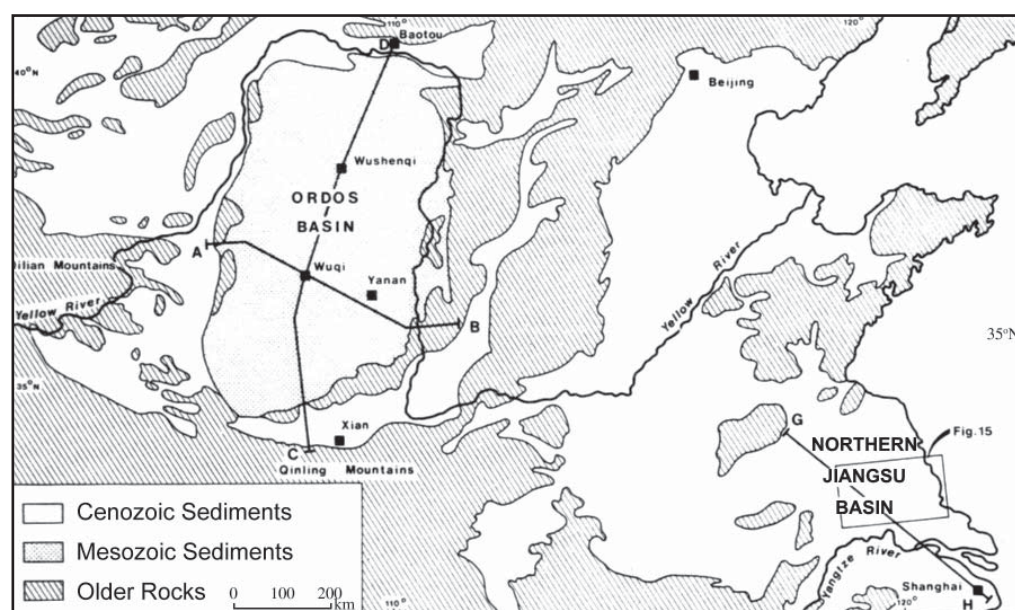


Figure A63.  
Jiangsu Basin  
map (from  
Moore et al.,  
1986)

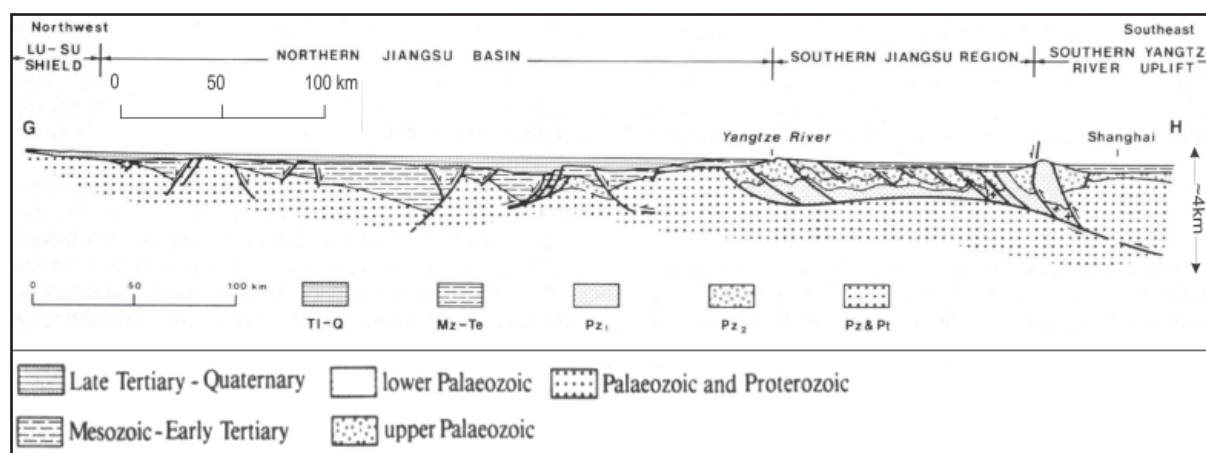


Figure A64. Generalised geological cross-section G-H showing Northern Jiangsu Basin. See Figure A63 for location of this section line (from Moore et al., 1986).

### A1.13.3 Basin Fill

Much of the information below relates to the Dongtai Sub Basin but is assumed that analogous geology occurs in the Yanhu and the offshore Subei Basin. The Tertiary stratigraphy of the Jiangsu Basin is depicted in Figure A65. Broad alluvial plains formed on the gently dipping margins of the half grabens. These alluvial sequences pass into deltaic sand/silt and prodelta shales. Well developed lacustrine shales are in the centre of the half grabens. The palaeogeography of the Funing and basal Dainan formations is depicted in Figure A67. Major deltaic episodes of the Funing Formation (members 1 and 3) and basal Dainan were deposited in times of regression (Moore, 1986). The depth to the base of the Dainan is 3000 to 3500 m. Porosity ranges from 10 to 15% and permeability ranges widely from 10 to 1000 mD. In general porosity and permeability of all formations is very poor below 4000 m. (Zhang et al., 1989). Seal is provided by lacustrine shale, which was deposited during subsequent higher water level events. Palaeogene to Neogene clastic reservoirs are also known offshore in the Yellow Sea (Vysotsky, 1999). These are presumed to be analogous in nature to the onshore Funing and Dainan Formations.

While oil discovered in Funing and Dainan proves there is a seal there might be other possibilities for reservoir-seal pairs in the Oligocene to Quaternary as shown in Figure A67. Details of these formations are not available. They are expected to be fluvial - lacustrine sediments.

Zhang, et al., (1989) predicted oil reservoirs in weathered Palaeozoic-Triassic carbonates in the basement of the Cenozoic rift. This hydrocarbon play exists in the Bohai Basin and it would also be a possible option for CO<sub>2</sub> storage.

### A1.13.4 Hydrocarbon Fields

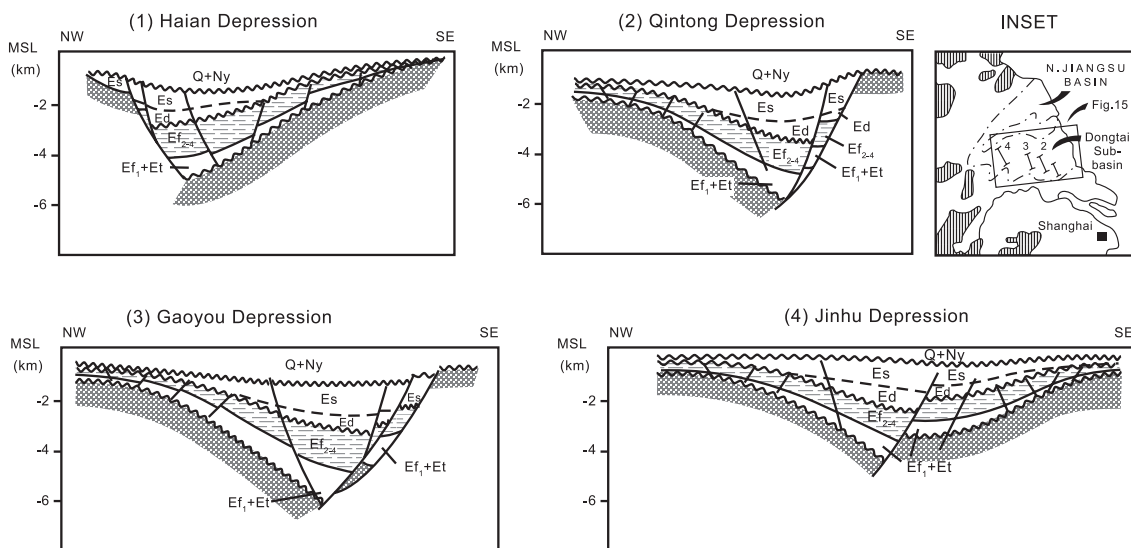
There is no data on field size distribution for this area in the USGS 2000 report. In 1986 the basin produced two million barrels of oil/year from over ten fields (Moore et al., 1986).

### A1.13.5 Coal Occurrence

Palaeozoic stratigraphy presented by Zhang et al., (1989) indicates coal is present at several levels but the shallowest of these, within the Permian Longtan Formation, lies at over 6000 m depth.

AGE	LITHO-LOGY	SEISMIC CODES	STRATIGRAPHY	SOURCE ROCK INTERVALS	OIL DISCOVERIES	COMMENTS
QUATERNARY		Q	Dongtai Formation			HIMALAYAN MOVEMENT EPISODE 2
Late Tertiary Pliocene & Miocene		Ny	Yanghang Formation			Partly oxidised and red. Gravolly and conglomeratic in part. Basalt interbed.
EARLY TERTIARY	Oligocene	Es	Sanduo Formation		●	SAMDUO MOVEMENT (HIMALAYAN MOVEMENT EPISODE 1) Interbedded sandstons, siltstone and shalo. Thin basalt interbed.
		Ed <sub>2</sub> Ed <sub>1</sub>	Dainian Formation		●	Interbedded sandstone, siltstone and dark shale. WUBAO MOVEMENT
	Eocene	Ef <sub>4</sub> Ef <sub>3</sub>	Funing Formation		●	Grey black mudstone with oil shale. Major source rock. Dolerite in middle.
		Ef <sub>2</sub>			●	Grey black to deep grety calcarnous shale with shaly limestone, thin tuffs and oil shale interbeds. Major source rock.
		Ef <sub>1</sub>			●	Interbedded sandstone, siltstone and minor grey shale.
Palaeocene	Et	Taizhou Formation		●	Sandy conglomerate grading upwards into mudstone.	
LATE CRETACEOUS		K <sub>2</sub> c	Chishan Formation		●	Sandstone with interbedded siltstone.

Cenozoic stratigraphy of the Dongtai Sub-basin.



Structure and stratigraphy of the four main fault depressions in the Dongtai Sub-basin. Location of each of the cross sections is shown in the inset.

Figure A65. Stratigraphy and half graben detail of the Dongtai sub-basin of the Jiangsu Basin (from Moore et al., 1986)

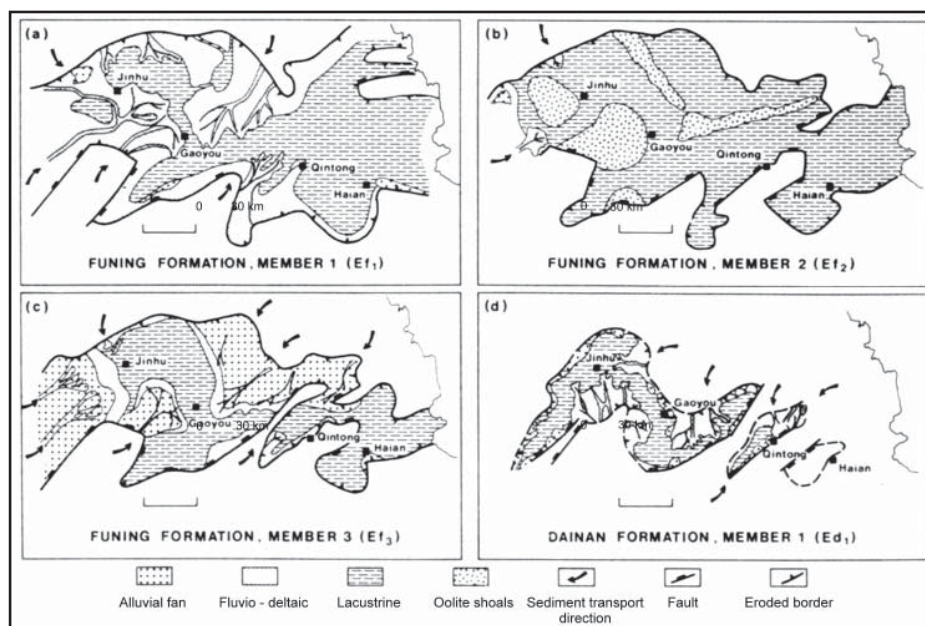


Figure A66. Interpreted environments of the Funing and lower Dainan formations of the Dongtai sub-basin, northern Jiansu Basin. Shale dominated Member 4 not shown (Moore et al., 1986).

### A1.13.6 Potential CO<sub>2</sub> Storage Options

By extension of the work of Moore et al., (1986) in the Dongtai sub Basin of the onshore Subei Basin, it is suggested there are several suitable reservoir-seal pairs for saline reservoir storage of CO<sub>2</sub> in the Tertiary, such as in the Funing and Dainan Formations. The production figures for 1986 of 2 million barrels from 10 fields (Moore 1986) suggest either quite small fields or poor well productivity or both. Triassic and Palaeozoic carbonates may be possible basement plays for CO<sub>2</sub> storage. Coal is present at several levels but the shallowest of these lies in the Palaeozoic basement at over 6000 m.

### A1.13.7 References

Moore, P. S., D. K. Hobday, H. Mai, and Z. C. Sun. Comparison of selected non-marine petroleum-bearing basins in Australia and China, *APEA Journal* 26[1], 285-309. 1986

Pang, X., M. Li, S. Li, Z. Jin, Z. Xu, and A. Chen. Origin of crude oils in the Jinhu Depression of North Jiangsu-South Yellow Sea Basin, eastern China. *Organic Geochemistry* 34[4], 553-573. 2003.

Yi, S., S. Yi, D. J. Batten, H. Yun, and S.-J. Park. Cretaceous and Cenozoic non-marine deposits of the Northern South Yellow Sea Basin, offshore western South Korea: palynostratigraphy and palaeoenvironments. *Palaeogeography, Palaeoclimatology, Palaeoecology* 191[1], 15-44. 2003.

Vysotsky, V. Oil and natural gas resources and potential in north-east Asia; mineral concentrations and hydrocarbon accumulations in the ESCAP region series. *Mineral Concentrations and Hydrocarbon Accumulations in the ESCAP Region*. United Nations Economic and Social Commission for Asia and the Pacific 10, 159p. 1999.

Zhang, Y., Z. Wei, W. Xu, R. Tao, and R. Chen. The North Jiangsu-South Yellow Sea Basin. In: Zhu, Xia (ed.), *Chinese sedimentary basins*. Elsevier Amsterdam, Netherlands, 107-123. 1989.

## A.1.14 Yinggehai Basin (China Section)

### A.1.14.1 CO<sub>2</sub> Sources

CO<sub>2</sub> emissions within 300 km in the coastal region adjacent to the Yinggehai Basin contributed approximately 32 Mt CO<sub>2</sub> /yr to China's estimated total stationary source CO<sub>2</sub> emissions of 2970 Mt/yr (IEA, 2000). This area includes Hainan Island.

### A.1.14.2 Basin Overview

The Yinggehai Basin is approximately 500 km long and just 50-60 km wide and strikes NW-SE (Zhang and Zhang, 1991)(Figure A67). There are from 12 to 17 km of Cenozoic sediments in the basin (Figure A68). Despite close proximity to the Qiongdongnan basins the Yinggehai Basin is not entirely related to the opening of the South China Sea. The basin is the result of strike slip motion on the Red River fault zone from the Palaeocene to Present Day together with the extensional motion of the South China Sea opening. This has resulted in locally thin crust and up-welling of the asthenosphere. Geophysical studies show the depth to Moho is 22 km. Cenozoic sediments are up to 17 km thick suggesting a Pre Cenozoic crustal thickness of only 5 km. (He et al., 2002). This resulted in a history of high subsidence rates and high geothermal gradients which continues to the Present.

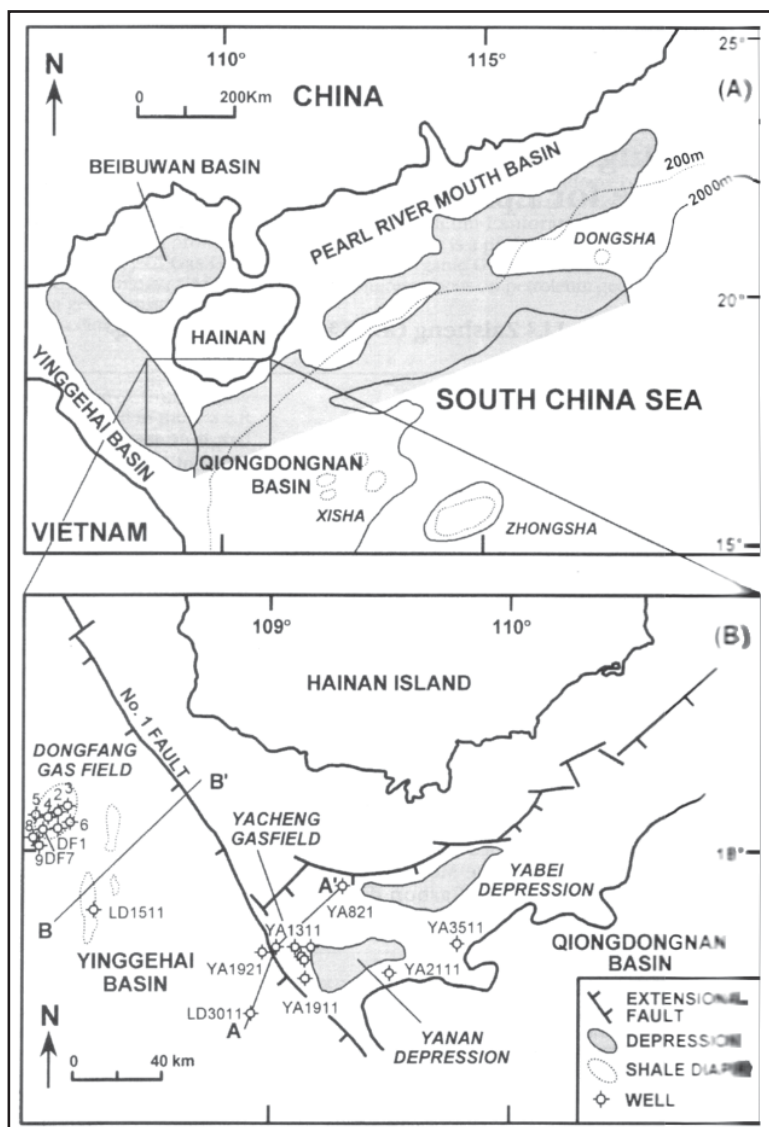


**Figure A67. Bathymetric map showing (a) the location of the study area and the four major offshore basins in the northern continental shelf of the South China Sea and (b) the locations of the wells from which samples were taken (from Hao et al., 2000).**

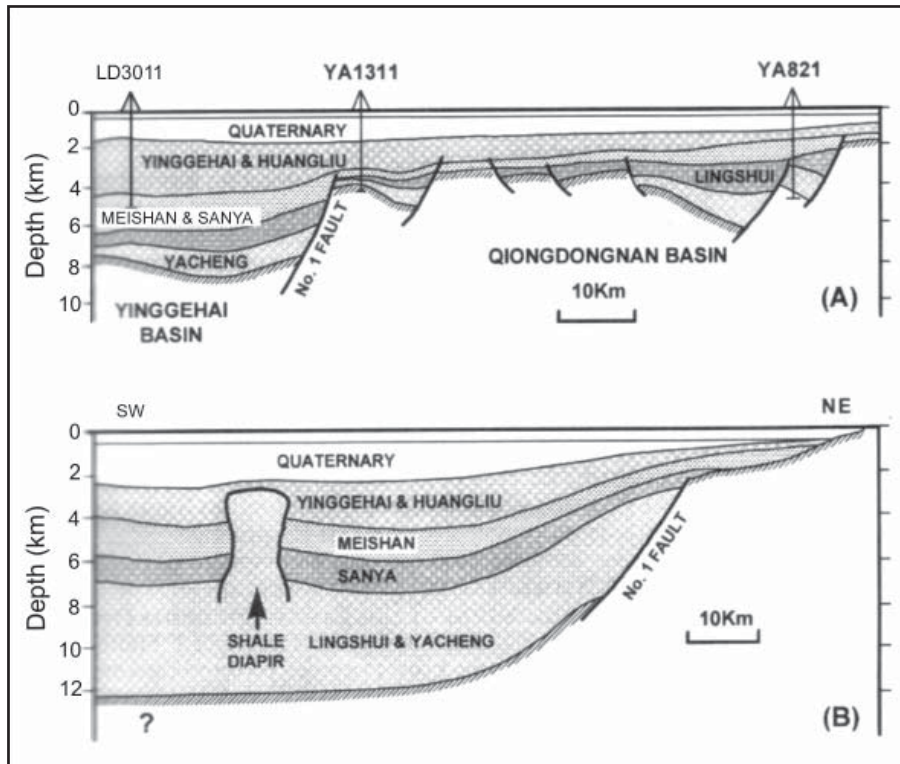


Figure A68. Cross-sections showing the structural differences between (a) the Qiongdongnan Basin and (b) the Yinggehai Basin (from Hao et al., 2000).

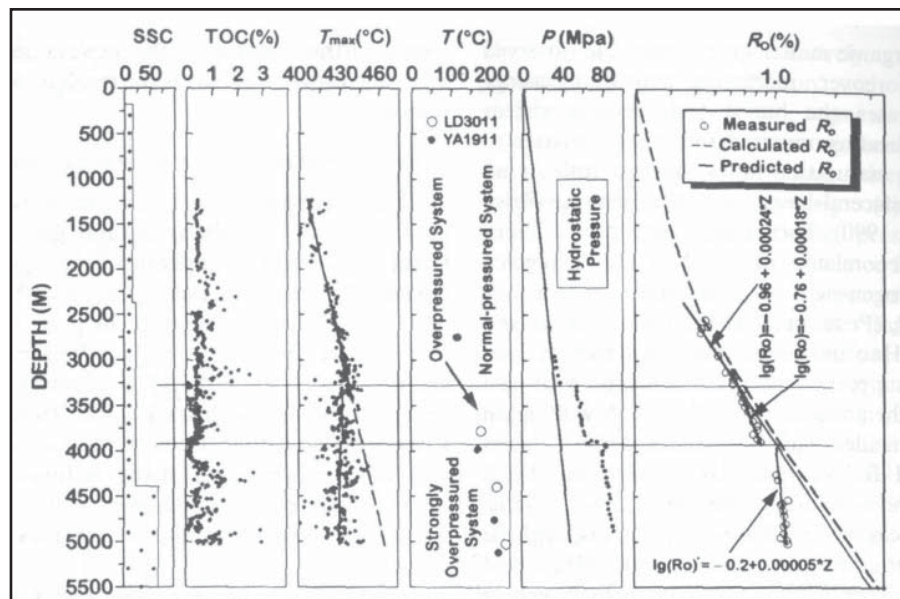


Figure A69. Organic chemistry and pressure profile for well LD301 Yinggehai Basin. Normal and over pressured zones are delineated (from Hao et al., 1996).

“The Yinggehai Basin is characterised by a high subsidence/sedimentation rate”, (Hao 1995). The average deposition rate from Miocene to present in the centre of the basin is 780 m/m.y (Hao et al., 1995). This resulted in pressure gradients up to 19.2 kPa/m (0.849 psi/ft) (Zhang and Zhang, 1991). However overpressure is not encountered until around 3200 m depth 3200 m depth in the Late Miocene Ying-Huang Fm (Figure A69). Extreme under compaction of rapidly deposited Palaeogene shales in the basin centre resulted in mud diapirs.

Geothermal gradients are estimated to vary from 31°C/km to 43°C/km, however some sources say 46°C/km . Surface heat flow at six sites in the Yinggehai Basin, range from 69 to 90 mW/m<sup>2</sup>, with a mean value of 79.7 mW/m<sup>2</sup> (He et al., 2002).

### A.1.14.3 Basin Fill

Little detail was located on the stratigraphy of the Yinggehai Basin. However a stratigraphic column (Figure A70) is presented by Hao et al., (1995). Sun et al., (2003) in a tectonics paper summarised the basin fill prior to 30 mya as alluvial, fluvial and lacustrine sediments. The period from 30 to 10 mya is generalised as a neritic environment and post 10 mya the water depth increased substantially to semi-abyssal. Hao (1995) points out five cycles of deposition (Figure A70). An inspection of Figure A70 suggests a progressive fining up or overall increase in accommodation space through cycles II to V. There appear to be sand prone intervals deposited at each unconformity (“sequence boundary”) which are potentially sealed by the succeeding fine grained sequences. This suggests tectonic activity reinvigorating coarse sediment supply against a background of on going high subsidence rates.

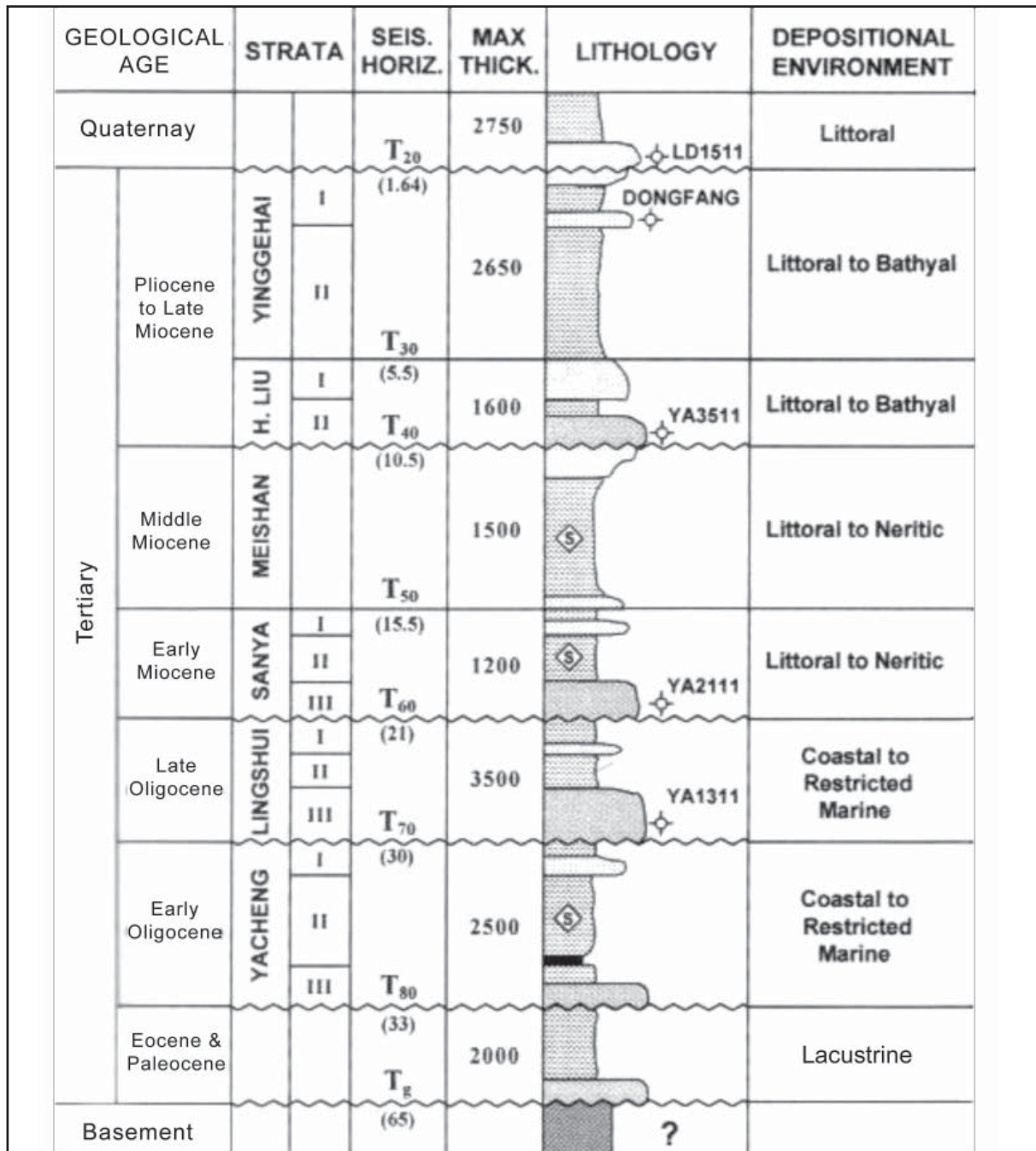


Figure A70. Generalised stratigraphy of the south eastern flank of the Yinggehai Basin. For location see Figure A67 (from Hao et al., 2000).

#### A.1.14.4 Hydrocarbon Fields

Dongfang is the major gas field in the Yinggehai Basin resulting from shale diapir structuring. Up to 50% of the subsurface accumulation volume is taken up by naturally occurring CO<sub>2</sub>. The recoverable hydrocarbon gas reserve is ~3.5 Tcf or 100 billion m<sup>3</sup> (Hao et al., 2000). The gases are contained in the Pliocene Ying-Huang Formation. The main reservoir lies between 1200 and 1600 m and has a deltaic environment of deposition (Figure A71). It will be some time before these fields are depleted. The presence of fields shows that there are sealing formations with high integrity. Without Palaeogeographic maps it is hard to imply anything about the lateral extent of reservoir facies. It is assumed the ancient equivalent of the Red River provided the sediment to the delta system which is the reservoir for the Dongfang field. Depositional dip would be expected to be to the SE (along structural strike). Given the length of this river system today one would imagine the areal extent of delta systems to be large. There may be opportunities for saline reservoir storage provided overpressure is not an issue. From Hao (1995) it appears overpressure onset occurs at around 3200 m in the basin centre. The basin is hot (46°C/km) and this will have an impact on storage capacity.

#### A.1.14.5 Coal Occurrence

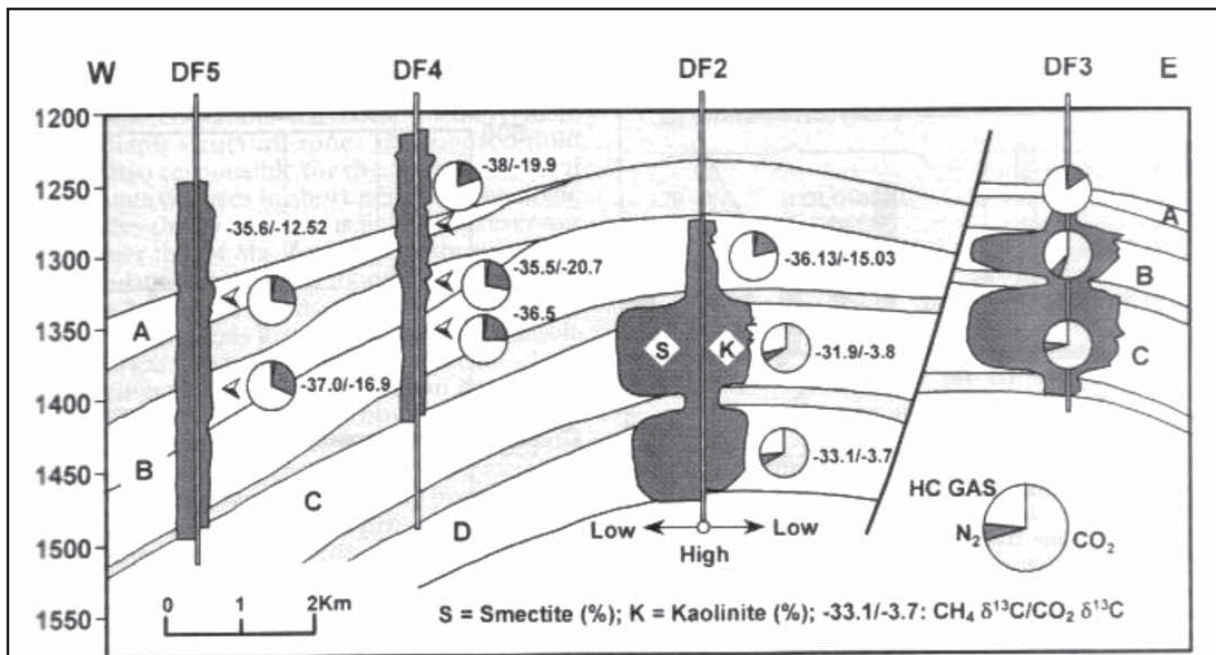
Coal is not a viable storage option in this basin. Any potential coal facies would be developed within Palaeocene to Mid Miocene lacustrine-littoral depositional environments. Most of these intervals lie very deep (> 4000 m) over most of the Yinggehai Basin.

#### A.1.14.6 Potential CO<sub>2</sub> Storage Options

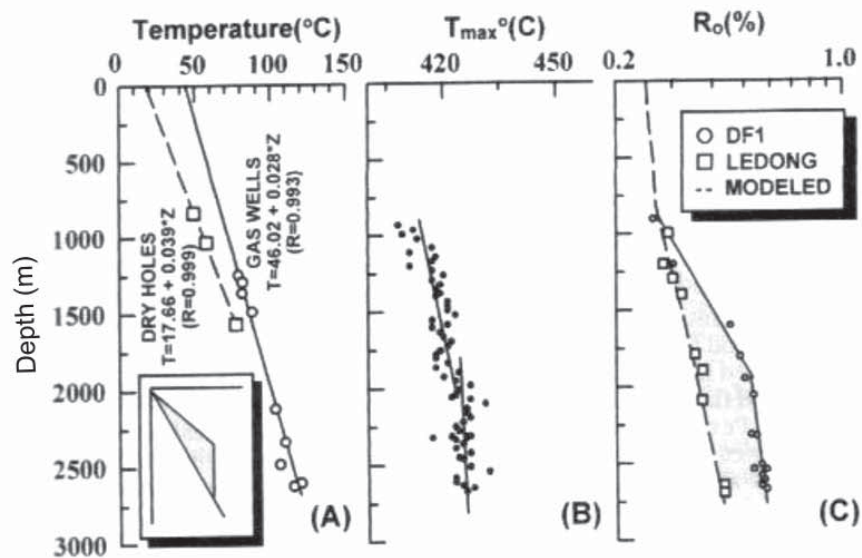
The basin may have potential in the Pliocene to Quaternary. Seals exist as shown by the existence of the Yinggehai field. While there are apparently reservoir-seal pairs there are a number of problems with the basin conditions. Rapid deposition means that the base Pliocene is at 2750 m and over pressure occurs from around 3200 m (Upper L. Miocene). A high geothermal gradient (up to 46°C/km in this case) will reduce the solubility of CO<sub>2</sub> in pore water.

There will not be depleted fields in the near future and the basin is still being explored.

Coal is not a viable option due to its projected occurrence in the deeper over pressured sections of this offshore basin.



Cross section of Dongfang gas field showing the interreservoir compositional heterogeneities and variation of clay mineral transformation profiles.



(A) Drill-stem test temperatures for wells in the diapair structure zone, (B) Rock-Eval  $T_{max}$ , and (C) vitrinite reflectance profiles for well DF1. Modeled  $R_o$  values are in reasonable agreement with  $R_o$  measured from well Df1. Both  $T_{max}$  and  $R_o$  profiles are segmented, with the deep segments having abnormally low  $T_{max}/R_o$  gradients; these results closely match those predicted for an idealized, convectively upwelling geothermal plume [insert in (A)].

Figure A71. Dongfang field cross-section showing heterogeneity of reservoir and temperature (from Hao et al., 2000).

## A.1.14.7 References

Hao Fang, Li Sitian, Sun Yongchuan, and Zhang Qiming. Characteristics and origin of the gas and condensate in the Yinggehai Basin, offshore South China Sea: evidence for effects of overpressure on petroleum generation and migration. *Organic Geochemistry* 24[3], 363-375. 1996.

He, L., L. Xiong, and J. Wang. Heat flow and thermal modelling of the Yinggehai Basin, South China Sea. *Tectonophysics* 351[3], 245-253. 2002.

Zhang Qiming. and Zhang Quanxing. A distinctive hydrocarbon basin—Yinggehai Basin, South China Sea. *Journal of Southeast Asian Earth Sciences* 6[2], 69-74. 1991.

Sun, Z., D. Zhou, Z. Zhong, Z. Zeng, and S. Wu. Experimental evidence for the dynamics of the formation of the Yinggehai Basin, NW South China Sea. *Tectonophysics* 372[1-2], 41-58. 2003.

Wang, P. Neogene stratigraphy and paleoenvironments of China. *Palaeogeography, Palaeoclimatology, Palaeoecology* 77[3-4], 315-334. 1990.

# A2. Indonesia

## A2.1 NW Java Basin

### A2.1.1 CO<sub>2</sub> Sources

The most concentrated CO<sub>2</sub> production in Indonesia occurs around Jakarta and the western part of Java. Oil and gas fuelled power stations in the area produce the majority of the emissions.

CO<sub>2</sub> emissions in the region directly overlying the onshore area of NW Java Basin contributed approximately 20 Mt CO<sub>2</sub>/yr to Indonesia's estimated total stationary source CO<sub>2</sub> emissions of 126 Mt/yr (IEA, 2000).

In a 300 km radius from the basin there are sources totalling approximately 42 Mt CO<sub>2</sub>/yr.

Note: The sum of sources within 300 km of a basin very crudely indicates the magnitude of emissions within reach of the basin. These "catchments" overlap for most basins and should not be summed.

### A2.1.2 Basin Overview

The NW Java Basin is a grouping of Tertiary sub basins; Sunda, Arjuna and several smaller onshore basins. Indonesia's basins formed along the southern edge of Sundaland during the Tertiary (Figure A72). The area is a prolific hydrocarbon province. Siliciclastic and carbonate reservoirs are present. The present day onshore basins contain a high proportion of carbonate formations because they were distal during most of the Tertiary (Figure A73). Sediment is 3000 m thick. The geothermal gradient is 40 to 50°C/km (Soenandar, 1997). The area of the basin is 140,870 sq km.

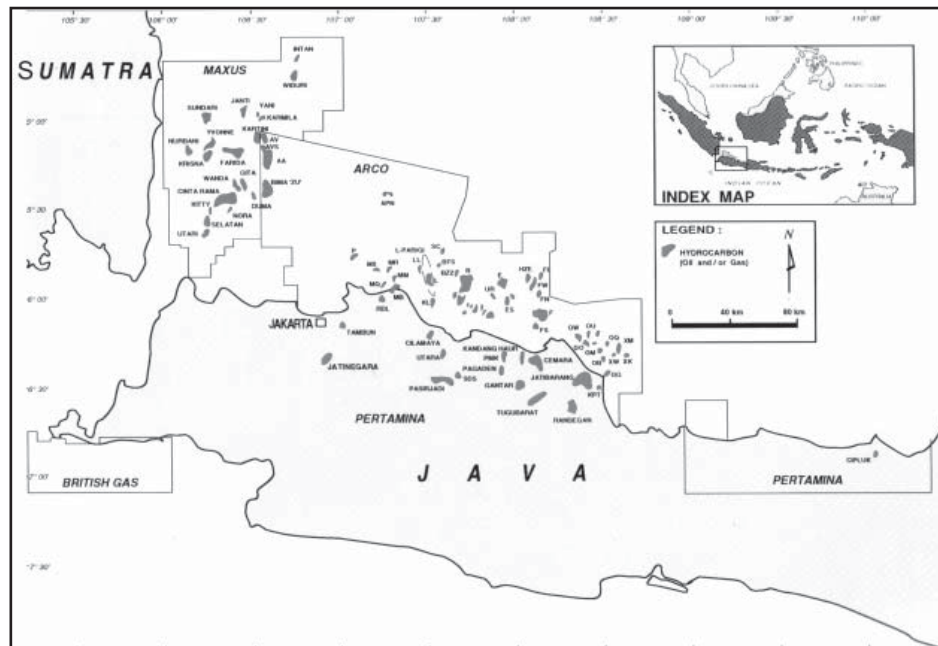
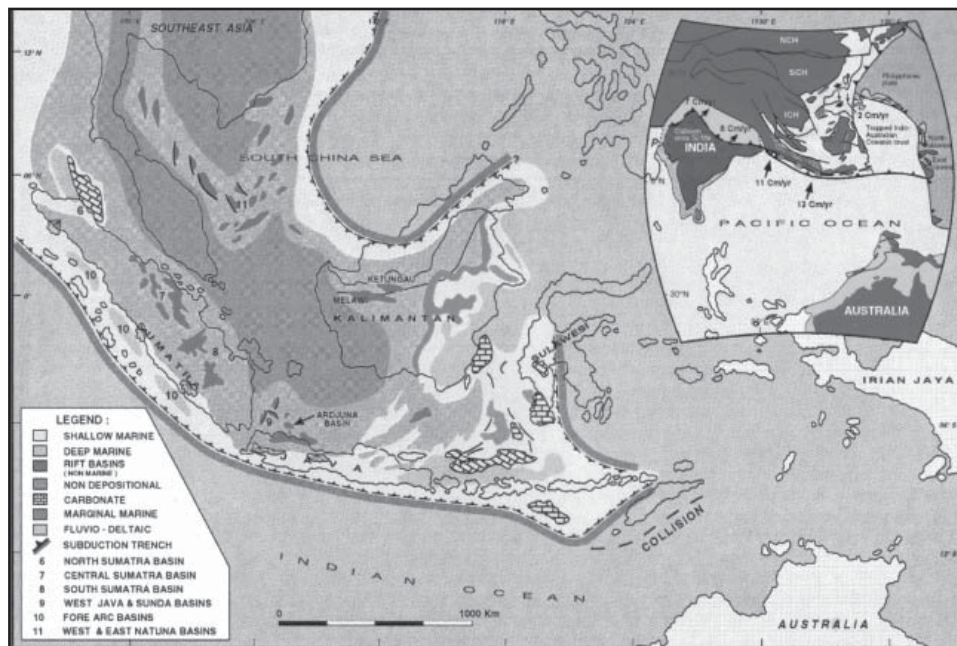


Figure A72. NW Java Basin with distribution of hydrocarbon fields (Noble et al., 1997).



**Figure A73.**  
**Sundaland**  
**palaeogeology (from**  
**Sundarmono et al.,**  
**1997 after Daly et al.,**  
**1987).**

### A2.1.3 Basin Fill

A generalised hydrocarbon stratigraphy of the NW Java Basin shows good quality siliciclastic and carbonate reservoirs, in both the offshore and onshore basins (Figure A74). A comparison of stratigraphy on and offshore in the NW and E Java basins yields many similarities (Figure A75).

More than three quarters of the discovered reserves are from late synrift Oligocene Talang Akar Formation (USGS, 2000).

The Talang Akar Formation is divided into a lower lacustrine unit and an upper fluvial deltaic unit. Stacked, sandy channels in the upper unit result in porosity from 23-35% and permeability of 150-2500 mD. The lower unit has porosity of 15 to 20% and good oil flow rates.

Early Miocene Batu Raja shallow marine reef carbonates are also an important reservoir. (USGS, 2000).

Arjuna Basin: E-M Miocene “Main” and “Massive” Formations consist of sandstones and limestones where clastic source was from the north and marine transgressions were from the south. The best reservoir quality clastic rocks are fluvial/deltaic, shoreline, and reworked, transgressive sandstones separated by thick, tuffaceous marine shale. Weathered granite basement is a minor reservoir rock.

Seal rocks include the Gumai Shale which is a regional seal and has equivalents in Sumatra basins. The Batu Raja Shale and intraformational seals in the Banuwati Shale, and the Talang Akar are also important. (USGS, 2000).

### A2.1.4 Hydrocarbon Fields

The total “known” gas volume is 8 Tcf (640 Mt stored CO<sub>2</sub>). Only 1 Tcf of the 8 Tcf is produced. The “known” oil volume is 3168 mmbbls (411 Mt stored CO<sub>2</sub>). About half of the known oil has been produced (USGS, 2000).

From work by the USGS (2000), the average field size is around 20 mmbbls (2.6 Mt) or less. The largest field has an estimated ultimate recovery of 600 mmbbls which is equivalent to 78 Mt of stored CO<sub>2</sub>. There are 10 other fields with ultimate recoverable volumes between 100 and 250 mmbbls. The top 11 fields account for 50% of known oil.

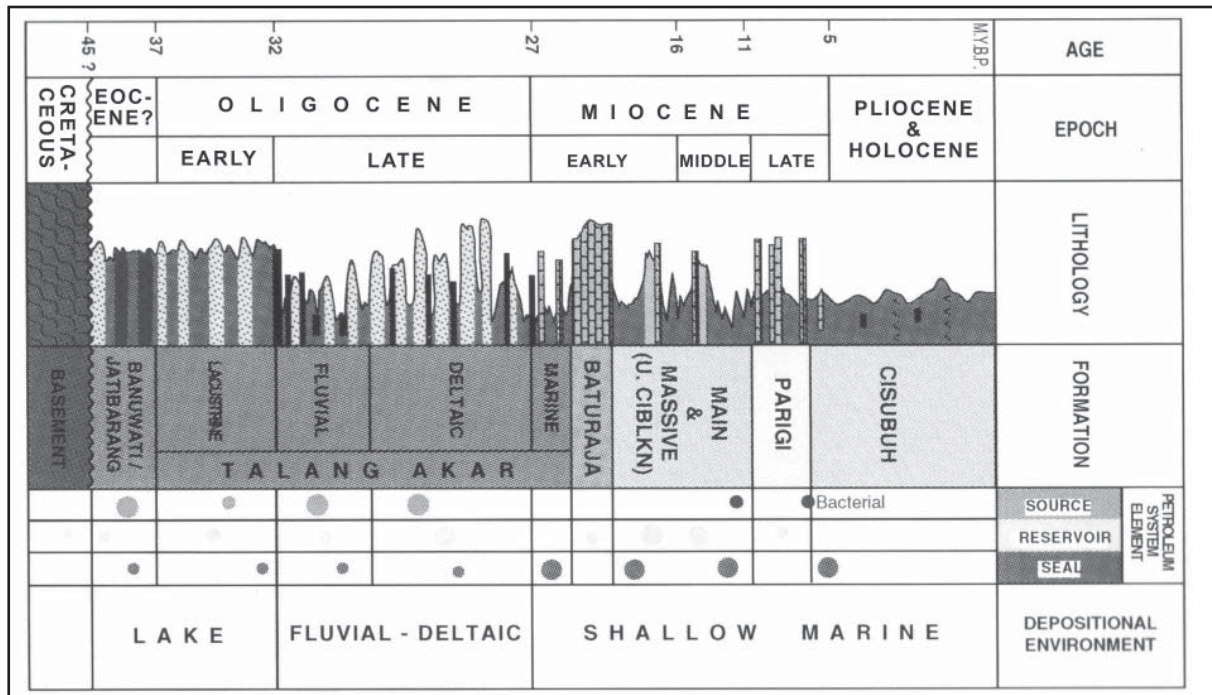


Figure A74. Generalised stratigraphic column of Northwest Java (from Noble et al., 1997)

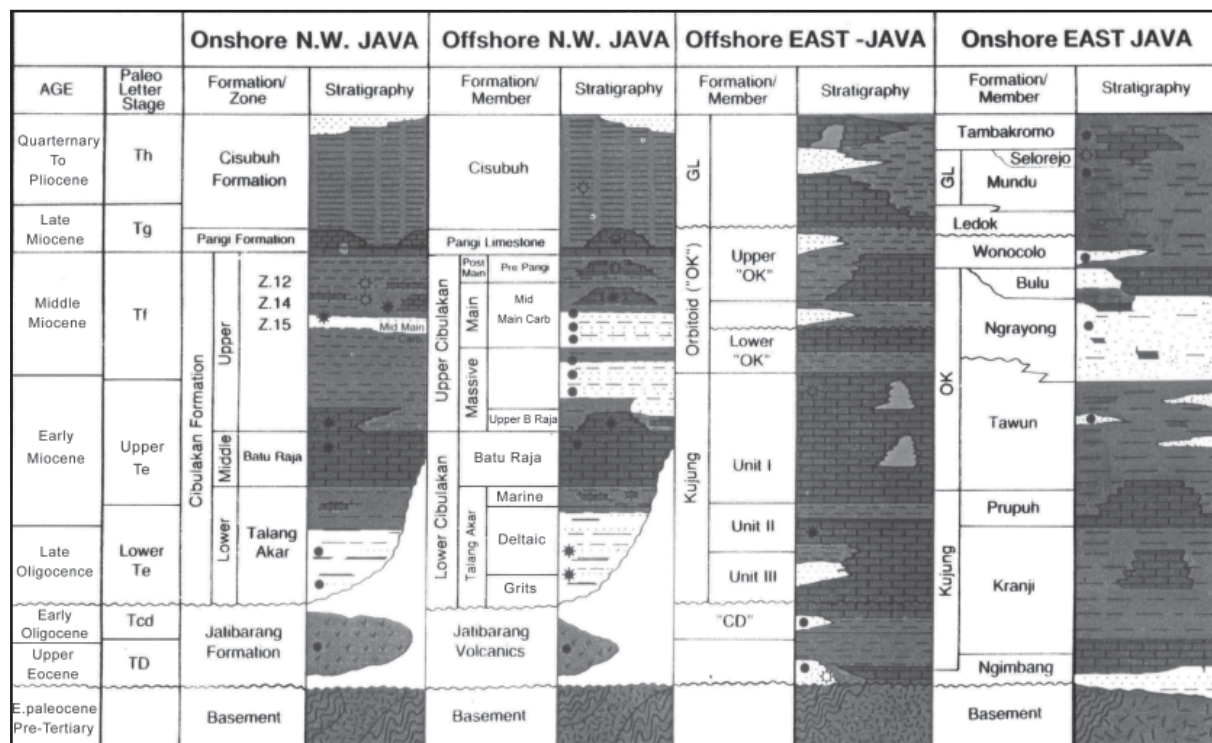


Figure A75. The geology and hydrocarbon potential of the Island of Java and its adjoining offshore areas (from Indonesian Petroleum Association Oil and Gas Fields Atlas IV, publication date unknown).

Most of the gas is in the Arjuna Basin. There is 8 Tcf of known gas, 3 Tcf is encompassed by the five largest fields. None of these fields is larger than 700 Bcf. The majority of known gas is contained in fields smaller than 300 Bcf (15 Mt CO<sub>2</sub>). The mode is very prominent and sits between 50 and 100 Bcf. (USGS, 2000). For reference 100Bcf is equivalent to around 8 Mt of stored CO<sub>2</sub>. The proportion of fields that are now depleted is unknown, but over all a large proportion of gas remains as reserves.

## A2.1.5 Coal Occurrence

Significant coal mining occurs at Bukit Asam and Tanjung Enim. Power generated at Tanjung Enim is transmitted to Java.

## A2.1.6 Potential CO<sub>2</sub> Storage Options

There are three main reservoir levels in the onshore and offshore NW Java Basin known from hydrocarbon exploration. They include the Late Oligocene Talang Akar siliciclastics, the Batu Raja Carbonates and the E-M Mioicene “Massive” and “Main” sandstone formations (Upper Cibulakan Group). Unfortunately, the Upper Cibulakan Formation sandstones are not as well developed in the onshore basins. Overall there appear to be plenty of good quality reservoir-seal pairs both onshore and offshore that could be exploited for CO<sub>2</sub> storage.

Oil and gas fields are relatively small but very plentiful. Many fields in the Arjuna Basin are onshore.

A well explored sub surface and the existence of hydrocarbon fields and known reservoir-seal pairs make the NW Java Basin a basin with good CO<sub>2</sub> storage prospectivity. However, high geothermal gradients, averaging 45°C/km, will reduce subsurface storage density.

## A2.1.7 References

Daly, M.C., Hooper, B.G.D., Smith D.G., and Christensen, R.M. Tertiary plate tectonics and basin evolution in Indonesia. *Proceedings of the 16th Annual Convention Indonesian Petroleum Association* , 399-428. 1987.

Indonesian Petroleum Association. *Exploration and Production History*. In: Indonesian Petroleum Association Oil and Gas Fields Atlas Vol IV. Indonesian Petroleum Association. Jakarta, Indonesia . 19??

Noble, R.A., Pratomo, K.H., Nugrahanto, K., Ibrahim, A.M.T., Prasetya, I., Mujahidin, N., Wu, C.H., and Howes, J.V.C. Petroleum systems of Northwest Java, Indonesia. In: Howes, J V C & Noble, R A (eds.), *Proceedings of the conference on Petroleum systems of SE Asia and Australasia*. Indonesian Petroleum Association. Jakarta, Indonesia , 585-600. 1997.

Soenandar, H.B. Thermal history of the western Indonesian basins (Sunda-Asri, Northwest Java, and Southwest Java); evidence from fission track geochronology apatite. In: Howes, J V C & Noble, R A (eds.), *Proceedings of the conference on Petroleum systems of SE Asia and Australasia*. Indonesian Petroleum Association. Jakarta, Indonesia , 601-629. 1997.

Sudarmono, Suherman, T., and Eza, B. Paleogene basin development in Sundaland and its role to the petroleum systems in western Indonesia. In: Howes, J V C & Noble, R A (eds.), *Proceedings of the conference on Petroleum systems of SE Asia and Australasia*. Indonesian Petroleum Association. Jakarta, Indonesia , 545-560. 1997.

USGS World Energy Assessment Team. *World Petroleum Assessment 2000*. United States Department of the Interior, U.S.Geological Survey Digital data series DDS-60[4 discs]. 2000.

Wright, A., Friestad, H., Anderson, I., Wicaksono, P., and Reminton, C.H. Exploration history of the offshore Southeast Sumatra PSC, Java Sea. In: Fraser, A.J., Matthews, S. J. & Murphy, R. W. (eds.), *Petroleum Geology of Southeast Asia*, Geological Society Special Publication 126[ ], 121-142. 1997.

## A2.2 East Java Basin

### A2.2.1 CO<sub>2</sub> Sources

CO<sub>2</sub> emissions in the region directly overlying the small onshore area of East Java Basin contributed approximately 5 Mt CO<sub>2</sub>/yr to Indonesia's estimated total stationary source CO<sub>2</sub> emissions of 126 Mt/yr (IEA, 2000).

In a 300 km radius from the basin there are sources totalling approximately 13 Mt CO<sub>2</sub>/yr.

Note: The sum of sources within 300 km of a basin very crudely indicates the magnitude of emissions within reach of the basin. These "catchments" overlap for most basins and should not be summed.

### A2.2.2 Basin Overview

The East Java Basin differs from the adjacent NW Java Basin in a number of ways. Some maps show maximum sediment thickness of 9 km (Hardy et al., 1997). The modal thickness of sediment in the East Java Basin is 3 km. From the basin's inception in the Eocene, marine or strongly marine influenced environments of deposition are predominant. The area is approximately 260,000 sq km. The geothermal gradient is 39°C/km (Hutchison, 1989).

In the Late Eocene the Cretaceous basement rifted into a series of SW to NE orientated troughs and ridges. During the late Oligocene and early Miocene the troughs were the focus of deposition for a thick series of deep marine clastics and limestones. In the middle Early Miocene, the basin was divided into a northern platform and a southern trough by a shelf edge. The shelf edge developed along an east-west trend which is still apparent today. (Figure A76).

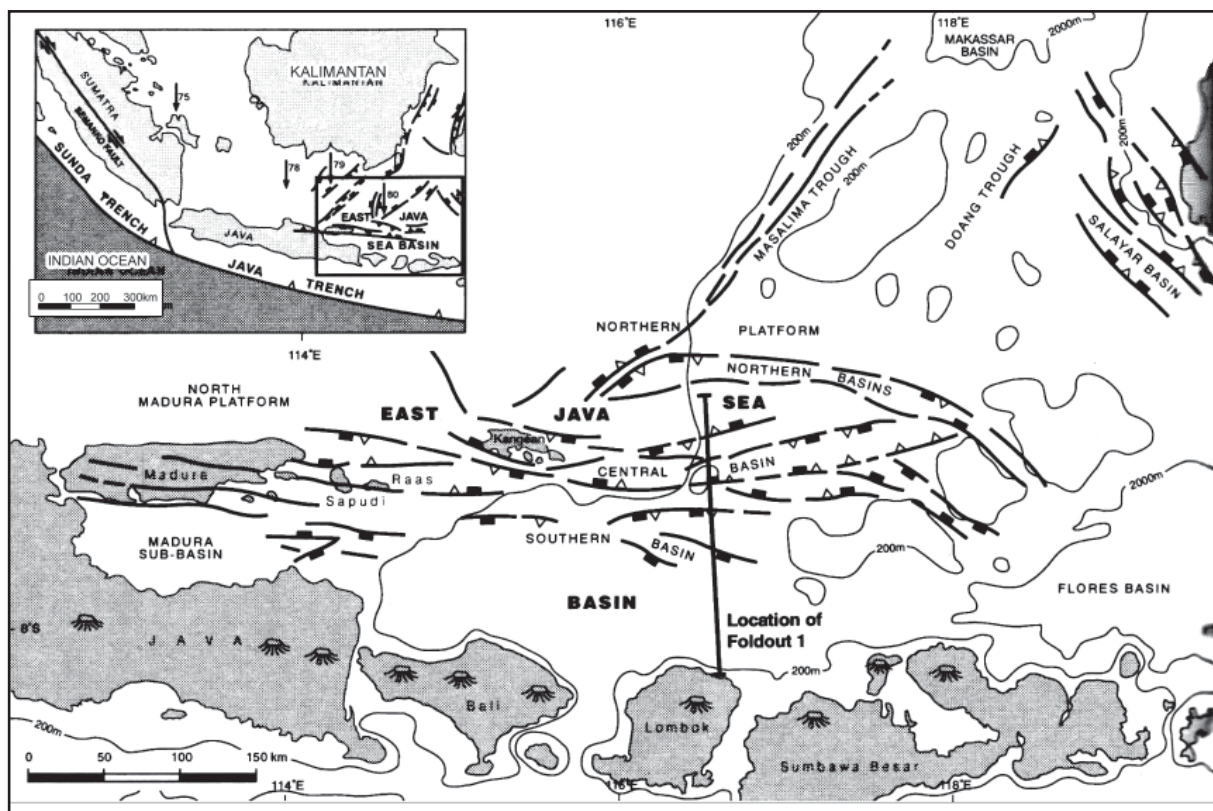


Figure A76. Tectono-stratigraphic development of the East Java Sea Basin (from Matthews and Brandsen, 1995).

## A2.2.3 Basin Fill

Like other basins along Java and Sumatra there are both siliciclastic and carbonate reservoirs (Figure A77 and Figure A78).

Carbonate reservoirs important to petroleum exploration are found in the Eocene-Oligocene Kujung Formation. These are high porosity reef zones on a carbonate shelf and isolated reef structures enclosed in intraformational mudstone. The parts of this formation targeted by hydrocarbon exploration lie at around 2700 m.

The main siliciclastic petroleum reservoirs are Middle to Late Miocene Marine Sandstones. Prominent reservoir is the Ngrayong Sandstone of the Kawengan Group. The Ngrayong Sandstone can be broadly correlated to the Upper Cibulakan Group in Western Java (Figure A78). The Ngrayong Formation represents a cycle of regression and transgression. The regressive section the cycle exhibits facies from shelfal sands through to various forms of debris flow sands. A subsequent transgression observed as hemipelagic mudstone seals all of these reservoirs. The facies of the Ngrayong Formation are diverse but excellent reservoir characteristics are reputed in the Cepu and Tuban areas. There is no reference to the facies encountered there.

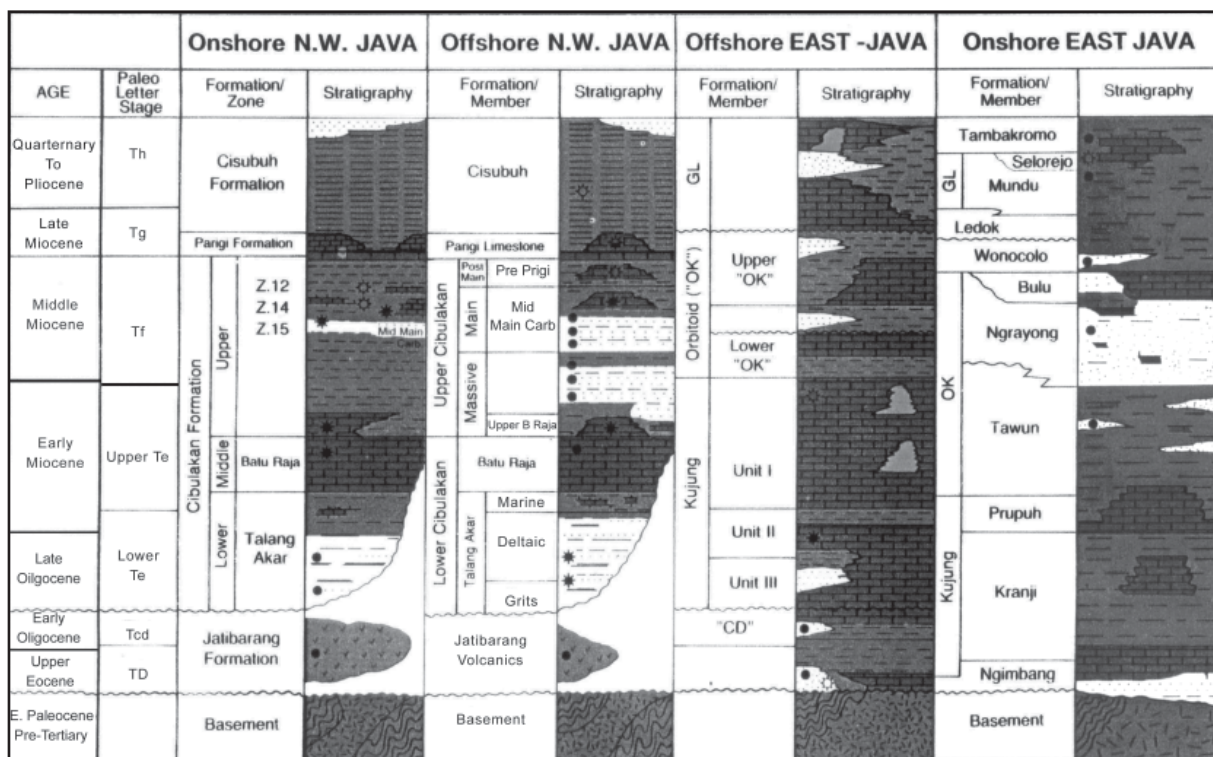


Figure A77. The geology and hydrocarbon potential of the Island of Java and its adjoining offshore areas (from the Indonesian Petroleum Association Oil and Gas Fields Atlas IV, publication date unknown.)

## A2.2.4 Hydrocarbon fields

The oil and gas fields of the East Java Basin are quite small. This is no doubt why the basin was omitted from the USGS World Petroleum assessment in 2000. Nearly all hydrocarbon bearing structures of note are Pliocene-Pleistocene reverse faulted anticlines.

Average field size is 6 mmbbls. Only field is over 100 mmbbls. Of the others only 4 are over 10 mmbbls in size. Up until 1993 approximately 200 mmbbls were produced from NE Java (equivalent stored CO<sub>2</sub> 26.6 Mt).

Gas discoveries onshore have total reserves of only 92 Bcf (equivalent to ~5 Mt of CO<sub>2</sub>)

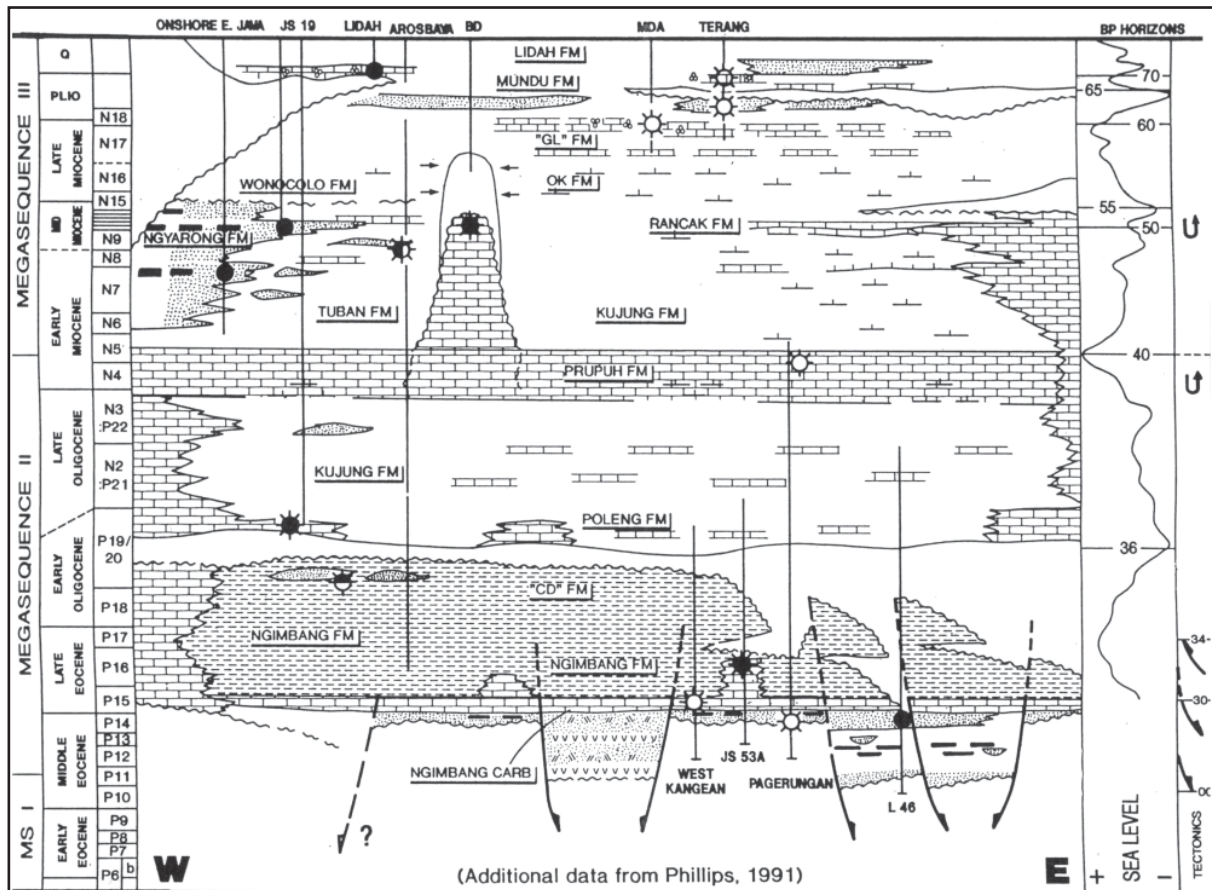


Figure A78. The geology and hydrocarbon potential of the Island of Java and its adjoining offshore areas (from Matthew and Brandsen, 1995).

### A2.2.5 Coal Occurrence

Coal occurs in mainly on Sumatra and Borneo. See section 4.2 in the main report for a discussion of coal occurrence in Indonesia and its relevance to CO<sub>2</sub> storage.

### A2.2.6 Potential CO<sub>2</sub> Storage Options

Hydrocarbon Fields are relatively small in the East Java Basin and do not appear to represent a large pore space. Discoveries since 1993 may have added some potential. In 2005 a 100+ mmbbl field was discovered in the East Java Basin. This aside, it is apparent pore space capacity of the fields is very limited.

Storage in saline reservoirs has much more potential. The Ngrayong Formation offers a high potential regression/transgression regional play. This play is best expressed in the smaller onshore portion of the basin. It appears the Middle to late Miocene Marine Sandstones may offer opportunities particularly the shelfal sands which may from larger bodies. The Kujung Formation provides carbonate reservoir targets for storage. The extent of these reef facies in the basin is unclear. No palaeogeography maps were located. From Figure A77 and Figure A78 it is inferred the reef limestones with good reservoir qualities occur in elongate belts parallel to the east-west structural trend.

The Ngrayong Sandstone of the Onshore East Java Basin appears to have very good geological potential. There are local emissions of ~ 10 Mt/yr. The Onshore East Java Basin is 450 km from the 25 Mt/yr emitted near Jakarta and Bandung.

## A2.2.7 References

Hardy, L.R., Muchsin, S., Ichram, L., Samuel, L. and Purmomo, E., Application of Petroleum System Concept to Reconnaissance Assessments of Mature and Emerging Basins, with Examples from Indonesia. In: Howes, J V C & Noble, R A (eds.), Proceedings of the conference on Petroleum systems of SE Asia and Australasia. Indonesian Petroleum Association. Jakarta, Indonesia , 127-140. 1997.

Matthews, S.J. and Bransden, P.J.E., Late Cretaceous and Cenozoic tectono-stratigraphic development of the East Java Sea Basin, Indonesia. *Marine and Petroleum Geology* 12[2], 499-510. 1995.

## A2.3 Kutei Basin

### A2.3.1 CO<sub>2</sub> Sources

Bongon gas refinery is the major stationary CO<sub>2</sub> source in the region with an annual estimated CO<sub>2</sub> emission of ~14 Mt.

CO<sub>2</sub> emissions in the region directly overlying the Kutei Basin contributed approximately 19 Mt CO<sub>2</sub>/yr to Indonesia's estimated total stationary source CO<sub>2</sub> emissions of 126 Mt/yr (IEA, 2000).

In a 300 km radius from the basin there are sources totalling approximately 20 Mt CO<sub>2</sub>/yr.

Note: The sum of sources within 300 km of a basin very crudely indicates the magnitude of emissions within reach of the basin. These "catchments" overlap for most basins and should not be summed.

### A2.3.2 Basin Overview

The Kutei Basin is the largest (165,000 km<sup>2</sup>) and the deepest (14 km) Tertiary sedimentary basin in Indonesia. The Kutei Basin was initiated by rifting during the Middle Eocene. The rift phase was succeeded by a basin sag phase that lasted until the Late Oligocene (Figure A79, Figure A80).

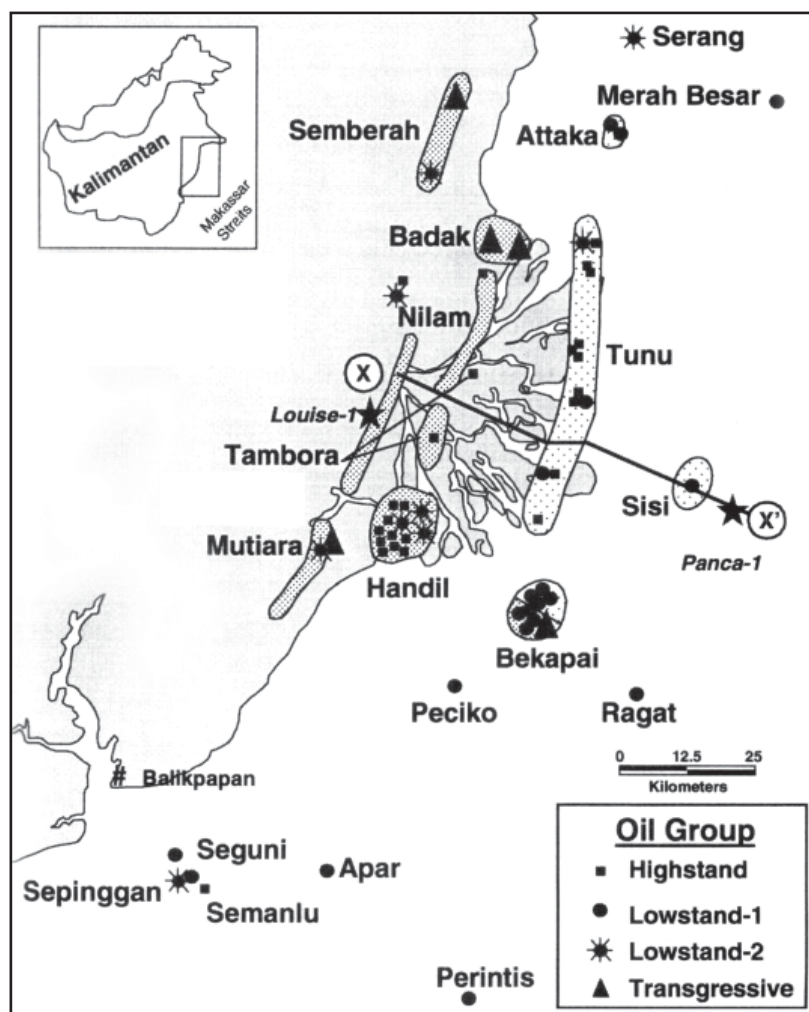
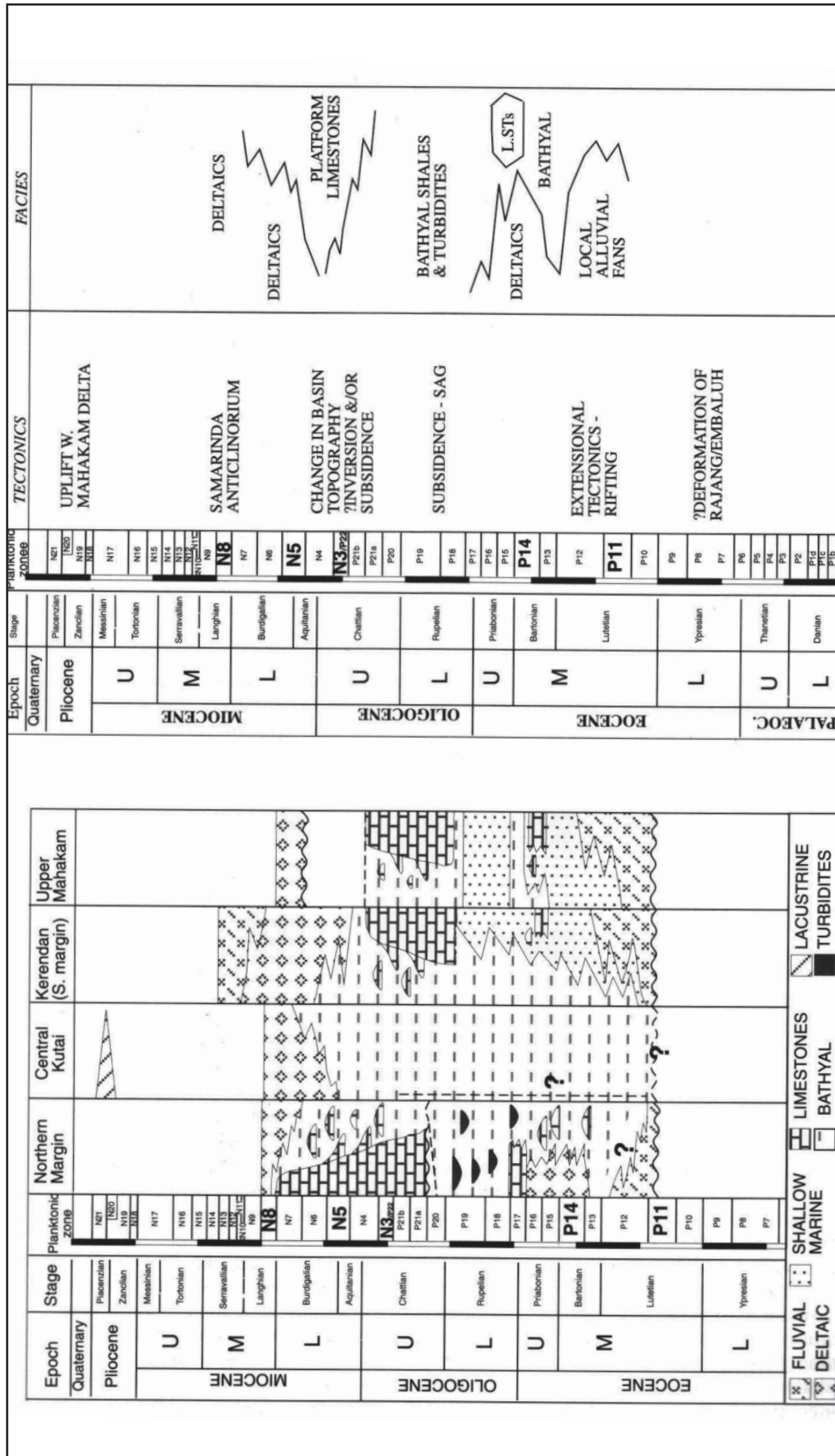


Figure A79. Map shows approximately north-south anticlinal trends (elliptical shapes) and locations of oil samples in the Mahakam-Makassar area, Kutei Basin. Inset upper left shows location of study areas in eastern Borneo, Kalimantan, Indonesia. Heavy stippling indicates oil trends and light stippling indicates gas trends within the anticlines. Genetic groups with symbols defined in the inset at lower right are based on statistical geochemical data. Stars indicate location of the Louise 1 and Panca 1 wells (text and figure from Peters et al., 2000).



Tertiary sedimentation in the basin has been fairly continuous since its inception in the Middle to Late Eocene. An extensive eastward pro-grading delta system existed from the Earliest Miocene to the present day. Sedimentation averaged 1000 m/m.y. and as a result the Palaeogene section is over pressured. The geothermal gradient is 32°C/km. The main lithologies are thick prodelta shale, shelf break and transgressive limestones and fluvial channel/deltaic and gravity flow sandstones. The basin was inverted in the earliest Middle Miocene. This created many anticline traps (Samarinda Anticlinorium) in what is now the eastern onshore area. This area has the most prolific hydrocarbon production in the basin.

### A2.3.3 Basin Fill

Heterogeneous sandstones in upper to middle Miocene lobes of the Mahakam Delta are prolific hydrocarbon reservoirs in the lower Kutei Basin. Sand bodies of the modern Mahakam delta are analogs for many of these reservoirs. Lowstand sandstones also form the most porous and permeable hydrocarbon reservoirs. The depth to hydrocarbon target reservoirs varies from under 500 m depth to 3000 m depth with a few targets between 3000 and 4000 m (USGS, 2000). Large fields are with in anticlines of the Samarinda Anticlinorium (Figure A81).

Some facies within the delta system have very good reservoir qualities. Cross-stratified, coarse-to fine-grained tidal/fluvial distributary channel sandstones are 3 to 17 m thick and <1.5 km wide. Distributary-channel sandstones are typically highly porous (20-35%) and permeable (100-10,000 mD), although tidal distributaries exhibit permeability heterogeneity, due to mud drapes and local burrows. Delta-front sandstones are extensive in area but have generally poorer reservoir quality than the distributary channel sandstones ( $k = <0.1-1000$  mD; porosity = 10-25%) (Trevena, Partono, & Clark 2003)

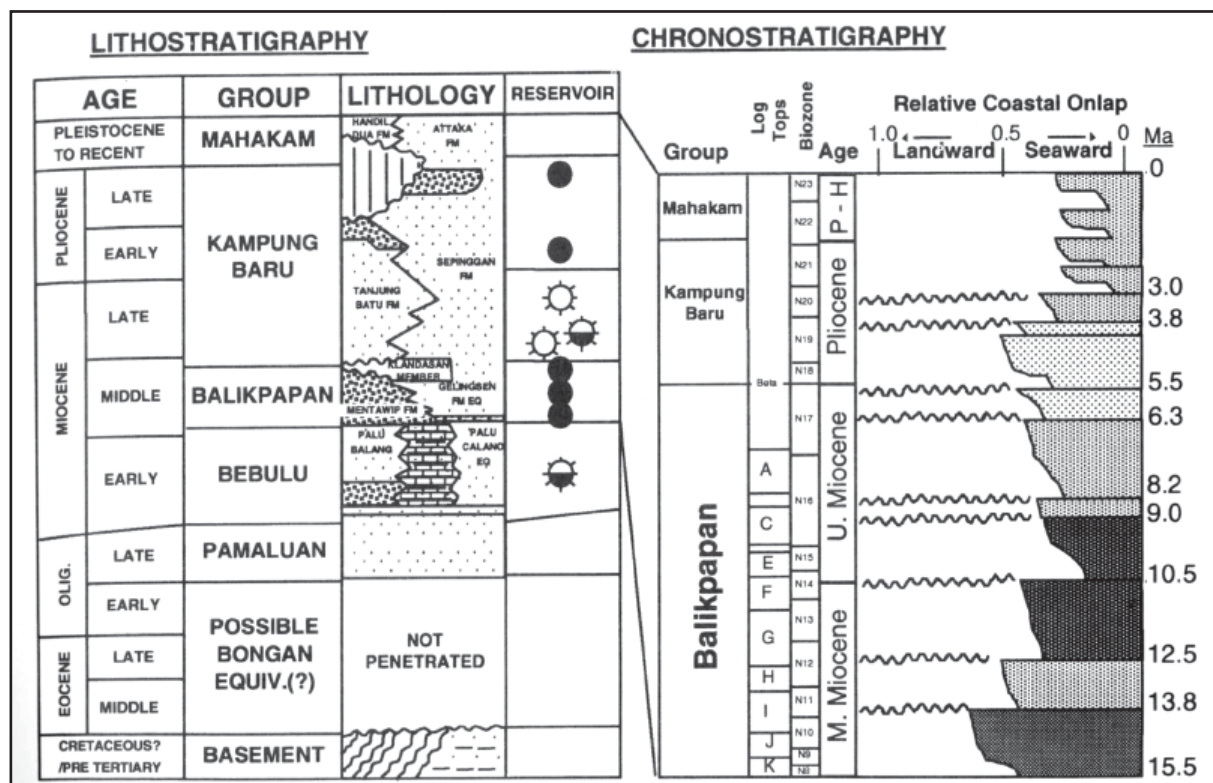


Figure A81. Generalised stratigraphic column (left) shows distribution of oil and rock samples and Neogene sequence lithostratigraphy, chronostratigraphy, and local zone names (right) of the Mahakam Delta and Makassar Slope (text and figure from Peters et al., 2000).

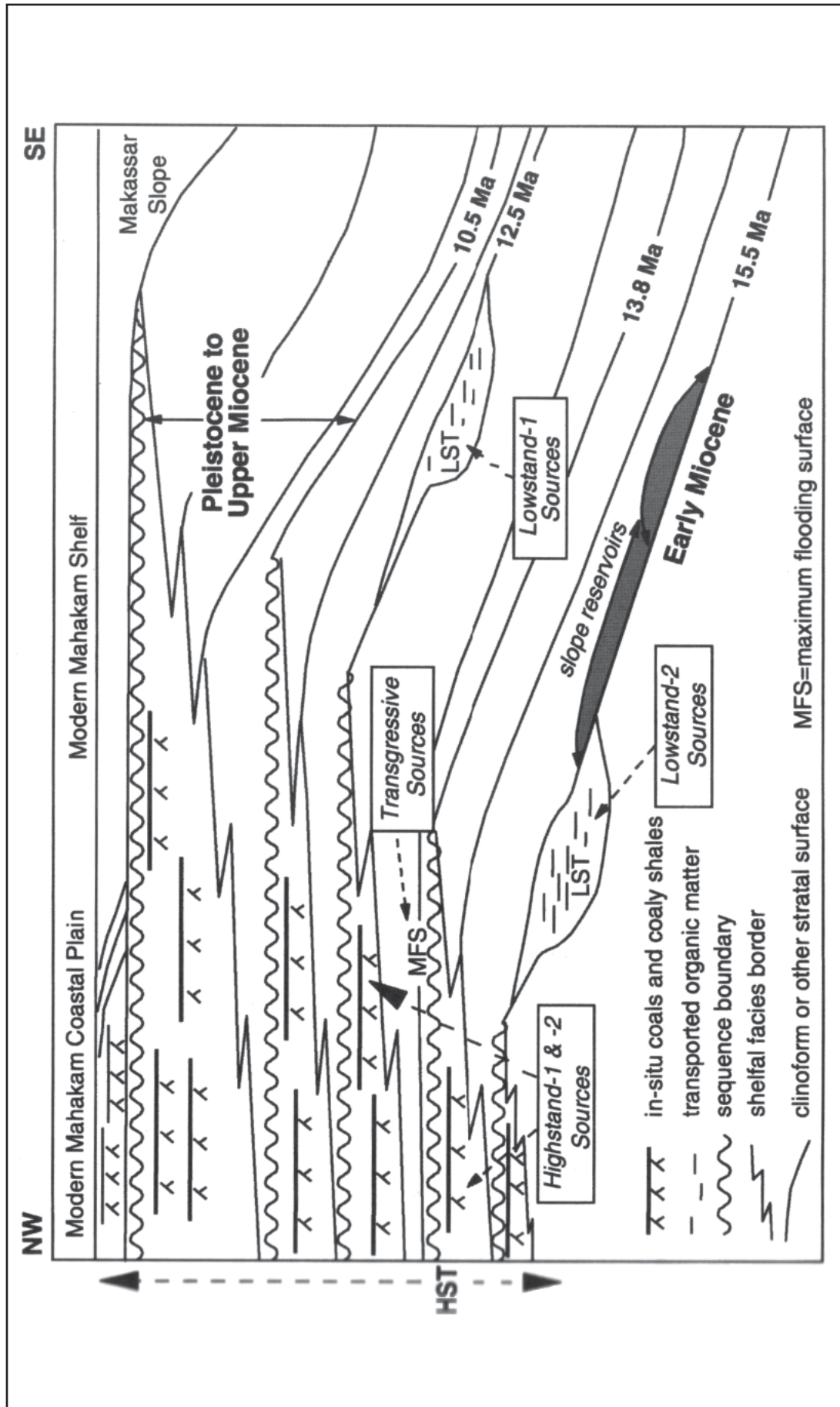


Figure A82. Schematic of the new geochemical-stratigraphic model and predicted distribution of the Mahakam-Makassar area source rocks. Faults, which provide inferred migration pathways from source rocks to reservoirs, are not shown. HST = highstand systems tract, TST = transgressive systems tract, LST = lowstand systems tract, MFS = maximum flooding surface (text and figure from Peters et al., 2000).

Seals on delta sands are inter-distributary shales and transgressive shales of marine flood events (Figure A82). There are also gravity flow sands isolated in deep water environments. Isolated sand body deposits are in principle less practical when considering injecting of CO<sub>2</sub> due to the likelihood of overpressure.

There is evidence of an extensive meteoric water invasion event around 3 Ma. Present Day there are fresh water sands at 6000 ft (1830 m) depth and 30 km offshore.(Paterson et al., 1997).

### A2.3.4 Hydrocarbon Fields

The Kutei Basin is a major hydrocarbon producing basin. Petroleum production began at the Sanga-Sanga field in 1898. Most of the production is currently centred on four, major north-trending anticlines. Oil and gas are currently being produced from about 20 onshore and offshore fields.

Various estimates of reserves can be located. The USGS (2000) estimated known oil volume of 2879 mmbbls (equivalent to 374 Mt stored CO<sub>2</sub>). The produced oil volume is equivalent to 285 Mt stored CO<sub>2</sub>.

Using the USGS (2000) data, the following characterisation of field sizes (Note: Field size NOT reserve) can be made: Oil fields range up to 1000 mmbbls. There are two fields of this size both discovered in the early 1970s. There are only four fields between ~100 and 300 mmbbls in size.

There is considerably more potential CO<sub>2</sub> storage capacity in gas fields. The USGS (2000) estimate “known” gas of 45.4 Tcf (equivalent to 3.6 Gt stored CO<sub>2</sub>). Only 8.7 Tcf has been produced. Of the known gas volume ~30 Tcf is within 6 fields over 1.5 Tcf in size. The largest field is 10 Tcf.

The produced volume of 8.7 Tcf equates to 696 Mt of CO<sub>2</sub> (Assuming 1Tcf = 80 Mt of CO<sub>2</sub>). The distribution of this depleted pore space is unknown.

### A2.3.5 Coal Occurrence

This is one of the main coal-producing basins with ECBM potential in Indonesia. Mining is mainly opencut, with a couple of underground operations. See section 4.2 in the main report for a discussion of coal occurrence in Indonesia and its relevance to CO<sub>2</sub> storage.

### A2.3.6 Potential CO<sub>2</sub> Storage Options

The majority of CO<sub>2</sub> emissions in Kalimantan are the result of hydrocarbon refining/processing operations. Given the source of the CO<sub>2</sub>, there are obvious technological synergies that favour saline reservoirs/depleted field storage over ECBM storage.

The Miocene to present day fluvial-deltaic system has high potential for extensive good reservoir quality sandstones with extensive transgressive seals. There is some evidence for fresh pore water down to 1830 m; increasing CO<sub>2</sub> solubility. The risk of CO<sub>2</sub> injection impacting on the extraction of hydrocarbons would need to be carefully assessed. A large proportion of “known” oil has been produced while much of the “known gas” is still held as reserves. Depleted fields (if such exist) within the Samarinda anticlines would provide extremely high confidence storage places.

### A2.3.7 References

Chambers, J.L.C. and Daley, T.E. A tectonic model of the onshore Kutai Basin, East Kalimantan. In: Fraser, A J, Matthews, S J & Murphy, R W (eds.), *Petroleum geology of Southeast Asia*. Geological Society Special Publications. Geological Society of London 126, 375-393. 1997.

Paterson, D.W., Bachtiar, A., Bates, J.A., Moon, J.A., and Surdam, R.C. Petroleum System of the Kutei Basin, Kalimantan, Indonesia. In: Howes, J V C & Noble, R A (eds.), *Proceedings of the conference on Petroleum systems of SE Asia and Australasia*. Indonesian Petroleum Association. Jakarta, Indonesia , 709-726. 1997.

Peters, K.E., Snedden, J.W., Sulaeman, A., Sarg, J.F., and Enrico, R.J. A New Geochemical-Sequence Stratigraphic Model for the Mahakam Delta and Makassar Slope, Kalimantan , Indonesia . *AAPG Bulletin* 84[1], 12-44. 2000.

Trevena, A.S., Partono, Y.J., and Clark, T. Reservoir Heterogeneity of Miocene-Pliocene Deltaic Sandstones at Attaka and Serang Feilds Kutei Basin, Offshore East Kalimantan, Indonesia. In: Sidi, F H, et al (eds.), *Tropical deltas of Southeast Asia; sedimentology, stratigraphy, and petroleum geology*. Special Publication - Society for Sedimentary Geology. Society for Sedimentary Geology (SEPM). Tulsa, OK 76, 235-254. 2003.



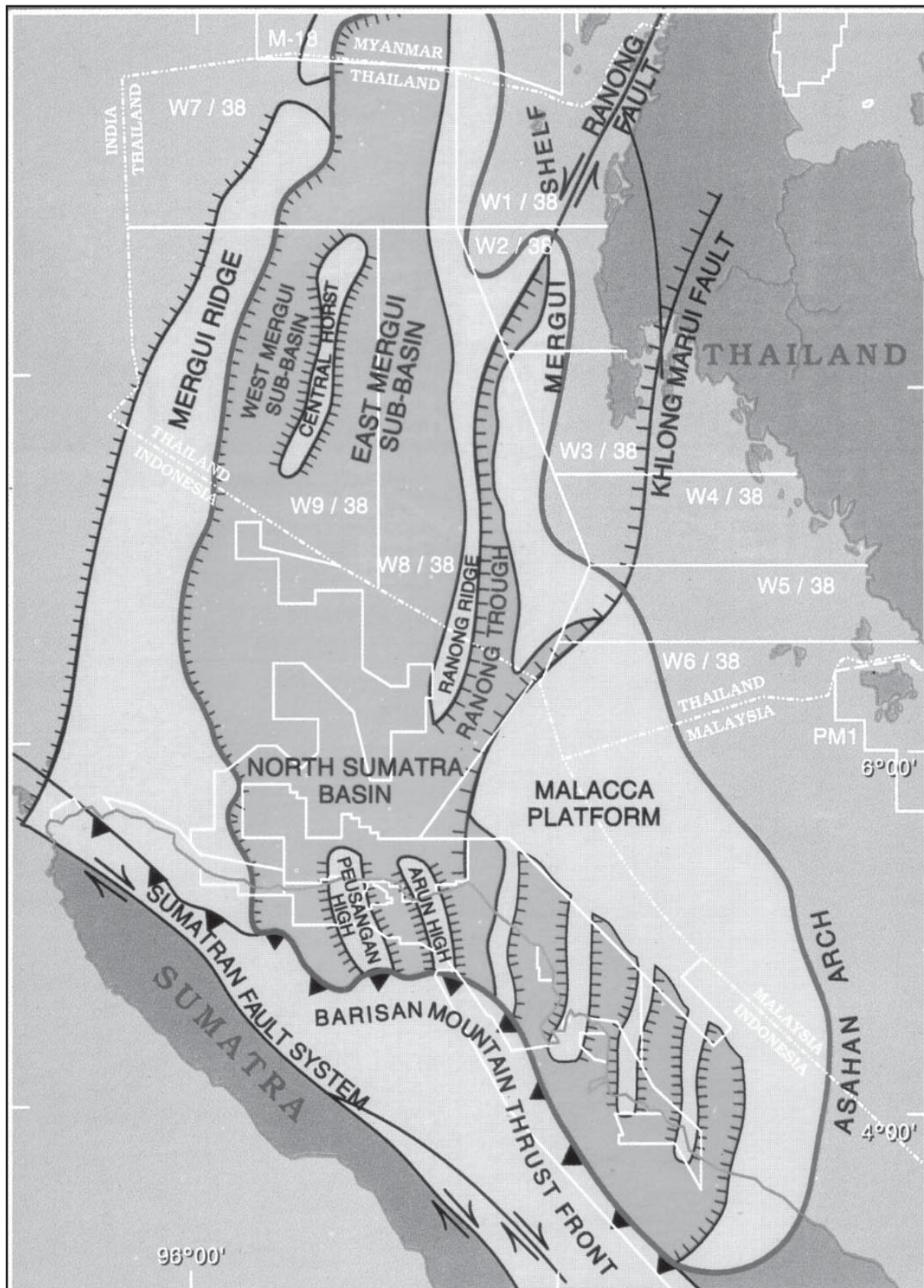


Figure A84. General physiography of the Mergui and North Sumatran basins showing the primary depocenters of the Thailand Andaman Sea: the West Mergui, East Mergui, and sub-basins (text and figure from Andreason et al., 1997).

### A2.4.3 Basin Fill

Clastic petroleum target reservoirs include lowstand fans, Oligocene Bampo fluvio-deltaics (observed porosities averaging 19 and 24%). These lowstand facies are sealed by Late Oligocene to Early Miocene transgressive black shales of the same group. This black mudstone facies was deposited in lacustrine to restricted marine environments up to 2000 m thick (USGS, 2000). The lacustrine rift environments gave way to a widespread shallow marine environment with strong carbonate deposition (Peutu Formation). (Figure A85, Figure A86 and Figure A87)

The most important petroleum reservoir rocks are Early Miocene platform carbonates and reefs of the Belumai and Peutu Formations. The Peutu Formation has good average porosity of 18%. In hydrocarbon reservoir sections porosity averages 25 to 30% (Andreason et al., 1997). Carbonate reservoir rocks are involved in anticline traps and combination faulted stratigraphic traps. Carbonate reefs and buildups are found on top of and around basement highs. Regional shales of the Middle Miocene Baong Formation seal most of the reservoirs. Intraformational seals also form important hydrocarbon traps (USGS, 2000). (Figure A85, Figure A86 and Figure A88)

The Miocene Keutapang Formation is a widespread siliciclastic reservoir sealed by the Seurula Formation. Fluvial to shallow marine facies of the Ketuapang are developed at the SE end of the North Sumatra Basin (Figure A85, Figure A86 and Figure A88).

### A2.4.4 Hydrocarbon fields

The USGS “known” hydrocarbon estimate is 674 mmbbls of oil (equivalent to 88 Mt stored CO<sub>2</sub>) and 25.5 Tcf (equivalent to 2 Gt stored CO<sub>2</sub>).

In 2000 the USGS reported the largest oil field to be approximately 300 million barrels. This field was an outlier with the rest of the known fields being no larger than 64 mmbbls with an average of only 16 mmbbls.

The area has a 14 Tcf gas field. The next four largest fields have a combined volume of 6 Tcf. All other fields are smaller than 1 Tcf in size. The individual depletion of these fields is unknown.

### A2.4.5 Coal Occurrence

There is little developed coal in the Northern Sumatra Basin or region. Coal mines are located in Central and Southern Sumatra regions. See section 4.2 in the main report for a discussion of coal occurrence in Indonesia and its relevance to CO<sub>2</sub> storage.

### A2.4.6 Potential CO<sub>2</sub> storage Options

The wide spread occurrence of the Baong Formation which is a regional seal for petroleum occurrence would be an ideal seal for all saline reservoir formations below it, most of which have some petroleum occurrence. Coarse alluvial to upper fluvial sediment of the early rift may be sealed by the Bampo Formation which is the main petroleum source rock in the basin.

Oil fields are relatively small and may not be material to CO<sub>2</sub> storage. There is only one very large gas field. The depletion status of all fields is unknown..

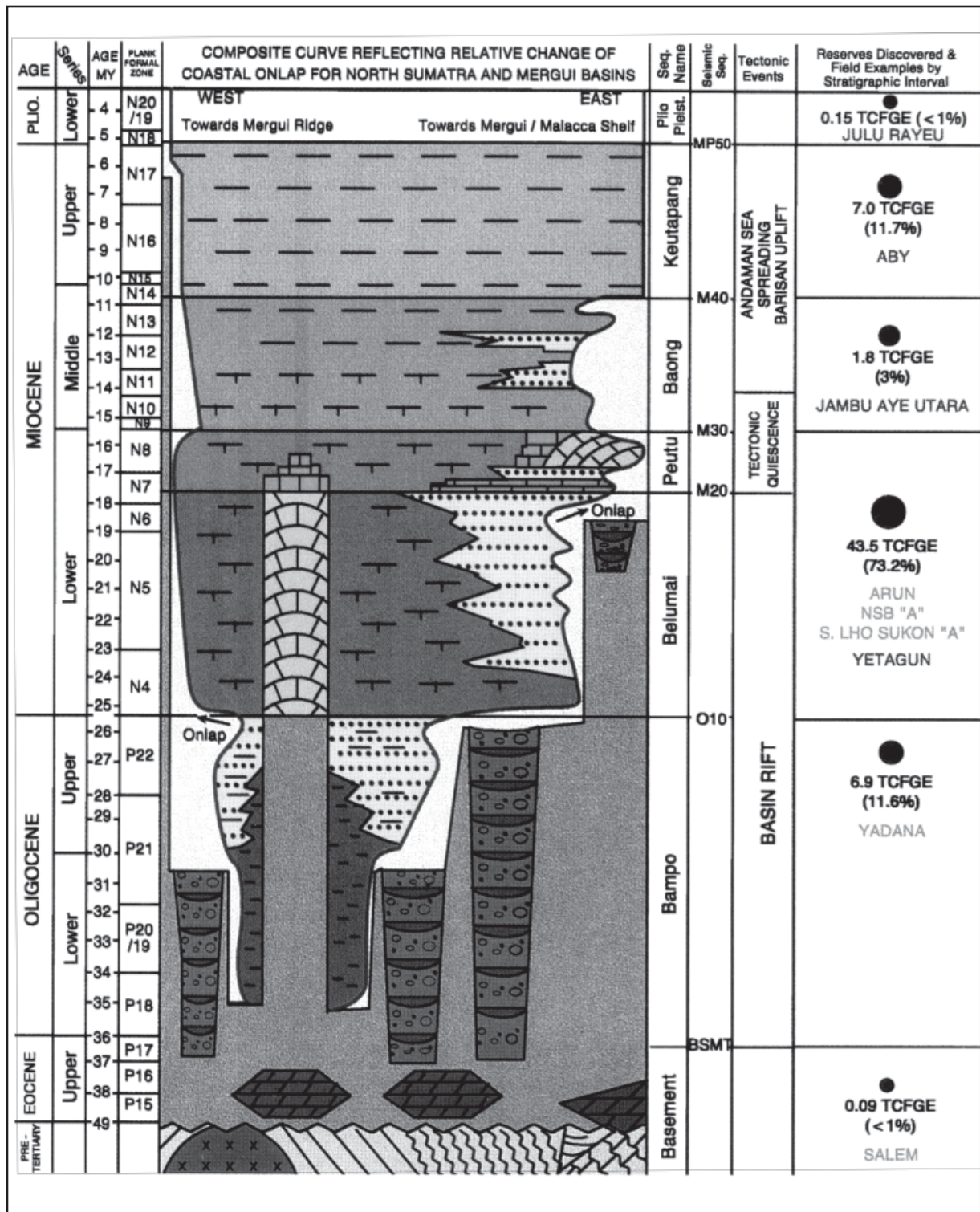


Figure A85. Generalised stratigraphic column for the Thailand sector of the Mergui and the North Sumatra basins showing the major sequences. Also shown is the volume of raw gas reserves and relative percentages discovered to date by sequence within the North Sumatra, Mergui and Martaban basins (from Andreason et al., 1997).

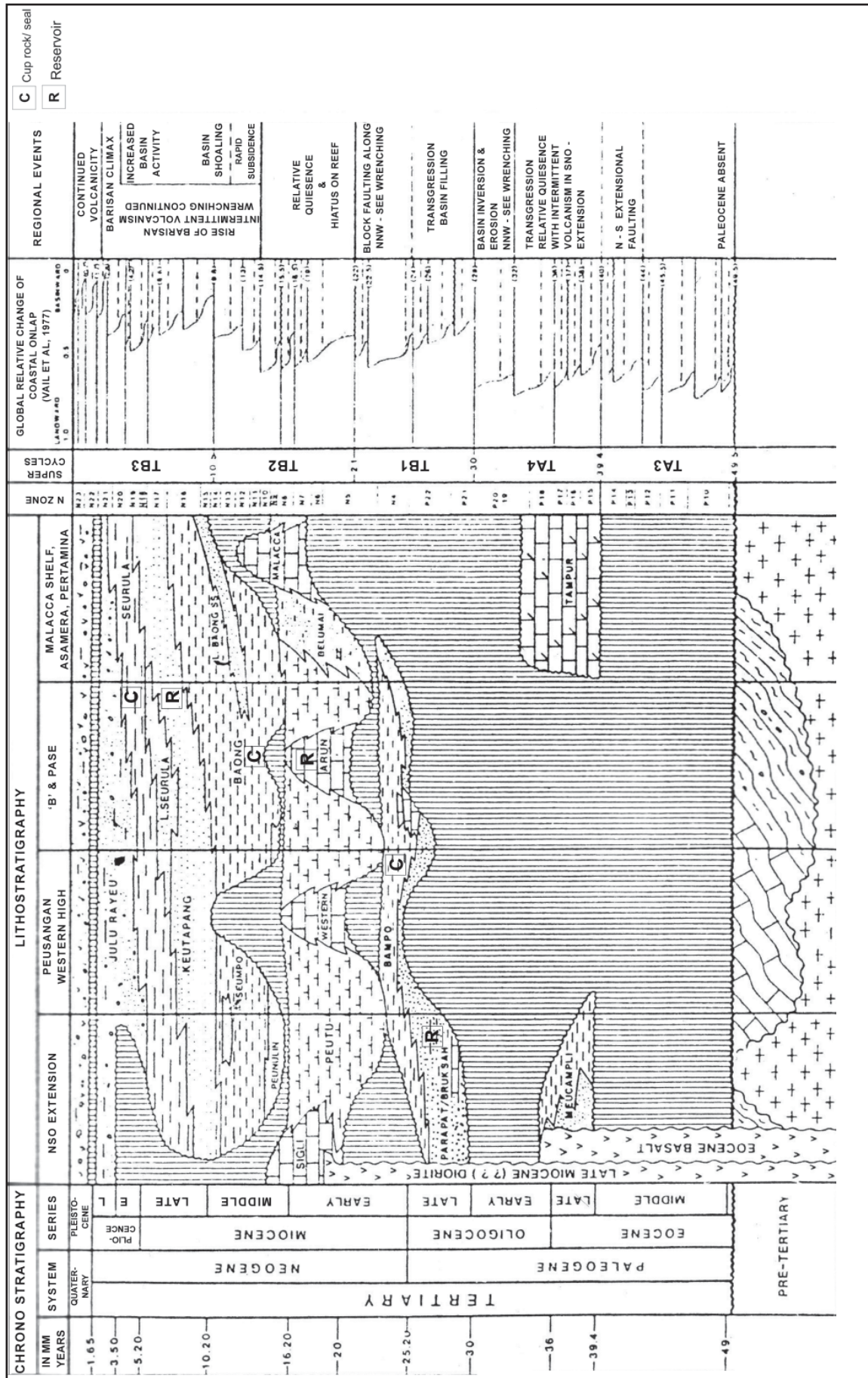


Figure A86. Stratigraphy of the North Sumatran Basin (from Ryacudu and Sjahbuddin, 1994).

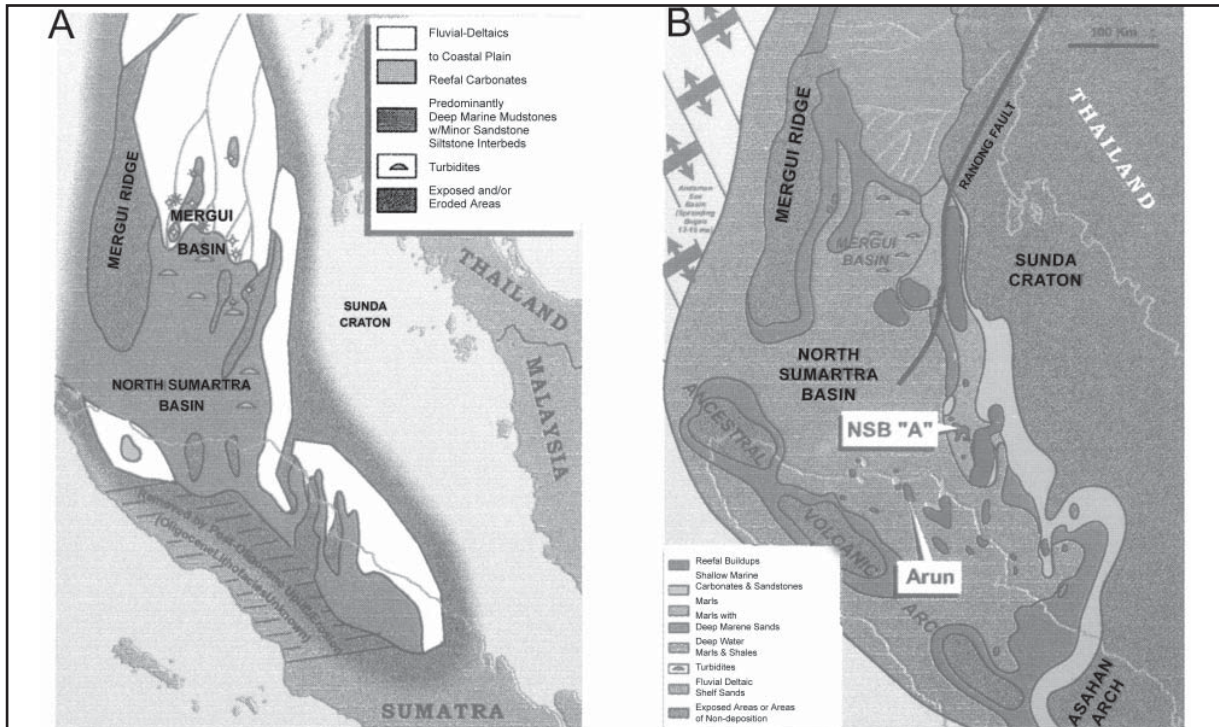


Figure A87. (a) Bampo sequence (Late Oligocene) lithofacies showing fluvial-deltaic sandstone deposition dominating the northern half of the Thailand Andaman Sea while shale deposition dominates the south. Thailand exploratory wells shown for reference (from Andreason et al., 1997). (b) Peutu sequence (Early Miocene) lithofacies. Reef growth is at a zenith during this time due to the tectonic calm, the sea-level maxima, and the suppression of clastic contamination (from Andreason et al., 1997).

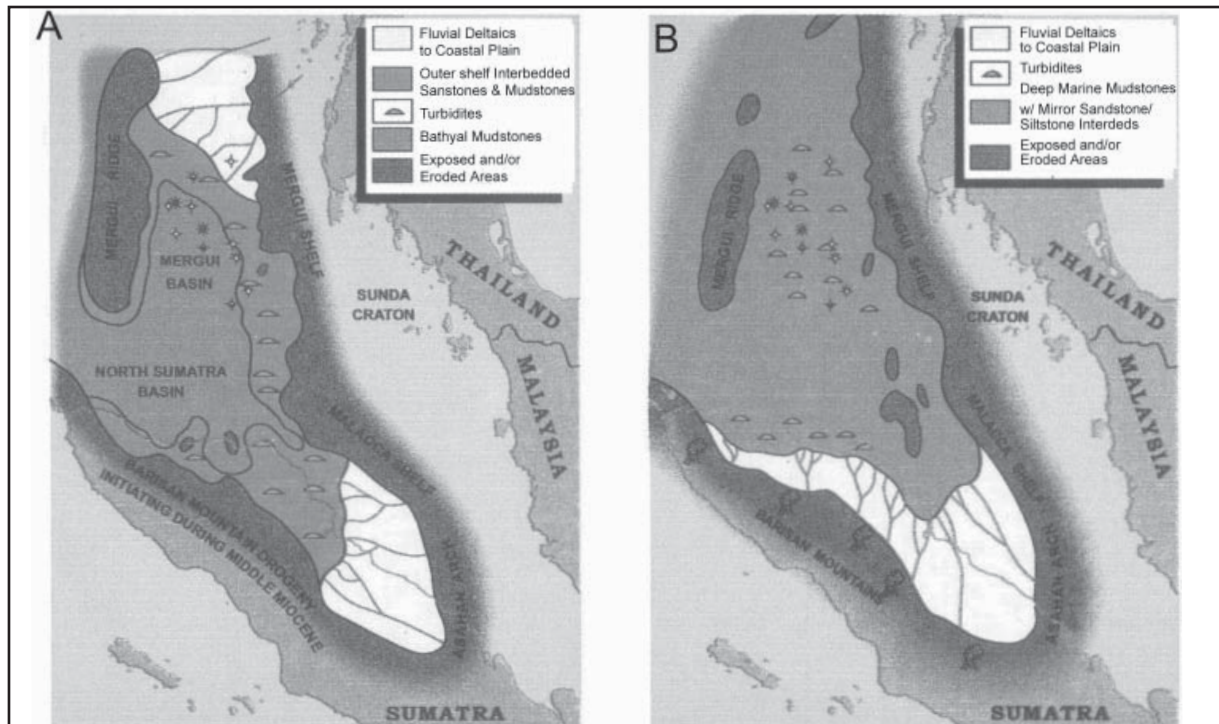


Figure A88. (a) Baong sequence (Middle Miocene) lithofacies. Deposition is generally restricted to rapidly subsiding basin centers while the shelves undergo subaerial exposure (from Andreason et al., 1997). (b) Keutapang sequence (Upper Miocene) lithofacies. Deep water deposition dominates the central basins while shelves remain regions of exposure (from Andreason et al., 1997).

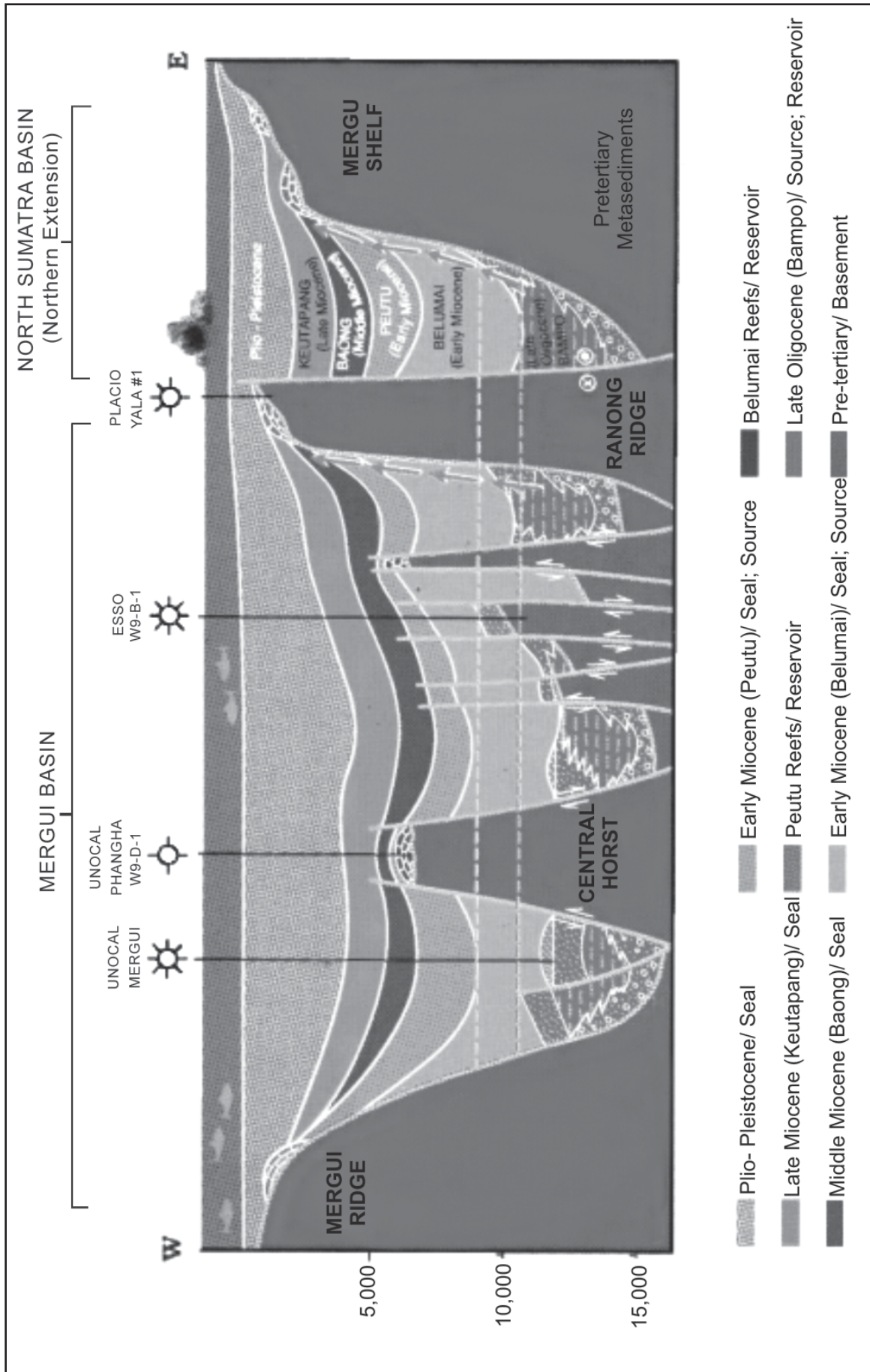


Figure A89. Generalised cross-section across the Thailand Andaman Sea and the North Sumatra Basin (from Andreason et al., 1997)

## A2.4.7 References

Andreason, M.W., Mudford, B., and St Onge, J.E. Geologic evolution and petroleum system of the Thailand Andaman Sea basins. In: Howes, J V C & Noble, R A (eds.), Proceedings of the conference on Petroleum systems of SE Asia and Australasia. Indonesian Petroleum Association. Jakarta, Indonesia , 337-350. 1997.

Buck, S.P. and McCulloh, T.H. Bampo-Peutu(!) petroleum system, North Sumatra, Indonesia. In: Magoon, L B & Dow, W G (eds.), The petroleum system; from source to trap. AAPG Memoir 60, 625-637. 1994.

Kirby, G.A., Morley, R.J., Humphreys, B., Matchette-Downes, C.J., Sarginson, M.J., Lott, G.K., Nicholson, R.A., Yulihanto, B., Widiastuti, R., Karmajaya, Sundoro, Fitris, F., Sofyan, S., and Wijaya. S. A re-evaluation of the regional geology and hydrocarbon prospectively of the onshore central North Sumatra Basin. In: Proceedings of the Twenty-first Annual Convention - Indonesian Petroleum Association. Jakarta, Indonesia 21[1], 243-264. 1993.

Ryacudu, R. and Sjahbudin, E. Tampur Formation, the Forgotten Objective in North Sumatra Baisn ? In: Strategic Management of Technology and Resources Proceedings of the 23rd Annual Convention - Indonesian Petroleum Association. Jakarta, Indonesia 1, 160-179. 1994.

## A2.5 Central Sumatra Basin

### A2.5.1 CO<sub>2</sub> Sources

CO<sub>2</sub> emissions in the region directly overlying the Central Sumatra Basin contributed approximately 3 Mt CO<sub>2</sub>/yr to Indonesia's estimated total stationary source CO<sub>2</sub> emissions of 126 Mt/yr (IEA, 2000).

In a 300 km radius from the basin there are sources totalling approximately 10 Mt CO<sub>2</sub>/yr.

Note: The sum of sources within 300 km of a basin very crudely indicates the magnitude of emissions within reach of the basin. These "catchments" overlap for most basins and should not be summed.

### A2.5.2 Basin Overview

The Central Sumatra Basin was initiated in the Eocene as a result of back arc extension and contains the largest oil fields in Indonesia (Figure A90). The basin is divided into a series of north to northwest trending, fault-bounded sub-basins, which have unique subsidence and sedimentary histories. The basin fill consists of a non-marine synrift sequence and a marine post-rift sequence. The major stratigraphic sequences are: Eocene-Oligocene syn-rift Pematang Group, post-rift Early Miocene Sihapas Group, Mid-Miocene-Pliocene Petani Group and Plio-Pleistocene Minas Formation (Figure A91). The basement depth averages 2.5 km in these half-graben and may reach 3 km. Up to 2 km of this fill may be post rift sequences. The average geothermal gradient in the basin is very high at an average of 60°C/km. Geothermal gradient ranges from to ~35°C/km in grabens up to ~90°C/km in areas of thin cover and shallow pre-Tertiary basement. The area of the basin is 117,300 sq km.

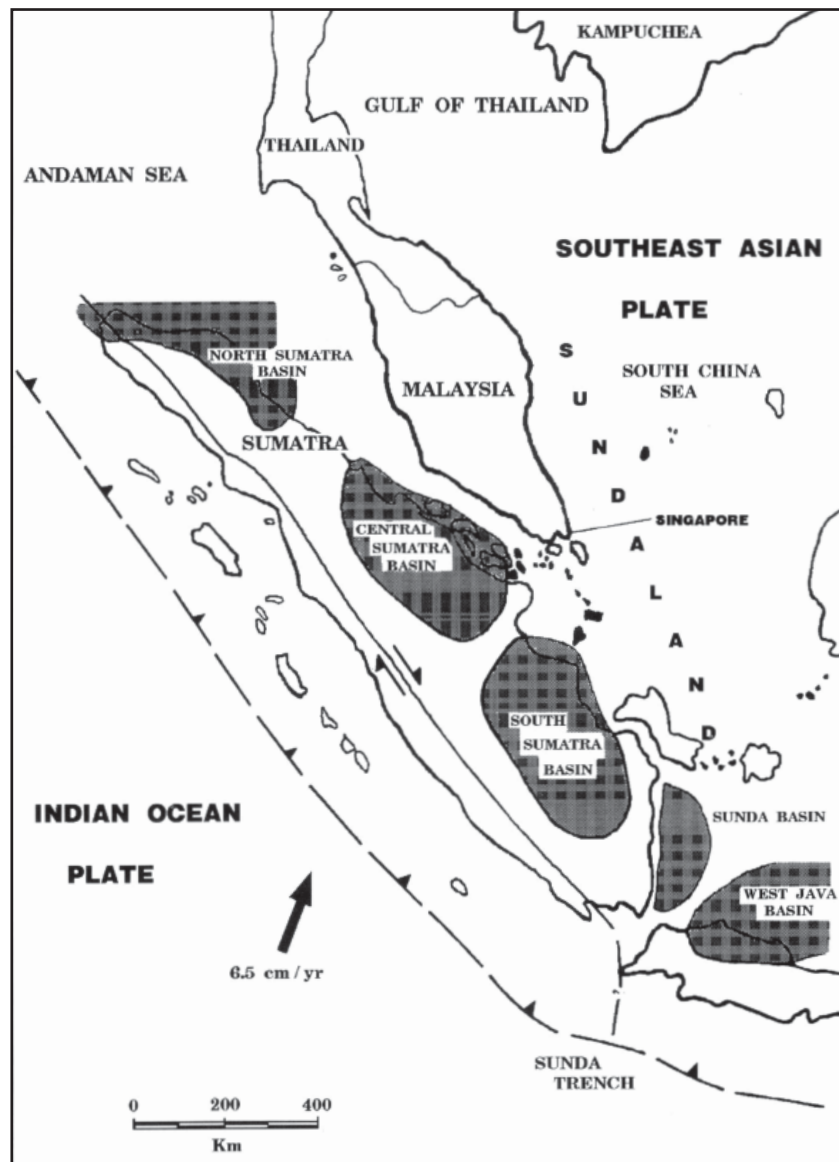


Figure A90. Central and Sumatran Basin regional map (from Williams and Eurbank, 1995).

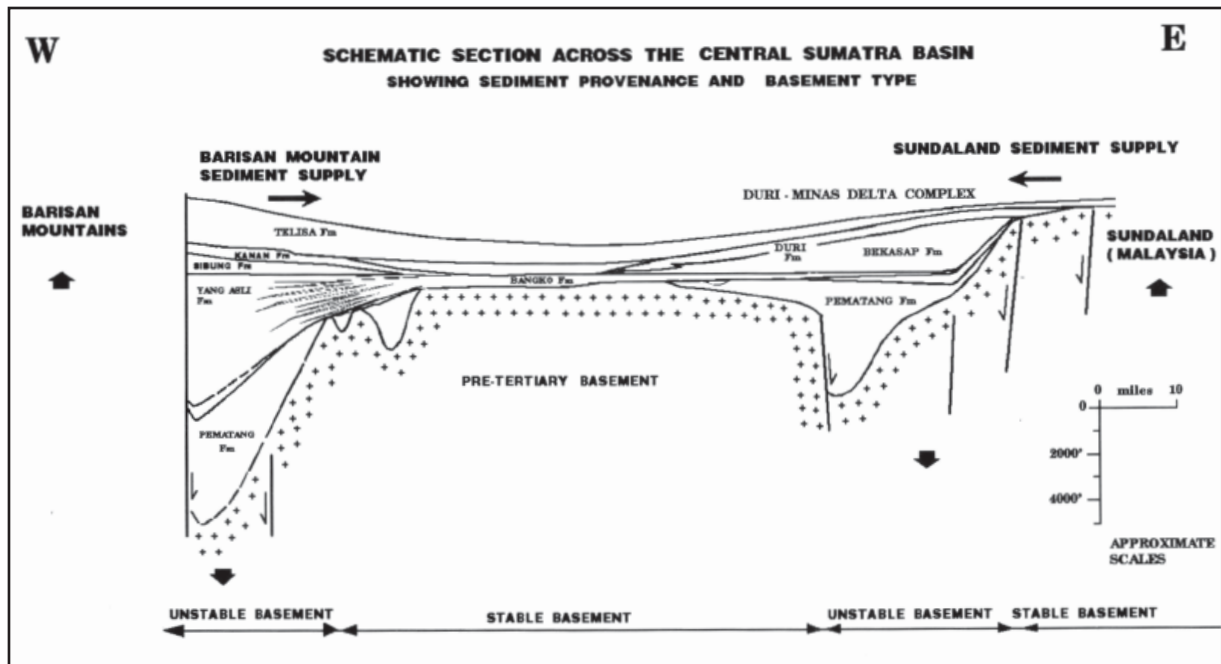


Figure A91. Schematic section across the Central Sumatra Basin (from Williams and Eurbank, 1995).

### A2.5.3 Basin Fill

Notably the Central Sumatra Basin lacks carbonate reservoirs in contrast to the North and South Sumatra basins (Williams and Eubank, 1995). The Sihapas Group post-rift marine sandstones are the principal reservoir units in the Central Sumatra Basin; fluvial-lacustrine sandstones within the syn-rift Pematang Group are subsidiary reservoirs (Figure A92). The Sihapas Group sediments were deposited in the Early Miocene during a period of rising relative sea level and form an overall fining-upward sequence. Deposition environment range from fluvial-deltaic to shallow marine facies; the sediment source is from the north in peninsula Malaysia. The extent of the Duri Formation of the Sihapas Group is shown in Figure A93. Well-sorted, quartz sandstones form excellent reservoir units, being composed of medium to coarse-grained with porosities >25% and permeability between 400-4500 mD and typically average about 1500 mD.

Siliciclastic reservoirs in the Pematang Group consist of braided fluvial and alluvial fan deposits along graben-bounding faults. These poorly to moderately well sorted feldspathic-quartzose sandstones have average porosities ranging from 15 -20% and average permeability of generally <100 mD; authigenic kaolinite has degraded the pore systems of these rocks.

The lower and middle Miocene Telisa Shale of the Sihapas Group represents the maximum transgression in the basin. These finely laminated marine shelf shales (equivalent of Gumai Fm to the east, offshore NW Java) form a regional seal on the hydrocarbon system. A 25-m thick paleosol in the Pematang Group is a good seal in some half-grabens as are thin marine shales within the Sihapas Group

### A2.5.4 Hydrocarbon Fields

The Central Sumatra Basin is the location of the largest oil fields in SE Asia, the Minas and Duri fields with total ultimately recoverable reserves of 8 and 4 billion barrels, respectively. Steam flood enhanced oil recovery is occurring at both fields.

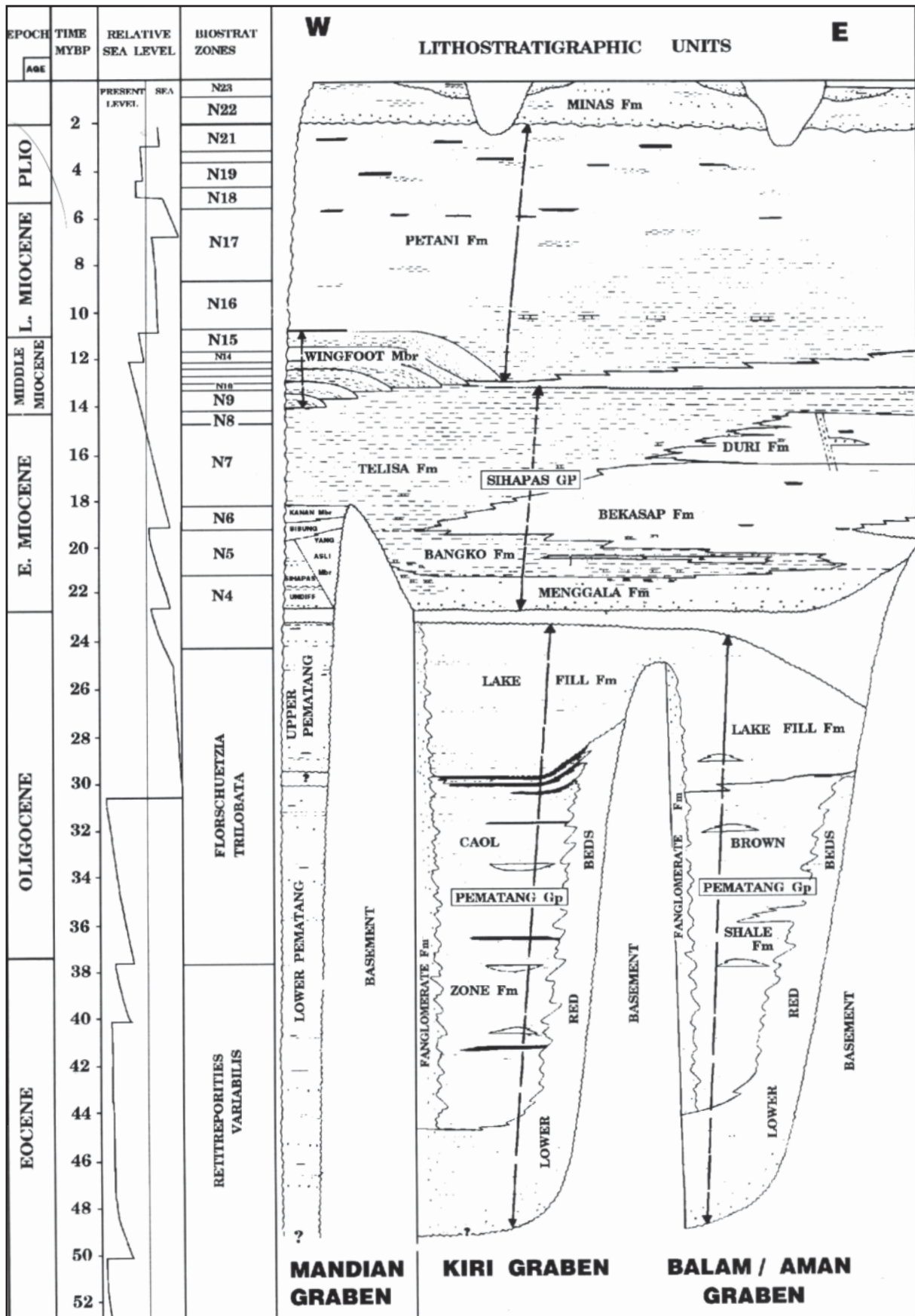


Figure A92. Stratigraphic chart of the Central Sumatra Basin (from Williams and Eurbank, 1995).

“Known” oil volumes in the basin are 13217 mmbbls (equivalent to 1718 Mt stored CO<sub>2</sub>). The majority (63%) of this known volume has been produced. “Known” gas volume is 3.8 Tcf (equivalent to 304 Mt stored CO<sub>2</sub>). An estimated 2.9 Tcf (76%) of this gas is still held as reserves (USGS, 2000).

Minor oil reservoirs also occur in weathered pre-Tertiary units. Traps are formed by late Miocene and Pliocene compressional tectonism accompanying uplift of the Barisan Mountains. Structural trap styles dominate and include drape-folds over palaeo-highs, faulted anticlines, wrench-faulted anticlines (flower structures), and graben-bounding, rollover anticlines. Locally, facies-change and truncation stratigraphic traps are also present. Miocene to Pliocene uplift, folding, wrenching and compression formed anticlinal traps for the oil and gas accumulations. The bulk of the hydrocarbon fields occur on the western graben hinge margin. Compressional stresses are occurring present day. Some of the many hydrocarbon plays are depicted in Figure A94. Note the regional seal.

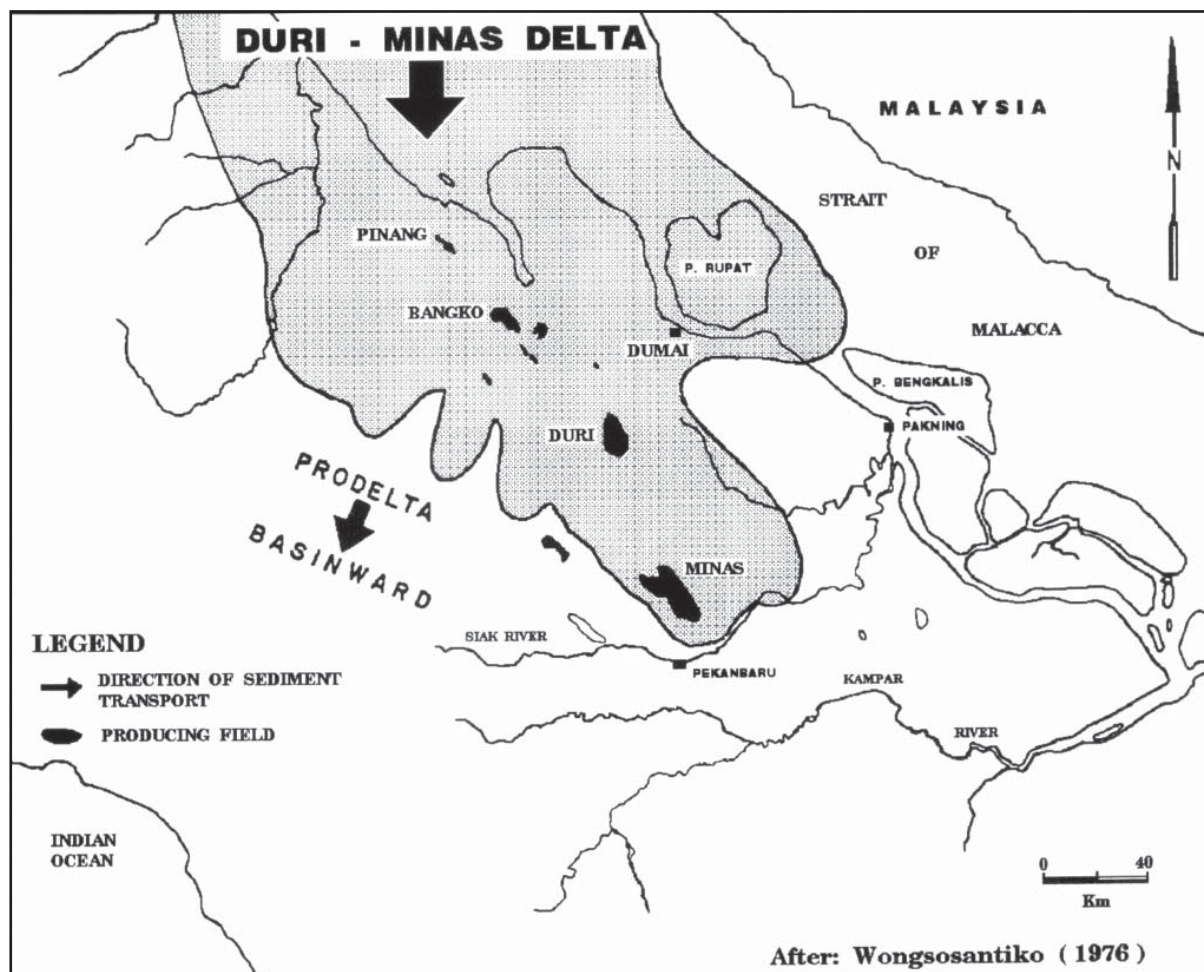


Figure A93. Extent of Miocene Duri-Minas sequence in the Central Sumatra Basin (from Williams and Eurbank, 1995).

### A2.5.5 Coal Occurrence

Coal seams occur at depth within synrift lacustrine clastics Pematang Group in the Kiri Graben in the SW part of the basin. Shallow coals also occur in Pliocene clastics. See section 4.2 in the main report for a discussion of coal occurrence in Indonesia and its relevance to CO<sub>2</sub> storage.

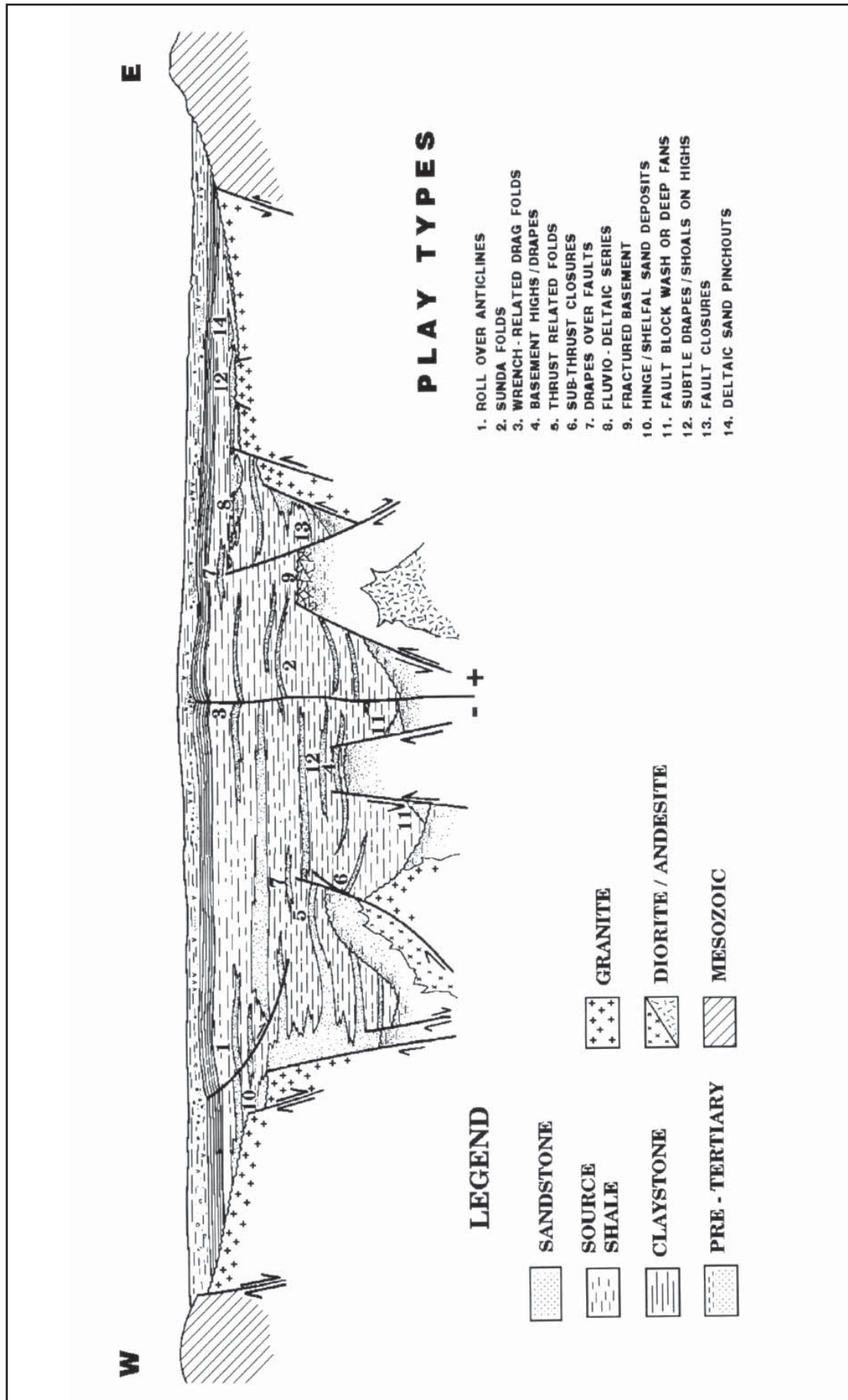


Figure A94. Diagrammatic cross-section of producing and prospective plays in Central Sumatra syn-rift sequences (from Williams and Eurbank, 1995).

## A2.5.6 Potential CO<sub>2</sub> Storage Options

CO<sub>2</sub> storage sites within the basin are probably restricted to Miocene or older units below the regional Early Miocene seal. The excellent permeability and porosity of the marine sandstones in the Sihapas Group are an obvious target horizon. The production phase of the oil fields is quite mature. The 63% of “known” oil already produced is equivalent to 1082 Mt stored CO<sub>2</sub>. Steam drive is being used for enhanced recovery. It is not known if CO<sub>2</sub> is being used for EOR in the basin. The basin has very good CO<sub>2</sub> storage potential but has relatively low local emissions and is distant from the higher emissions in the Jakarta area.

## A2.5.7 References

Williams, H. H. and Eubank R. T., Hydrocarbon habitat in the rift graben of the Central Sumatra Basin, Indonesia. In: Lambiase, J J (eds.), Hydrocarbon habitat in rift basins. Geological Society Special Publications; Geological Society of London 80, 331-371. 1995

## A2.6 Southern Sumatra Basin

### A2.6.1 CO<sub>2</sub> Sources

CO<sub>2</sub> emissions in the region directly overlying the Central Sumatra Basin contributed approximately 7 Mt CO<sub>2</sub>/yr to Indonesia's estimated total stationary source CO<sub>2</sub> emissions of 126 Mt/yr (IEA, 2000).

In a 300 km radius from the basin there are sources totalling approximately 34 Mt CO<sub>2</sub>/yr.

Note: The sum of sources within 300 km of a basin very crudely indicates the magnitude of emissions within reach of the basin. These "catchments" overlap for most basins and should not be summed.

It is proposed to generate power on the southern end of Sumatra and transmit it to Java by sub sea cable.

### A2.6.2 Basin Overview

The Southern Sumatra Basin is approximately 133000 sq km in area (Figure A95). Sediment thickness is locally up to 5000 m, but generally averages 2500m. The average geothermal gradient is 49°C/km (Hutchison, 1989). Tertiary rift basins oriented north-south formed on the southern edge of the Sunda Shelf with early lacustrine depositional history followed by marine incursion from the south and carbonate platform deposition and reef formation on palaeo-highs. Late Miocene compression resulted in a foreland basin with clastic input from the rising mountains to the south. Pliocene -Pleistocene faulting and detached folding related to the formation of the Barisan Mountains. The area of the basin is 133,700 sq km.

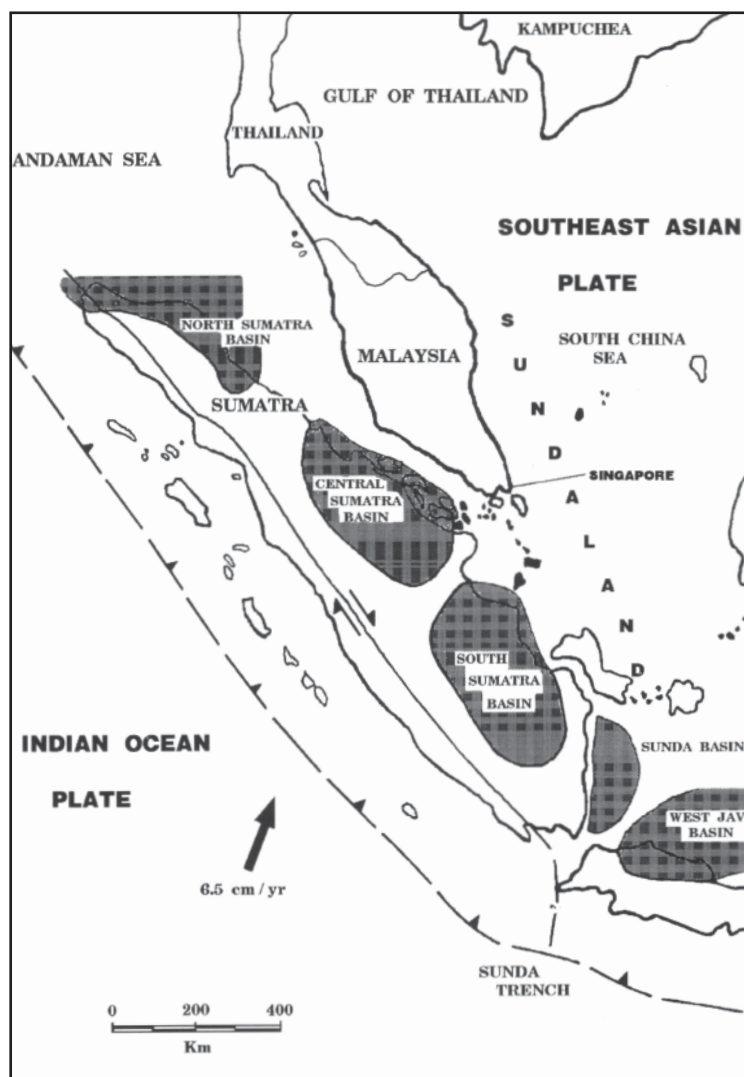


Figure A95. South Sumatra Basin regional location map (from Williams and Eurbank, 1995).

### A2.6.3 Basin Fill

There are numerous sequences that are hydrocarbon reservoirs which could be useful as CO<sub>2</sub> stores. These include: Palaeocene to Early Oligocene coarse clastics of the Lahat Formation, Oligocene to Miocene deltaic and marine sandstones of the Talang Akar Formation (Figure A96). Early Miocene platform carbonates and local carbonate build-ups of the Batu Raja Limestone, Miocene transgressive shoreline sands of the Telisa Formation, and Late Miocene to Pliocene shallow marine to non-marine sandstones of the Lower and Middle Palembang Formations serve as hydrocarbon reservoirs (USGS, 2000). These are formations similar to those found in the NW Java Basin. The Telisa Formation (also known as Gumai Shale) is a regional seal to both the Central and Southern Sumatra basins.

Anticlines are the primary hydrocarbon trap followed by fault block and carbonate build-up stratigraphic traps.

### A2.6.4 Hydrocarbon fields

The Southern Sumatra Basin is apparently gas prone, unlike the Central Sumatra Basin. The total Known gas volume is 10.2 Tcf (equivalent to 816 Mt stored CO<sub>2</sub>). Only 3 Tcf of the 10 Tcf is produced. Known Oil volume is 2429 mmbbls (equivalent to 315 Mt stored CO<sub>2</sub>). Most of this has been produced 1842 mmbbls (equivalent to 239 Mt stored CO<sub>2</sub>) (USGS, 2000).

Work by the USGS (2000) shows a bi-modal distribution in discovered oil fields. The primary mode is just 4-8 mmbbls another mode occurs at 32-64 mmbbls. There are only three fields larger than 128 mmbbls. Of the approximately 10 Tcf known gas, 4 Tcf is encompassed by the eight largest fields. None of these fields is larger than 768 Bcf. The majority of known gas is contained in fields smaller than 300 Bcf (USGS, 2000).

### A2.6.5 Coal Occurrence

It is assumed that deep coals would be present in the Talang Akar within lower delta-plain sequences as in the NW Java Basin. See section 4.2 in the main report for a discussion of coal occurrence in Indonesia and its relevance to CO<sub>2</sub> storage.

### A2.6.6 Potential CO<sub>2</sub> Storage Options

Early rift and transgressive Tertiary siliciclastic and carbonate reservoirs are present. Like the Central Sumatra Basin the basin has good saline reservoir potential due an excellent regional seal. Anticlinal structures are formed in the basin.

From basin wide production data it is estimated that the storage potential of depleted oil fields is equivalent to 239 Mt stored CO<sub>2</sub>. The actual depletion of individual fields is unknown. The oil fields are not large (up to 64 mmbbls or 8 Mt stored CO<sub>2</sub>). The gas fields in the basin are yet to be significantly depleted.

The local CO<sub>2</sub> sources are relatively small (this may increase as gas resources are developed). The Jakarta area lies within 300 km of the southern portion of the basin.

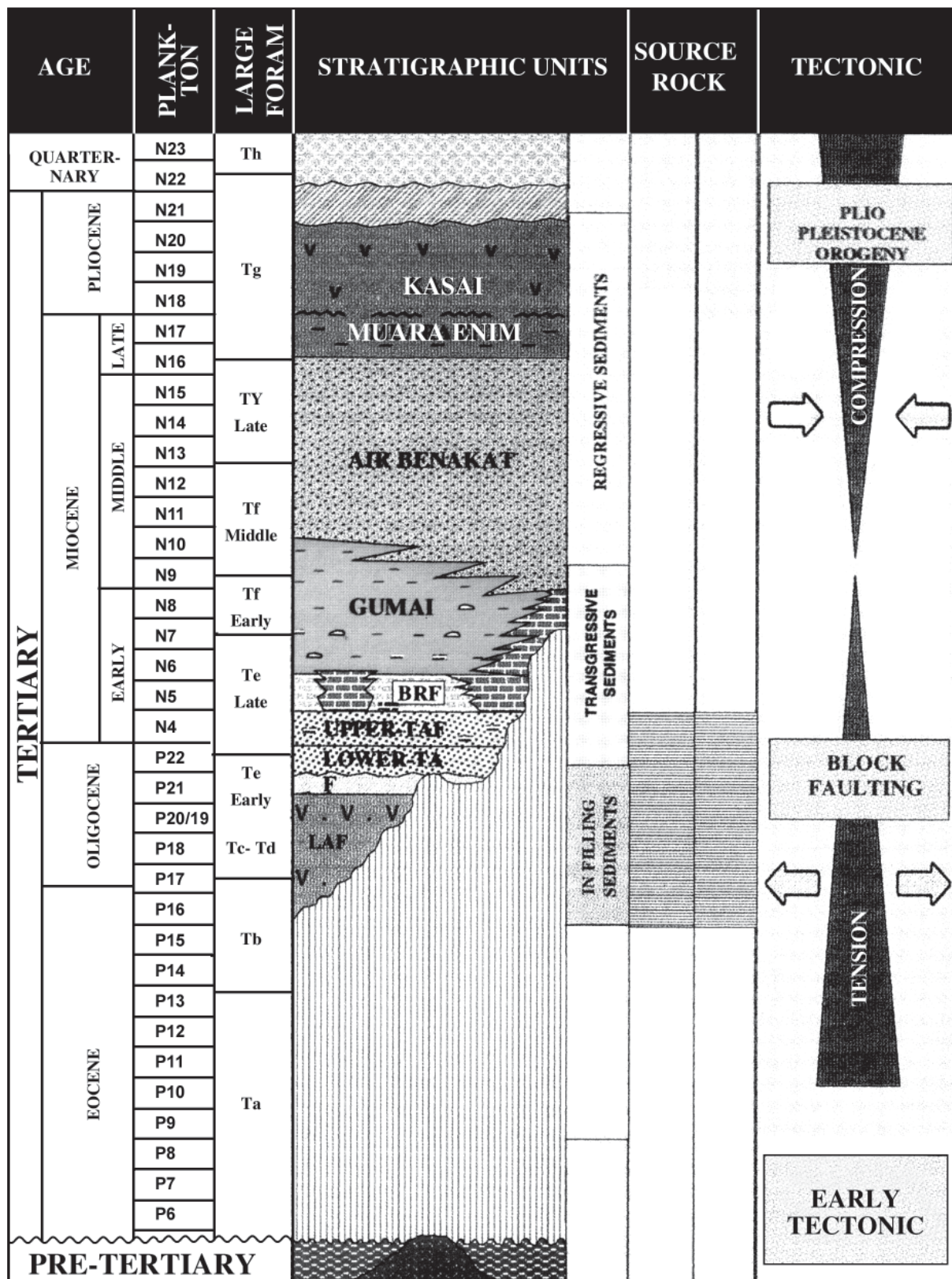


Figure A96. Stratigraphy and tectonics of the South Sumatra Basin (from Tamtomo et al., 1997).

## A2.6.7 References

de Costa, G.L. The Geology of the Central and South Sumatra basins. In: Proceedings of the 3rd Annual Convention - Indonesian Petroleum Association. Jakarta, Indonesia , 77-110. 1974.

Hutchison, C.S. Geological evolution of South-East Asia. Clarendon Press, Oxford, 1989 .

IEA GHG (International Energy Agency Greenhouse Gas R & D programme). Greenhouse Gas Emissions from Major Industrial Sources . 2000.

Tamtomo, B., Yuswar, I., and Widiyanto, E. Transgressive Talang Akar sands of the Kuang area, South Sumatra Basin; origin, distribution and implication for exploration play concept. In: Howes, J V C & Noble, R A (eds.), Proceedings of the conference on Petroleum systems of SE Asia and Australasia. Indonesian Petroleum Association. Jakarta, Indonesia , 699-708. 1997.

USGS World Energy Assessment Team. World Petroleum Assessment 2000. United States Department of the Interior, U.S.Geological Survey Digital data series DDS-60[4 discs]. 2000.

Williams, H.H. and Eubank, R.T. Hydrocarbon habitat in the rift graben of the Central Sumatra Basin, Indonesia. In: Lambiase, J J (eds.), Hydrocarbon habitat in rift basins, Geological Society Special Publications, Geological Society of London 80, 331-371. 1995.

## A3. South Korea

### A3.1 Kunsan Basin [South Korean Sector: North Yellow Sea Basin]

#### A3.1.1 CO<sub>2</sub> Sources

The area of the Kunsan Basin is 50 to 150 km offshore from CO<sub>2</sub> sources on the west coast of South Korea. South Korea has sources of CO<sub>2</sub> totalling 314 MT/yr (IEA, 2000). Emissions totalling 120 Mt CO<sub>2</sub> /yr are within 300 km of the Kunsan Basin (Korean Sector Of North Yellow Sea). Three closely located large power stations south of Seoul on the west coast contribute 78 Mt CO<sub>2</sub>/yr (25%) to total emissions.

Note: The sum of sources within 300 km of a basin very crudely indicates the magnitude of emissions within reach of the basin. These “catchments” overlap for most basins and should not be summed.

#### A3.1.2 Basin Overview

There are several basins in the Yellow Sea including Bohai Bay and the North Yellow Sea (= West Korea Bay) in the north, and the South Yellow Sea and Subei in the south. The South Yellow Sea Basin, which is located between East China and the Korean peninsula, is subdivided into the Northern and Southern South Yellow Sea basins by a central uplifted area Figure A97 (Yi et al., 2003).

The Northern South Yellow Sea Basin (NSYSB), is one of a number of Mesozoic Cenozoic, non-marine, back-arc, transtensional rift or pull-apart basins that are distributed along a general NE-SW trend in China and the Yellow Sea. It is filled with mainly Cretaceous and Cenozoic non-marine clastic sediments. The eastern part of it is divided into the South-West, Central and North-East sub-basins by structural highs and faults within the basin. In South Korea the eastern part of the NSYSB is called the Kunsan Basin. (Yi et al., 2003)

The development of the basin was initiated during the Late Jurassic or Early Cretaceous and continued through the Palaeogene. A period of regional scale erosion took place towards the close of the Palaeogene, mainly in the Oligocene. Neogene sediments rest unconformably on the older Cenozoic deposits (Yi et al., 2003). The geological history is very similar to the onshore and offshore Subei (Southern Yellow Sea Basin). (Yi et al., 2003)

#### A3.1.3 Basin Fill

The Yellow Sea area was subjected to compressional tectonic movements caused by the subduction of the South China Block under the North China Block from the Jurassic Period onwards. A small-scale rift basin developed during the Late Jurassic-Early Cretaceous and continued through the Eocene. The Late Cretaceous and Palaeogene deposits that it contains were predominantly deposited in alluvial, fluvial-lacustrine environments of deposition. Half-grabens developed in the NSYSB during the Palaeogene and a unified pan-like depression formed in the Neogene (Zhang et al., 1989). Maximum regional subsidence of the basin occurred during the Early-Middle Eocene. In the Late Eocene the rate of subsidence decreased and eventually ceased altogether when basin inversion and erosion took place, leading to a hiatus in deposition, now manifested by an unconformity between the Upper Eocene and Miocene deposits. During the Early Miocene there was further uplift but a small amount

of sedimentation took place in the basin, and from the Middle Miocene onwards regional subsidence again led to widespread sedimentation, although in parts of the basin Late Miocene deposits are missing from the succession. The basin was uplifted once more in the Early Pliocene. Subsidence followed during the Late Pliocene, and the basin finally succumbed to marine deposition in the Pleistocene (Yi et al., 2003).

Palaeogeographic maps of the Kunsan Basin were not located. It is clear from Yi et al., (2003) that deposition was in non-marine environments including fluvial and lacustrine. This is similar to the depositional systems in other extensional Cenozoic basins in the region. The lithological column (Figure A98) indicates numerous potential reservoir-seal pairs. An environmental interpretation of palaeogeography would better illustrate the potential for saline reservoir storage.

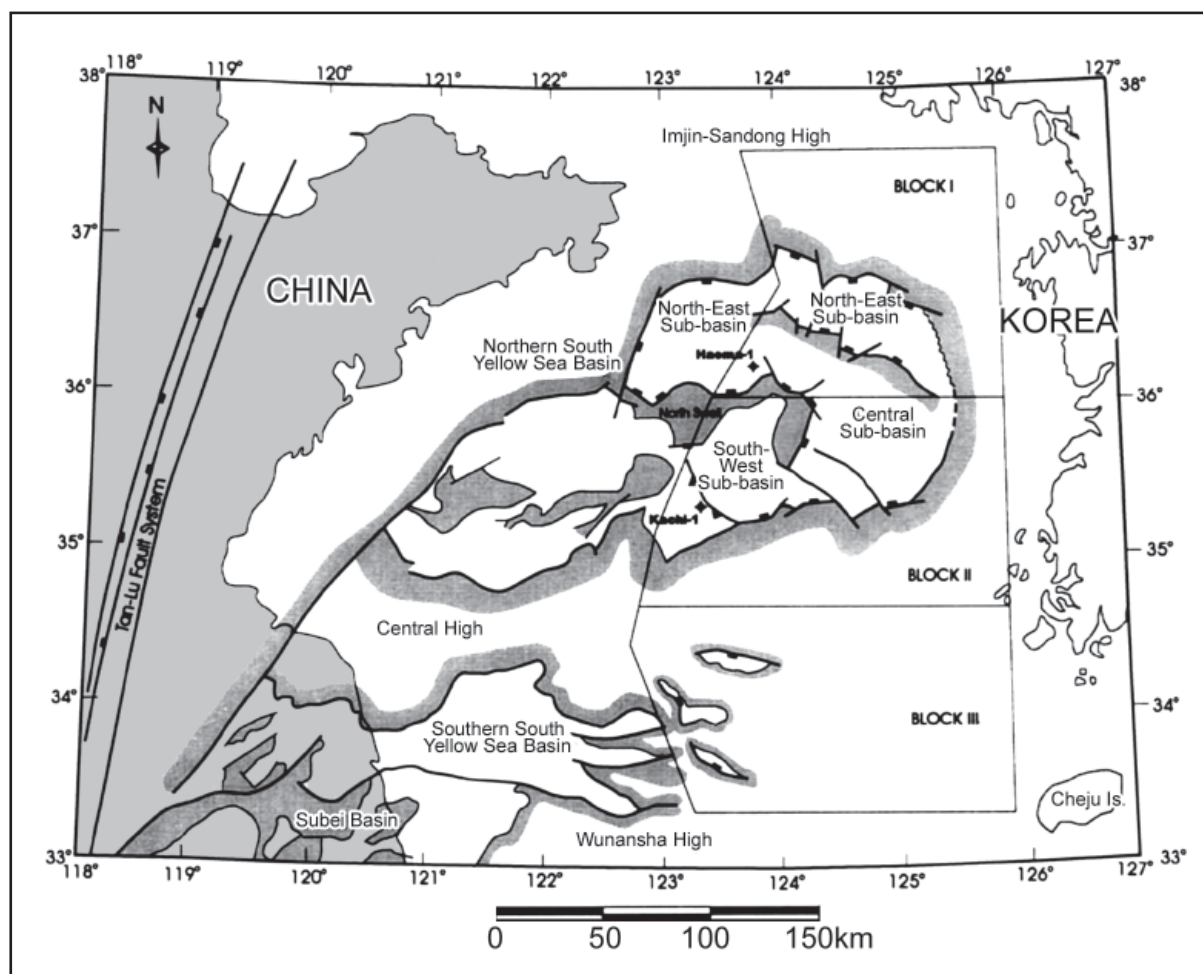


Figure A97. Structural framework of the South Yellow Sea Basin, offshore western Korea, and location of the wells examined (from Yi et al., 2003).

### A3.1.4 Hydrocarbon Fields

Unknown.

### A3.1.5 Coal Occurrence

Unknown.

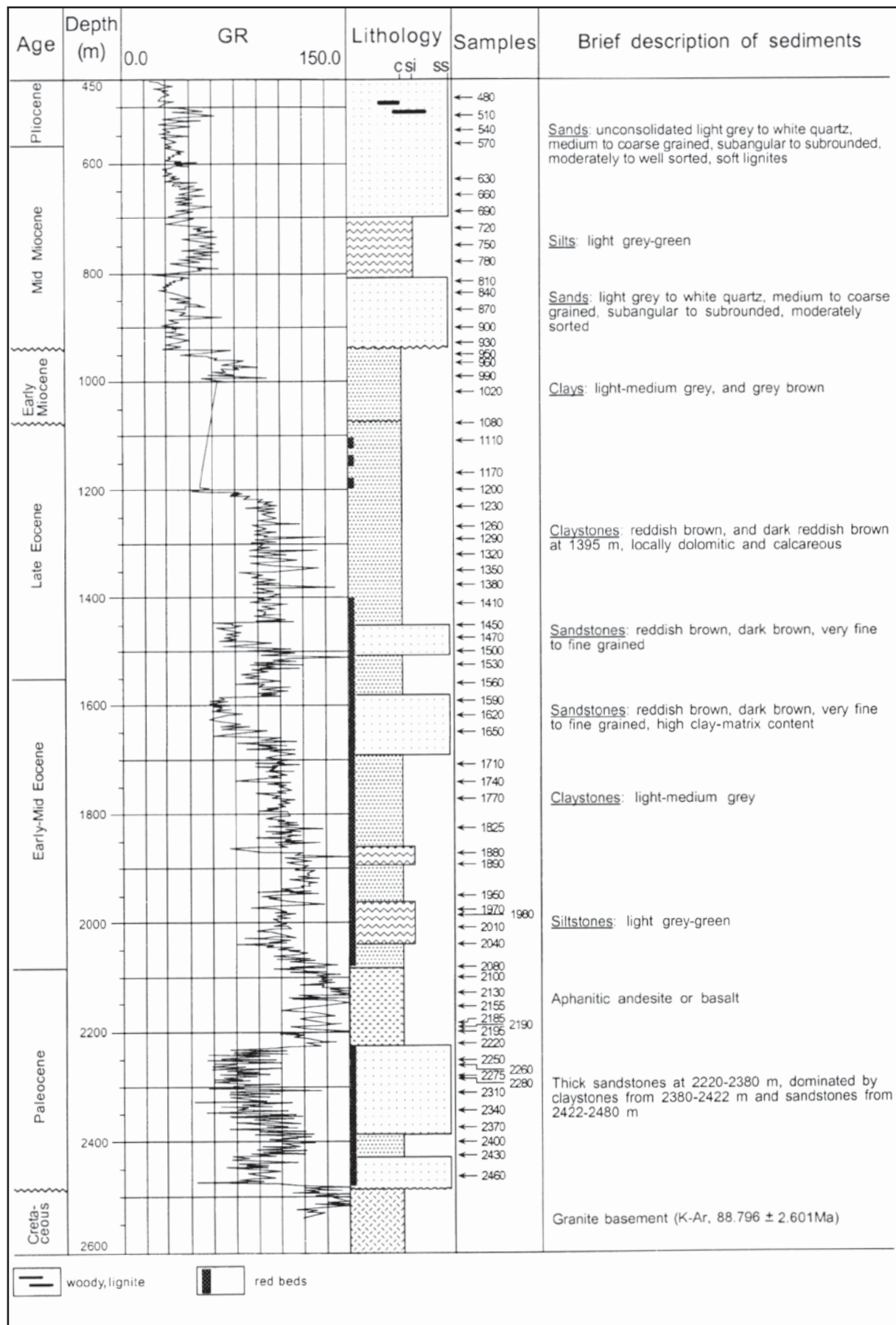


Figure A98. Generalised lithological log of the Haeme-1 well showing sample horizons (from Yi et al., 2003)

### A3.1.6 Potential CO<sub>2</sub> Storage Options

Information is limited but there appear to be good potential reservoir-seal pairs in the offshore area west of the Korean peninsula which could allow “saline reservoir” storage. No indication of reservoir quality was located in the literature. From stratigraphic columns and logs provided in Yi et al., (2003) it appears likely to have acceptable reservoir characteristics, similar to the fluvial-deltaic sandstones in the Cenozoic rift basins of onshore China.

It appears from information available there are no producing or depleted oil/gas fields in the area. From reading Yi et al., (2003) it is clear that there are at least two exploration wells drilled in the area.

While coal may be present it very unlikely to be a viable target for storage in this offshore setting.

Unfortunately building infrastructure in an offshore setting will always carry additional expense. However, the combined emissions of the closely co-located power stations south of Seoul might present economies of scale in the capture and storage processes.

### A3.1.7 References

Kwon, Y.I. and Boggs, S. Provenance interpretation of Tertiary sandstones from the Cheju Basin (NE East China Sea); a comparison of conventional petrographic and scanning cathodoluminescence techniques. Abstracts with Programs - Geological Society of America 33[3], 44. 2000.

Sturt, D.C. and Quinton, N.A. South Korea; an overlooked hydrocarbon province?. Oil and Gas Journal 91[44], 85-88. 1993.

Yi, S., Yi, S., Batten, D.J., Yun, H., and Park, S.-J. Cretaceous and Cenozoic non-marine deposits of the Northern South Yellow Sea Basin, offshore western Korea: palynostratigraphy and palaeoenvironments. Palaeogeography, Palaeoclimatology, Palaeoecology 191[1], 15-44. 2003.

Zhang, Y., Wei, Z., Xu, W., Tao, R., and Chen, R. The North Jiangsu-South Yellow Sea basin. In: Zhu, Xia (ed.), Chinese sedimentary basins. Elsevier Sci. Publ.. Amsterdam, Netherlands, 107-123. 1989.

## A3.2 Northern most East China Sea Basin

### A3.2.1 CO<sub>2</sub> Sources

South Korea has sources of CO<sub>2</sub> totalling 314 MT/yr (IEA, 2000). Emissions totalling 114 Mt CO<sub>2</sub> /yr are within 300 km of Korean sector the East China Sea Basin.

Note: The sum of sources within 300 km of a basin very crudely indicates the magnitude of emissions within reach of the basin. These “catchments” overlap for most basins and should not be summed.

### A3.2.2 Basin Overview

The basin known in South Korea as the Cheju Basin, lies adjacent to the very northern end of the East China Sea Basin. This basin is divided between South Korea and Japan. This area is in fact the northern most sub basin in the East China Sea Basin (Figure A99). The basin is 130 km long and 70 km wide with a sediment thickness of four to five kilometres (Jang, 2003). A few wells have been drilled in the basin and there are hydrocarbon shows. The seismic interpretation and stratigraphy by Sturt and Quinton (1993) (Figure A100, Figure A101, Figure A102) indicates the presence of extensive reservoirs and seals.

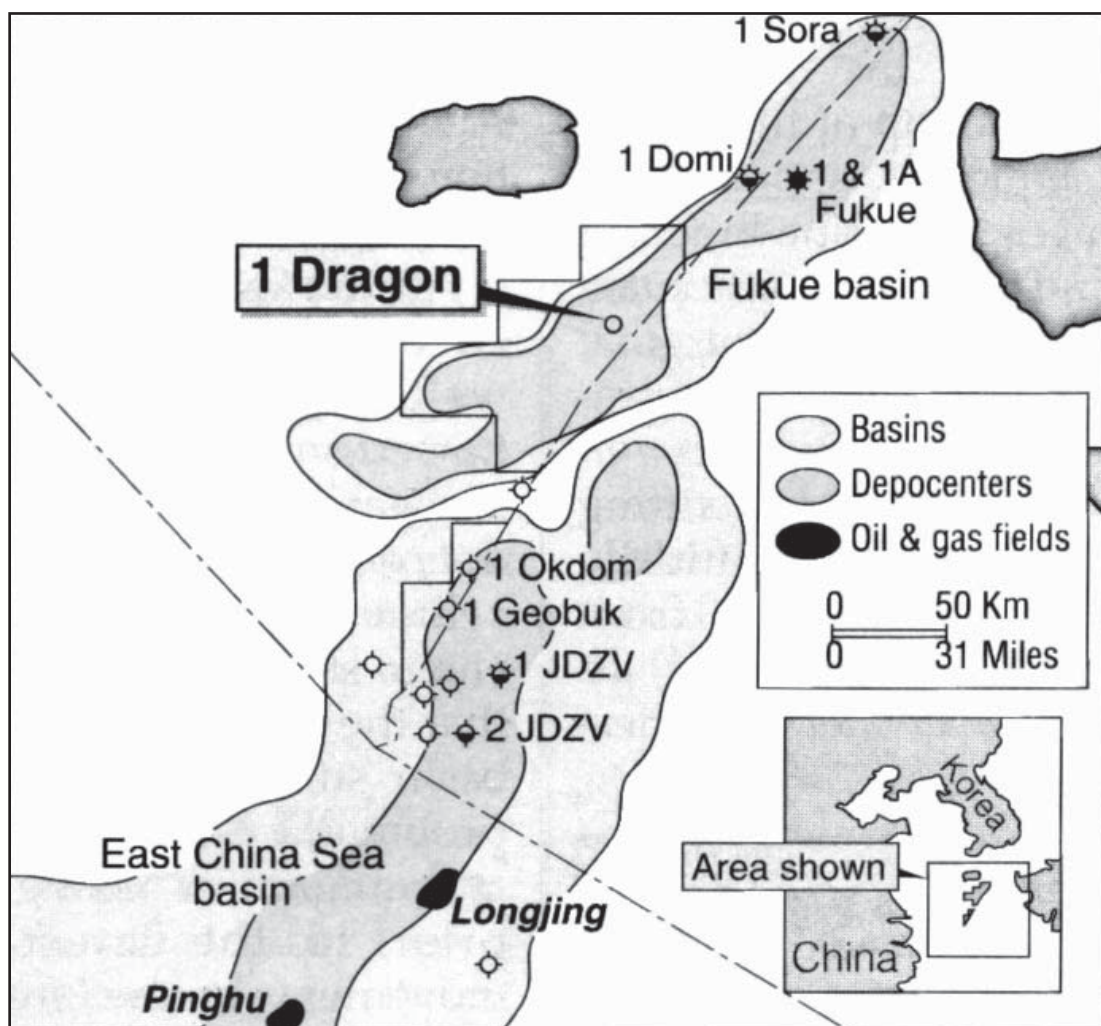


Figure A99. Cheju (Fuke) Basin location (from Sturt and Quinton, 1993).

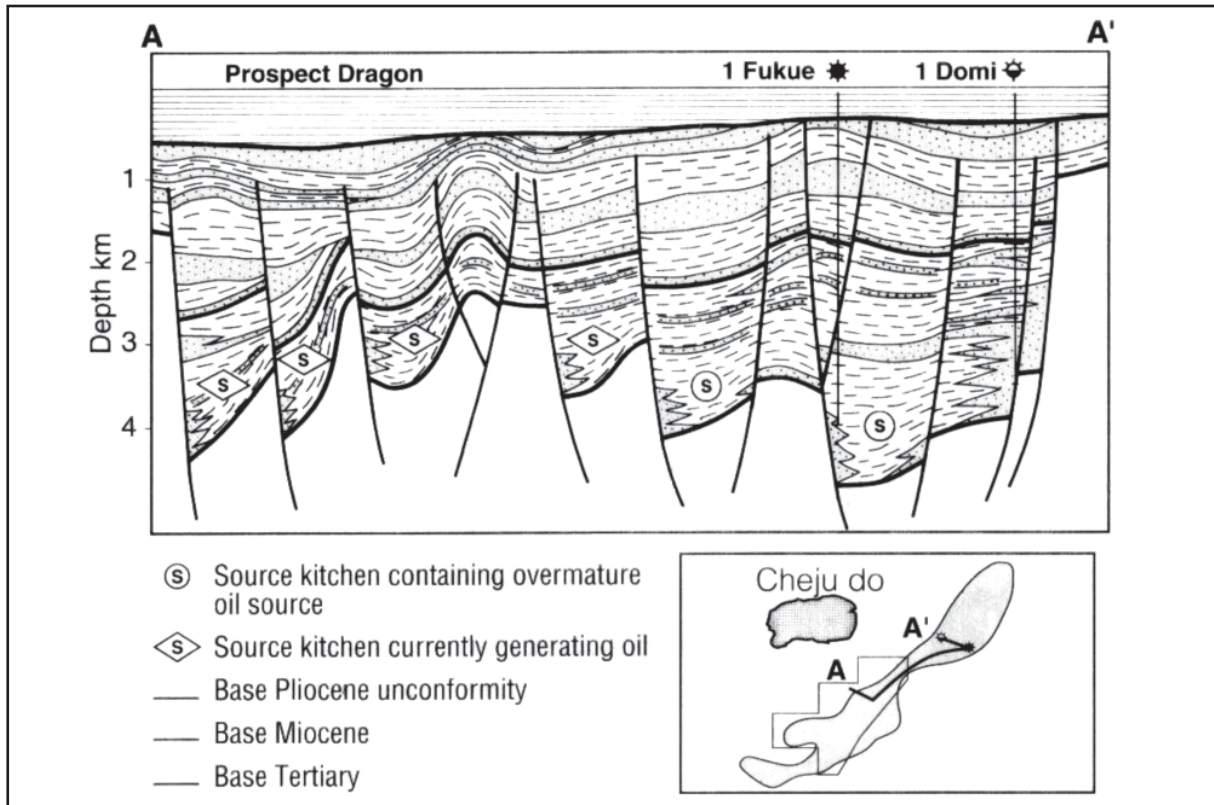


Figure A100. Cheju (Fuke) Basin cross-section (from Sturt and Quinton, 1993).

Epoch	Age (ma)	Lithology	Environment	Formation	Seismic horizons	Tectonics
Pliocene-Recent	5		Neritic	Utsube	Orange*	Post rift 2
	11	R	Continental to marginal marine	Tai	Blue*	
Miocene	15	C, R	Transitional	Shiira	Green*	Synrift 2
	19	C, R	Fluvial-marine	U. Claystone	Yellow	
	22	R	Marine-deltaic	Sayori ss		
				L. Claystone		
Oligocene		C/R	Fluvial deltaic	Kasago	Yellow	Synrift 1
		S	Lacustrine-deltaic			
Eocene	39	S	Lacustrine?	Chinu	Brown	
	43	S	Transitional/alluvial fan	Arakabu		
			Restricted marine			

\*Sequence boundary      Ⓢ Source      R Reservoir      C Cap

Figure A101. Cheju stratigraphy (from Sturt and Quinton, 1993).

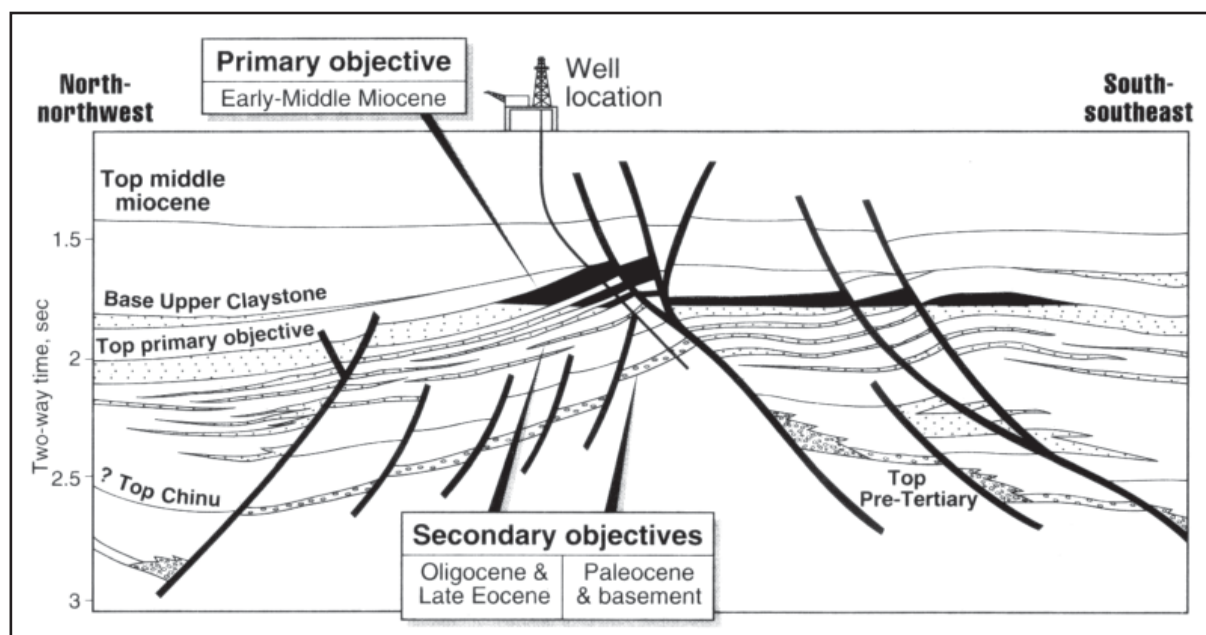


Figure A102. Seismic section line with overlaid geological interpretation A (from Sturt and Quinton, 1993).

### A3.2.3 Basin Fill

During the Palaeogene, rifting occurred on the extensional regime and half-grabens were developed that provided the sites for a thick succession ~2 km of clastic sediments forming alluvial fan or lacustrine fan delta. In the Early to Mid Miocene, as extension was taken over by transtension, the rate of basin extension reduced and thermal subsidence followed. Movement on the basin forming faults continued in the northern depression. Sediments were deposited extensively and lacustrine environments gradually turned into fluvial. After the Mid Miocene, extension ceased but subsidence continued. In this phase, sedimentation is not related to the preceding evolution of the basin but related to the eastward tilting of the Eurasian plate. Sediments are composed of channel sandstones, overbank mudstones and coals deposited in floodplains. The end of the Late Miocene is characterized by strong inversion caused by widespread uplift and erosion. Until the Mid Miocene, sedimentation in the basin was mainly controlled by local tectonics, and the basin filling continued with regional subsidence from the Late Miocene (Jang, 2003).

It would appear from the stratigraphy (Figure A101) presented in Sturt and Quinton (1993) that there are two extensive reservoir-seal pairs in the Miocene. The first pair is the Lower Claystone of the Sayori group seal and the Miocene Basal Sandstone. The Basal sandstone is 50-60 m thick. The Sayori Sandstone is 175 to 280 m thick and sealed by the Upper Claystone. Porosity of both sandstones ranges from 18 to 30%.

### A3.2.4 Hydrocarbon Fields

Few wells have been drilled in the basin. It appears that the elements for a hydrocarbon play do exist. There are shows but no commercial success.

### A3.2.5 Coal Occurrence

While Jang (2003) mentions the presence of coal in the Mid to Late Miocene the details of are unknown.

### A3.2.6 Potential CO<sub>2</sub> Storage Options

The interpretation by Sturt and Quinton (1993) indicates there are two extensive reservoir-seal pairs in the Miocene.

### A3.2.7 References

Jang, H.R. Structural Evolution and Its Influence on Sedimentation of the Domi (Fukue) Basin, Offshore Korea . Presentation abstract AAPG Annual Convention May 11-14, 2003. [http://aapg.confex.com/aapg/sl2003/techprogram/paper\\_78689.htm](http://aapg.confex.com/aapg/sl2003/techprogram/paper_78689.htm)

Kwon, Y.I. and Boggs, S. Provenance interpretation of Tertiary sandstones from the Cheju Basin (NE East China Sea); a comparison of conventional petrographic and scanning cathodoluminescence techniques. Abstracts with Programs - Geological Society of America 33[3], 44. 2000.

Sturt, D.C. and Quinton, N.A. South Korea; an overlooked hydrocarbon province?. Oil and Gas Journal 91[44], 85-88. 1993.

## A3.3 Ulleung Basin

### A3.3.1 CO<sub>2</sub> Sources

South Korea has sources of CO<sub>2</sub> totalling 314 MT/yr (IEA, 2000). Emissions totalling 123 Mt CO<sub>2</sub> /yr are within 300 km of the Ulleung Basin.

Note: The sum of sources within 300 km of a basin very crudely indicates the magnitude of emissions within reach of the basin. These “catchments” overlap for most basins and should not be summed.

### A3.3.2 Basin Overview

The Ulleung Basin lies in the Sea of Japan, east of the Korean Peninsula (Figure A103). The basin began with the opening of the Sea of Japan in the late Oligocene and was compressed as the Sea of Japan began to close again in the middle Miocene (12 Ma). The area is approximately 56,000 sq km.

This slope basin has two main depocentres the northern one contains only 4-5 km of mainly distal pelagic sediments (Figure A103, Figure A104). The southern depocentre is up to 10 km thick containing mass-flow Oligocene-Miocene deposits that originated near the southern basin edge (Figure A105). The sea closing event at 12 Ma results in a shift from mass flow deposition to shelfal marine and even coastal plain environments on the southern edge of the basin.

Much of the basin lies on oceanic crust around 9.5 km thick. Lee and Kim (2002) performed thermal basin modelling using geothermal gradient, 38°C/km. No data was located for the southern portion of the basin which is underlain by continental crust of Cretaceous to Palaeogene age.

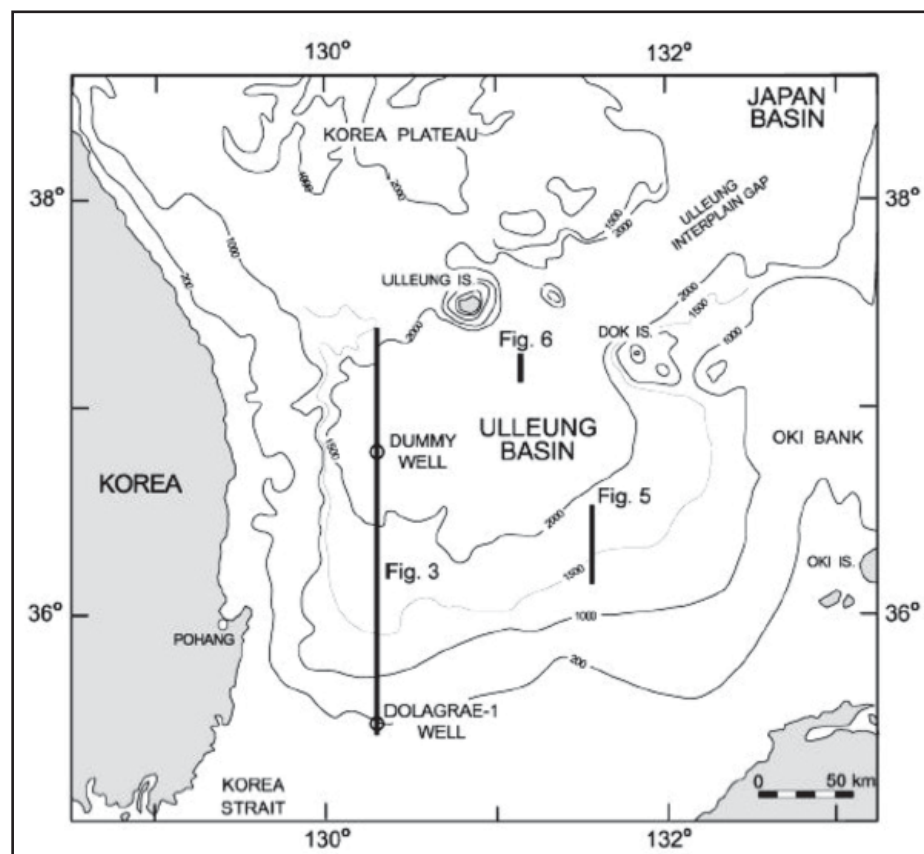


**Figure A103.**  
Bathymetry of the  
Ulleung Basin. Contor  
intervals in metres  
(from Lee and Kim,  
2002).

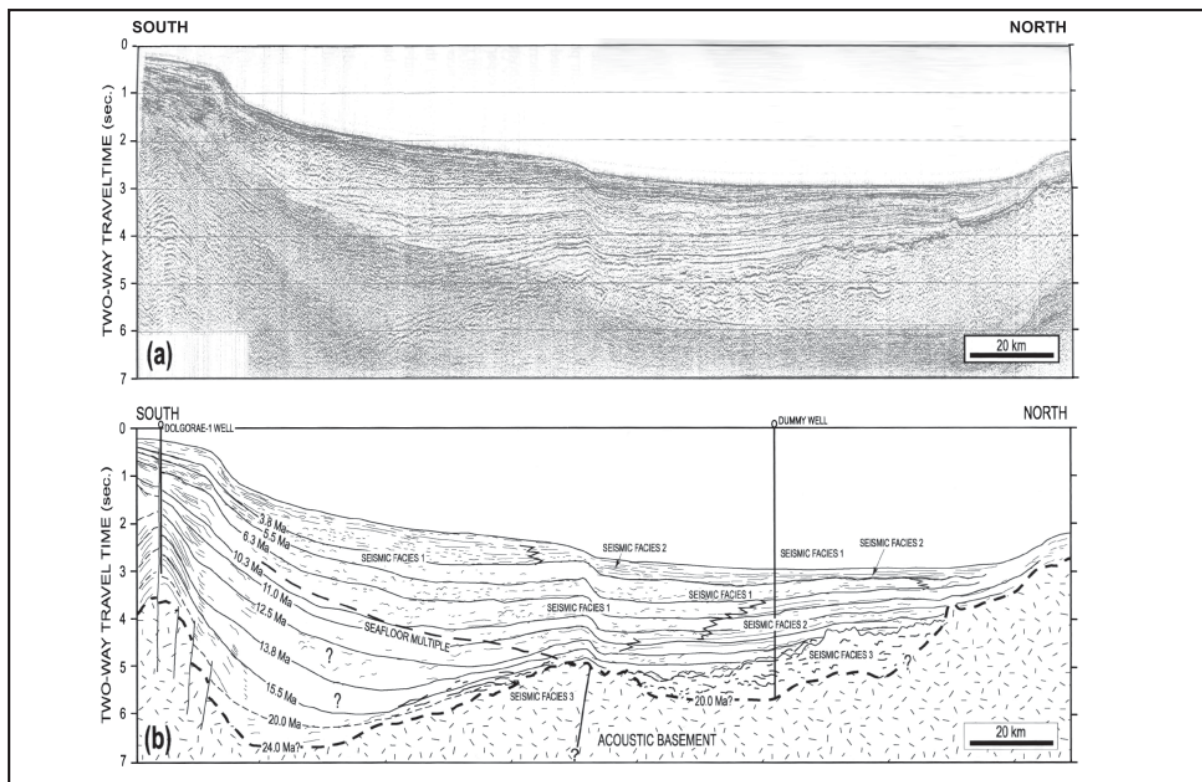


**Figure A104. (a) Regional N-S seismic profile (b) and its stratigraphic interpretation. Two sub basins or depocenters are separated by a basement high. The basin fill is thickest in the southern basin and thins northward, suggesting that southern basin margin was the main sediment source. Much of the southern basin and the southern part of the northern basin are characterised by seismic facies 1 (mass-transport deposits). The northern, distal part of the basin is dominated by seismic facies 2 (distal turbidites/ hemipelagic sediments). Seismic facies 3 (volcanic sill/ flow-sediment complexes) occurs immediately above the acoustic basement in the northern basin, indicating extensive volcanic activity during the early phase of basin spreading (text and figures from Lee and Kim, 2002).**

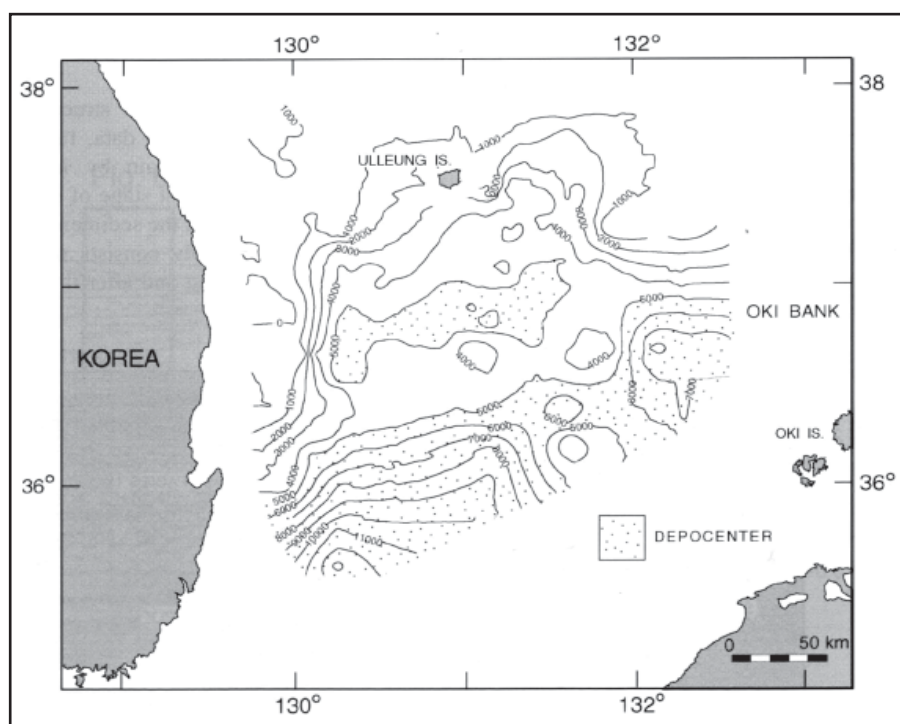


**Figure A105. Total sediment thickness (isopach) between the top of the acoustic basement and the seafloor. Two depocenters separated by an intervening region of thinner basin fill can be recognized. The basin fill is thickest in the southern depocenter, suggesting that the southern basin margin has been the main sediment source. Contour interval in metres (from Lee and Kim, 2002).**

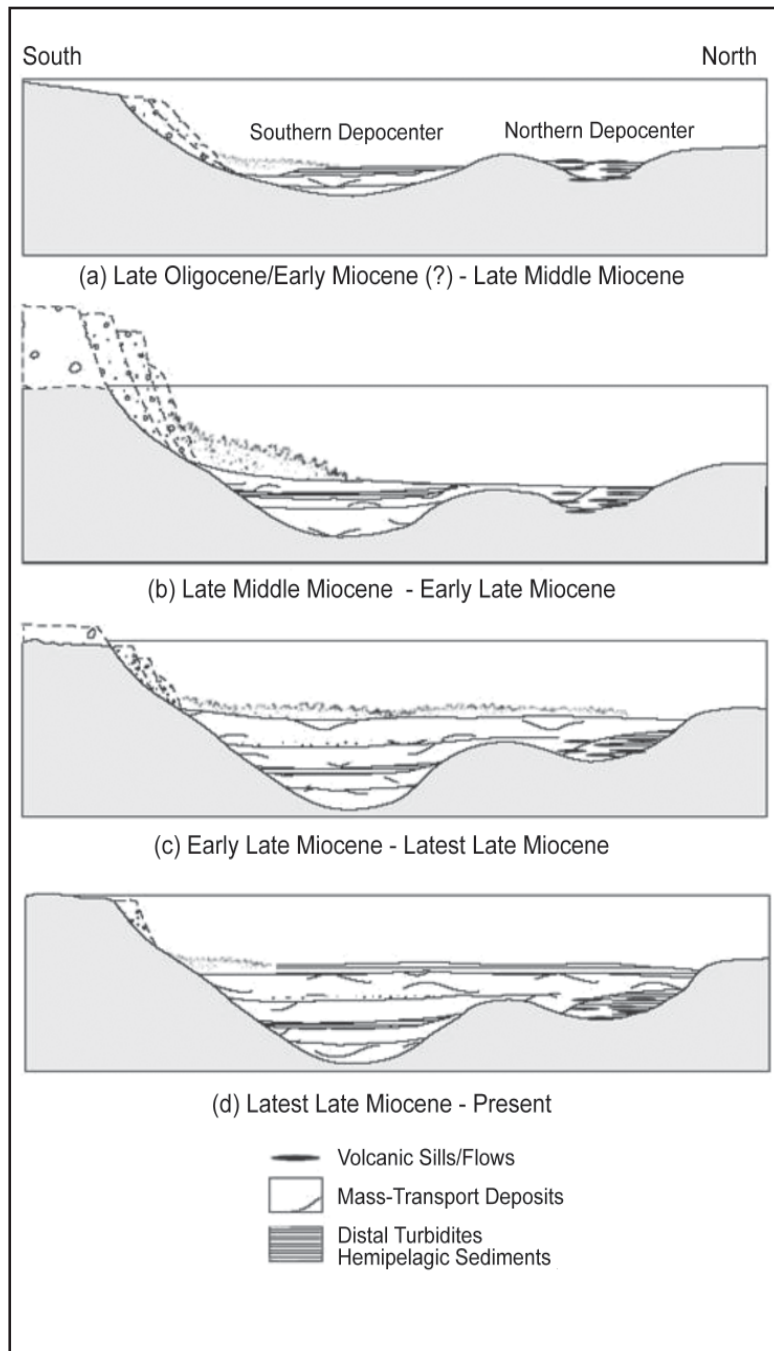


**Figure A106.** A schematic model illustrating the stratigraphic evolution of the Ulleung Basin. (a) Early Miocene(?) - Late Middle Miocene - a larger portion of sediments from the southern sources was deposited in the southern depocenter as the southern basin subsided rapidly, while finer-grained materials burried and/overtopped the intervening high, reaching the northern depocenter. (b) Late Middle-Early Late Miocene - uplift along the southern and southeastern basin margins, caused by the back-arc closure, brought large volumes of sediments into the basin. Mass-transport processes bypassed the shelf and slope and deposited these sediments directly into the deep basin. The northern and northeastern basins are dominated by distal turbidites and hemipelagic sediments, (c) Early Late - Latest Late Miocene - as the subsidence of the southern basin decreased, sediments from the southern and southeastern sources gradually filled the southern basin. Mass-transport processes, although reduced in scale and frequency, travelled farther north, depositing sediments in the northern basin. (d) Latest late Miocene-present - as the tectonic activity along the basin margins waned significantly, mass-transport deposits retreated rapidly in an updip direction, resulting in radical changes in sedimentary facies in the central basin (text and figure from Lee and Kim, 2002).

### A3.3.3 Basin Fill

The northern area appears to have little or no reservoir. In the south, the very proximal mass flow deposits originating from a volcanically active area suggests that reservoir porosity and permeability will be poor. Shales deposited between gravity flow events may provide seals (Figure A106, Figure A107). One well on the higher southern basin margin (on continental crust) displays a major sequence boundary at 12 Ma (Mid Miocene) as the basin filled with gravity flow debris and water depth reduced. The environment in this marginal position then became shallow marine (with a coastal plain interlude) until the Pliocene. The water depth increased again in the Pliocene to depths comparable with the Present Day water depths. While no lithological column was located it seems likely that reservoir quality and seal will be a problem.

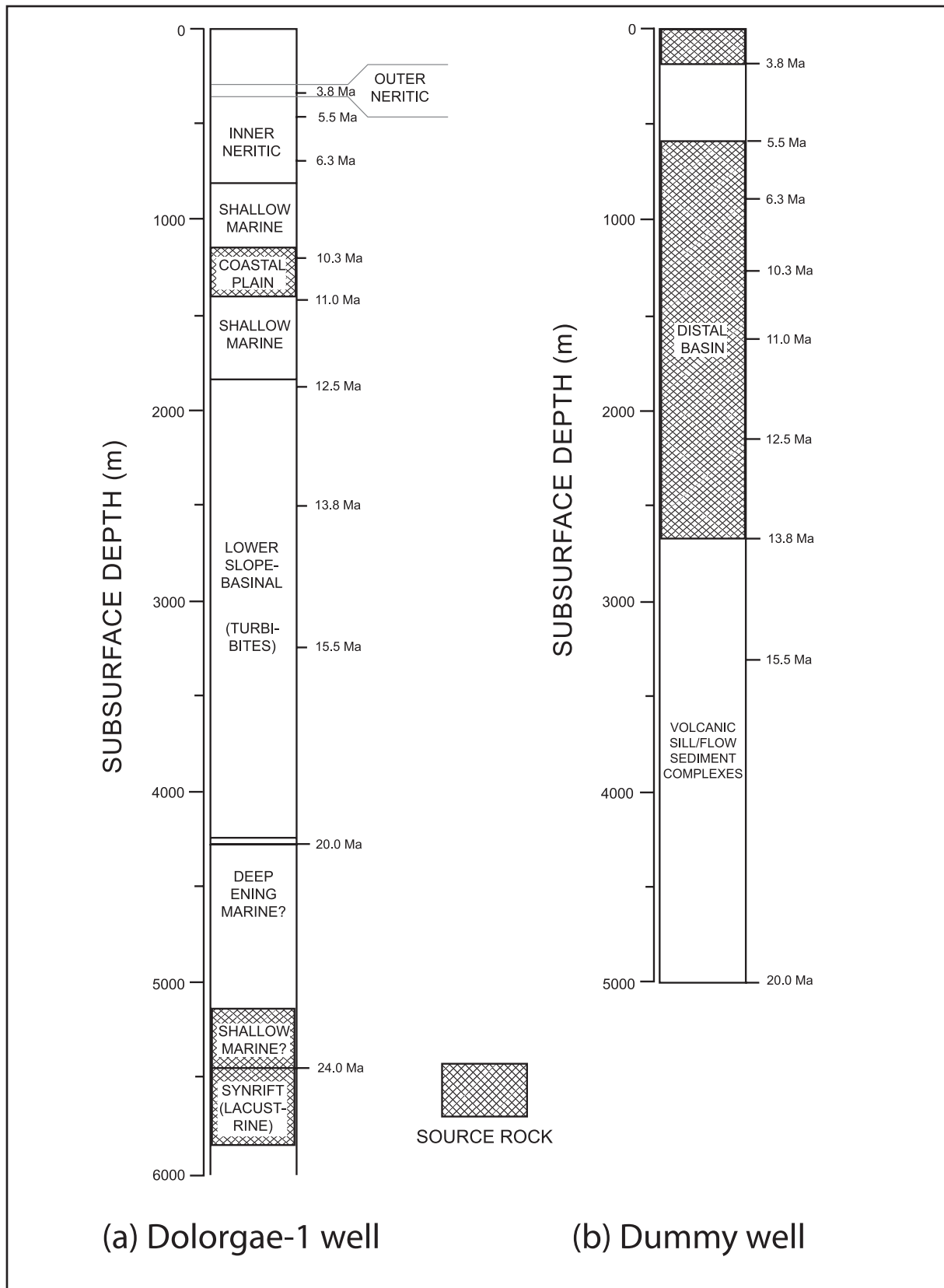


Figure A107. Lithologic columns of (a) the Dolgorae-1 well and (b) the dummy well. The Dolgorae-1 well was extended beyond the actual bottom depth (4265 m) to the basement and assumed to have penetrated synrift sequence. The sedimentary section above the volcanic sill/flow-sediment complexes at the dummy well site is dominated by basinal muds for mass-transports of the early Pliocene intervals (5.5-3.8 Ma) (text and figure from Lee and Kim 2002).

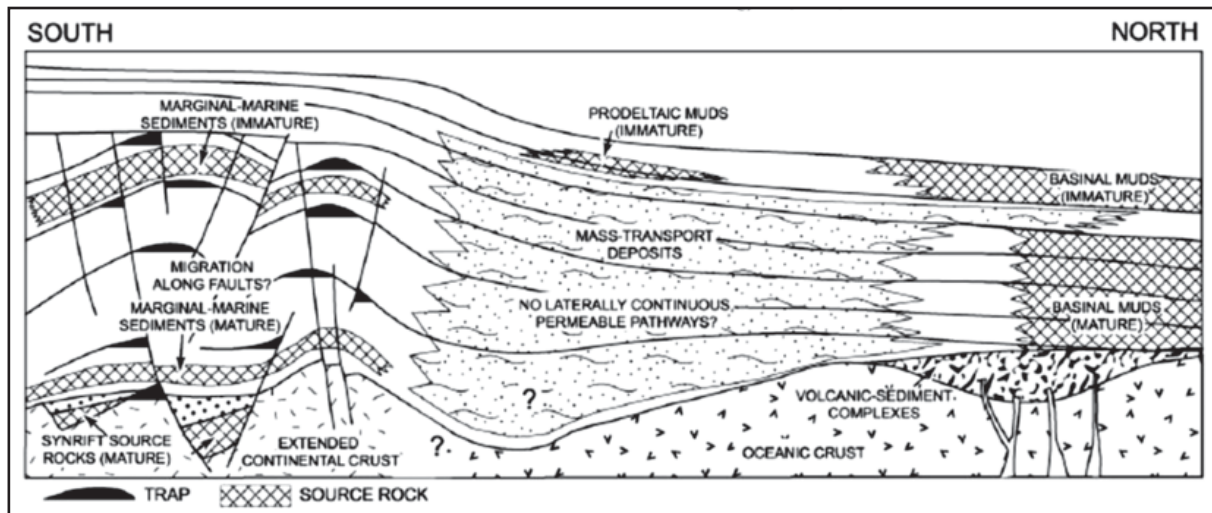


Figure A108. Schematic cross-sectional diagram showing main rock types (from Lee and Kim, 2002).

### A3.3.4 Hydrocarbon Fields

Much of the basin is in deep water (1000-2000 m) and has not been examined by drilling. There are a few exploration wells on the southern edge of the basin. About half of these wells have recovered gas while oil has not been recovered. There is apparently one commercial gas/condensate field (Lee and Kim 2002). The hydrocarbon field is some form of stratigraphic trap related to an ancient sub marine canyon (Choi and Jang, 2000).

### A3.3.5 Coal Occurrence

Coal is postulated as a possible gas source rock in the basin by Lee and Kim (2000). The period of time suitable for coal formation appear to be brief. Given the water depths coal is not considered an option for geological storage.

### A3.3.6 Potential CO<sub>2</sub> Storage Options

Much of the basin is currently in water depths over 1000 m making it expensive to drill wells. The ancient gravity flow sandstones are difficult to investigate as they lie in this area of Present Day deep water. Sub marine gravity flow processes can lead to sand bodies that are completely encased in sealing formations. The pressure isolation of such sands would limit the amount of CO<sub>2</sub> that could be safely injected without fracturing the seal formation.

The water depth decreases to the south of the basin. There may be saline reservoir opportunities on the southern depocentre if reservoir quality could be shown to be adequate and if it was shown that there was an ultimate seal over the “marginal” deposits which are thick on the southern basin edge (Figure A107).

### A3.3.7 References

Choi, B. and Jang, H. Hydrocarbon exploration in the Ulleung (Tsushima) Basin, offshore Korea and the recent gas discovery. AAPG Bulletin 84[9], 1411-1412. 2000.

Lee, G.H., Kim, H.J., Han, S.J., and Kim, D.C. Seismic stratigraphy of the deep Ulleung Basin in the East Sea (Japan Sea) back-arc basin. Marine and Petroleum Geology 18[5], 615-634. 2001.

Lee, G.H. and Kim, B. Infill history of the Ulleung Basin, East Sea (Sea of Japan) and implications on source rocks and hydrocarbons. *Marine and Petroleum Geology* 19[7], 829-845. 2002.

Yoon, S.H., Chough, S.K., and Park, S.J. Sequence model and its application to a Miocene shelf-slope system in the tectonically active Ulleung Basin margin, East Sea (Sea of Japan). *Marine and Petroleum Geology* 20[10], 1089-1103. 2003.

## A4. Malaysia

Malaysia is located in southeast Asia. Its 330,242 km<sup>2</sup> of territory includes Peninsular Malaysia and the states of Sabah and Sarawak on the island of Borneo.

Malaysia has significant conventional energy resources such as oil, gas and coal. Renewable energy sources in use include, hydro, biomass and solar. Malaysia has 29,000 MW of hydropower capacity.

Given the distribution of Malaysia's CO<sub>2</sub> emissions the main basin of interest is the Malay Basin. The population near the Greater Sarawak-East Natuna Basin of East Malaysia is relatively small compared to that of the Malay Peninsular, as a result power generation facilities are few.

### A4.1 Malay Basin

#### A4.1.1 CO<sub>2</sub> Sources

Power generation within peninsular Malaysia is the main source of CO<sub>2</sub>. The majority of Malaysia's stationary CO<sub>2</sub> emissions are generated on the west coast of Peninsular Malaysia (West Malaysia).

The combined CO<sub>2</sub> emissions within 300 km in the coastal region adjacent to the Malay Basin (i.e. the Malay Peninsula) are 86 Mt CO<sub>2</sub>/yr. Malaysia's estimated total stationary source CO<sub>2</sub> emissions are 113 Mt/yr (IEA, 2000).

Note: The sum of sources within 300 km of a basin very crudely indicates the magnitude of emissions within reach of the basin. These "catchments" overlap for most basins and should not be summed.

#### A4.1.2 Basin Overview

The basement of the Malay Basin consists of Mesozoic to Carboniferous carbonates or Mesozoic granites and sits on continental lithosphere (Ngah et al., 1996). Sediment may be 10,000 m to 12,000 m thick. The basin is a rift basin generated by transtensional forces. The basin has an area of 83,000 sq km. It is 500 km long and 200 km wide and strikes NW (Figure A109). It was initiated in the Oligocene. In general, Oligocene deposition was in a lacustrine environment. During the Miocene an extensive fluvial to delta system flowed into the incipient South China Sea Basin (Figure A110). The Thai Gulf and Malay Basin were part of this system. The basin was inverted in the Middle to Late Miocene after which fully marine conditions prevailed. The present day geothermal gradient of the Malay Basin ranges from 35 to 55°C/km with higher gradient in the north (Hutchinson, 1989).

#### A4.1.3 Basin Fill

Often the stratigraphy of the Malay Basin is known by letters.

A synthesis of the various schemes was made by Bishop (2002) of the USGS (Figure A111). Below is an edited extract on hydrocarbon reservoir quality by Bishop (2002).

Depositional facies and burial diagenesis influence the reservoir quality in the Malay Basin. Oligocene and Early Miocene deposits are represented by mainly clean, medium-grained sandstones, and the Middle Miocene shallow marine deposits of fine to medium-grained sandstones with porosity of 10% to 15%. The oldest producing reservoir

rocks are upper Oligocene, M and L group, fluvial sandstones. These are generally coarse to medium-grained sandstones with porosity of 10% to 27% and permeability averaging 400 mD.

The K Group is interpreted to be of late Oligocene to early Miocene age. The reservoir rocks in this group are mostly fluvial sandstone with porosity of 10-30% and permeability of up to 3000 mD

The overlying J Group reservoirs consist of fluvial and shoreline deposited sandstones of early Miocene age. The J Group produces lacustrine sourced oil, gas, and condensate from reservoirs with porosity ranging from 11-30% and permeability of up to 2000 mD The lower to upper Miocene E Group was deposited in an estuarine depositional environment. The lower to middle Miocene I Group reservoir rocks are described as shallow marine. Reservoir rocks have 25-30% porosity and up to 1000 mD permeability

The middle to upper Miocene H to D groups contain reservoir rocks of medium- to very fine-grained, shallow marine sandstones. The upper Miocene rocks from the Jerneh field in the northern portion of the Malay Basin include abundant coal beds and marine-influenced deltaic and coastal plain sandstones and glauconitic sandstones. These sandstones are interpreted to have been deposited in mangrove swamps and tidal channels. These reservoirs have up to 30% porosity, 1000 mD permeability.

The Malay Basin has intraformational and regional seals. There is regional marine shale flooding surface between I and H groups which seals the reservoirs. Other transgressive marine shales may occur between H and F, primarily in the eastern part of the basin (Bishop, 2002).

Work by Worden et al., (1997) addresses the concern that ductile lithic grains may occlude porosity and limit permeability in sediments of the Thai and Malay basins. However, data gathered by the USGS (2000) from hydrocarbon field data suggests there is often good porosity and permeability, at least in the Malay Basin.

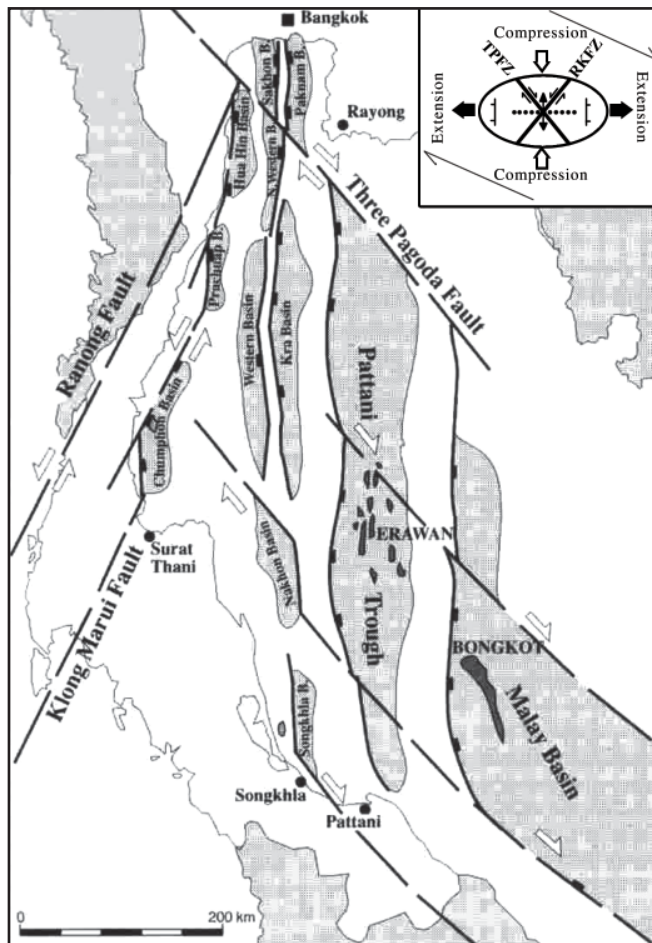


**Figure A109. Simplified structural map of the Gulf of Thailand and Malay Basins (from Leo, 1997).**

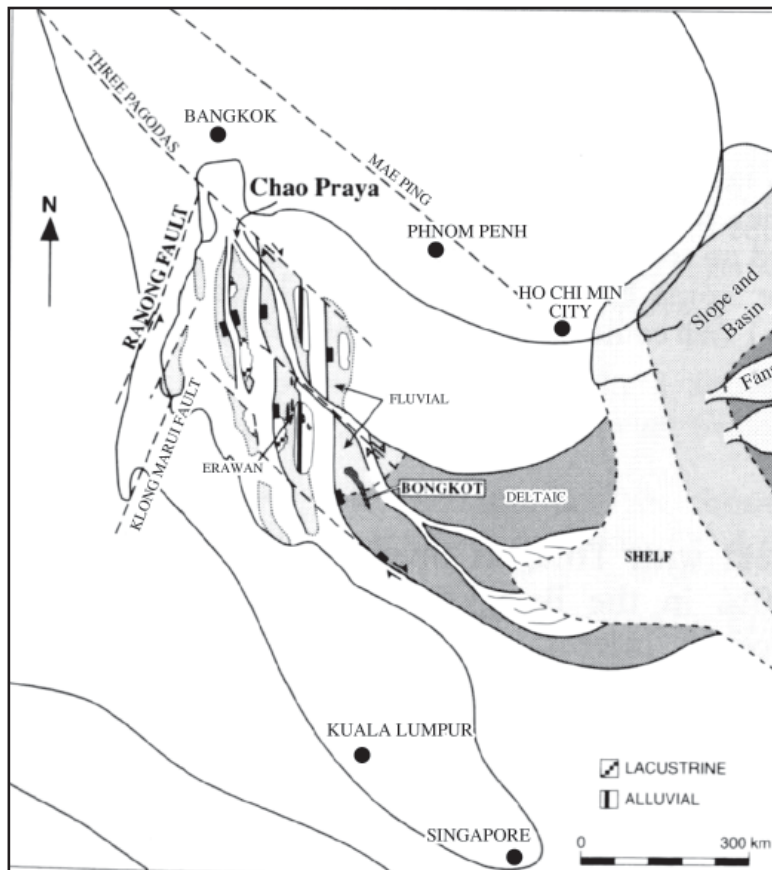


Figure A110. Palaeogeographic map of the Oligocene to Miocene period in the region of the Thai and Malay basins (from Leo, 1997).

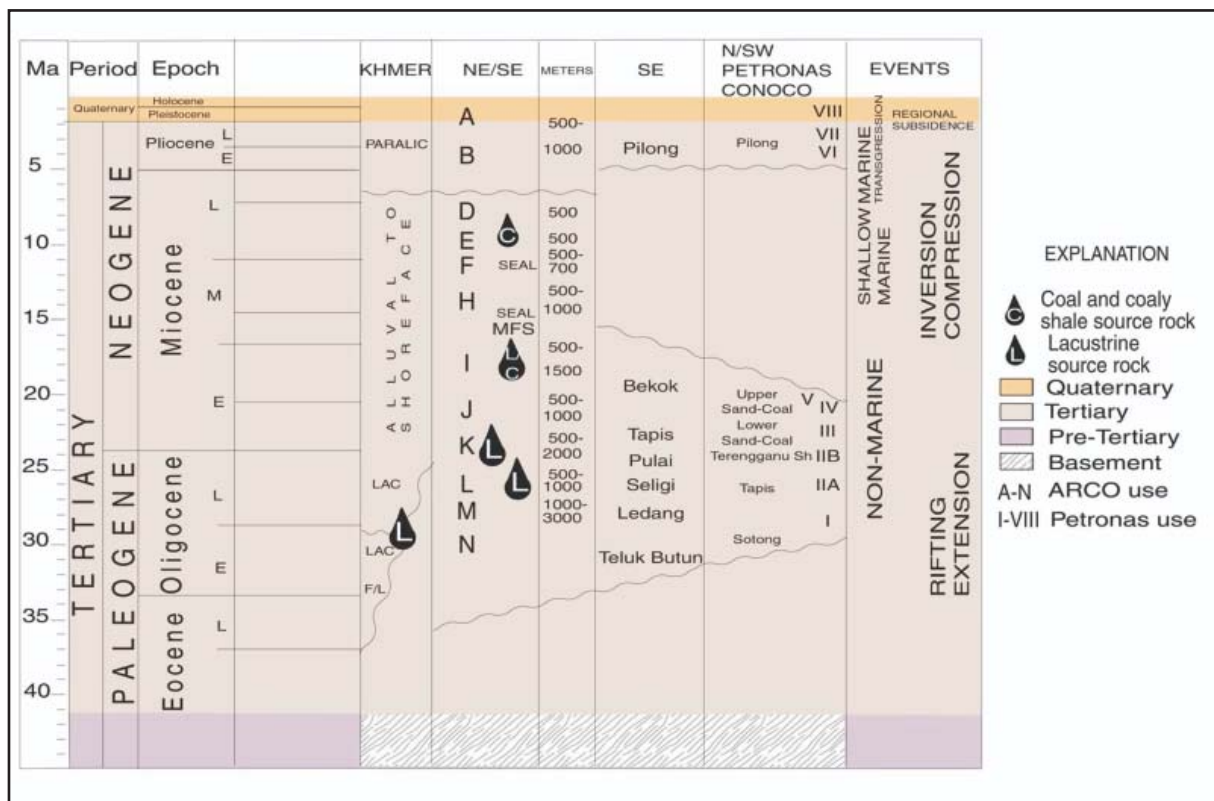


Figure A111. Malay Basin composite stratigraphy (from Bishop, 2002).

## A4.1.4 Hydrocarbon Fields

Malaysia's total hydrocarbon pore space is considerable. The USGS estimate for Malaysia's "known" (cumulative production plus reserves) hydrocarbon in the Malay and Greater Sarawak basins is 4.4 billion bbls of oil and 126 Tcf of gas.

The USGS (2000) estimates Malay Basin "known" oil of 3608 mmbbls. Of this 1518 mmbbls is produced and 2090 mmbbls is still in reserves. The "known" volume of 3608 mmbbls is equivalent to ~ 469 Mt of stored CO<sub>2</sub>.

The USGS (2000) estimates the Malay Basin has "known" gas reserves of ~48Tcf. Only 492 Bcf is produced leaving 47.6 Tcf in reserves. The "known" volume of 48 Tcf is equivalent to 3840 Mt of stored CO<sub>2</sub> (assuming 80 Mt CO<sub>2</sub> stored per 1Tcf of gas).

Depletion status of specific fields is unknown. However it is important to note that very little of the large "known" gas volume has been produced. This pore space will not be available for storage for some time.

## A4.1.5 Coal Occurrence

Coal occurs in the Malay Basin but it is assumed the offshore setting would prevent ECBM development. As of December 2001 Malaysia had coal reserves of 1,483 million tonnes (Mt) mainly in the Sarawak Basin.

## A4.1.6 Potential CO<sub>2</sub> Storage Options

The Malay Basin is proximal to 76% of Malaysia's CO<sub>2</sub> sources. The Malay Basin has compressional structuring resulting from a Miocene inversion. Anticlinal structures would have high structural integrity whether they are depleted hydrocarbon fields or water wet (saline reservoir). The high geothermal gradients will reduce storage density. Data gathered by the USGS (2000) from hydrocarbon field data suggests there is often good porosity and permeability.

The major Miocene transgression provides a generally claystone marine section into the Pliocene, representing a regional seal in the basin. There is a large known hydrocarbon pore space. It is apparent that oil and gas reserves are far from spent and the access to depleted gas fields in particular may not occur for some time.

Setting aside the offshore location the Malay Basin seems to have moderate potential.

## A4.1.7 References

Bishop, M.G. Petroleum Systems of The Malay Basin Province, Malaysia , Open-File Report 99-50T, U.S. Geological Survey . 2002.

Hutchison, C.S. Geological evolution of South-East Asia. Clarendon Press, Oxford, 1989.

Leo, C. T. A. M. Exploration in the Gulf of Thailand in deltaic reservoirs, related to the Bongkot field. In: Fraser, A J, Matthews, S J & Murphy, R W (eds.), Petroleum geology of Southeast Asia. Geological Society Special Publications. Geological Society of London 126, 77-87. 1997.

Worden, R.H., Mayall, M.J., and Evans, I.J. Predicting reservoir quality during exploration: lithic grains, porosity and permeability in Tertiary Clastic rocks of the South China Sea basin. In: Fraser, A J, Matthews, S J & Murphy, R W (eds.), Petroleum geology of Southeast Asia. Geological Society Special Publications. Geological Society of London 126, 107-115. 1997.

# A5. Philippines

## A5.1 Luzon Basin

### A5.1.1 CO<sub>2</sub> Sources

The Philippines has falling use of coal and is increasingly using gas. Efforts are being made to use geothermal and wind power. According to IEA data (2000) the Philippines as a whole produced an estimated 45 Mt/yr of CO<sub>2</sub>. The region near Manila generated 24 Mt/yr. Manila sits on the Luzon Central Valley fore-arc basin (Figure A112, Figure A113).



Figure A112. Phillipines stationary CO<sub>2</sub> emissions and Luzon Basin.

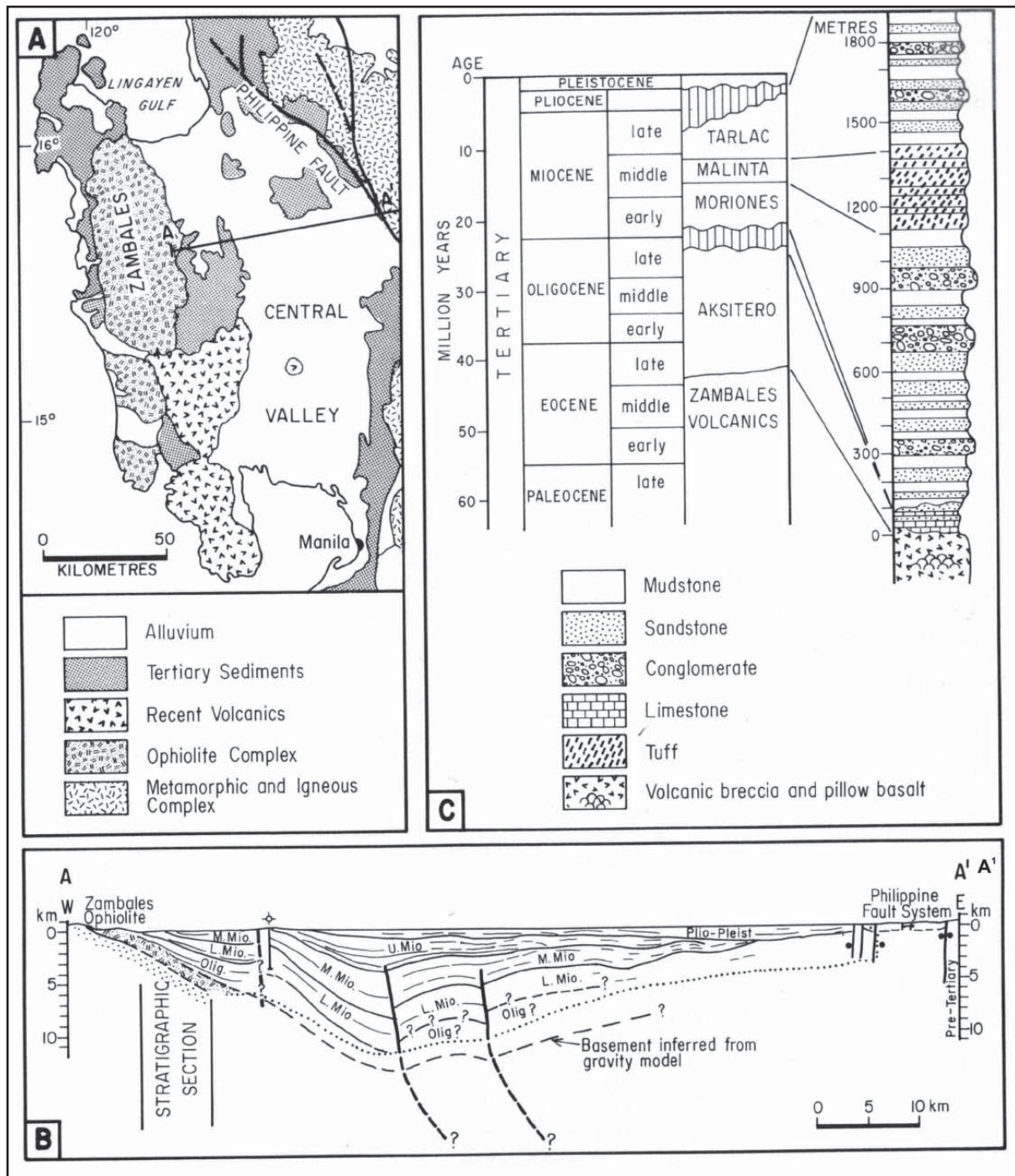


Figure A113. The Luzon Central Valley fore-arc basin. (a) Generalised geological map. (b) Cross-section based on outcrop, well data, seismic, and gravity modelling. (c) Stratigraphic column for the sequence which overlies the eastern flank of the Zambales ophiolite complex (from Hutchison, 1989).

## A5.1.2 Basin Overview

The Philippines is located near the junction of three major tectonic plates, and contains about eighteen sedimentary basins. These basins are related to the current subduction of the South China Sea in the north and the Philippines tectonic plate in the central and southern part of the archipelago. There are fore-arc, intra-arc and back-arc basins.

The Luzon Basin is a fore-arc basin located on the western margin of Luzon Island, the northern-most island in the Philippines archipelago (Figure A113). The basin covers an area of 20,000 km<sup>2</sup>. The basin forms a north-south structural terrace on the landward side of the West Luzon Trench. It contains 14 km of Cenozoic sediments (Figure A113) and the geothermal gradient is 16-24°C/km (Hutchison, 1987). The basins of the Philippines archipelago have a range of geothermal gradients: Visayan (31°C/km), Ragay-Samar (41°C/km) (Hutchison, 1987).

## A5.1.3 Basin Fill

The Luzon Basin sits between the Zambales uplifted ophiolite complex to the west and a volcanic arc called the Cordillera Central (Hutchison, 1987). The basin is floored with oceanic crust of Early Tertiary age. Pelagic and hemiplegic sedimentation occurred interspersed with ash from late Eocene to Miocene. In the late Palaeogene the eastern side of the basin received 8 km of arc derived sediments. In the middle Miocene the Central valley had a north south elongated shape and shelf deposits on the eastern and western sides. The high sediment inflow continued to reduce the water depth until non-marine deposition occurred in the Pliocene. Folding occurred in the eastern side of the basin adjacent to the Philippine fault during the Late Miocene to Holocene (from Hutchison, 1987).

A stratigraphic column is provided in Figure A113. Please note this column represents the fill at the shallow western edge of the basin. The history of copious erosion from near- by volcanic provinces suggests poor reservoir quality up until the mid Miocene. Relatively better reservoir may be possible in shelfal to fluvial and lacustrine environments of the post Mid Miocene non-marine section.

There are a few shows of hydrocarbon in the basin. If a geothermal gradient of 16-24 km is truly representative of the basin the notion that the basin is too cool for hydrocarbon generation (Hutchison, 1987) is credible. The lack of hydrocarbon resources makes it difficult to locate any porosity and permeability data.

## A5.1.4 Hydrocarbon Fields

The Philippines has proven oil reserves across all basins of 178 mmbbls and 3.7 Tcf of gas (Oil and Gas Journal, 2002). This equates to approximately 23 Mt and 296 Mt of stored CO<sub>2</sub> respectively. This does not present a large storage opportunity even when compared to the Philippines moderate emissions of 32 Mt/yr.

## A5.1.5 Coal Occurrence

Coal is a declining part of the Philippines fuel mix (EIA web site). In 2002, coal production was 1.7 Mt.

### A5.1.6 Potential CO<sub>2</sub> Storage Options

The Philippines location near a subducting boundary produces complex geology. The Luzon Basin is beneath Manila and thus is near a major concentration of CO<sub>2</sub> sources. Poor reservoir quality is expected in most of the formations of the basin due to the inflow of physically and chemically immature sediments from the nearby volcanic regions. The shelfal deposits from the Middle Miocene to Pliocene and the non-marine deposition from the Pliocene may present possibilities for better quality clastic reservoirs. The low geothermal gradient is a substantial positive for the efficiency of CO<sub>2</sub> storage. The folding on the eastern flank may create structurally closed areas for storage.

### A5.1.7 References

Bachman, S. B., Lewis, S. D. and Schweller W. J., Evolution of a forearc basin, Luzon Central Valley, Philippines. AAPG Bulletin 67[7], 1143-1162. 1983.

Gallagher, J. J. Jr. Philippine microplate tectonics and hydrocarbon exploration. In: Transactions of the Fourth Circum-Pacific energy and mineral resources conference , 103-119. 1987.

Hutchison, C. S. Geological Evolution of South-East Asia, Oxford University Press, Oxford. 1989.

Radler, M., Worldwide reserves increase as production holds steady, Oil and Gas Journal, 113-145, December 2002.

# A6. Chinese Taipei

## A6.1 West of Chinese Taipei

### A6.1.1 CO<sub>2</sub> Sources

Chinese Taipei's estimated total stationary source CO<sub>2</sub> emissions are 253 Mt/yr (IEA, 2000). All of these emissions are located well within 300 km of the west Chinese Taipei basins.

### A6.1.2 Basin Overview

There are three main basins to the west of Chinese Taipei. These are the Penghu, Taihsi and Tainan basins (Figure A114, Figure A115). The Taihsi and Tainan partly underlie Chinese Taipei Island. In terms of regional geology all three basins have a similar history. The sediment thickness is 8 km in the Tainan Basin.

Lin et al., (2003) defined three major unconformities that define the geological frame work of the area (Figure A116). Rifting began in the area around 58 Ma and is marked by the ROU (rift onset unconformity). It is assumed the rifting is a later result of the crustal thinning that underlay the development of NE trending rift basins in eastern China around the late Cretaceous.

At around 30 Ma the South China sea opened forming a major regional "break up" unconformity (BU). The area under went thermal subsidence and a "passive" margin developed until a collision with the Philippine plate around 6.5 Ma. This collision produces a late foreland basin phase in the Taihsi and Tainan basins.

### A6.1.3 Basin Fill

Stratigraphy of Lin et al., (2003) (Figure A116) suggests the Penghu Basin is quite sand prone and may lack extensive seals. It seems likely that the fluvial facies belts lay in the region of the Penghu Basin during the post break up period (30 Ma – 6.5 Ma).

In the Tainan Basin, an upper Oligocene transgressive sand deposited on the Break Up Unconformity is apparently well sealed by marine shales (Figure A116). No palaeogeography maps were located in the literature surveyed. Figure A115 shows the the transgressive sand is located at depths from 4 km to less than 1 km. Other possible saline reservoirs include the prograding Late Miocene formations and the over lying transgressive formations which follow the Basal Foreland Unconformity (BFU). The ultimate seal of these formations appears to be the Hinshui Shale which is interpreted to be a maximum flooding period in the foreland basin.

### A6.1.4 Hydrocarbon Fields

In 2003 the oil proven hydrocarbon reserves of Chinese Taipei were estimated at 4 million barrels of oil (equivalent to 0.5 Mt of Stored CO<sub>2</sub>) and 2.7 Tcf of gas (equivalent to 112 Mt of Stored CO<sub>2</sub>)(EIA [http://www.eia.doe.gov/emeu/cabs/Chinese Taipei.html](http://www.eia.doe.gov/emeu/cabs/Chinese%20Taipei.html)). It is apparent that storage in depleted hydrocarbon fields is a quite limited option when compared to annual emissions of 253 Mt/yr.

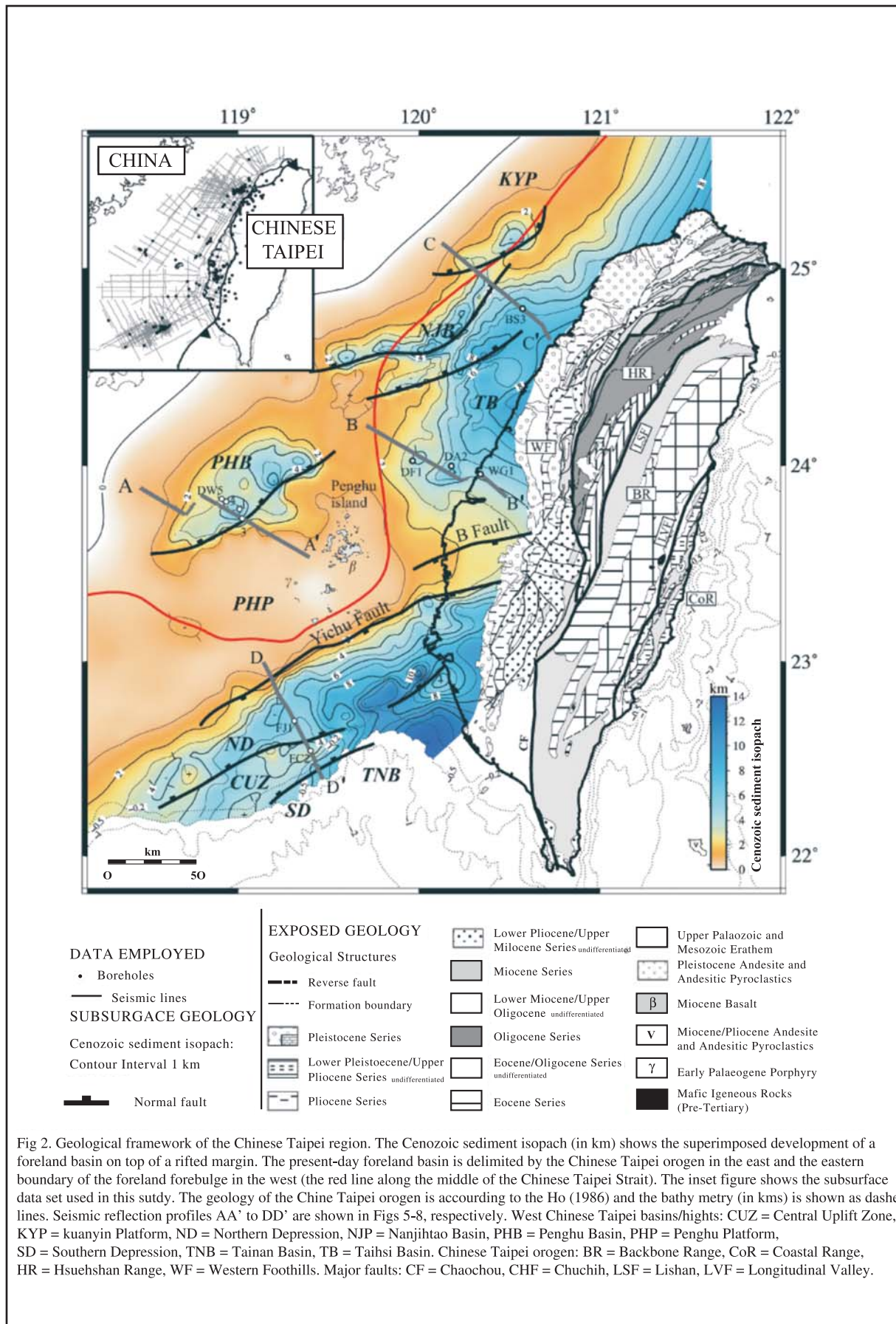
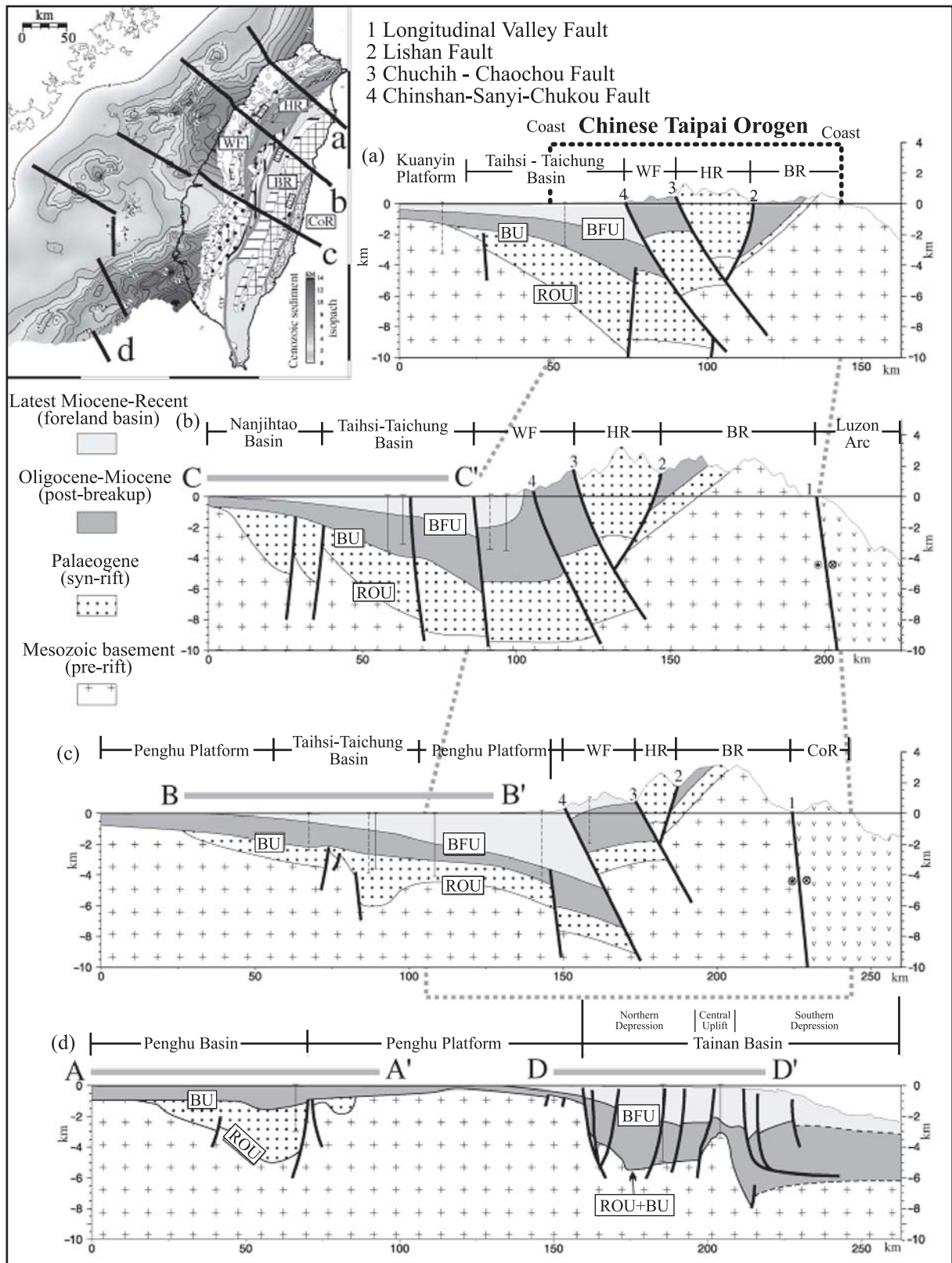


Figure A114. Basins in the Chinese Taipei region (from Lin et al., 2003)



**Figure A115.** Profiles showing the upper crustal structures across the northern margin of the South China Sea in the Chinese Taipei region. The profiles in offshore regions are from depth- converted seismic sections and the structures beneath the Taiwan orogen are schematic plots. The inset figure shows the locations of the profiles. ROU = rift-onset unconformity, BU = breakup unconformity, BFU = basal-foreland unconformity (text and figure from Lin et al, 2003).

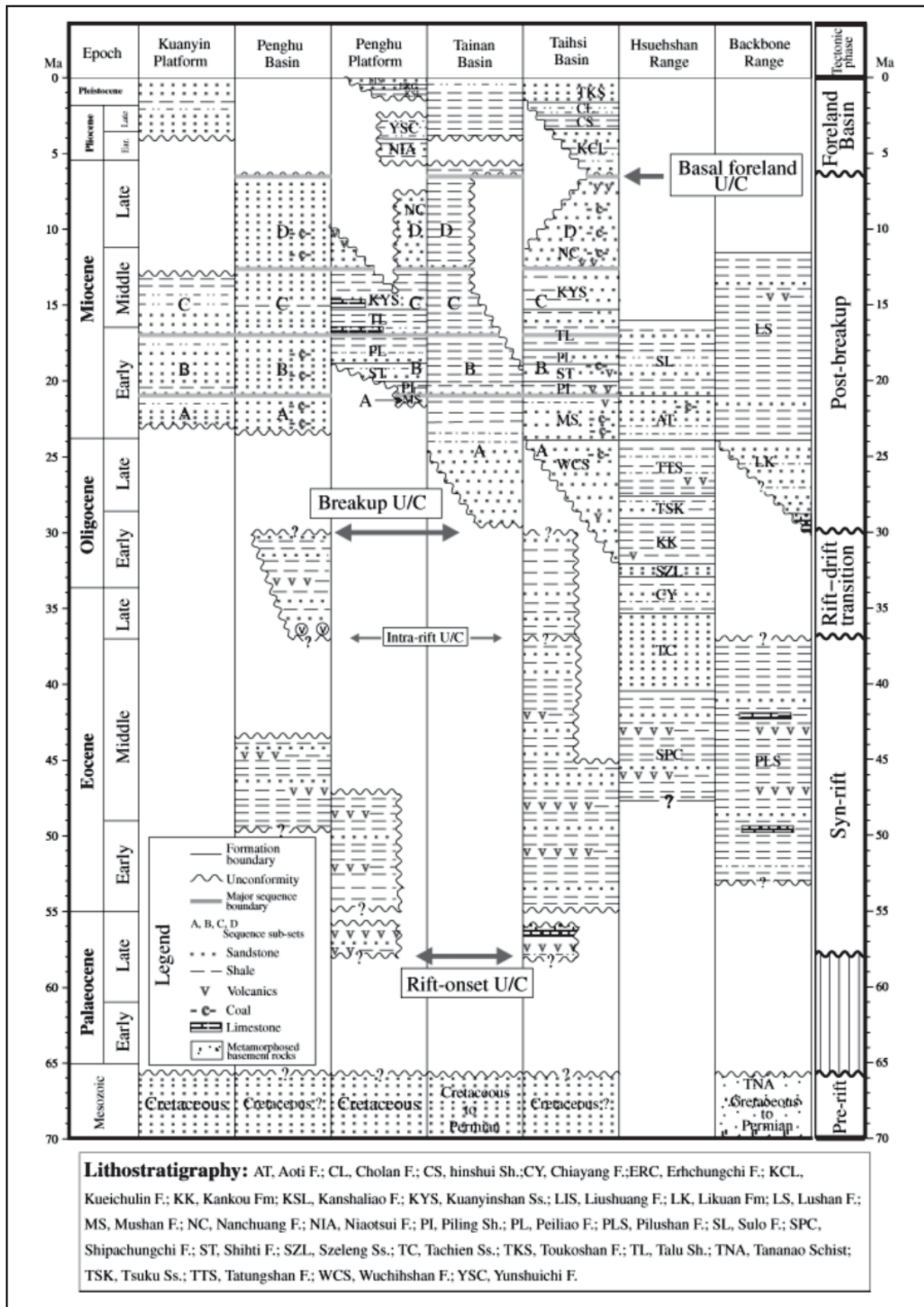


Figure A116. Cenozoic and tectonic phases in the Chinese Taipei region suggested in this study. the post-breakup succession is divided into four (A,B,C and D) sequence sets. U/C = unconformity (text and figure from Lin et al., 2003).

### A6.1.5 Coal Occurrence

Coal occurrence on Chinese Taipei Island is limited. Production ceased in 2000 (EIA [http://www.eia.doe.gov/emeu/cabs/Chinese Taipei.html](http://www.eia.doe.gov/emeu/cabs/Chinese%20Taipei.html)). Coal occurs in the Penghu and Taihsi basins during the post break up period (30 ma to 6 ma) at over 1 km deep.

### A6.1.6 Potential CO<sub>2</sub> Storage Options

The Tainan Basin in particular may offer a few reservoir-seal pairs with prospectivity for CO<sub>2</sub> storage. Some of these may be accessible from an onshore location. Depleted hydrocarbon fields are very few. Shallow coal occurrence is also limited.

### A6.1.7 References

Kong, F., Lawver, L. A. and Lee, T.-Y., Evolution of the southern Chinese Taipei-Sinzi Folded Zone and opening of the southern Okinawa trough. *Journal of Asian Earth Sciences* 18[3], 325-341. 2000

Lin, A.T., Watts, A.B. and Hesselbo, S.P., Cenozoic stratigraphy and subsidence history of the South China Sea margin in the Chinese Taipei region. *Basin Research* 00015[00004], 453-479. 2003



# A7. Thailand

## A7.1 Thai Gulf Basin (NW Basins & Pattani)

### A7.1.1 CO<sub>2</sub> Sources

Nearly all of Thailand's emissions of 120 Mt CO<sub>2</sub>/yr are within 300 km of the Gulf of Thailand Basin (IEA, 2000).

Note: The sum of sources within 300 km of a basin very crudely indicates the magnitude of emissions within reach of the basin. These "catchments" overlap for most basins and should not be summed.

### A7.1.2 Basin Overview

The main basin to be considered is the Gulf of Thailand Basin which developed in the early Tertiary. Two major strike slip fault systems cut the area (Three Pagodas and Ranong). These faults frame an area of north south grabens (Leo, 1997) (Figure A117). The Gulf of Thailand has two main structural regions: to the western half is a region of many small basins. The eastern half contains two large basins the Pattani trough and the Malay Basin (Leo, 1997). The basement is Mesozoic to Carboniferous carbonates and Mesozoic granites (Leo, 1997). Sediment thickness is a maximum 3500 m. The geothermal gradient is 50°C/km (Hutchison, 1989).

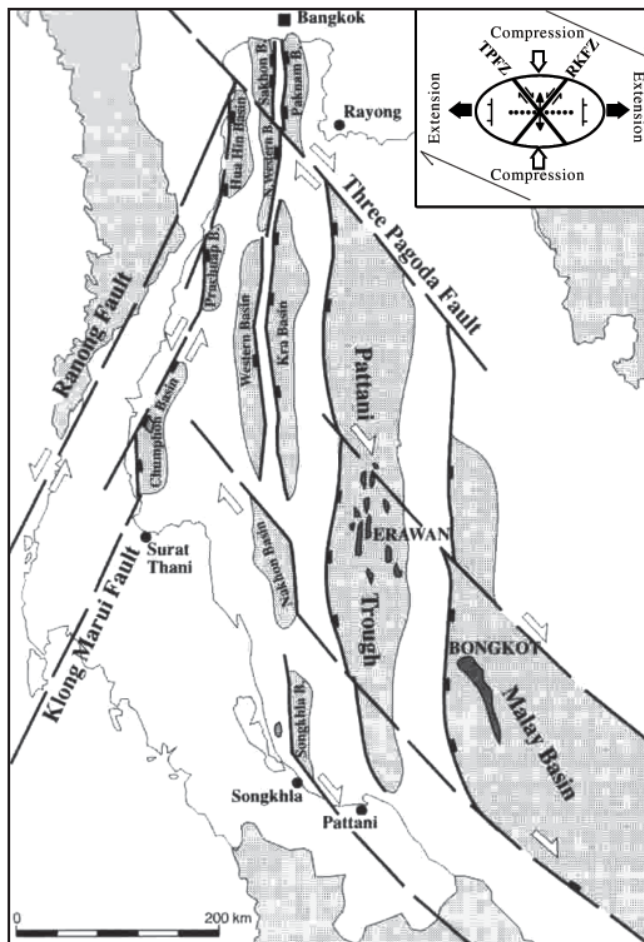


Figure A117. Simplified structural map of the Gulf of Thailand and Malay Basins (from Leo, 1997).

### A7.1.3 Basin Fill

The NW basins and the Pattani are dominated by lacustrine deposition in the Oligocene and by fluvial environments in the Miocene and Pliocene. There is little or no marine influence in this area unlike the Malay Basin immediately to the south (Figure A118). The Late Miocene regional transgression shifted the environments of deposition to paralic, marine delta and open marine (Figure A119). There are gas accumulations in the Gulf of Thailand in the Oligocene/Miocene sequences. The fluvial point bars which reservoir the gas can have very low interconnectivity. These accumulations have intra-formational seals (and source rocks).

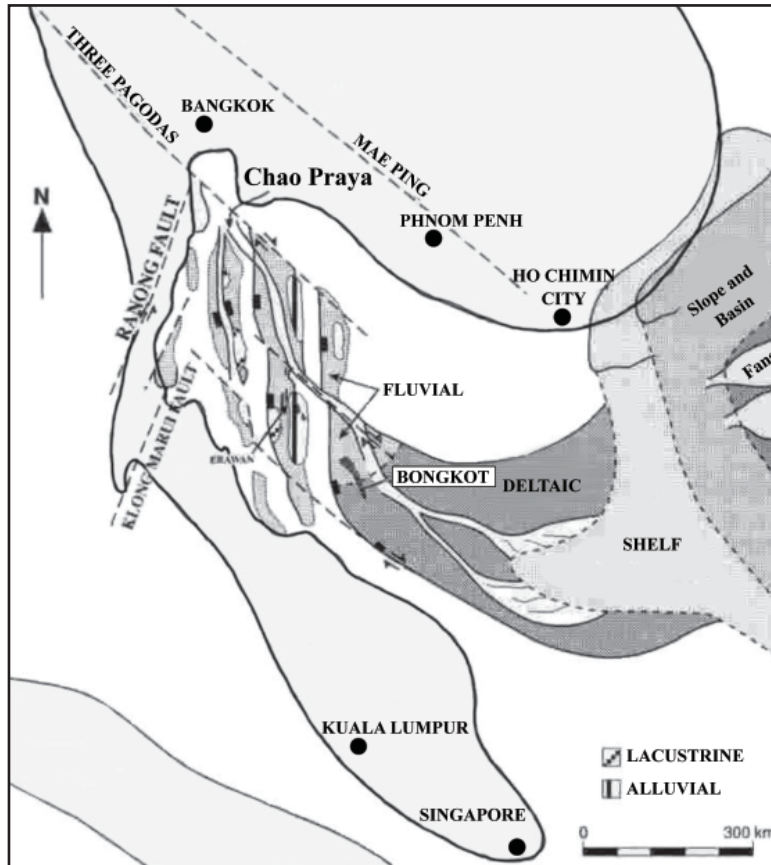


Figure A118. Depositional environment during the Oligocene and Miocene (from Leo, 1997).

### A7.1.4 Hydrocarbon Fields

The Pattani Trough contains several large gas fields developed since 1979. The Pailin Field, is located in the southern Pattani Trough, and contains up to 65% CO<sub>2</sub> (Martens et al., 2000).

Gas accumulations in the Gulf of Thailand are contained in quite discontinuous fluvial reservoirs (Figure A120)

### A7.1.5 Coal Occurrence

Coal occurs in the basin but it is assumed the offshore setting would prevent ECBM development.

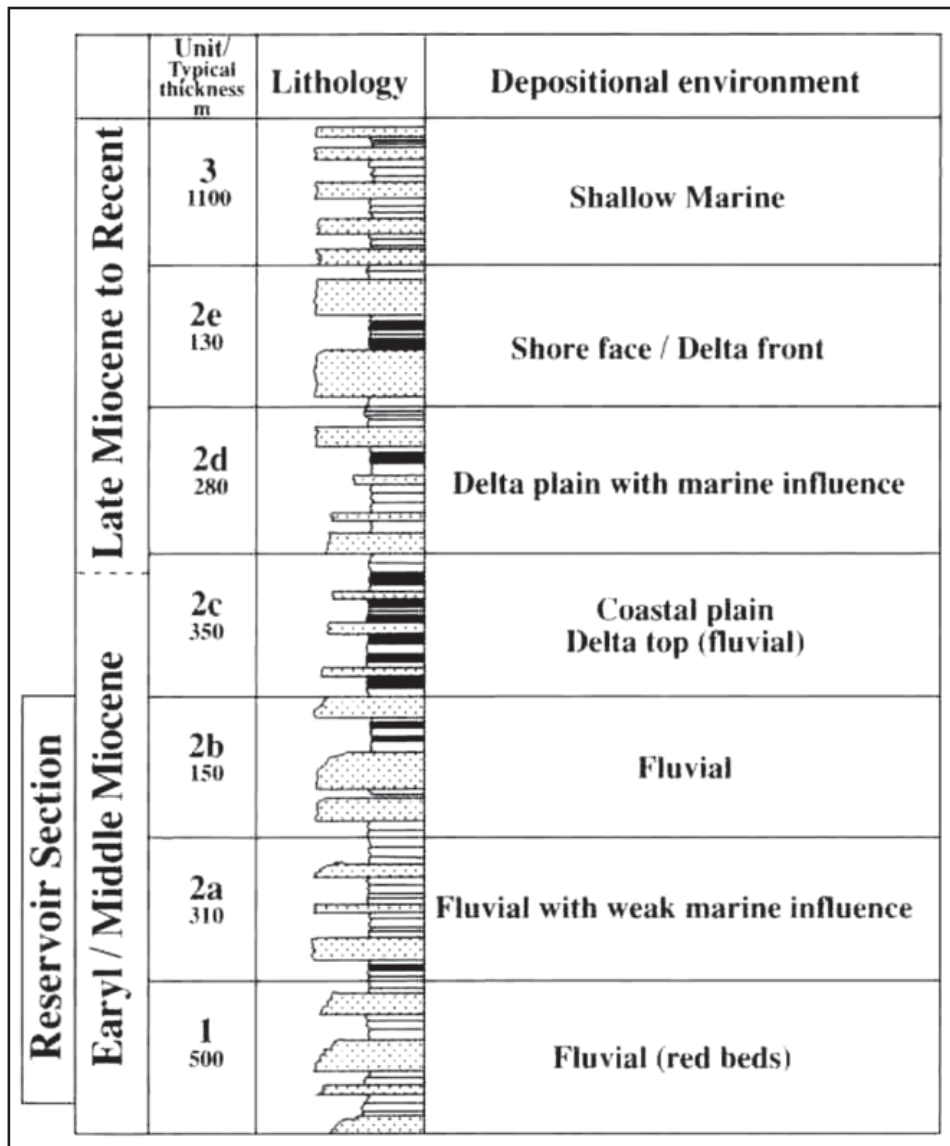
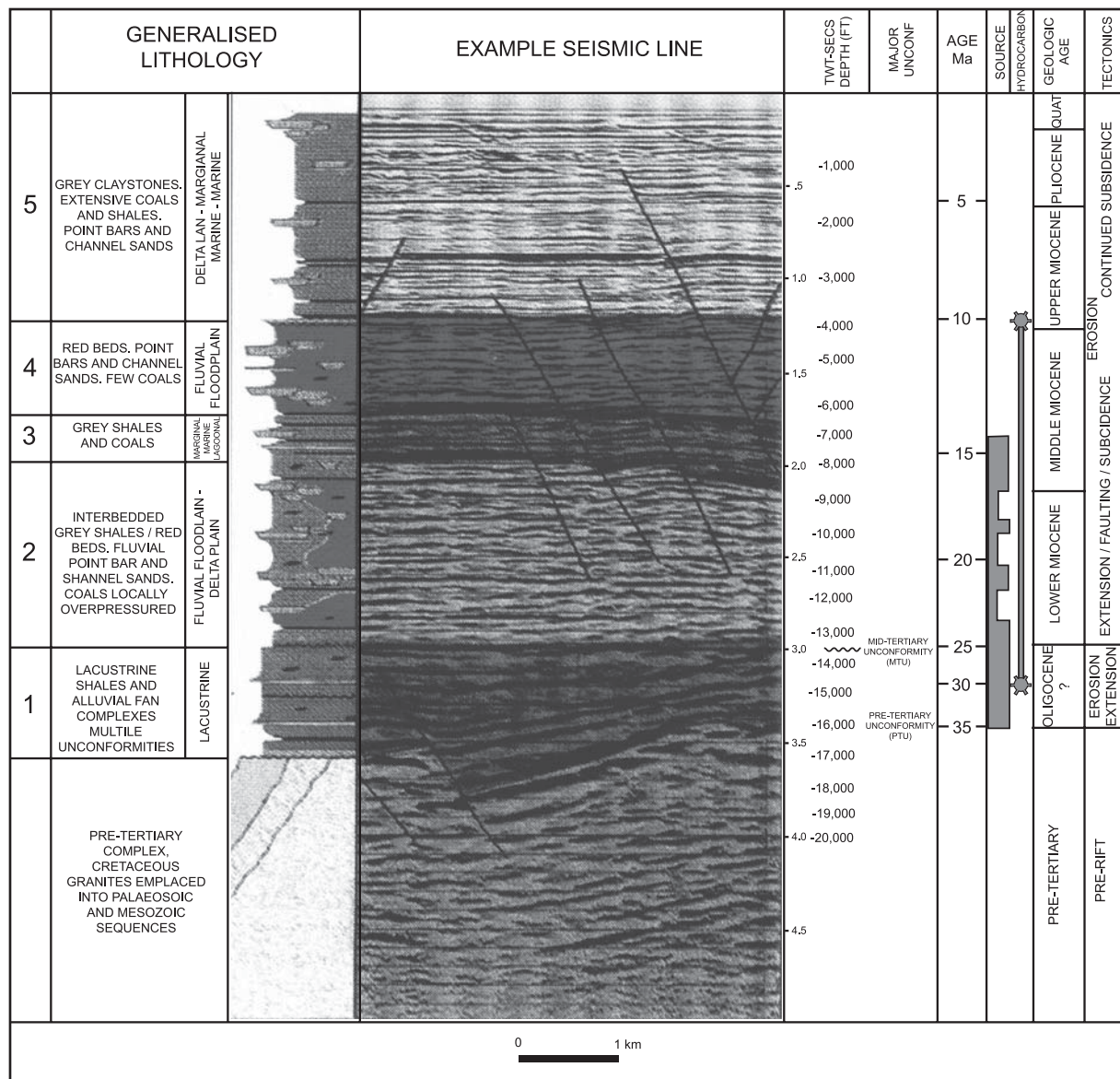


Figure A119. Litostratigraphic column of the Bongkot Field (from Leo, 1997).

### A7.1.6 Potential CO<sub>2</sub> Storage Options

The discontinuity of sandstones in the hydrocarbon rich areas of the basin is not ideal for CO<sub>2</sub> injection. Better connected more closely stacked sandstones are expected up depositional dip toward the head of the Gulf of Thailand (Figure A118). Obviously intraformational seals would decrease. However Late Miocene marine facies may potentially provide seals. The very high geothermal gradient of 50°C/km will reduce CO<sub>2</sub> storage density.

It may be possible to inject CO<sub>2</sub> into the carbonate basement. Depth to basement is up to 3500 m. However at this depth with a geothermal gradient of 50°C/km temperatures in the basement will be high, reducing CO<sub>2</sub> storage density.



**Figure A120. Stratigraphic summary of the major depositional sequences within the Pattani Basin. Shown from left to right are primary lithologies, depositional environments, a stratigraphic column and seismic character example, average depths, age source and productive intervals, and major tectonic events controlling basin evolution (from Jardine, 1997).**

## A7.1.7 References

Hutchison, C. S. Geological Evolution of South-East Asia, Oxford University Press, Oxford. 1989.

Jardine, E. Dual petroleum systems governing the prolific Pattani Basin, offshore Thailand. In: Howes, J V C & Noble, R A (eds.), Proceedings of the conference on Petroleum systems of SE Asia and Australasia. Indonesian Petroleum Association. Jakarta, Indonesia , 351-363. 1997.

Leo, C. T. A. M. Exploration in the Gulf of Thailand in deltaic reservoirs, related to the Bongkot field. In: Fraser, A J, Matthews, S J & Murphy, R W (eds.), Petroleum geology of Southeast Asia. Geological Society Special Publications. Geological Society of London 126, 77-87. 1997.

Martens, D., R. Lin, and R. G. Hickman. Source, migration and CO<sub>2</sub> occurrences in the Pailin Field, Gulf of Thailand. AAPG Bulletin 84[9], 1459-1460. 2000.

# A8. Table of Basin Attributes

Member Economy	Basin Name	Basin Sequence &	Area (Km <sup>2</sup> )	Basin Depth km	Temperature Gradient (°C/Km <sup>2</sup> )	Reservoir lithology & age	Porosity range in %	Permeability Range (md)	Traps & sealing rocks	Remarks
China	Songliao	Jurassic & Cretaceous	261,000	7 km	31—78	Non marine fine-grained sandstone, Middle Cretaceous	20—25	100—8,000	Plunging anticlinal folds, and stratal pinch outs; sealed shale & mudstone of Middle to late Cretaceous age	Supergiant field (Daqing); production ranks first in country. Basin evolved from the Variscan folded cratonic basement by extensional tectonics followed by filling depressions formed above basement lineaments (Wang & others, 1983; Yang, 1985; Yang, Li, & Gao, 1985; Lee, 1986c; Qiu & others, 1987).
China	Bohaiwan	Tertiary & Quaternary	200,000	4-7 km	33—50	Sandstones, Eocene and Oligocene	16—32	100—2,440	Fault blocks, rollover & drape anticlines, stratigraphic overlaps, unconformities, stratal pinch outs,	Gudao oil & gas field of the Jiyang depression is characterized by deltaic reservoir sandstone with porosity 30 to 32 percent & permeability for oil ranging from 510—2,440 md (Cheri & Wang, 1980, p. 486; Qiu & others, 1987).
China	North China-Buried Hill Basement Reservoirs	Tertiary & Quaternary	200,000	various	33—50	Reef-limestone, Oligocene	36—46	n.a.		Pinofangwang oil & gas field of the Jiyang depression (Lee, 1986b; Petroconsultants, Ltd, 1982)
						Dolomite & limestone, Ordovician, Cambrian & Late Proterozoic	n.a.	n.a.	Buried hill highs; sealed by Palaeogene shale, mudstone & gypsum-rock salt beds.	Renqiu & Guxinzhuang oil & gas fields of the Jizhong depression produce from buried fractures of hills (Lee, 1986b, p. 26—28).
						Quartzite, Late Proterozoic	0.4—7.7	5—10		Dujiatai oil field of the Liaodong Gulf-Liao River depression (Lee, 1986b).
						Granite, gneiss, Archaean deeply weathered,	8	n.a.		Dongshengpu & Xinglongtai oil fields of the Liaodong Gulf-Liao River depression (Lee, 1986b, p. 26—28).
China	Subei/ Yellow Sea Basin	Tertiary and Quaternary	Total 130,000 (onshore 41,000)	6 km	30—32	Sandstone Late Mesozoic & Palaeogene. Cavernous carbonate rocks, Early Tertiary	n.a.	n.a.	Stratal pinch outs & fault blocks; sealed by Palaeogene & Neogene shale & evaporite beds.	Zhenwu oil field (personal communication with Wang-on, Chu, Pemzoi International Co., 1986). In addition to Tertiary beds, production reported from Jurassic & Cretaceous strata; oil & gas shows occur in Palaeozoic strata (Wang & others, 1983).

A8. Table of Basin Attributes

Member Economy	Basin Name	Basin Sequence	Area (Km <sup>2</sup> )	Basin Depth km	Temperature Gradient (°C/Km <sup>2</sup> )	Reservoir lithology & age	Porosity range in%	Permeability Range (md)	Traps & sealing rocks	Remarks
China	Jianghan	Tertiary	28,000	10 km	31—32	Sandstone, Palaeogene	n.a.	n.a.	Plunging anticlinal folds, fault blocks, & sandstone pinch outs; sealed by Palaeogene shale, mudstone, & gypsum-rock salt beds.	Excluding the Dongting Hu depression on the south. Oil reported from Upper Cretaceous strata in small amounts (Wang & others, 1983).
China	Taikang Heifei (Dabie-shan)	Jurassic foreland	~100,000	6 km	?	Sandstone, braided stream to lake	n.a.	n.a.	No hydrocarbon fields	Complex poly basin region near the Dabie-shan. The foreland basin deposits are eroded at the end of the Cretaceous.
China		Tertiary rift		?	?	Sandstone, fluvial to lacustrine	n.a.	n.a.	No hydrocarbon fields	Complex poly basin region near the Dabie-shan. Not a hydrocarbon basin. No source rock.
China	Nanyang/Nanxiang	Tertiary	17,000	9 km	43	Sandstone, Palaeogene	n.a.	n.a.	Fault blocks & stratal pinch-outs; sealed by Palaeogene shale, mudstone, & gypsum beds.	Producing fields located in east & central parts of the basin (Wang & others, 1983).
China	East China Sea Basin	Cret., Tert., Quaternary	770,000	1 - 10 km	32 (shelf basin)	Sandstone	n.a.	n.a.	Drape over basement & other stratigraphic	Xihu trough is the main area of hydrocarbons & therefore sub surface knowledge. Hydrocarbon gas produced from the Xihu trough is piped 400 km to Shanghai. A lot of uncertainty - not enough known about areas nearer to shore.
China	South China Sea - pearl River Mouth	L.Cret,Tert, Quaternary	147,000	up to 10 km	34 (Zhu III)	Sandstone	20-36	360 - 450	Enhanced drape over basement faults & other stratigraphic traps	steady transgression from the Neogene may have resulted in some semi regional reservoir seal pairs ?
China	South China Sea- Yinggehai (China Section)		~25,000	12 to 17	31—46	Sandstone	n.a.	n.a.	Dongfang gas field contains 50% natural CO <sub>2</sub>	The presence eof Dongfang shows there are effective seals & traps. However Hard overpressure onset is at 3200 m & geothermal gradient is 46 deg C/km. These are significant negatives that are compounded by offshore location.

A8. Table of Basin Attributes

Member Economy	Basin Name	Basin Sequence	Area (Km <sup>2</sup> )	Basin Depth km	Temperature Gradient (°C/Km <sup>2</sup> )	Reservoir lithology & age	Porosity range in%	Permeability Range (md)	Traps & sealing rocks	Remarks
China	Ordos	Late Triassic, Jurassic, and Cretaceous	320,000	10 km	27—28	Non marine sandstone, Late Triassic and Jurassic	10—15	6—100	Stratal pinch outs, stratigraphic overlaps, drag of imbricated thrust-faulted beds; sealed by shale & mudstone of Late Triassic & Jurassic age.	Crude oil production dominantly from Upper Triassic & Middle Jurassic rocks. Upper Palaeozoic coal series is identified as potential gas resource. Evolved on western central part of the Sino-Korean platform (Wang & others, 1983; Lee, 1986a; Qiu & others, 1987).
China	Sichuan	Late Triassic, Jurassic, and Cretaceous	230,000	6-12 km	22—27	Non marine sandstone and bioclastic limestone, Triassic & Jurassic Carboniferous & Permian bioclastic limestone dolomite	10—15 12—18	10—20	Stratal pinch outs, stratigraphic overlaps, anticline, drag of imbricated thrust-faulted beds; sealed by shale, mudstone & evaporite beds of Palaeozoic, Triassic & Jurassic age.	Natural gas production ranks first in country. Dominant reservoir rocks are Palaeozoic carbonates with fractures & solution cavities. Area lies in north-western part of the Yangtze platform (Wang & others, 1983; Masters & others, 1980).
China	Nanpanjiang Depression	Cambrian to Triassic Carbonates	100,000	?	?	No known reservoirs. Oil seeps at margins. Bitumen in rock samples. Possibility of fractured carbonate reservoirs.	Cemented. Very little porosity.	None	n.a.	n.a.
China	Sanshui	Tertiary and Quaternary	2,600	3-4 km	31—45	Sandstone & volcanic rock, Late Cretaceous, Palaeocene & Eocene	n.a.	n.a.	Stratal pinch outs, fault blocks; sealed by Cretaceous & Palaeogene shale, mudstone, & gypsum-rock salt beds.	Eocene volcanism caused the formation of high purity of carbon dioxide (99.5 percent) pools in areas near the volcanic flows (Tang, 1984).
China	Shiwan Dashan Basin	na	11,600	na	na	na	n.a.	n.a.	n.a.	n.a.

A8. Table of Basin Attributes

Member Economy	Basin Name	Basin Sequence	Area (Km <sup>2</sup> )	Basin Depth km	Temperature Gradient (°C/Km <sup>2</sup> )	Reservoir lithology & age	Porosity range in %	Permeability Range (md)	Traps & sealing rocks	Remarks
China	Bose (Baise)	Tertiary	1,400	3 km	30—40	Sandstone, Palaeogene	n.a.	n.a.	Sandstone pinch outs, faults & anticlines; sealed by Palaeogene shale & mudstone.	Small amount of crude oil produced from structural-lithologic pools (Lee, 1984).
Indonesia	North Sumatra Basin	Oligocene - Quaternary	~258000	av 2.6 km & up to 5 km	45	Oligocene sandstone (e.g. Bampo fluvio-deltaic) Miocene carbonate (eg Peutu Fm)	19-24 av 18 (up to 25-30)	n.a. n.a.	L.Oligocene to E.Mio black shale seal M. Mio Baong Fm Seal	The basin has three major reservoir seal pairs. Sandstone facies not common in North Sumatra at this time. Mostly shale Isolated reefs around the central onshore N. Samatra & carbonate shelf at SE end of the basin.
Indonesia	Central Sumatra Basin	Oligocene - Quaternary	~117300	av 2.5 km & up to 5 km in grabens	60	Sihapas Grp Sandstones (deltaic) Pematang Fm	> 25% 15-20	400-4500 < 100 md	Miocene Telisa Shale (Sihapas Grp) Immediate seal in the Bangko Fm.	Widespread sandstone at this time. With terrestrial drainage from Sumatra into the greater North Sumatra/Mergui basin This reservoir seal pair contains the largest fields in Indonesia. Minas & Duri. Poorly sorted feldspathic fluvial/alluvial sandstones. Poor permeability is due to au-
Indonesia	South Sumatra Basin	Oligocene - Quaternary	~133700	av 2.6 km & up to 5 km	49	Reef Carbonate (Batu Raja F m) Oligocene Miocene marine deltaic Sandstone (Talang Akar Fm) E. Oligocene Lahat Fm	n.a. n.a. n.a.	n.a. n.a. n.a.	Sealed by Gumai (Telisa Eq) Ultimate seal is Gumai Fm (Telisa Fm equivalent)	Quality of this reservoir is unknown. Assume it is similar to that found in NW Java Basin. Deltaic sandstones. No data. Expect fair to good porosity. Quality of this reservoir is unknown. Assume it is analogous to the Pematang Fm of the early rift in the North Sumatra basin.

A8. Table of Basin Attributes

Member Economy	Basin Name	Basin Sequence	Area (Km <sup>2</sup> )	Basin Depth km	Temperature Gradient (°C/Km <sup>2</sup> )	Reservoir lithology & age	Porosity range in %	Permeability Range (md)	Traps & sealing rocks	Remarks
Indonesia	Northwest Java Basin	Oligocene - Quaternary	~140870	av 2.6 km & up to 5 km	40—50	E-M Miocene "Main" & "Mas-sive" Sandstones	n.a.	n.a.	Gumai Shale seal	The main & massive sands are fluvial deltaic sandstones deposited in a transgressive period with a thick marine shale (alaealous to Sihapas Grp)
						Reef Carbonate (Batu Raja Fm)	n.a.	n.a.	Bantu Raja Shale	Quality of this reservoir is unknown. Assume it is similar to that found in NW Java Basin.
						Oligocene Miocene marine deltaic Sandstone (Talang Akar Fm)	23-35	150-2500	Intraformational	Deltaic sandstone.
						Eocene Banuwati Fm	n.a.	n.a.	Intraformational	Quality of this reservoir is unknown. Assume it is analogous to the Pematang Fm of the early rift in the North Sumatra basin.
Indonesia	East Java Basin	Eocene - Quaternary	260,000	av 3 km	39	Ngrayong Sandstone	n.a.	n.a.		Reservoir properties are reported excellent in places.
						Carbonate in the Kujung Group	n.a.	n.a.		
Indonesia	Kutei Basin	Eocene - Quaternary	165,000	14 km	32	Miocene Delta Sandstones	20-35	100-10000	Intraformational & transgressive shales. Large Anticlines on shore (Samarinda Anticlines)	Prolific oil & gas basin. Very good reservoirs.
Korea	Cheju	Cenozoic	~9,100	4-5 km	?	Sayori Sandstone (Shiira Grp)	18-30	n.a.	Upper Claystone (Shiira Grp)	Synrift. Transition from fluvial to marine.
						Basal Miocene Sandstone (Shiira Grp)	18-30	n.a.	Lower Claystone (Shiira Grp)	Synrift. Transition from fluvial to delta-marine.
Korea	Ulleung	L. Olig-Quaternary	est 56,000	5 km	38	Miocene debris flows	n.a.	n.a.	marine shale between debris flow events	Speculative reservoirs. Little data. There is also a more proximal play in southern basin where a coastal plain environment briefly occurs in the late Miocene.
Korea	Kunsan (Rep. Korea portion of N. Yellow Sea Basin)	Cret. to Quaternary	est 10,000	max 6 km	?	Sandstone Fluvial & Lacustrine	n.a.	n.a.	Intraformational	Speculative. Little data specific to this area of the northern Yellow Sea Basin. Another Fluvial lacustrine system.

A8. Table of Basin Attributes

Member Economy	Basin Name	Basin Sequence	Area (Km <sup>2</sup> )	Basin Depth km	Temperature Gradient (°C/Km <sup>2</sup> )	Reservoir lithology & age	Porosity range in%	Permeability Range (md)	Traps & sealing rocks	Remarks
Malaysia	Malay Basin	Oligocene-Quaternary.	83,000	10-12 km	35(south) — 55 (north)	Sandstone (H-D Groups) Sandstone (I Group) Sandstone (J Group)	up to 30 25—30 11—30	up to 1000 up to 1000 up to 2000	Intraformational/mi-nor marine flood Seal : Miocene maximum flood. Regional marine shale. Intraformational/mi-nor marine flood	
Philippines	Zambales/Central Luzon Basin	Eocene - Quaternary	20,000	14 km	16—24 (?)	Fluvial Sandstone (K Group) Fluvial Sandstone (M & L Group)	10—30 10—27	up to 3000 av. 400	Intraformational/mi-nor marine flood Intraformational	No major hydrocarbon data. Speculative reservoirs in the Mid Miocene to Quaternary.
Chinese Taipei	West of Taiwan	Palaeocene - Quaternary	Tainan & Taihsi est 27,000	8-10 km	?	Late Miocene Sandstones Oligocene Sandstone (Transgressive ?)	n.a. n.a.	n.a. n.a.	Hinshui Shale ? Transgressive Shale	
Thailand	Thai Gulf Basin	Tertiary-Quaternary	~112680	3.5 km	50	Fluvial Sandstone	n.a.	n.a.	Intraformational	Reservoirs often discontinuous in the Patani Trough. More continuous reservoir may be found up depositional dip in the north of the basin. However intraformational seal will decrease as reservoir continuity increases.

Modified after Lee, K. Y. and C. D. Masters. Geologic framework, petroleum potential, and field locations of the sedimentary basins in China. Miscellaneous Investigations Series - U. S. Geological Survey, 1988.

# Appendix B: Depleted Field Calculations and Data

Hydrocarbon reserves data and estimated equivalent stored CO<sub>2</sub> are in Table A1.

## Hydrocarbon to Stored CO<sub>2</sub> Conversion estimates

These calculations assume perfect replacement of hydrocarbons volumes with CO<sub>2</sub> volumes. Multiple phase behaviour is very complex; given our limited data we have assumed pure CO<sub>2</sub> in the reservoir.

Pure CO<sub>2</sub> density in the subsurface becomes asymptotic between 2 and 4 km deep under normal pressure gradient and geothermal gradient of 30-35°C/km (surface temperature 15°C). The density of CO<sub>2</sub> is between 600 and 700 kg/m<sup>3</sup>. Reserves numbers are an amalgamation of field volumes. The specific depth, pressure, temperature and volume of each field is unknown.

As there are some many factors that are unknown or very uncertain the authors see no value in attempting to apply multiple geothermal gradients or pressure regimes to compute numbers that still have considerable residual uncertainty.

## Conversion of GAS STP volumes to Equivalent CO<sub>2</sub> tonnage stored

To convert methane volumes to CO<sub>2</sub> volumes greater compressibility of CO<sub>2</sub> must be considered. Volumes of methane at standard conditions (ie reserves) where converted to volumes of CO<sub>2</sub> at standard conditions by applying a factor of 1.6. This factor is the average ratio of the expansion factor of methane and the expansion factor of CO<sub>2</sub> in the average case where CO<sub>2</sub> is stored in a depleted gas field between 2 and 4 km deep under normal pressure gradient and geothermal gradient of 30-35°C/km.

The CO<sub>2</sub> volume is then multiplied by the density of CO<sub>2</sub> at standard conditions to give a mass that could be expected to be stored in the reservoir.

For ease of computation we have used:

**1 Tcf (Trillion standard Cubic Feet) of methane ≈ 80 Mt CO<sub>2</sub> stored underground**

Conversion of OIL STP volumes to Equivalent CO<sub>2</sub> tonnage stored

When removed from the subsurface oil expands from 1 to 1.4 times. Unlike gas the density (and volume) of oil in the sub surface is fairly similar to density (and volume) at the surface. The Formation volume factor is used to compensate for this difference.

Volume of underground oil = Volume (std m<sup>3</sup>) \* FVF

Equivalent CO<sub>2</sub> mass stored = (Volume (std m<sup>3</sup>) \* FVF) \* density of CO<sub>2</sub> (reservoir)

Assumed average values were adopted from Holloway et al., (1996) for FVF and CO<sub>2</sub> density.

FVF = 1.2

CO<sub>2</sub> density in the subsurface = 700 kg/m<sup>3</sup> (approximate asymptotic limit for CO<sub>2</sub> density between 1.5 and 4 km assuming 30-35°C/km and 10.5 MPa/km.)

Again for ease of computation we used:

**100 mmbbl oil (stock tank barrels) 13 Mt CO<sub>2</sub> stored underground**



Indonesia	Kutei Basin	2195	285	684	89	2879	76	374	8,711	697	36,762	2941	45,473	19	3638	982	3030	4012	24	USGS 2000	Indonesia	Kutei Basin	2879	374	45.47	3638	4012	24
Indonesia	North Sumatra Basin	496	64	178	23	674	74	88	13,977	1118	11,582	927	25,559	55	2045	1183	950	2132	55	USGS 2000	Indonesia	North Sumatra Basin	674	88	25.56	2045	2132	55
Indonesia	Northwest Java Basin	1555	202	1613	210	3168	49	412	1,026	82	7,028	562	8,055	13	644	284	772	1056	27	USGS 2000	Indonesia	Northwest Java Basin	3168	412	8.06	644	1056	27
Indonesia	South Sumatra Basin	1842	239	587	76	2429	76	316	3,125	250	7.08	566	10,204	31	816	489	643	1132	43	USGS 2000	Indonesia	South Sumatra Basin	2429	316	10.20	816	1132	43
Indonesia	Total	14437	1877	7930	1031	22367	65	2908	27,749	2220	65,408	5233	93,157	30	7453	4097	6264	10360	40		Indonesia	Total	22367	2908	93.16	7453	10360	40
South Korea	Total	-	0	-	0	0	0	0	-	0	0.21	17	0.21	0	17	0	17	17	0		South Korea	Total	0	0	0.21	17	17	0
Malaysia	Greater Sarawak Basin	168	22	649	84	817	21	106	3,731	298	78,433	6275	82,164	5	6573	320	6359	6679	5	USGS 2000	Malaysia	Greater Sarawak Basin	817	106	82.16	6573	6679	5
Malaysia	Malay Basin	1518	197	2090	272	3608	42	469	0,492	39	47,657	3813	48,149	1	3852	237	4084	4321	5	USGS 2000	Malaysia	Malay Basin	3608	469	48.15	3852	4321	5
Malaysia	Total	1686	219	2739	356	4425	38	575	4,223	338	126,09	10087	130,313	3	10425	557	10443	11000	5		Malaysia	Total	4425	575	130.31	10425	11000	5
Philippines	Total	-	0	178	23	178	0	23	-	0	3.7	296	3.7	0	296	0	319	319	0	Oil and Gas Journal Dec 2002	Philippines	Total	178	23	3.70	296	319	0
Chinese Taipei	Total	-	0	4	1	4	0	1	-	0	2.7	216	2.7	0	216	0	217	217	0	IEA website 2004	Taiwan	Total	4	1	2.70	216	217	0
Thailand	Total	726	94	700	91	1426	51	185	7.4	592	15.4	1232	22.8	32	1824	686	1323	2009	34	BP world energy 2004	Thailand	Total	1426	185	22.80	1824	2009	34

1. In 2000 the USGS assessed the hydrocarbon volumes in ~200 basins that represent 90+% of the world's hydrocarbon reserves.

2. "Tarim and Junggar basins do not match with significant sources of CO<sub>2</sub> and were not studied in this report. However they are included totals for figures 29 and 30 of the main report which is attempt to estimate the ultimate potential of depleted field storage."

3. According to the IEA 2000 emissions data used in this study, there are no major sources of CO<sub>2</sub> in Eastern Malaysia (ie adjacent to the Sarawak Basin) and so it was not studied. However it is included in this attempt to estimate ultimate depleted storage potential



# Glossary

This glossary defines a selection of terms used in this report.

**Alluvial:** Pertaining to the subaerial (as opposed to submarine) environment. Products of a stream or river formed where its velocity has slowed on the upper floodplain, usually consisting of clastic sediments. Distinct from subaqueous deposition in lakes or oceans and lower energy fluvial deposition. Sediments deposited in an alluvial environment can be subject to high depositional energy, such as fast-moving flood waters, and may be poorly sorted or chaotic.

**Bioherm:** A mound-like mass of rock built by organisms such as colonial corals and calcareous algae.

**CCS:** Carbon Capture and Storage.

**Clastic sediments:** Sediment consisting of broken fragments derived from preexisting rocks and transported elsewhere and re-deposited before forming another rock. Examples of common clastic sedimentary rocks include rocks such as conglomerate, sandstone, siltstone and shale. Carbonate rocks can also be broken and reworked to form clastic sedimentary rocks.

**Carbonate:** A class of sedimentary rock whose main mineral constituents are calcite and dolomite. Limestone, dolomite and chalk are carbonate rocks. Although carbonate rocks can be clastic in origin, they are more commonly formed through processes of precipitation or the activity of organisms such as coral and algae. Carbonates form in marine settings, evaporitic basins, lakes and windy deserts. Carbonate rocks can serve as hydrocarbon reservoir rocks, particularly if their porosity has been enhanced through dissolution. They often rely on fractures for permeability.

**Coal Bed Storage:** Coals are known to adsorb CO<sub>2</sub> more strongly than methane (which commonly occurs in coals) and to have a substantially greater capacity to store CO<sub>2</sub> than methane (at least twice as much). The storage capacity for coal seams can't be calculated using pore volumes and gas compressibility as for conventional porous reservoirs, as the gas in coals is stored in the coal matrix on the surface of micropores, in a free state in the coal cleats or is dissolved in water. To calculate CO<sub>2</sub> storage capacity in coals requires knowledge of the adsorption isotherms and pressure, which vary for each coal type. There are concerns that storage of CO<sub>2</sub> in coals may not actually produce any net greenhouse gas mitigation when it is associated with production of methane (ECBM - Enhanced Coal Bed Methane). The range of permeability typical of coal beds is at the lower end of the range of permeability possible in siliciclastic and carbonate rocks. Storage of CO<sub>2</sub> in coals is an emerging science, and more research is required to fully understand the processes and interactions involved, such as the effect of swelling of coals during injection of CO<sub>2</sub>. The trapping mechanism operates immediately.

**CBM:** Coal Bed Methane is process where by methane is extracted from coal seams for energy generation. ECBM Enhanced Coal Bead Methane is an experimental process in which coals' preferred adsorption of CO<sub>2</sub> over methane is used to produce methane while trapping CO<sub>2</sub>. See *Coal Bed Storage* for further details.

**Crust:** The thin, outermost shell of the earth that is typically 5 to 75 km thick. Generally divided into continental crust and oceanic crust; crustal- adjective.

**Delta:** A low, nearly flat accumulation of sediment deposited at the mouth of a river or stream generally into a marine or lake environment, commonly triangular or fan-shaped; *deltaic* - adjective.

**Depositional environment:** The area in which and physical conditions under which sediments are deposited, including sediment source; depositional processes such as deposition by wind, water or ice; and location and climate, such as desert, swamp or river.

**Depositional system:** The three-dimensional array of sediments or facies that fills a basin. Depositional systems vary according to the types of sediments available for deposition as well as the depositional processes and environments in which they are deposited e.g. fluvio-deltaic system.

**Facies:** The overall characteristics of a rock unit that reflect its depositional origin and differentiate the unit from others around it, e.g. river channel facies, floodplain facies and reef facies.

**Fluvial:** Pertaining to an environment of deposition by a river or running water. Fluvial deposits tend to be well sorted, especially in comparison with alluvial deposits, because of the relatively steady transport provided by rivers.

**Geothermal Gradient:** Rocks lying deeper in the earth are at high temperatures than the rocks above. The rate of temperature change is called the geothermal gradient. This gradient varies from place to place and is dependant on the crustal thickness and thermal conductivity of the rocks in area. Reservoirs that are at higher temperatures will store CO<sub>2</sub> at a lower density and will be somewhat less efficient as storage sites.

**Hydrocarbon Pore Space:** pore space in the subsurface that contains (or has contained) hydrocarbons. i.e. pore space within a hydrocarbon field or a depleted hydrocarbon field.

**“Known” Hydrocarbons:** A term used by the USGS (2000) meaning the sum of the cumulative produced hydrocarbons in an area plus the reserves.

**Lacustrine:** Pertaining to an environment of deposition in lakes, or an area having lakes.

**Oil/Gas field:** Most porous rocks in the sub surface contain saline water. If a “trap” exists and other conditions are favourable hydrocarbons can accumulate in a porous rock displacing most of the saline water. (See also *Saline reservoir; Reservoir-seal pair*).

**Petroleum system:** Geologic components and processes necessary to generate and store hydrocarbons, including a mature source rock, migration pathway, reservoir rock, trap and seal.

**Permeability:** Ability to flow or transmit fluids through a porous solid such as rock, typically measured in the petroleum industry in darcies or millidarcies (one thousandths of a darcy). Rocks that transmit fluids readily, such as sandstones, are described as permeable and tend to have many large, well-connected pores. Impermeable formations, such as shales and siltstones, tend to be finer grained or of a mixed grain size, with smaller, fewer, or less interconnected pores.

**Platform:** See *shelf*.

**Pore:** A discrete void within a rock that can contain air, water, hydrocarbons or other fluids. In a body of rock, the percentage of pore space is the porosity.

**Porosity:** The percentage of pore volume or void space, or that volume within rock that can contain fluids.

**Prospectivity:** A term used in the exploration for any geological resource, in this case pore volume for CO<sub>2</sub> storage. Prospectivity is a perception in the mind of a geoscientist/explorer of the likelihood that a resource is present in a given area based on the available information. This perception is developed through; examining data (if possible), examining existing knowledge, application of established conceptual models and ideally the generation of new conceptual models or applying an analogue from a neighbouring basin or some other geologically similar setting.

Often prospectivity assessment involves an element of professional judgement (experience) and is influenced considerably by the level of uncertainty associated with absence and/or presence of conflicting or confirming data for a concept. When the level of uncertainty is very high (as in this report) the prospectivity of an area can and will change with new knowledge and changes in economic and technological factors.

In the case of this study, some specific aspects that enter into consideration include; distance to sources of CO<sub>2</sub>, rate of CO<sub>2</sub> emission of near-by sources, presence of reservoir-seal pairs, extent of reservoir-seal pairs, heterogeneity/homogeneity, porosity and permeability, coal presence, coal rank, availability of depleted hydrocarbon fields, basin structure, basin age, basin history, pore water salinity, geothermal gradients and pressures. The list is not exhaustive. Availability of information on these factors in the literature for any given basin will vary markedly. Detailed investigation of these matters is not possible in a “desk top” study such as this report.

**Reserve:** A volume of hydrocarbon that is expected to be recovered from an area in the future with a high confidence.

**Reservoir:** Subsurface rock having sufficient porosity and permeability to store and transmit fluids.

**Reservoir-seal pair:** To prevent the upward migration of CO<sub>2</sub> due to buoyancy, any porous rock (saline reservoir) used to store CO<sub>2</sub> requires the existence of an overlying impermeable “seal” or “caprock”. A reservoir formation and seal formation stratigraphically related in this way is called a reservoir-seal pair. Use of this term does not necessarily imply the presence of a structure or trap. (See also *Saline Reservoir; Oil/Gas Reservoir*).

**Saline Reservoir:** A reservoir containing saline formation water. Nearly all porous rock formations in the subsurface contain saline water. Some contain fresh water. A few contain hydrocarbons. (See also *Reservoir; Oil/Gas Reservoir; Reservoir-seal pair*).

**Seal (or Caprock):** A relatively impermeable rock that forms a barrier or cap above and around reservoir rock preventing the migration of fluids beyond the reservoir (See also *Reservoir; Reservoir-seal pair*).

**Siliciclastic:** Silica-based sediments that are broken from pre-existing rocks, transported elsewhere, and re-deposited before forming another rock. Examples of common siliciclastic sedimentary rocks include conglomerate, sandstone, siltstone and shale.

**Shelf:** Continental shelf, or the area at the edges of a continent from the shoreline to a depth of 200 m, where the continental slope begins. The shelf is commonly a wide, flat area with a slight seaward slope; *shelfal* – adjective.

**Subduction:** A geologic process in which one edge of one crustal plate is forced below the edge of another.

**Terrane:** A crustal block or fragment that preserves a distinctive geologic history that is different from the surrounding areas and that is usually bounded by faults.

**Tectonic:** Describing the forces that cause the movements and deformation of Earth's crust on a large scale, also describes the resulting structures or features from these forces.

**Transgression:** A rise in sea level relative to the land.

**Trap:** A configuration of rocks suitable for containing hydrocarbons and sealed by a relatively impermeable formation through which hydrocarbons will not migrate. Traps can be either structural traps (in deformed strata such as folds and faults) or stratigraphic traps (in areas where rock types change) or a combination of these.

**Turbidite:** The sediments or rocks that formed as a result of a flow of dense, muddy water due to a fast-flowing current that moves down a slope, depositing suspended sediments over the floor of a body.

# Acronyms and Units

barrel	0.1589873 m <sup>3</sup> of oil at standard temperature and pressure (short for stock tank barrel)
Bcf	Billion (10 <sup>9</sup> ) standard cubic feet
billion	petroleum field definition:10 <sup>9</sup>
CO <sub>2</sub>	Carbon dioxide
FVF	Formation Volume Factor
Gt	Giga tonnes (10 <sup>9</sup> tonnes)
kg	kilograms
km	kilometre
m <sup>3</sup>	cubic metre
mmbbls	million barrels
MPa	Mega pascals (1 MPa = 10.1 atmospheres)
Mt	Mega tonnes (10 <sup>6</sup> tonnes)
sq km	square kilometre
stb	(stock tank barrel ie the basic petroleum field unit of oil volume at surface conditions or Standard conditions see STP and barrel)
STP	standard temperature and pressure
t	metric tonnes
Tcf	Trillion standard cubic feet
trillion	petroleum field definition:10 <sup>12</sup>





an emission free vision for the future





Prepared by  
**Innovative Carbon Technologies Pty Ltd.**  
on behalf of  
**the Cooperative Research Centre for  
Greenhouse Gas Technologies (CO2CRC)**

GPO Box 463, Canberra, ACT 2601  
Tel: +61 2 6200 3366 Fax: +61 2 6230 0448  
Email: [dhilditch@ictpl.com.au](mailto:dhilditch@ictpl.com.au) Website: [www.ictpl.com.au](http://www.ictpl.com.au)

**FOR THE ASIA-PACIFIC ECONOMIC COOPERATION  
SECRETARIAT**

35 Heng Mui Keng Terrace Singapore 119616  
Tel: (65) 6775-6012 Fax: (65) 6775-6013  
Email: [info@apec.org](mailto:info@apec.org) Website: [www.apec.org](http://www.apec.org)

© 2005 APEC Secretariat  
APEC#205-RE-01.6.

